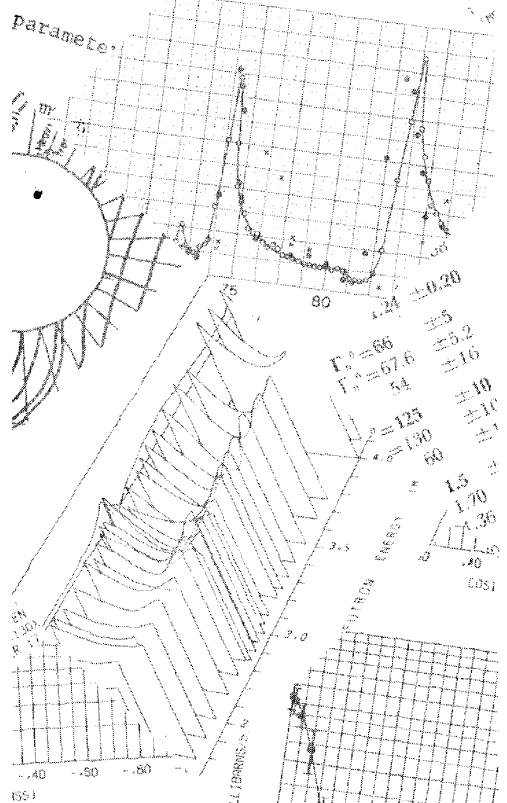


- nucleus
of cylindrical symmetry is defined as:
 $B_{\lambda} Y_{\lambda 0}(\theta')$
 $B_{\lambda} Y_{\lambda 0}(\theta')$



NATURAL OXYGEN
DIFF ELASTIC
E = 3.910 MEV
HELV PHYS 11 35 351 82
BASEL ΔEₐ = 0.35 MEV
3-ND ORDER LOG-NORM FIT

TELETYPE
=FNDF SERVICE ROOM
FORTRAN
LABEL
INCREMENTED RCD IDENT
SUBROUTINE INK(X,M)
A IS OF THE FORM ANNN.
M MAY BE A NUMERIC OR
N IS A NUMERIC CHARACTER
R IS THE BLANK CHARACTER
M IS THE NUMBER OF NON-
=3 FOR SEQUENCE OF NON-
=5 FOR RECORD ID NUMBER
ON RETURN X IS INCREMENTED
DIMENSION L(6)
CALL SPLIT(X,L)
M=M-1
Pₐ(eV)MP

BNL-NCS-50451
(ENDF-217)
NEACRP-L-147
NEANDC(US)-192/L
INDC(US)-69/L

SEMINAR ON ²³⁸U RESONANCE CAPTURE

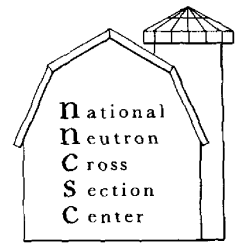
JOINTLY SPONSORED BY THE
ELECTRIC POWER RESEARCH INSTITUTE
AND U.S. ENERGY RESEARCH
AND DEVELOPMENT ADMINISTRATION

Edited by
S. PEARLSTEIN

March 18-20, 1975

INFORMATION ANALYSIS CENTER REPORT

HELD AT THE
NATIONAL NEUTRON CROSS SECTION CENTER
BROOKHAVEN NATIONAL LABORATORY
UPTON, NEW YORK 11973



NOTICE

This report was prepared as an account of work sponsored by the United States Government. Neither the United States nor the United States Energy Research and Development Administration, nor any of their employees, nor any of their contractors, subcontractors, or their employees, makes any warranty, express or implied, or assumes any legal liability or responsibility for the accuracy, completeness or usefulness of any information, apparatus, product or process disclosed, or represents that its use would not infringe privately owned rights.

Printed in the United States of America
Available from
National Technical Information Service
U.S. Department of Commerce
5285 Port Royal Road
Springfield, VA 22161

Price: Printed Copy, Domestic \$8.75;
Foreign \$11.25; Microfiche \$1.45

August 1975

800 copies

BNL-NCS-50451
(ENDF-217)
(Physics-General - TID-4500)

SEMINAR ON ^{238}U RESONANCE CAPTURE

**JOINTLY SPONSORED BY THE ELECTRIC POWER RESEARCH INSTITUTE
AND U.S. ENERGY RESEARCH AND DEVELOPMENT ADMINISTRATION**

**Edited by
S. PEARLSTEIN**



March 18-20, 1975

**HELD AT THE
NATIONAL NEUTRON CROSS SECTION CENTER**

**BROOKHAVEN NATIONAL LABORATORY
ASSOCIATED UNIVERSITIES, INC.**

**UNDER CONTRACT NO. E(30-1)-16 WITH THE
U.S. ENERGY RESEARCH AND DEVELOPMENT ADMINISTRATION**

TABLE OF CONTENTS
SEMINAR ON ²³⁸U RESONANCE CAPTURE

	Page
SPONSORS' STATEMENTS	iv
INTRODUCTION	vi
PROGRAM	viii
AGENDA	ix
EPILOGUE	xi
SUMMARIES	
A. SESSIONS I AND IV	xiii
I. ANALYSIS OF CRITICAL AND SUBCRITICAL EXPERIMENTS - F. J. McCrosson	
IV. INTEGRAL MEASUREMENT ANALYSIS - J. Hardy, Jr.	
B. SESSIONS II AND III	xxiv
II. EXPERIMENTAL DIFFERENTIAL DATA - G. deSaussure	
III. RESONANCE ANALYSIS - M. R. Bhat	
C. SESSION V	xxx
V. METHODS FOR CALCULATING ENERGY AND SPATIAL SELF-SHIELDING EFFECTS - R. Karam	
LIST OF PARTICIPANTS	xxxiv
CONTRIBUTED PAPERS	
1. DISCREPANCIES IN THERMAL REACTOR LATTICE ANALYSIS - W. Rothenstein	2
2. MONTE CARLO ANALYSIS OF TRX LATTICES WITH ENDF/B VERSION 3 DATA - J. Hardy, Jr.	18
3. S ₀ ANALYSIS OF THE TRX METAL LATTICES WITH ENDF/B III DATA - F. J. Wheeler	35
4. THE CURRENT UK POSITION ON URANIUM-238 RESONANCE CAPTURE - J. R. Askew	45

	Page
5. ANALYSIS OF THE "FOUR-FUEL" EXPERIMENTS USING HAMMER - D. S. Craig	72
6. EFFECTIVE U-238 RESONANCE INTEGRALS IN CLUSTERS OF NATURAL URANIUM FUELPINS DERIVED FROM ORNL LATTICE MEASUREMENTS - J. Griffith	81
7. ADJUSTMENT OF THE EFFECTIVE ²³⁸ U RESONANCE INTEGRAL TO FORCE AGREEMENT WITH INTEGRAL DATA - M. Edenius	87
8. PRECISE MEASUREMENT AND CALCULATION OF ²³⁸ U NEUTRON TRANSMISSIONS - D. K. Olsen et al.	95
9. THE ²³⁸ U(n,γ) CROSS SECTION ABOVE THE RESONANCE REGION - R. B. Perez et al.	103
10. EVALUATION OF ²³⁸ U CROSS SECTIONS FOR ENDF/B-IV - F. J. McCrosson	122
11. COMMENT ON THE U-238 DISCREPANCY - R. E. Chrien	147
12. ANALYSIS OF ORNL CAPTURE DATA - G. deSaussure	151
13. COMMENTS ON ²³⁸ U NEUTRON WIDTH EVALUATIONS - H. Derrien	156
14. REVIEW OF BENCHMARK EXPERIMENTS - R. Sher and S. Fiarman	163
15. REACTIVITY AND REACTION RATE MEASUREMENTS IN U-D ₂ O LATTICES WITH COAXIAL FUEL - D. J. Pellarin and B. M. Morris	167
16. INTERFERENCE SCATTERING EFFECTS ON INTERMEDIATE RESONANCE ABSORPTION AT OPERATING TEMPERATURES - R. Goldstein	189
17. INTERACTIVE APPROACHES TO EVALUATING METHODS AND DATA FOR SELF-SHIELDED RESONANCE ABSORPTION - M. Becker	200
18. EFFECTS OF THE FREE-GAS, SLOWING-DOWN MODEL ON RESONANCE CROSS SECTIONS IN ²³⁸ U - R. A. Karam	204
19. TECHNIQUE FOR SIMULTANEOUS ADJUSTMENT OF LARGE NUCLEAR DATA LIBRARIES - D. R. Harris et al.	215
20. ENDF/B-IV THERMAL REACTOR LATTICE BENCHMARK ANALYSIS WITH MONTE CARLO RESONANCE TREATMENTS - W. Rothenstein	222
21. A DISCUSSION OF U-238 RESOLVED RESONANCE PARAMETERS AND THEIR INFLUENCE ON CAPTURE CROSS-SECTIONS - M. R. Bhat	255

SPONSOR'S COMMENTS

O. Ozer

Electric Power Research Institute

The Electric Power Research Institute (EPRI) is an organization established by the U.S. utility industry in order to conduct and administer research in areas related to the generation, transmission, distribution and utilization of electric power. About a quarter of the institute's budget (\$36.2 million in 1975) is assigned to research projects related to the development of nuclear power.

In the area of neutron cross sections and associated nuclear constants, EPRI's objective is to provide the utility industry with a standard data base acceptable for use in power reactor applications and compatible with the requirements of ANSI standard N411.

The ENDF/B library, developed primarily under fast reactor funding, could provide the basis for such a standard provided its performance in thermal reactor applications can be improved. The major problem along this path concerns the apparent inability of the ENDF/B data to predict observed uranium-238 resonance capture rates in critical lattice experiments.

Since it is not clear whether the basic data, the methods of analysis, or the interpretation of lattice experiments is at fault, EPRI is supporting the National Neutron Cross Section Center to organize a working seminar of experts in each of the above areas in a format conducive to free discussions and exchange of ideas.

It is hoped that such a seminar will result in a better determination of areas where further research is most likely to yield a solution.

P. Hemmig (in absentia)

Energy Research and Development Administration

I consider the meeting to be an important one with considerable promise of being productive. It is a milestone in technology when a large number of people get together to try to investigate discrepancies, accelerate understanding and the application of that understanding. EPRI is to be commended for their endorsement of this work. I wish you all a very successful meeting.

INTRODUCTION

The National Neutron Cross Section Center is interested in U-238 resonance capture as part of its responsibility for development of the Evaluated Nuclear Data File (ENDF/B), a library of microscopic data useful to both the research and applied communities. It is a prime objective that ENDF/B be application independent. Consistent results should be obtained when the best differential data are used to analyze integral experiments in configurations which average the nuclear properties of many nuclides over energy and space.

Assembly of a comprehensive library of evaluated data is too massive a task for any one group. ENDF/B is developed with the help of the Cross Section Evaluation Working Group (CSEWG), a group of measurers, evaluators, and reactor physicists that meet regularly to plan, evaluate, and test nuclear data. In addition special groups of scientists are mobilized at times to study important problems. Part of CSEWG's program is the validation of ENDF/B data in the calculation of integral benchmark experiments. The attention of this Seminar is directed to the poor agreement obtained using ENDF/B data in the calculation of low enrichment uranium lattices. This is not a new problem but since configurations of this type continue to play an important role in nuclear power, a field which is being increasingly scrutinized for technical flaws, all discrepancies should be tenaciously investigated until understood.

In the CSEWG experience, good cooperation among measurers, evaluators, and reactor physicists has been instrumental in bringing about improvements in ENDF/B. Each disciplinary group has shown a mutual respect for the potential precision inherent in differential and integral experiments and in calculational methods. These areas are sufficiently developed that it is now reasonable to expect that low enrichment uranium lattices should be well calculated from first principles. At present however this has not been done and the fault lies somewhere among the nuclear data derived from measurements of basic data, the parameters interpreted from integral measurements, and the calculational methods.

In view of the past extensive investigations of this problem perhaps this Seminar cannot expect to develop any new insight. However, this Seminar does have the advantage of a time perspective of older information and consists of a large group of experts gathered in one place to have extended interactive discussion dedicated to this subject. The objective of this Seminar is to review past efforts, describe work in progress, and recommend new investigations aimed at understanding the inconsistency between differential and integral data. The Seminar is jointly sponsored by the Electric Power Research Institute, 3412 Hillview Avenue, P. O.Box 10412, Palo Alto, CA 94304 and the U. S. Energy Research and Development Administration, Washington, D. C. 20545.

PROGRAM

There were five Sessions each devoted to an aspect of the effect of U-238 data on uranium lattice calculations. The Sessions and chairmen were selected with the help of the Thermal Data Testing Group, headed up by F. J. McCrosson, operating within the Cross Section Evaluation Working Group.

The Sessions were divided according to the following topics:

<u>Session</u>	<u>Topic</u>	<u>Chairman</u>
I	Analysis of Critical and Subcritical Experiments	F. J. McCrosson, SRL
II	Experimental Differential Data	G. DeSaussure, ORNL
III	Resonance Analysis	M. R. Bhat, BNL
IV	Integral Measurements and Analysis	J. Hardy, Jr., BAPL
V	Methods for Calculating Energy and Spatial Self-Shielding Effects	R. Karam, GIT

Each Session chairman was responsible for making arrangements with the speakers and organizing the discussion. After all speakers were heard the participants divided into working groups to prepare Session summaries and recommendations for future work. Papers submitted in the form of photo-ready copy are included in these proceedings.

AGENDA

Seminar on ^{238}U Resonance Capture

March 18-20, 1975
National Neutron Cross Section Center
Conference Room, Bldg. 197

Tuesday, March 18

- 9:00 AM Introduction S. Pearlstein, BNL
Sponsor's remarks O. Ozer, EPRI
Sponsor's remarks P. B. Hemmig, ERDA (in absentia)
- 9:30 AM Comments on Sessions Session Chairmen
- 9:45 AM Session I Analysis of Critical and Subcritical Experiments -
F. J. McCrosson, SRL - Chairman
1. Historical Review, W. Rothenstein, BNL
 2. Monte Carlo Analysis of TRX Lattices with ENDF/B
Version III Data, J. Hardy, Jr., BAPL
 3. S_n Analysis of TRX-Metal Lattices, F. Wheeler, ANC
 4. The Current UK Position on U-238 Resonance Capture,
J. R. Askew, AEEW
 5. Analysis of the "Four-Fuel" Experiments using HAMMER
D. S. Craig, AECL
 6. Effective U-238 Resonance Integrals in Clusters of
Natural Uranium Fuelpins Derived from ORNL Lattice
Measurements, J. Griffiths, AECL
 7. Adjustment of the Effective U-238 Resonance Integral
to Force Agreement with Integral Data, M. Edenius,
AB ATOMENERGI, Studsvik
- Discussion
- 12:30 PM Break
- 2:00 PM Session II Experimental Differential Data - G. DeSaussure, ORNL-
Chairman
1. Average Resonance Parameters for U-238, W. W. Havens, Jr., COL
 2. Resonance Parameter Correlations, J. Felvinci, COL
 3. Transmission Measurements for U-238, D. Olsen, ORNL
 4. Self Indication Measurements with Filtered Beams, R. Block, RPI
 5. Capture Cross Section above the Resonance Region, R. Perez
and R. Spencer, ORNL
 6. Evaluation of U-238 for ENDF/B-IV, F. J. McCrosson, SRL
 7. Filtered Beam Measurements of U-238 Capture, R. E. Chrien, BNL
 8. Geel-Mol Measurement Program, G. Rohr, Geel
 9. Harwell Measurement Program, D. Gayther, AERE
- Discussion
- 5:30 PM Break

EPILOGUE

After the Seminar there was an immediate exchange of information internal to the reactor physics calculations, the comparison of which would show where the reported disagreement between similar calculational methods entered. After correction of some differences in interpretation and some minor errors in long-standing versions of processing codes, most of the available reactor physics analyses of the benchmark lattices are in substantial agreement. At the Seminar confidence was not shaken in the parameters relating to uranium capture derived from lattice and rod measurements. Therefore, nuclear data continues to be suspected as the major source of the discrepancy although this is not obvious from examination of the measurements and their quoted uncertainty.

A useful background for the long standing discrepancy is presented in Paper No. 1 by Rothenstein. Monte Carlo calculations using ENDF/B-III data by Hardy in Paper No. 2 show that the discrepancy between calculation and experiment from previous values is reduced but not removed for TRX lattices even though thorough investigative techniques are employed. Monte Carlo methods reported by Rothenstein in Paper No. 20 were checked in part against Hardy's methods and showed that there were further small improvements using ENDF/B-IV data. In summary, there was relatively good agreement between calculated and measured reaction rate ratios and criticality for a wide range of metal to water ratios if Monte Carlo methods were used corresponding to a reduction in the disagreement between calculated and measured self shielded integrals from about 10 percent to 3 or 4 percent. The constant criticality bias and favorable calculated spectrum dependent reaction rate ratios gave strong indication that corrections to the data alone to accommodate remaining discrepancies would be severely restricted to avoid worsening calculated reaction rate ratios or introducing a composition dependent tilt in the criticality comparisons.

In the area of nuclear data future work is expected to concentrate on new experiments and reanalysis of existing data. New measurements are recommended that focus on the determination of resonance widths for the first few resonances for U-238, the magnitude of the capture cross section in the valleys between resonances and the transmission of neutrons through thick samples. Existing data will be examined for possible alternate choices of U-238 data that will lead to consistency within experimental uncertainties, differential cross sections and dilute and self shielded

resonance integrals. For improved understanding of the discrepancy between calculation and experiment the sensitivity of the lattice benchmarks to reasonable choices of U-238 and other data will be investigated. As a result of the Seminar discussion, three papers by Bhat, Chrien, and deSaussure were submitted for inclusion in this compendia bearing on nuclear data and its analysis.

For more detailed comments the Session Summaries and Contributed Papers should be consulted.

Summary of Sessions I and IV

I. Analysis of Critical and Subcritical Experiments

IV. Integral Measurements and Analysis

F. J. McCrosson, SRL

J. Hardy, Jr., BAPL

1. SUMMARY OF LATTICE ANALYSES

Results of ENDF/B-III benchmark lattice calculations were summarized.

These included calculations by the following (Tables 1 and 2):

F. Wheeler (ANG) - S_n / RABBLE

J. Hardy, Jr. (BAPL) - Monte Carlo (MUFT leakage corrections)

D. S. Craig and M. Hughes (CRNL) - Integral Transport/Nordheim

D. Mathews (GGA) - S_n / GAND3

L. Petrie (ORNL) - Monte Carlo

F. J. McCrosson (SRL) - Integral Transport/Nordheim

These results consistently indicate that criticality for low enrichment uranium lattices is underpredicted by approximately 2% and ρ^{28} , the ratio of epithermal-to-thermal ^{238}U captures, is overpredicted by approximately 10%. These discrepancies can be removed by a 1.0 ± 0.3 barn reduction of the effective resonance integral above 0.625 eV. The reasonably good prediction of criticality for the ORNL spheres of uranyl nitrate (93 wt % ^{235}U) indicates there are no significant deficiencies in the ^{235}U cross sections.

TABLE 1

Criticality

BENCHMARK	DESCRIPTION	k _{eff} (ENDF/B-II)				k _{eff} (ENDF/B-IV)	
		ANC	BAPL	CRNL	GGA	ORNL	SRL
ORNL	Unref. spheres of uranyl nitrate sol.						
-1	H/U-235=1378; R=34, 595 cm		0.9965		0.9999		0.9996
-2	H/U-235=1177; R=34, 595 cm		0.9963		0.9995		
-3	H/U-235=1033; R=34, 595 cm		0.9933		0.9963		
-4	H/U-235= 971; R=34, 595 cm		0.9947		0.9980		0.9976
-10	H/U-235=1835; R=61.011 cm		0.9931		0.9956		0.9951
TRX	H ₂ O moderated U lattices						
-1	Mod/Fuel = 2.35	0.9741	0.9872	0.9808	0.9791	0.985	0.9875
-2	Mod/Fuel = 4.02	0.9823	0.9913	0.9876	0.9924	0.998	0.9941
MIT	D ₂ O moderated U lattices						
-1	Mod/Fuel = 20.74		0.9674	0.9801	0.9888	0.984	0.9883
-2	Mod/Fuel = 25.88		0.9739	0.9804	0.9925	0.974	0.9888
-3	Mod/Fuel = 34.59		0.9705	0.9826	0.9996	0.975	0.9911

TABLE 2
Ratio of Epithermal-to-Thermal ²³⁸U Captures*

<u>BENCHMARK</u>	<u>EXP</u>	<u>ANC</u>	<u>²³⁸U (ENDE/B-III)</u>			<u>²³⁸U (ENDE/B-IV)</u>		
			<u>BAPL</u>	<u>ORNL</u>	<u>GGG</u>	<u>ORNL</u>	<u>SRL</u>	<u>SRL</u>
TRX-1	1.311 ±0.020	1.438	1.422	1.419	1.416	1.44	1.454	1.417
TRX-2	0.830 ±0.015	0.906	0.899	0.874	0.877	0.91	0.890	0.868
MIT-1	0.498 ±0.008		0.534	0.5319	0.534	.535	0.5683	0.5464
MIT-2	0.394 ±0.002		0.437	0.4365	0.435	.430	0.4659	0.4483
MIT-3	0.305 ±0.004		0.345	0.3400	0.334	.346	0.3624	0.3490

*Thermal cutoff energy = 0.625 eV

J. Askew described the extensive Winfrith experience in this area, which was first reported in the United States at the 1966 San Diego meeting on reactor physics in the resonance and thermal regions. With the U.K. cross section library, a reduction of about 0.5 b in effective resonance integral is required to predict ^{238}U capture in a large number of lattices. M. Edenius found the U.K. library to be 0.5 b lower than ENDF/B-III in effective capture integral. Hence, the Winfrith studies support the ~ 1.0 b reduction of ENDF/B-III effective capture integral suggested by CSEWG benchmark analyses.

The SRL results in Tables 1 and 2 provide a measure of the magnitude of the changes in going from ENDF/B-III to ENDF/B-IV. Although the improvement is substantial, much of the discrepancy remains. One of the primary objectives of the ENDF/B-IV ^{238}U cross section evaluation was to improve the prediction of thermal benchmark experiments, but accuracy of the differential measurements, as reported in the literature, gave little leeway for such improvement.

Because of the high degree of consistency among the hundreds of benchmarks considered over a wide range of leakages, pitches, enrichments and moderator types, it was concluded that there is a real discrepancy in the ^{238}U epithermal capture cross sections which yields effective resonance integrals which are about 1.0 barn too high, and that our objective should be to localize where the deficiencies lie in the epithermal region. Reactor analysts have generally agreed that the reduction should be made in unshielded regions of the cross section, and this has been accomplished by a variety of artifices, e.g., a constant reduction in the capture cross section throughout the resonance region, or a reduction of keV p-wave cross sections.

The consistency of the thermal reactor calculations can also be extended to the large plutonium fueled fast reactor benchmarks. Here the U-238 capture to Pu-239 fission rate ratios are, for the most part, high by 2-8 percent whereas the calculated eigenvalues are low by about 0.5 percent. There is also evidence that the agreement between the calculated and measured parameters gets worse as the U-238 isotopic concentration increases (summary of CSEWG Meeting, October 23-24, 1974). It should be noted, however, that in fast reactor systems modifications to cross sections other than the U-238 capture cross section (e.g., the U-238 inelastic cross section) can improve the agreement between the calculated and measured values of the U-238 capture to Pu-239 fission rate ratios and the eigenvalues.

Two new calculational programs were presented at the meeting. W. Rothenstein (BNL) presented results from HAMMER calculations, but with the resonance reaction rates calculated by Monte Carlo (REPC). These calculations yielded good prediction of k and ρ^{28} using ENDF/B-IV. D. Finch (SRL) also presented results using integral transport theory and a new resonance treatment, similar to RABBLE, which yielded promising results. These new results offer the possibility that the problems with ρ^{28} might lie in the lattice analysis techniques and not in the differential cross sections (or the integral measurements). However, at this point this is rather improbable due to the good consistency among many previous calculations using similar techniques. For example, F. Wheeler's calculations used RABBLE for the resonance treatment, which should be similar to the new approach presented by D. Finch. J. Hardy used Monte Carlo (RECAP) calculations, which should include the advantages of the Rothenstein technique.

The Wheeler and Hardy calculations are consistent within themselves and support the need for a 1.0 barn reduction in the effective resonance integral. A comparison of the two methods is given below for the zero leakage cell calculations for TRX-1:

<u>Parameter</u>	<u>Hardy</u>	<u>Wheeler</u>	<u>% Diff.</u>
k	1.155	1.151	.3
ρ^{28}	1.375	1.407	2.3
δ^{28}	0.0835	0.0835	0
δ^{25}	0.1002	0.0999	.3
CR	0.814	0.796	2.3

2. SUMMARY OF INTEGRAL MEASUREMENTS

R. Sher reviewed some of the activation methods used to measure ^{238}U capture, ^{238}U fission, and ^{235}U fission rates in lattices. Emphasis was placed on the cadmium ratio method for ρ^{28} , the ratio of epithermal/thermal ^{238}U capture. Among the sources of possible systematic error are neutron streaming, flux and source perturbation by experimental loadings, and calculation of the cadmium cutoff energy.

S. Fiarman and R. Sher presented calculational results for streaming effects caused by use of aluminum shields on ^{238}U detector foils.

J. Hardy, Jr. discussed ^{238}U capture experiments in TRX lattices. ρ^{28} was measured by the cadmium ratio technique and also by thermal subtraction, which avoids the use of cadmium-covered ^{238}U foils (and associated questions of systematic error). The two methods gave consistent results.

D. Pellarin and W. Morris described recent parameter experiments in exponential assemblies of concentric-tube ^{238}U lattices moderated with D_2O . Included were measurements of ^{238}U fission, ^{235}U fission, ^{238}U capture, and B^2 . These lattices strongly emphasized spatial heterogeneity effects.

The following points were noted in the discussions:

a. Lattice Experiments

Overall consistency of results from a large number of experiments at different laboratories suggests that there are no serious systematic errors associated with ^{238}U capture measurements in lattices. (Because of the varied techniques employed, and the extreme range of lattice types and pitches covered, any such errors would have to be of a fundamental nature.) This conclusion is supported by the consistent calculation of low k_{eff} values, correlated with the amount of ^{238}U resonance capture. Consistency of the CSEWG benchmark experiments with those analyzed at Winfrith can be inferred from the fact that both indicate the need for a ^{238}U capture integral ~ 0.6 b below that required for isolated rod experiments (see Item c).

b. Isolated Rod Shielded Capture Experiments

These were reviewed by E. Hellstrand at the 1966 San Diego meeting. For UO_2 rods, the average recommended values are slightly lower than Hellstrand's own measurements; for metal rods, the recommended values are appreciably higher. Calculations indicate that Hellstrand's own results are more consistent as to slope, and between UO_2 and metal rods.

Overall uncertainty is $\pm 3.5\%$. This type of measurement is subject to uncertainty of normalization and flux spectrum. Interpretation is less straight forward than for lattice measurements.

c. Consistency of Lattice and Isolated Rod Experiments

Analyses of lattice capture measurements and isolated rod shielded integrals have been made at Winfrith and by the CSEWG data testing committee. Both analyses conclude that the lattice experiments require ~ 0.6 b less ^{238}U effective capture integral than do the isolated rod experiments. (This differs by only 0.1 b between Hellstrand's recommended values and his own results, but the latter give better overall consistency.) This difference is compatible with uncertainties assigned to the respective experiments. Lattice measurements are considered to be more cleanly interpretable, although they show some sensitivity to nuclear data other than the ^{238}U capture cross section.

Discussion of integral experiments, and additional references, may be found in the following reports:

1. M. L. Mikhail, "Elaboration d'un ensemble de donnees coherentes pour le calcul des reacteurs nucleaires ...," GEA-N-1773, December 1974.
2. F. J. Fayers, et al., "An Evaluation of Some Uncertainties in the Comparison between Theory and Experiment for Regular Light Water Lattices," *Journal Brit. Nucl. Energy Soc.*, 6, 2, April 1967.
3. P. B. Kemshell, "Some Integral Properties of Nuclear Data Deduced from WIMS Analyses of Well-Thermalized Uranium Lattices," AEEW-R786, April 1972.

4. E. Hellstrand, "Measurement of Resonance Integrals," in Reactor Physics in the Resonance and Thermal Regions, Vol, II, p. 151, M.I.T. Press, 1966.

3. RECOMMENDATIONS

A. Sensitivity of ρ^{28} to the resonance parameters of the first few ^{238}U resonances should be reviewed. It was indicated by experimentalists at this meeting and also the Saclay Specialists Meeting on Resonance Parameters of Fertile Nuclei and ^{239}Pu (e.g. NEANDC (E) 163U, p. 149) that uncertainties in Γ_n and Γ_γ for the first few resonances may be significantly greater than previously reported in the literature. Any revisions to the resonance parameters should be consistent with the measured value of the dilute resonance integral and should provide effective resonance integrals consistent with the Hellstrand data for isolated rods. Analyses of Doppler measurements, e.g., the work presented by M. Edenius in Session I, should be helpful in evaluating the merit of revisions to the cross sections.

B. The effects on ρ^{28} due to the proper inclusion of interference scattering from bound levels and the very high energy resonances should be further examined. The proper analysis was described in a paper by B. R. Leonard given at the 1972 Kiamesha Lake Conference (CONF-720901, P. 81). Presently ENDF/B ignores these effects which can be discerned in transmission measurements (see, for example, the presentation by D. Olsen (ORNL), Session II).

C. There should be a coordinated effort to qualify the calculational methods themselves. A systematic comparison of the techniques used by D. Finch, J. Hardy, W. Rothenstein, and F. Wheeler would provide valuable information concerning the inter-relationships of the various methods. Also, a documented comparison of the edits of ENDF/B to multigroup processing codes on a common group structure would serve to better define the starting point of the lattice calculations and provide valuable information to the developers of processing codes. Some limited work in this area has been done, but none of it has been adequately documented for thermal reactor applications.

D. The above work has been carried out to some extent, but the questions are still raised within the reactor community because the results have been inadequately published. This clearly suggests that, to avoid duplication and provide a more cohesive program, these efforts should be coordinated through specific funding to a single responsible organization, and the results made known to the general reactor community.

E. A detailed review should be made of the current most important techniques for measuring ^{238}U capture in lattices (e.g., modified conversion ratio; cadmium ratio and thermal subtraction methods for ρ^{28}). Sources of systematic error should be evaluated and compared. Work in this area, funded by EPRI, is now in progress at Stanford.

F. A review should be made of the major integral measurements of ^{238}U capture in reactor lattices. This should include a comparison of techniques and results as well as an evaluation of reliability. Results should be compiled according to reactor types and the quality of the measurements. Comparison should be made with isolated rod results.

G. Three experiments were proposed for analyzing the ^{238}U capture cross section under heavily shielded conditions and localizing the discrepancy in energy:

- 1) Self-indication transmission measurements on a resonance-by-resonance basis through thick samples of uranium. An experiment of this type was performed at RPI and analyzed by T. Byoun and R. Block in the unresolved resonance region. Data exists in the resolved region down to approximately 20 eV. Thus, the data for selected resonances could be analyzed at little cost to evaluate the merit of the information provided by this technique.
- 2) An experiment in which a small Cf^{252} source drives a surrounding homogeneous mixture of ^{238}U and moderator. The moderator/ ^{238}U ratio would be varied to progressively soften the spectrum. The ^{238}U capture/ source neutron would be measured and calculated. A liquid system (uranyl nitrate in H_2O or D_2O ?) would greatly simplify the experiment, if feasible.
- 3) Time of flight spectrum measurements in heavily shielded ^{238}U samples.

Summary for Sessions II and III
EXPERIMENTAL DIFFERENTIAL DATA AND RESONANCE ANALYSIS

G. de Saussure
Oak Ridge National Laboratory

M. R. Bhat
Brookhaven National Laboratory

Bill Havens stressed the importance of systematic errors and the lack of detailed information on such errors in published reports. Experimentalists should be encouraged to report in detail the main features of the experiment and analysis so as to allow an evaluator to independently determine errors and correlations among errors.

J. Felvinci reported on correlations between successive Γ_n^0 . Statistical tests (using runs statistics and autocorrelations tests) show "intermediate structure" with 200 eV and 300 eV spacings. Such structure is not observed when the tests are applied either to random data or to the neutron widths of ^{232}Th . Apparent correlations between Γ_n^0 and Γ_γ have also been observed.

D. K. Olsen reviewed the transmission measurements made since 1963 and reported the results of recent 40-m measurements from ORELA. A comparison of the ORELA transmissions with transmissions obtained from ENDF/B-IV showed a serious discrepancy in the total cross section between resonances. It was shown that a correct R-matrix calculation using ENDF/B-IV parameters reproduced the experimental differential data.

R. C. Block discussed the filtered beam technique using an 8-in Fe filter; a peak is obtained around 24 keV with FWHM of 2 keV and a signal-to-background ratio of 200. Block also reported on self-indication measurements done at RPI on samples at 80°K, 300°K, and 900°K.

R. B. Perez summarized the present status of ^{238}U capture above the resonance region. The various measurements agree in shape but there are large normalization uncertainties. Intermediate structure in the unresolved range was also discussed.

F. J. McCrosson reported on the ENDF/B-IV evaluation of the resonance parameters. There were not much more data available to the ENDF/B-IV evaluator than had been available for ENDF/B-III, however, the version III data tests results which were available underpredicted eigenvalues. Some p-wave levels of version III were eliminated from version IV.

Gert Rohr reported recent p-wave assignments made at the BCMN by looking at the high and low bias measurements of the gamma transitions. Also the experimental program on ^{238}U at Geel was discussed. This program includes measurements of scattering, transmission with sample cooled to liquid nitrogen temperature, self-indication and capture.

Derek Gayther discussed recent transmission measurements made by Moxon at Harwell through a 9-cm depleted uranium metal sample. Preliminary indications are that at least one small resonance previously assigned to be p-wave shows signs of a resonance-potential interference effect. It is planned to make further measurements with a 14-cm thick sample. Measurements to study Doppler effects in 16-cm thick UO_2 samples are currently under way. Initially, transmission measurements will be made with the sample heated up to $\sim 1800^\circ\text{C}$. It is hoped to also measure capture with a Moxon-Rae detector.

R. Chrien reported on measurements of capture cross sections for ^{238}U and other nuclei through an iron filter using activation techniques. The ^{238}U measurement was in excellent agreement with the RPI and Kyoto Univ. filtered beam results.

R. N. Hwang discussed the effect of level spacing correlations on the Doppler coefficient. A comparison of calculations using the Dyson statistics with calculations using the uncorrelated Wigner distribution was made. The effect of corrections was small except perhaps at extremely high temperatures.

Bo Leonard stressed the importance of doing an unbiased R-matrix calculation of scattering. The proper treatment for this is described in a paper at the 1970 Kiamesha Lake Conference and also in ENDF-153 (71).

H. Derrien could not attend the seminar but sent some "Comments on ^{238}U Width Evaluations" which were distributed to the participants and are included in the proceedings.

Recommendations

We suggest that the errors of the first few levels of ^{238}U be critically reevaluated.

A review of the transmission measurements of Jackson and Lynn on the 6.7-eV resonance reveals that their resonance parameters primarily depend on data obtained at 4°K combined with an Einstein phonon frequency distribution. Thus, the interpretation of this experiment differs from the gas model used in most differential and reactor neutronics interpretations of Doppler broadening. Jackson and Lynn obtained

$$\Gamma = 28.5 \pm 1.5 \text{ meV}$$

$$\Gamma_n = 1.52 \pm 0.01 \text{ meV}$$

Note that the Γ (and Γ_Y) values of this experiment were misquoted in BNL-325 with errors of ± 0.4 meV. This error assignment was not a result of the measurement. The high accuracy of Γ_n is not supported by any details reported in the paper and is judged by this group to be unrealistic. We further note that there are four other experimental values reported in BNL-325 (1965) all of which report Γ_Y values lower than Jackson and Lynn with comparable precisions (21.2 - 26 meV). The average (unweighted) value of Γ_Y of the five experiments would be about 25 meV. We further note that de Saussure *et al.* reported, Nucl.Sci. Eng. 51, 385 (73), measurements of capture in a thick sample of this resonance. Doppler-broadened, Monte Carlo corrected calculations of this resonance line with ENDF/B-III gave a broader resonance in the wings than observed in the experiment. Since ENDF/B-III gave $\Gamma_Y = 25.6$ meV, the implication is that perhaps the true value of Γ_Y is smaller than this.

We further note that the Γ_Y values deduced from analyses of different experiments of the next few strong s-wave resonances produce a significantly large spread of values. The plots of Γ_n vs Γ_Y , *e. g.*, shown by Poortmans *et al.* [NEANDC(E) 163U, pp 155-156] typically show ranges of experimental values of 5 meV for resonances between $E_0 = 36.7$ eV and 116.8 eV. Thus, it appears that evaluated Γ_Y values for these resonances have produced uncertainties which are unrealistically small. Thus, this group feels that values in the range 20 to 25 meV for the first few s-wave resonances do not violate the existing differential data.

The group recommends studies of benchmark experiments in which the Γ_γ values of these resonances are systematically and uniformly perturbed to determine quantitatively the effect on the benchmark parameters. In performing these perturbations, care should be taken to adjust the $1/v$ component of capture in the smooth file to provide continuity with the ENDF/B-IV thermal smooth capture file at 1 eV.

B. We recommend that a proper R-matrix treatment of the total cross section be adopted by ENDF/B, and that this treatment be tested by comparison with experimental differential data over the entire resolved resonance range and below.

C. We recommend that the systematic discrepancies between Columbia, the BCMN and JAERI neutron widths above 1.5 keV be further investigated, in particular, by using the same method of analysis on all sets of data (as suggested by H. Derrien).

D. We recommend that all observed p-wave levels be included in the ENDF/B file and that a p-wave strength function of $2.2 \pm .2 \times 10^{-4}$ be used to make up missed levels in the resolved range and in the unresolved range.

E. The present ENDF/B-IV strength functions appear low compared to the most recent experimental evidence.

F. We recognize that there is a possibility that there are capture and scattering width correlation, those correlations could possibly explain the discrepancy between calculation and data. If the discrepancy can be explained entirely by the correlation, we recommend that an intensive study be done.

G. Recent measurements of gamma transitions by Ed Journey (LASL) indicate that there is probably no p-wave level below the Cd cutoff.

H. We recommend a careful measurement of the shape of the 6.7-eV capture resonance to see if any asymmetry is present.

I. We recommend performance of self indication (S.I.) measurements with different sample thicknesses and temperature. We recommend that RPI S.I. measurements be further analyzed.

J. We recommend that a group of experimentalists and reactor physicists collaborate in designing a set of S.I. measurements to be used as benchmarks to test ^{238}U data and calculation methods.

K. The two alternate data adjustments used as a contrivance by reactor physicists to make the differential data in agreement with integral experiments are (1) subtract about .2 b of capture cross section from 4 eV to 9.12 keV; (2) reduce the p-wave capture integral by about 1b. These adjustments appear totally incompatible with our present knowledge of differential data.

Summary for Session V

R. A. Karam, GIT

METHODS OF CALCULATING ENERGY AND SPATIAL SELF-SHIELDING EFFECTS

Members of the committee on "Methods for Calculating Energy and Spatial Self-Shielding Effects," Session V, made the recommendations given below which were adopted by all attendees of the Seminar. Members of the Committee were Don R. Finch, Savannah River Laboratory; Richard Hwang and Phil Kier Argonne National Laboratory; Rubin Goldstein, Combustion Engineering; Wolfgang Rothenstein and Arthur Buslik, Brookhaven National Laboratory; R. A. Karam (chairman), Georgia Institute of Technology.

A. There is a need to investigate the possible effects of the use of the free gas model in neutron slowing down in tightly bound atoms in crystal-line lattices on resonance capture. This will require a study of the phonon spectrum in the uranium metal, uranium oxide, and uranium carbide lattices. If this theoretical investigation suggests that there are significant effects, the possibility of defining a relevant experimental program should be looked into. In addition a study should be made of the influence of this effect on Doppler broadening. (See "Effects of the Free-Gas, Slowing-Down Model on Resonance Cross Sections in ^{238}U .")

B. The treatment of the Unresolved Resonance Region appears to be adequate for thermal reactor analysis.

C. Discrepancies have been noted during the Seminar on ^{238}U Resonance Capture between the results of various codes. The discrepancies of most concern refer to different Monte Carlo codes which have been used for some

benchmark studies. Some of the differences may be due to the use of ENDF/B-III in some calculations and ENDF/B-IV in others; the effect of the cross section changes will be evaluated. However, apart from cross section data differences, there appear to be anomalies which must be resolved. Of prime importance is the calculated value of the capture fraction of neutrons in ^{238}U in a simple benchmark lattice normalized similarly in the Monte Carlo codes used at Westinghouse and BNL. In this connection the resonance profiles in both Monte Carlo codes, as well as the energy grids and Doppler broadening techniques employed in their generation, should be compared in detail. Additional parameters that can be computed by all codes using the same data base are the following:

1. The thermal neutron captures in ^{238}U per neutron slowing down past 0.625 eV.
2. The thermal fissions in ^{235}U per neutron slowing down past 0.625 eV.
3. The ratio of A and B represents a number that can be used as a consistency check between experiment and calculation (see E below).
4. The ^{238}U fission per neutron from thermal fission injected into the lattice.

D. With regard to the advantages and disadvantages of different calculational procedures the following points should be noted:

1. The Nordheim resonance treatment may not be sufficiently accurate for thermal reactor benchmark calculations. Some of the reasons for this are the isolated resonance approximation, the limited extent of the numerical integration covering each resonance with

the need for simple algorithms to cover wing corrections, and the flat flux approximation.

2. Integral transport and Monte Carlo methods do not have these difficulties.

The integral transport method has the advantages of computing detailed flux distributions in space and energy. A leakage buckling term can be used if desired. Running times are relatively short compared to the Monte Carlo method. The shortcomings of integral transport methods include the difficulty of including anisotropic scattering in the laboratory system, the use of a cylindrical outer boundary with an isotropic return boundary condition in a one-dimensional code, and the use of cosine currents to evaluate collision probabilities in some of the codes currently employed.

Monte Carlo methods have the advantage of treating complex geometries, anisotropic scattering, and can in general model the physical problem accurately. On the other hand small regions in space or energy may present statistical problems unless special methods, such as adjoint Monte Carlo, are employed. The advantages are, however, offset to some extent by the long running times required to attain adequate statistics. If Monte Carlo methods are used in conjunction with other codes, such as multigroup codes, care must be exercised in how they are interfaced.

A full three-dimensional Monte Carlo study of some of the lattice benchmarks might be useful.

It was noted that Monte Carlo methods might be used to study streaming and flux depression effects in foil activation experiments.

E. With regard to the choice of benchmarks, attention must be paid to the methods used to ensure that the most accurate integral parameters are

obtained. One suggested consistency check is the ratio of thermal captures in ^{238}U , C^{28} to the thermal fissions in ^{235}U , F^{25} . This quantity should be calculated accurately by any thermal spectrum code. It can also be related to the measured integral parameters by the expression:

$$\frac{C^{28}}{F^{25}} = CR^* \frac{(1 + \delta^{25})}{(1 + \zeta^{28})}$$

where

CR^* = total capture in ^{238}U to total fissions in ^{235}U ,

δ^{25} = the epithermal to thermal fissions in ^{235}U ,

ζ^{28} = the epithermal to thermal captures in ^{238}U .

Additional benchmarks involving non Cd-covered as well as Cd-covered reaction ratios would be useful. The range of moderator to fuel ratios should also be extended.

LIST OF PARTICIPANTS
Seminar on ^{238}U Resonance Capture

Askew, J., A.E.R.E.- Winfrith
Becker, M., Rensselaer Polytechnic Institute
Bhat, M. R., Brookhaven National Laboratory
Block, R., Rensselaer Polytechnic Institute
Bohn, E. M., Argonne National Laboratory
Bowman, C., National Bureau of Standards
Buslik, A., Brookhaven National Laboratory
Cheng, S., Brookhaven National Laboratory
Cowan, C., General Electric Co.-Fast Breeder Reactor Development
Craig, D. S., Atomic Energy of Canada, Ltd.
deSaussure, G., Oak Ridge National Laboratory
Edenius, M., AB Atomenergi
Felvinci, J., Columbia
Fiarman, S., Stanford Univ.
Finch, D. R., Savannah River Laboratory
Gayther, D., A.E.R.E.-Harwell
Goldstein, R., Combustion Engineering
Griffiths, J., Atomic Energy of Canada Ltd.
Hardy, J. D., Jr., Bettis Atomic Power Laboratory
Harris, D., Los Alamos Scientific Laboratory
Havens, W. W., Jr., Columbia
Howerton, R. J., Lawrence Livermore Laboratory
Hwang, R. N., Argonne National Laboratory
Jenquin, U., Battelle Northwest Laboratory
Karam, R. A., Georgia Inst. Technol.
Kier, P., Argonne National Laboratory
LaBauve, R., Los Alamos Scientific Laboratory
Leonard, B. R., Jr., Battelle Northwest Laboratory
Livolsi, Z., Babcock and Wilcox
McCrosson, F. J., Savannah River Laboratory
Moore, M. S., Los Alamos Scientific Laboratory
Morris, W., Savannah River Laboratory
Olsen, D. K., Oak Ridge National Laboratory
Ozer, O., Electric Power Research Institute
Pearlstein, S., Brookhaven National Laboratory
Pellarin, D. J., Savannah River Laboratory
Perez, R. B., Oak Ridge National Laboratory
Rahn, F., Electric Power Research Institute
Raymund, M., Westinghouse Nuclear Energy Systems
Rohr, G., EURATOM-GEEL
Rose, P., Brookhaven National Laboratory
Rothenstein, W., Brookhaven National Laboratory
Sher, R., Stanford Univ.
Spencer, R. R., Oak Ridge National Laboratory
Stewart, L., Los Alamos Scientific Laboratory
Wade, D. C., Argonne National Laboratory
Wheeler, F., Aerojet Nuclear Company

CONTRIBUTED PAPERS

March 1975

Discrepancies in Thermal Reactor Lattice Analysis

W. Rothenstein
Brookhaven National Laboratory
Upton, New York 11973

Abstract

Experience gained over recent years has shown that the consistent use of ENDF/B data leads to discrepancies, when the results of analysis of thermal reactor lattices containing Uranium fuel of low enrichment are compared with experiment. Typically the effective multiplication factor is less than unity by one or two percent, and even as much as three percent for very tight water moderated lattices. Similar trends have been observed by investigators at Winfrith using their multigroup data.

It is the purpose of the seminar on U-238 Resonance Capture to examine the different areas which might lead to the observed discrepancies, and in particular to determine whether the problem is due to the quality of the microscopic nuclear data, the accuracy of the integral experiments, the approximations inherent in the lattice analysis, or a combination of all of these factors.

In the present paper the previous studies of clean thermal reactor lattices will be reviewed. The principal features of the calculational methods, which make full use of ENDF/B data, will be outlined and compared with other treatments specially as regards the resonance capture calculations.

The information which can be obtained from comparisons of measured integral lattice parameters and their calculated values will be discussed, together with attempts which have been made to use this information to reduce or eliminate the gap between theory and experiment.

I. INTRODUCTION

Thermal reactor lattices have been analyzed quite satisfactorily for many years. It might seem strange therefore that a seminar should be devoted to this topic at the present time.

It is of interest to note that those concerned with thermal reactor design report no problems regarding the agreement between their calculations and experiment. In particular, V. O. Uotinen of Babcock and Wilcox, in a review paper⁽¹⁾ at a recent Conference on Nuclear Cross Sections and Technology in Washington, D.C., March 1975, referred to the successful analysis of 17 UO_2 uniform lattices and 14 uniform UO_2 - PuO_2 lattices, which led to values of k_{eff} differing from unity by not more than about 2 tenths of one percent. Similar accuracy was also reported in the analysis of non uniform lattices.

It was admitted however, that the analysis involved a certain amount of adjustment of the nuclear data and the calculational procedures in order to attain this degree of agreement between the experiments and the calculations.

At the APS meeting on Nuclear Cross Sections and Technology, the need for bias factors was also referred to by N. C. Paik⁽²⁾ of Westinghouse in the analysis of LMFBR's, and J. Y. Barre of Cadarache⁽³⁾ stressed the approach of relying heavily on integral data in Fast Breeder development.

On the other hand for a thorough understanding of reactor behavior, and in particular thermal reactors, it seems unsatisfactory that even the simplest lattices cannot be analyzed from the basic microscopic data without resorting to adjustments of one kind or another.

It was pointed out about six years ago, by J. Chernick, that in any attempt to reconcile calculations and experiments the three basic ingredients involved should be carefully investigated: the basic nuclear data, the integral experiments, and the approximations inherent in the lattice analysis. Clearly any discrepancies might be due to any one of these ingredients or to all in different proportions. It is frequently difficult to pin down exactly where the trouble lies. It is the aim of the Seminar on U-238 Resonance Capture to throw light on the causes responsible for the existing discrepancies and to stimulate further work in these areas.

II. THE MAGNITUDE OF THE DISCREPANCIES

The discrepancies between lattice analysis and integral experiments have been evident since the early versions of the ENDF/B library. Table 1 shows some k_{eff} values for clean light water moderated lattices.⁽⁴⁾ These were based on ENDF/B-I from which multigroup libraries were prepared for the HAMMER analysis code.⁽⁵⁾ It is apparent that the multiplication factor gets progressively worse the tighter the lattice.

TABLE 1
1.3% ENRICHED U-H₂O (HEXAGONAL LATTICES)

	Rod Diameter	0.387"
	Gap Thickness	0.005"
	A ℓ Clad Thickness	0.028"
V_w/V_u	B^2 (M ⁻²)	K_{eff} (ENDF/B-I)
1.0	20.98	0.9773
1.5	40.51	0.9843
2.0	52.19	0.9861
3.0	59.25	0.9884
4.0	54.69	0.9991

A similar trend is observed in the case of some Würenlingen D₂O lattices⁽⁴⁾ which are shown in Table 2.

TABLE 2
NATURAL URANIUM - D₂O (SQUARE LATTICES)

Rod Radius	1.0 CM	
Gap Thickness	0.025 CM	
Al Clad Thickness	0.075 CM	
Pitch (CM)	B ² (M ⁻²)	K _{eff} (ENDF/B-I)
8.0	7.80	0.9814
10.0	8.40	0.9840
12.0	7.57	0.9873
14.0	6.47	0.9893
16.0	5.06	0.9884

It was realized at the outset that a weak link - and probably the weakest link - in the analysis is the resonance capture calculation. The shielding in these systems containing rods having very high U-238 density is very large, and small errors in its evaluation can influence the results of the analysis very considerably. The methods used at Brookhaven National Laboratory for evaluating the shielded resonance integrals are based on the Nordheim procedure,⁽⁶⁾ which is relatively straightforward and rapid on a fast computer. The method involves a number of simplifications and assumptions, however, the most important of which are:

- 1) In the resolved resonance region each resonance is treated separately as though it were entirely isolated.
- 2) A 1/E flux is assumed to be the asymptotic flux above the resonance, i.e., complete flux recovery between resonances is assumed.
- 3) In order to emphasize the energy variable by constructing a very fine energy grid, the spatial aspects of the problem are reduced to the use of two region collision probabilities for which tables are prepared.

- 4) The collision density is calculated over the central part of each resonance only by numerical integration of the slowing down integral equation. Unshielded end or wing contributions are used beyond this region.
- 5) The shielded resonance integral is generally assumed to contribute to the capture only in the energy group in which the peak is located.⁽⁷⁾

In order to treat the resonance events more realistically without the need for simplifying assumptions, comparisons with Monte Carlo calculations have frequently been made. Such comparisons are also not free from problems quite apart from the statistical uncertainties of the Monte Carlo calculations. The results shown in Tables 1 and 2 for H₂O and D₂O lattices were in fact corrected so as to bring the Nordheim shielded resonance integrals in line with Monte Carlo estimates. The latter were obtained with a code⁽⁸⁾ based on the Breit-Wigner Single Level formalism for which parameters are given in the ENDF/B files. The code used was quite cumbersome as a number of neighboring resonances had to be used to calculate the neutron cross sections at each energy point. Doppler Broadening line shape functions had to be evaluated for each contributing resonance. In addition it was necessary to use a simple algorithm to include the effect of distant resonances. The magnitude of the corrections which were applied to the calculated Nordheim resonance integrals are shown for U-238 in Fig. 1. They amount to a reduction of the shielded resonance integral by up to 10 percent for the D₂O lattices. For the light water lattices the corrections were smaller⁽⁴⁾ about half this amount. The corrections applied to the U-235 resolved resonance integral are considerable as shown in Fig. 2. They were not determined very accurately at the time, but their effect on the lattice analysis is rather small, since

most of the U-235 events occur at thermal energies. The reason for the large corrections in the case of U-235 lies in the fact that they are shielded by the U-238 resonances, an effect which is not taken into account in the Nordheim calculations.

Notwithstanding the fact that corrections to the shielded resonance integrals were applied, they were insufficient to bridge the gap between lattice analysis and experiment. Consistent use of ENDF/B data underpredicted the reactivity in every case.

III. DETAILED EXAMINATION OF THE U-238 DISCREPANCY

Very detailed studies of the clean H₂O moderated lattices using ENDF/B data were made by J. Hardy of BAPL.^(9,12) Kemshell⁽¹⁰⁾ and others at Winfrith analyzed the problem for a wider range of well thermalized lattices with the data on the UKAEA library. Papers will be presented at the present seminar about these investigations, but some of the most important conclusions will be given in the present review, specially in as far as they relate to the U-238 capture problem.

In 1970 Hardy⁽⁹⁾ compared shielded resonance integral calculations (based on Nordheim's method) coupled to a more sophisticated procedure below 200 eV, with Monte Carlo estimates. The same data were used throughout. Agreement was good, although there was a bias in that the Monte Carlo values were consistently slightly in excess of the other values (1.5 - 2%). The author referred to the possibility that this trend may be due in part to the way resonance integrals are inferred from the captures.

The main problem arose however in the comparison with experiment. In order to obtain agreement with Hellstrand's measured resonance integrals of

isolated rods, more resonance capture was needed than in order to fit the measured values of ρ_{28} , the ratio of epithermal to thermal captures in U-238, in water moderated lattices. The results were interpreted in terms of the smooth capture, i.e., that part of the resonance cross sections which was handled by equivalent smooth cross sections. The principal conclusions are shown in Table 3.

TABLE 3
U-238 RESONANCE CAPTURE
 Hardy et al (Westinghouse).

	p-wave Dilute Resonance Integral $\int \sigma_c du$ (barns)
Value required to make calculated value of ρ_{28} agree with experiment:	0.65
Value required to make the calculated effective resonance integral of isolated rods agree with Hellstrand's experiments:	1.45
ENDF/B-IV Nuclear data (McCrosson)	
Resolved resonance region 0.70	
Unresolved resonance region <u>0.84</u>	1.54

The values clearly show the magnitude of the discrepancy and should be compared with the capture integrals of the p-wave resonances which are practically unshielded and are treated usually by equivalent smooth cross sections. McCrosson⁽¹¹⁾ who examined the p-wave resonances in detail in 1973 concluded that the ENDF/B-III p-wave capture resonance integral of 1.83 barns should be reduced by 0.28 barns, but nevertheless the ENDF/B-IV values are clearly greatly in excess of the value required to match the measured lattice values of ρ_{28} . Of course it is not necessary to look only at the contributions of the p-wave resonances as the cause of the discrepancy, but its magnitude

is certainly very large. Subsequent sensitivity studies with ENDF/B-III data⁽¹²⁾ helped to indicate where (at what energies) the reduction of the U-238 capture integral should be made, but did not explain the cause of the discrepancy.

Kemshell⁽¹⁰⁾ in 1972 examined the prescription used at Winfrith to evaluate the resonance capture in U-238 in detail. He referred to previous comparisons between the WIMS⁽¹³⁾ calculations and Monte Carlo values which had been in good agreement. On the other hand, a scaling procedure was required to make the results of calculations based on a detailed tabulation of cross section against energy agree with integral evidence. The scaling is shown in Table 4.

TABLE 4
U-238 RESONANCE CAPTURE

<u>Winfrith</u>	<u>R.I. (Hellstrand)-R.I. (Lattice)</u>
	(barns)
Askew	1.2
Kemshell* H ₂ O lattices (1972)	0.8
D ₂ O Lattices	0.4
C Lattices	0.6

*Based on:

	σ_s	
	<u>Winfrith</u>	<u>(ENDF/B-IV)</u>
H	20.3	(20.45)
D	3.35	(3.35)
C	4.68	(4.73)

The resonance integral scaling was originally 1.2 barns. By referring to experimental evidence on the relative conversion ratio, the ratio of U-238 captures to U-235 fissions in the lattice relative to the same value in a thermal column, Kershell suggested modifications to the scaling factor. These depend to some extent on the moderator and are influenced by its scattering cross section in the resonance region. The scaling necessary to make calculations agree with the measured conversion ratio, now amounts to much less than before, but it is still not negligible. The scattering cross sections used at Winfrith are close to the present ENDF/B-IV values.

Kershell and later Chawla⁽¹⁴⁾ drew further conclusions about nuclear data from these studies. In particular they suggested that a harder fission spectrum might be indicated by the measured values of δ^{28} which were higher than the WIMS calculations. This ratio of the U-238 to U-235 fissions will clearly increase if the temperature of the U-235 fission spectrum is raised. Chawla used a temperature of 1.43 MeV which is greatly in excess of the current ENDF/B-IV value of 1.323 MeV. He did not consider that the harder fission spectrum would lead to discrepancies between calculated and measured neutron ages in the three principal moderators greatly in excess of the experimental errors.

In addition Chawla sought to account for the low values of k_{eff} in their D₂O lattice calculations (even when compared to the other moderators) by changing the very low energy α values of U-235. A reduction would enhance the k_{eff} of the most thermalized, i.e. the D₂O lattices, and have a smaller effect in the H₂O lattices. The proposed change, which was thought to be reasonable in the light of the available experimental thermal

nuclear data would extrapolate α to 0.157, instead of 0.173 in ENDF/B-IV, as the neutron energy tends to zero.

IV. POSSIBLE SOURCES OF THE DISCREPANCIES

Previous studies of the discrepancies between thermal reactor lattice calculations and experiments for assemblies containing natural Uranium or fuel of low enrichment have been conducted according to the following pattern. For a given microscopic data set the best theoretical procedures were used in the lattice analysis. The resulting integral lattice parameters were compared with experiment and the discrepancies attributed to the quality of the basic nuclear data.

Recalling the three ingredients which contribute to such comparisons, the question must be asked whether it is certain that the integral experiments and the methods of lattice analysis can be ruled out entirely as contributing factors to the differences that have been observed.

The major area of doubt is clearly the U-238 resonance capture which is strongly influenced by the heavy shielding of the large resonances in the heterogeneous assemblies.

Resonance capture rates have been studied very extensively in the past. Good agreement has frequently been reported between different calculational procedures using the same data base. The tendency of adjusting the data in order to force agreement between theory and experiment was then a natural consequence.

On the other hand it appears desirable to approach the problem at the present stage with an open mind and with full regard to what is currently

available both as regards lattice analysis codes, computer facilities, and experimental data.

Following the procedures previously adopted, one might first of all, question the codes used for the calculations. In order to compare different theoretical approaches it is essential that the comparisons refer to quantities defined in an identical manner. An example of an area of doubt is the resonance integral. Its definition is unambiguous at infinite dilution, but in the presence of heavy shielding the definition must be clarified. It is not certain that the most appropriate definition for an analytical evaluation of the shielded resonance integral for one calculational procedure is also directly applicable to other numerical methods, such as Monte Carlo calculations.

As regards the use of a given data base, further questions arise. The data base should contain an unambiguous procedure for specifying all cross sections at every energy point. Of special interest is the resonance region. The procedure agreed upon to calculate the resonance cross section from the resonance parameters in the data base may be too cumbersome for some methods of calculation of the shielded resonance reaction rates, and simplifications are frequently introduced for each method separately. Even when very detailed resonance profiles are used, questions arise regarding the energy mesh and interpolation procedures used to represent them and the manner in which they have been Doppler broadened. Comparisons between different methods of calculation for the same data base, such as Monte Carlo versus Integral Transport, certainly merit detailed re-examination, even when close agreement has been reported.

Turning to the basic nuclear data, there is the problem of how well the cross sections and resonance parameters are known. In particular one may ask whether the use of a constant radiation width for all resonances is justified, or should be replaced by different values, according to the best measurements, specially in the case of the first few resonances of U-238 which contribute most to the total resonance capture. What accuracy can be expected in the calculated integral parameters in the light of the present uncertainties in the basic data? Is the overprediction of resonance capture of U-238 to the extent reported in the literature consistent with the quality of the basic data? As regards the resonance formalisms used, some fundamental problems also remain. U-238 is an isotope with well separated resonances so that little difficulty is expected from the use of the single level Breit-Wigner formulae. On the other hand these formulae appear to be applied, according to current ENDF specifications, in a manner which is inconsistent with certain basic theoretical considerations. In particular negative scattering cross sections and even total cross sections are not excluded even after Doppler broadening. Although these problems occur only over a few narrow energy regions the question remains how well the cross section measurements are fitted by the currently recommended resonance formalisms, specially at energies in the valleys between the large resonance peaks.

Finally, the measured integral lattice parameters might need further study. Confidence limits, allowing for experimental error are generally quoted in the literature, but the measurements might be subject to possible systematic errors which had not been sufficiently well analyzed at the time the experiments were performed. In addition, frequent reference is made to

rather old experiments, in which the measuring techniques were less refined than at present. The selection of the most reliable experimental information on integral parameters from the reported measurements, and a re-examination of sources of systematic errors appear to be of considerable importance.

It may well be that one or more of the problems mentioned can be ruled out as a contributory factor to the existing discrepancies, from studies already reported or those currently in progress. On the other hand the objective of the specification of a single data base, which when properly used will be adequate for the widest range of applications, provides a strong incentive for a fuller understanding of the causes which lead to the current overprediction of U-238 resonance capture in thermal reactor lattices.

References

1. Uotinen, V. O., Robertson, J. D., Tulenko, J. S., The Light Water Reactor Industry - Nuclear Data Needs. APS Conference on Nuclear Cross Sections and Technology, 1975. To be published by National Bureau of Standards. (Bulletin of the APS, p. 134, February 1975)
2. Paik, N. C., Significance of Nuclear Data on Neutron Monitoring of an LMFBR. APS Conference on Nuclear Cross Sections and Technology, 1975. To be published by National Bureau of Standards. (Bulletin of the APS, p. 135, February 1975)
3. Barre, J. Y., Bouchard, J., After PHENIX, What is the Importance of Nuclear Data Programs for Fast Breeder Development? APS Conference on Nuclear Cross Sections and Technology, 1975. To be published by National Bureau of Standards. (Bulletin of the APS, p. 136, February 1975)
4. Rothenstein, W., Analysis of Heavy and Light Water Moderated Thermal Reactor Lattices Using ENDF/B Data and the HAMMER Code System. BNL-RP-1001, 1961
5. Suich, J. E., Honeck, H. C., The HAMMER System. DP-1064, 1967
6. Kuncir, G. F., A Program for the Calculation of Resonance Integrals. GA-2525, 1961
7. Jabbawy, S., Karni, J., Rothenstein, W., Velner, S., Water-Moderated Reactor Analysis with ENDF/B Data. Nuclear Data in Science and Technology, Vol. II, 147, 1973
8. Rothenstein, W., Monte Carlo Code for the Calculation of Resonance Reaction Rates and Effective Resonance Integrals Based on ENDF/B Data (REPCDC). BNL 13851, 1969
9. Hardy, J., Klein, D., Volpe, J. J., A Study of Physics Parameters in Several H₂O-Moderated Lattices of Slightly Enriched and Natural Uranium. J. Nucl. Sci. and Eng. 40, 101, 1970
10. Kemsshell, P. B., Some Integral Properties of Nuclear Data Deduced from WIMS Analyses of Well Thermalized Uranium Lattices. AEEW-R 786, 1972.
11. McCrosson, F. J., U-238 p-Wave Resonance Parameters. Private Communication February 1973.
12. Hardy, J., Analysis of TRX Lattices with ENDF/B - Version 3 Data Proc. U-238 Seminar March 1975. (in process)

13. Askew, J. R., Fayers, F. J., Kemshell, P. B., A General Description of the Lattice Code WIMS. J. Brit. Nucl. En. Soc., 5, 564, 1966.
14. Chawla, R., Improvements in the Prediction of Reactivity and Reaction Rate Ratios for Uranium Lattices. J. Nucl. Energy, 27, 797, 1973.

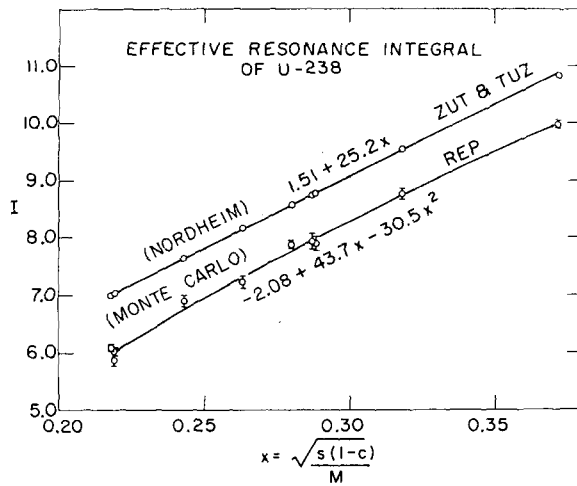


Figure 1

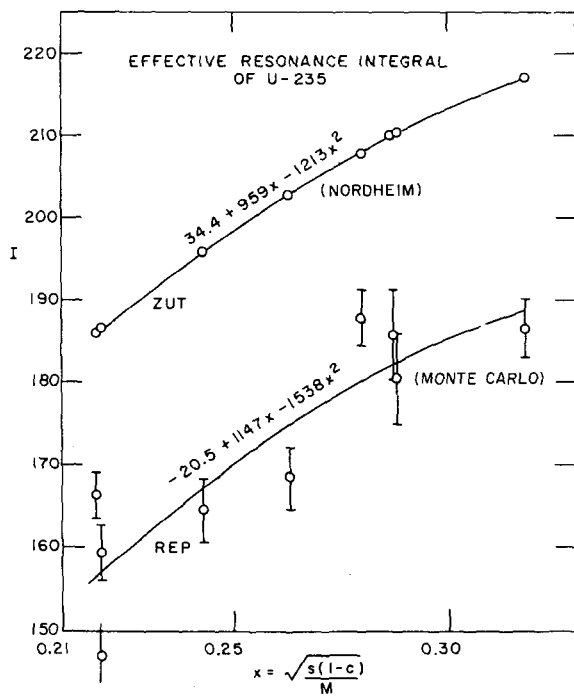


Figure 2

Monte Carlo Analysis of TRX Lattices
with ENDF/B Version 3 Data

J. Hardy, Jr.

I. INTRODUCTION

Four TRX water-moderated lattices of slightly enriched uranium rods have been re-analyzed with consistent ENDF/B Version 3 data by means of the full-range Monte Carlo program RECAP (Reference 1). The parameter measurements and the original analysis are described in References 2 and 3.

The following measured lattice parameters were studied:

- ratio of epithermal-to-thermal U^{238} captures (ρ^{28}),
- ratio of epithermal-to-thermal U^{235} fissions (δ^{25}),
- ratio of U^{238} captures to U^{235} fissions (CR^*),
- ratio of U^{238} fissions to U^{235} fissions (δ^{28}), and
- multiplication factor (λ).

In addition to the base calculations, some studies were done to find sensitivity of the TRX lattice parameters to selected variations of cross section data.

Finally, additional experimental evidence is afforded by effective U^{238} capture integrals for isolated rods. Shielded capture integrals were calculated for U^{238} metal and oxide rods. These are compared with the measurements of Hellstrand (Reference 4).

II. LATTICE CALCULATIONS

The TRX fuel rods were of uranium metal (enriched to 1.3% U^{235}) clad in aluminum. They were 48 inches long and of 0.387 inch diameter, arranged in hexagonal arrays at four water-to-fuel volume ratios: 1.00, 2.35, 4.02, and 8.11. The two intermediate arrays were full lattices for which measured buckling values were available. The other two arrays were run as inner lattices surrounded by a

driver region of TRX high density UO₂ rods. At the center, where parameters were measured, the flux spectra were essentially asymptotic. All these lattices were fully reflected, and their perimeters were made as nearly circular as possible.

In the analysis, Monte Carlo cell calculations were done, with leakage corrections obtained from homogenized, multigroup full-core calculations. The RECAP Monte Carlo program described the lattice cell geometry explicitly and neutrons were followed over the full energy range below 10 MeV.

ENDF/B cross sections were processed with ETOMX and FLAN2, which are Bettis versions of ETOG (Reference 5) and FLANGEIII (Reference 6), respectively.

Above 0.625 eV. smooth cross sections, including the inelastic scattering transfer matrix, were described in the 54-group MILC energy structure. Doppler broadened resonance profiles were described at ~25,000 energies. Smooth thermal cross sections were described at 25 energies.

For U²³⁸, all p-wave resonance capture was treated as smooth. The first set of unresolved S-wave resonance parameters was used over the entire unresolved range (4 KeV - 45 KeV), with suitable adjustment of the smooth capture. For U²³⁵, all unresolved resonance absorption was treated as smooth.

Leakage corrections were obtained by means of a multigroup calculation, with cross sections closely matching those of the Monte Carlo. For the two full lattices, the epithermal calculation used MUFT (Reference 7), which treated a homogenized, simply-buckled lattice in the B1 approximation. An "L-factor" was used to force the U²³⁸ capture in the zero-buckling MUFT calculation to match that of RECAP above 0.625 eV. A single L-factor was applied to U²³⁵ absorption (fission plus capture) in a similar manner.

Thermally, a DPl calculation was done in 25 energy groups. Thermal disadvantage factors were used to force the zero-buckling thermal reaction rates to match

those in the RECAP calculation, and a fast advantage factor was applied similarly to obtain the proper U^{238} fission rate.

Leakage corrections for the two-region lattices were obtained with P3MG (Reference 8), which performed one-dimensional, 54-multigroup calculations in cylinder geometry. The calculations were P3 epithermally and double P-1 thermally. There was one thermal group, with constants condensed from a 25-group calculation for each homogenized core region.

In all cases, leakage correction factors for the RCP-calculated reaction rates were obtained as the ratio of reaction rate in the leaking, homogenized lattice to that in the homogenized lattice with zero-buckling. For the relative reaction rates, the largest such correction was 7% (on δ^{28} in the 2.35/1 lattice) and corrections were usually much less than this. The k_{∞} values from the Monte Carlo cell calculations were 1.0290, 1.1551, 1.1432, and 1.0099, respectively, for the 1.00/1, 2.35/1, 4.02/1, and 8.11/1 lattices.

Results for the TRX lattices are summarized in Tables 1 and 2 along with the measured parameters. For completeness, Version 2 ENDF/B results are also included. Calculated reaction rates are tabulated in the Appendix.

The following points are noteworthy:

- 1) Both Version 2 and Version 3 produce high ρ^{28} and CR^* values, indicating ~10% too much epithermal U^{238} capture in all lattices. As will be seen from the sensitivity studies, this implies about 1.3 ± 0.3 b too much smooth capture integral.
- 2) The increased $\sigma_f^{U^{238}}$ in Version 3 has brought δ^{28} into good agreement with the experiment. δ^{28} is also sensitive to $\sigma_{in}^{U^{238}}$ and to the U^{235} fission spectrum. These quantities appear reasonable -- especially the lower U^{238} inelastic scattering compared to Version 1. The trend

in δ^{28} observed in the original analysis (Reference 2) was attributed to too high $\sigma_{in}^{U^{238}}$ (Version 1 ENDF was used).

- 3) The U^{235} epithermal fission in Version 3 is from 2% to 9% high compared to experiment (δ^{25}). It averages ~2% higher than Version 2, slightly greater than would be expected from the dilute fission integrals (above 0.625 eV): $RI(\text{Version 2}) = 266$ b and $RI(\text{Version 3}) = 269$ b. Although within the uncertainties, these are somewhat high compared to direct measurements of the U^{235} fission integral (Reference 9). In particular, the TRX value for the dilute fission integral of U^{235} is 276 ± 11 b above 0.5 eV, or 260 ± 11 b above 0.625 eV (Reference 10). In any case, Bettis deck 718 with $RI = 259$ b gives better δ^{25} results than either Version 2 or 3. All these cross section sets show a trend toward high values in the tighter lattices.
- 4) Eigenvalues are low by ~1% (.7% to 1.3%). This is about what one expects from the excess U^{238} capture.

To determine sensitivity of the lattice parameters to selected cross sections, the full core P3MG calculations were repeated for each of the following variations:

- 1) Reduction of U^{238} smooth capture integral by 1.0 b in the range 5.5 KeV to 25 KeV.
- 2) Reduction of U^{238} smooth capture integral by 1.0 b in the range .625 eV to 6 eV.
- 3) Reduction of U^{235} smooth fission integral by 10 b in the range .625 eV to 6 eV.

Results of these variations are shown in Table 3. A reduction of 1.3 b in the low KeV range coupled with 10 b reduction of the U^{235} fission integral would bring

σ^{28} into line, and eigenvalues as well. δ^{25} would be brought into better agreement, although the tendency to calculate high in tight lattices would persist. A reduction of U^{238} smooth capture in the low eV range (Variation 2), rather than higher up, would help to reduce the drift in δ^{25} .

III. SHIELDED CAPTURE INTEGRALS

Effective resonance capture integrals for U^{238} metal and oxide rods were calculated with the RESQ Monte Carlo program (Reference 11). Doppler broadened resonance profiles were described at 24,000 energies from 5 eV to 325 eV. Bettis versions of L. W. Nordheim's ZUT and TUZ were used respectively for the remaining resolved S-wave resonance (up to 4 KeV) and in the unresolved range (up to 45 KeV). Smooth capture integral was added to account for resonance tails omitted in the resolved range, and to cover the energy ranges 0.5 eV - 5 eV and 45 KeV-10 MeV.

In the interval 200 - 325 eV, both RESQ and ZUT were used and gave good agreement:

$$ZUT-RESQ \approx .005 \text{ b.}$$

Results are shown in Table 4, along with Hellstrand's measured values (Reference 4). The experiment is uncertain to 3.5%. There is good agreement as to slope, but the calculation is high by 0.75 ± 0.54 b on the average.*

* Compared to Hellstrand's recommended isolated rod resonance integrals, it averages high by 0.67 b. This is not very different, but overall consistency is less favorable than for Hellstrand's own experiments (see Table 4).

IV. CONCLUSIONS

Version 3 ENDF/B U^{238} produces too much capture in TRX lattices by 1.3 ± 0.3 b. Compared to E. Hellstrand's measured isolated rod resonance integrals, it averages high by 0.75 ± 0.54 b. These two comparisons are consistent within the uncertainties. It is felt that the lattice comparison is the more reliable, and that Version 3 U^{238} capture needs to be reduced by slightly more than 1.0 b of smooth capture integral. In addition, a 10 b reduction of the U^{235} fission integral would considerably improve the δ^{25} prediction. In other respects, the Version 3 data work well in these lattices.

REFERENCES

1. N. R. Candelore and R. C. Gast, "RECAP-2, A Monte Carlo Program for Estimating Epithermal Capture Rates in Rod Arrays," WAPD-TM-427, 1964.
2. J. Hardy, Jr., et al., Nucl. Sci. Eng. 40, 101 (1970).
3. J. Hardy, Jr., D. Klein, and J. J. Volpe, "A Study of Physics Parameters in Several Water-Moderated Lattices of Slightly Enriched and Natural Uranium," WAPD-TM-931, March 1970.
4. E. Hellstrand, "Measurement of Resonance Integrals" in "Reactor Physics in the Resonance and Thermal Regions. Volume II. Proceedings of the National Topical Meeting of the American Nuclear Society, San Diego, February 7-9, 1966, A. J. Goodjohn and G. C. Pomraning, Eds., pp. 151-173, The M.I.T. Press, Cambridge, Mass., 1966.
5. D. E. Kusner, S. Kellman, and R. A. Dannels, "ETOG-1, A Fortran IV Program to Process Data from the ENDF/B File to the MUFT, GAM and ANISN Formats," WCAP-3845-1 (ENDF 114), December 1969.

REFERENCES (Cont'd)

6. H. C. Honeck and D. R. Finch, "FLANGEII (Version 71-1). A Code to Process Thermal Neutron Data from an ENDF/B Tape," DP-1278, October 1971.
7. H. Bohl, Jr., et al, "MUFT-5 - A Fast Neutron Spectrum Program for the Philco-2000", WAPD-TM-218, 1961.
8. H. Bohl, Jr., et al, "POMG-1, A One-Dimensional Multigroup P-3 Program for the Philco-2000 Computer", WAPD-TM-272, 1963.
9. F. Feiner and L. J. Esch, "Survey of Capture and Fission Integrals of Fissile Materials" in "Reactor Physics in the Resonance and Thermal Regions, Volume II", pp. 299-318 (see Ref. 4).
10. J. Hardy, Jr., Nuclear Science and Engineering, 27, 131 (1967).
11. B. L. Anderson, E. M. Gelbard and J. Spanier, "RESQ-2: A Combined Analytic-Monte Carlo Calculation of Resonance Absorption Based on Superposition", WAPD-TM-665, June 1967.

Table 1

Analysis of TRX Lattice Parameters with ENDF/B Data
(1.3% Enriched, .387-Inch Diameter Uranium Fuel Rods in H₂O)

Parameter**	W/M = 8.11			W/M = 4.02			W/M = 2.35			*W/M = 1.00		
	Exp.	Ver. II	Ver. III	Exp.	Ver. II	Ver. III	Exp.	Ver. II	Ver. III	Exp.	Ver. II	Ver. III
ρ												
ρ												
epi/thermal U ²³⁸ capture	.466 ±.01	.515 ±.005	.521 ±.005	.830 ±.015	.896 ±.004	.899 ±.004	1.311 ±.02	1.425 ±.013	1.422 ±.013	3.01 ±.05	3.28 ±.01	3.30 ±.01
β												
epi/thermal U ²³⁵ fission	.0352 ±.0004	.0354 ±.0004	.0359 ±.0004	.0608 ±.0007	.0628 ±.0008	.0649 ±.0008	.0981 ±.001	.1020 ±.0005	.1031 ±.0005	.230 ±.003	.244 ±.001	.251 ±.001
β												
U ²³⁸ fission/U ²³⁵ fission	.0452 ±.0007	.0445 ±.0004	.0458 ±.0004	.0667 ±.002	.0620 ±.0004	.0654 ±.0004	.0914 ±.002	.0856 ±.0005	.0894 ±.0005	.163 ±.004	.156 ±.001	.164 ±.001
CR* U ²³⁸ capture/U ²³⁵ fission	.526 ±.004	.545 ±.003	.546 ±.003	.646 ±.002	.667 ±.001	.667 ±.001	.792 ±.008	.831 ±.007	.829 ±.007	1.255 ±.011	1.329 ±.005	1.328 ±.005
λ												
k _{eff}	1.000	.9902 ±.0030	.9925 ±.0030	1.000	.9929 ±.0015	.9913 ±.0015	1.000	.9821 ±.0030	.9872 ±.0030	1.000	.9917 ±.0030	.9889 ±.0030

*W/M = water/fuel volume ratio.

**Thermal cut energy is 0.625 ev in all cases.

Table 2

Summary of Parameter Results*
Calculation/Experiment

Parameter	ENDF/B Version	W/M = 8.11			W/M = 4.02			W/M = 2.35			W/M = 1.00		
		Calculation	Experiment	Ratio	Calculation	Experiment	Ratio	Calculation	Experiment	Ratio	Calculation	Experiment	Ratio
ρ ²⁸	II	1.105 ± .023	1.080 ± .019	1.087 ± .017	1.087 ± .017	1.087 ± .017	1.087 ± .017	1.087 ± .017	1.087 ± .017	1.087 ± .017	1.087 ± .017	1.087 ± .017	
	III	1.118	1.083	1.085	1.085	1.085	1.085	1.085	1.085	1.085	1.085	1.085	
δ ²⁵	II	1.006 ± .015	1.033 ± .017	1.040 ± .001	1.040 ± .001	1.040 ± .001	1.040 ± .001	1.040 ± .001	1.040 ± .001	1.040 ± .001	1.040 ± .001	1.040 ± .001	
	III	1.020	1.068	1.051	1.051	1.051	1.051	1.051	1.051	1.051	1.051	1.051	
δ ²⁸	II	.985 ± .017	.930 ± .031	.937 ± .023	.937 ± .023	.937 ± .023	.937 ± .023	.937 ± .023	.937 ± .023	.937 ± .023	.937 ± .023	.937 ± .023	
	III	1.013	.981	.978	.978	.978	.978	.978	.978	.978	.978	.978	
CR*	II	1.036 ± .010	1.033 ± .004	1.049 ± .013	1.049 ± .013	1.049 ± .013	1.049 ± .013	1.049 ± .013	1.049 ± .013	1.049 ± .013	1.049 ± .013	1.049 ± .013	
	III	1.038	1.033	1.046	1.046	1.046	1.046	1.046	1.046	1.046	1.046	1.046	
λ	II	.990 ± .003	.993 ± .002	.982 ± .003	.982 ± .003	.982 ± .003	.982 ± .003	.982 ± .003	.982 ± .003	.982 ± .003	.982 ± .003	.982 ± .003	
	III	.993	.991	.987	.987	.987	.987	.987	.987	.987	.987	.987	

*Uncertainties are standard deviations. Same values apply to the Version III comparison.

Table 3

Effect of Cross Section Variations on Parameters

Parameter	Cross Section Variation*	Percent Change of Parameter		
		W/M = 8.11	W/M = 4.02	W/M = 2.35
²⁸ P	1	-6.02	-6.56	-7.27
	2	-5.61	-5.87	-6.36
	3	-.05	-.11	-.18
⁶²⁵ P	1	-.08	-.08	-.14
	2	-.36	-.66	-1.13
	3	-3.88	-3.68	-3.69
⁶²⁸ P	1	-.52	-.89	-1.50
	2	-.48	-.81	-1.33
	3	+.08	+.10	+.14
CR*	1	-2.06	-3.09	-4.26
	2	-1.91	-2.74	-3.63
	3	+.11	+.17	+.23
λ	1	+.63	+.83	+1.10
	2	+.57	+.76	+1.21
	3	-.08	-.10	-.13
W/M = 1.00	1	-8.78	-7.27	-7.27
	2	-7.41	-6.36	-6.36
	3	-.45	-.18	-.18
W/M = 1.00	1	+.18	-.14	-.14
	2	-2.37	-1.13	-1.13
	3	-3.52	-3.69	-3.69
W/M = 1.00	1	-2.29	-1.50	-1.50
	2	-1.99	-1.33	-1.33
	3	+.20	+.14	+.14
W/M = 1.00	1	-6.77	-4.26	-4.26
	2	-5.24	-3.63	-3.63
	3	+.35	+.23	+.23
W/M = 1.00	1	+1.03	+1.10	+1.10
	2	+.89	+1.21	+1.21
	3	-.10	-.13	-.13

*Variation 1: 1.0b reduction of ²³⁸U smooth capture integral (5.5 kev-25 kev).

2: 1.0b reduction of ²³⁸U smooth capture integral (.625 ev-6 ev).

3: 10b reduction of ²³⁵U smooth fission integral (.625 ev-6 ev).

Table 4

Shielded Capture Integrals for U^{238} Metal and Oxide Rods
(Version 3 ENDF/B)

Radius (cm)	Uranium Metal			UO ₂				
	.3430	.4915	.7620	1.588	.3534	.7044	1.111	
RESQ 5-101 ev	10.832±.081	8.931±.064	7.115±.075	4.747±.067	15.907±.085	13.682±.074	11.488±.080	9.248±.068
RESQ 101-200 ev	1.311±.012	1.126±.012	.976±.012	.699±.013	1.840±.013	1.618±.011	1.426±.011	1.209±.014
RESQ 200-325 ev	.575±.003	.488±.003	.414±.002	.330±.006	.833±.003	.717±.003	.616±.003	.524±.003
ZUT 200-325 ev	.578	.495	.419	.334	.836	.723	.624	.532
ZUT 0.325-4 Kev	2.066	1.821	1.578	1.295	2.701	2.433	2.175	1.909
TUZ 4-45 Kev	.654	.653	.651	.650	.687	.687	.687	.687
Total* .5 ev - 10 Mev	19.354	16.935	14.650	11.637	25.884	23.053	20.308	17.493
Experiment 1†	18.71	16.31	13.94	10.96	25.20	22.21	19.43	16.58
Experiment 2††	19.15	16.69	14.25	11.19	24.90	21.98	19.28	16.49
Smooth integral: .625 ev - 10 Mev (includes ENDF/B pointwise data plus smoothed p-wave resonances, resolved and unresolved).					3.720			
Smooth integral: .5 ev - .625 ev plus resonance tails not accounted for by RESQ and ZUT					.196			
								3.916

*Using RESQ result 200 ev-325 ev; includes 3.916 b of smooth integral. A statistical uncertainty of ~.08b applies.

†Hellstrand's own experiments.

††Hellstrand's recommended values.

APPENDIX

TABULATED REACTION RATES

Major Cell Reaction Rates (Ver. 3 ENDF) - TRX Lattices

	8.11/1	4.02/1	2.35/1	1.0/1
↑ Thermal ↓				
U238 fission	.01815	.02733	.03625	.05440
ν fission	(.6%)	(.4%)	(.9%)	(.5%)
Capture	(ν=2.8222)	(ν=2.8180)	(ν=2.8136)	(ν=2.8051)
	.07393	.13512	.20477	.35800
	(1.0%)	(.8%)	(.5%)	(.3%)
U235 fission	.01371	.02621	.03955	.07107
ν fission	(.8%)	(.8%)	(.5%)	(.2%)
Capture	(ν=2.4414)	(ν=2.4386)	(ν=2.4368)	(ν=2.4348)
	.03347	.06392	.09638	.17304
	.00604	.01141	.01746	.03090
	(.9%)	(.8%)	(1.3%)	(.3%)
Q (.625 ev)	.88053	.79327	.69639	.48204
	(.1%)	(.2%)	(.2%)	(.2%)
↑ Thermal ↓				
U238 Capture	.14208	.15471	.14900	.11226
	(.2%)	(.2%)	(.2%)	(.3%)
U235 fission	.38186	.41364	.39484	.29028
ν fission	(.2%)	(.2%)	(.2%)	(.2%)
Capture	(ν=2.4230)	(ν=2.4230)	(ν=2.4230)	(ν=2.4230)
	.92525	1.00225	.95670	.70335
	.06615	.07201	.06913	.05168
	(.2%)	(.2%)	(.2%)	(.3%)
H Capture	.28481	.14660	.07776	.02356
	(.2%)	(.2%)	(.4%)	(.5%)
K _∞ (tot ν fission)	1.0099	1.1432	1.1551	1.0290

Rates are normalized to one neutron born of all fission. Q(.625) is slowing down rate across .625 ev. Uncertainties are % standard deviations. ν values are from the MUFT calculations.

Leakage Corrected Reaction Rates (Ver. 3 ENDF) - TRX Lattices

	8.11/1	4.02/1	2.35/1	1.0/1
U238 fission	.01779	.02486	.03298	.05626
U238 fission Capture	.05016 .07280	.06995 .12001	.09267 .17952	.15781 .34923
U235 fission	.01349	.02318	.03448	.06879
U235 fission Capture	.03293 .00595	.05652 .01008	.08403 .01519	.16754 .02982
Q(.625 ev)	.86547	.69190	.59637	.45476
U238 Capture	.13965	.13350	.12625	.10590
U235 fission	.37532	.35692	.33451	.27384
U235 fission Capture	.90940 .06502	.86482 .06214	.81052 .05857	.66351 .04876
H Capture	.27994	.12650	.06588	.02222

↑ epithermal
↑ thermal

↑ thermal

ADDENDUM

Preliminary results with ENDF/B-IV, obtained since the Seminar, are shown in tables below.

(PRELIMINARY)
TRX LATTICE PARAMETERS CALCULATED WITH ENDF/B-IV DATA

Parameter	W/M = 8.11		W/M = 4.02		W/M = 2.35		W/M = 1.00	
	Exp.	Calc.	Exp.	Calc.	Exp.	Calc.	Exp.	Calc.
ρ^{28} (epi/thermal ^{238}U capture)	.466 + .01	.500 + .005	.830 + .015	.859 + .007	1.311 + .02	1.362 + .009	3.01 + .05	3.19 + .02
δ^{25} (epi/thermal ^{235}U fission)	.0352 + .00004	.0373 + .00003	.0608 + .0007	.0610 + .0004	.0981 + .001	.0992 + .0004	.230 + .003	.244 + .001
δ^{28} (^{238}U fission/ ^{235}U fission)	.0452 + .0007	.0477 + .0006	.0667 + .002	.0678 + .0006	.0914 + .002	.0948 + .0004	.163 + .004	.177 + .001
CR^* ($^{238}\text{C}_{\text{capture}}/^{235}\text{U}$ fission)	.526 + .004	.530 + .002	.646 + .002	.646 + .002	.792 + .008	.798 + .003	1.255 + .011	1.283 + .007
K_{eff}	1.000	.9994 + .0013	1.000	1.0022 + .0014	1.000	.9997 + .0014	1.000	1.0001 + .0024

(PRELIMINARY)
MAJOR CELL REACTION RATES (ENDF/B-IV) - TRX LATTICES ($\beta^2 = 0$)

	W/M = 8.11	W/M = 4.02	W/M = 2.35	W/M = 1.00
↑ U238 fission v fission Capture	.01907 (.5%) .05397 (v=2.8301) .07035 (.8%)	.02873 (.5%) .08115 (v=2.8246) .12943 (.5%)	.03896 (.5%) .10981 (v=2.8185) .19621 (.5%)	.05908 (.3%) .16583 (v=2.8069) .34769 (.3%)
↑ U235 fission v fission Capture	.01357 (.5%) .03311 (v=2.4399) .00601 (.5%)	.02501 (.5%) .06091 (v=2.4354) .01135 (.5%)	.03865 (.4%) .09408 (v=2.4342) .01764 (.5%)	.07044 (.3%) .17134 (v=2.4324) .03151 (.4%)
↑ Epithermal Q(.625 eV)	.88313 (.1%)	.79859 (.1%)	.70288 (.1%)	.48792 (.2%)
↑ Thermal U238 capture	.14090 (.1%)	.15489 (.1%)	.14885 (.1%)	.11246 (.2%)
U235 fission v fission Capture	.38508 (.1%) .93141 (v=2.4188) .06573 (.1%)	.42032 (.1%) 1.01667 (v=2.4188) .07209 (.1%)	.40075 (.1%) .96933 (v=2.4188) .06919 (.1%)	.29541 (.2%) .71454 (v=2.4188) .05187 (.2%)
H capture	.28578 (.2%)	.14517 (.1%)	.07819 (.1%)	.02381 (.2%)
K_{∞} (tot v fission)	1.0185	1.1587	1.1732	1.0517

Rates are normalized to one neutron born of all fission. Q(.625 eV) is the slowing-down rate across 0.625 eV. Uncertainties are % standard deviations. v values are from the MUFT calculations.

(PRELIMINARY)
LEAKAGE CORRECTED REACTION RATES

ENDF/B-IV TRX LATTICES

	<u>w/M = 8.11</u>	<u>w/M = 4.02</u>	<u>w/M = 2.35</u>	<u>w/M = 1.0</u>
U238 fiss.	.01866	.02604	.03527	.06065
v fiss.	.05275	.07344	.09929	.17027
Capture	.06918	.11458	.17126	.33486
U235 fiss.	.01334	.02205	.03355	.06731
v fiss.	.03254	.05370	.08168	.16378
Capture	.00591	.00999	.01529	.03002
Q(.625)		.69480	.60004	
U238 capture	.13829	.13334	.12573	.10483
U235 fiss.	.37793	.36179	.33848	.27537
v fiss.	.91414	.87510	.81872	.66606
Capture	.06451	.06206	.05844	.04835
H capture	.28047	.12497	.06605	.02219

(PRELIMINARY)
LEAKAGE CORRECTED REACTION RATES AND PARAMETERS
FOR THE w/M = 1.0 CELL, SIMPLY BUCKLED ($B^2 = 20.98 \text{ M}^{-2}$)

U238 fiss.	.05698
v fiss.	.15988
Capture	.32676
U235 fiss.	.06598
v fiss.	.16051
Capture	.02948
Q (.625)	.45253
U238 capture	.10382
U235 fiss.	.27268
v fiss.	.65955
Capture	.04788

Parameters:	ρ_{28}	3.15
	ρ_{25}	.242
	ρ_{28}	.168
	CR*	1.271
	K_{eff}	.9799

S_n ANALYSIS OF THE TRX METAL LATTICES
WITH ENDF/B VERSION III DATA

F. J. Wheeler
Aerojet Nuclear Company
Idaho Falls, Idaho

(A) Introduction

Two critical assemblies, designated as thermal-reactor benchmarks TRX-1 and TRX-2 for ENDF/B data testing, were analyzed using the one-dimensional S_n -theory code SCAMP*. The two assemblies were simple lattices of aluminum-clad, uranium-metal fuel rods in triangular arrays with H₂O as moderator and reflector. The fuel was low-enriched (1.3% ²³⁵U), 0.387-inch in diameter and had an active height of 48 inches. The volume ratio of water to uranium was 2.35 for the TRX-1 lattice and 4.02 for TRX-2. Detailed parameter measurements have been reported⁽²⁾ for these lattices. Full-core S_n calculations based on Version III data were performed for these assemblies and the results obtained were compared with the measured values of the multiplication factors (k), the ratio of epithermal-to-thermal neutron capture in ²³⁸U (ρ^{28}), the ratio of epithermal-to-thermal fission in ²³⁵U (δ^{25}), the ratio of ²³⁸U fission to ²³⁵U fission (δ^{28}), and the ratio of capture in ²³⁸U to fission in ²³⁵U (CR). Reaction rates were obtained from a central region of the full-core problems. Multigroup cross sections for the reactor calculation were obtained from S_n cell calculations with resonance self-shielding calculated using the RABBLE⁽³⁾ treatment. The results of the analyses are generally consistent with results obtained by other investigators. The calculated multiplication factors were 1.8 to 2.6% low for the critical assemblies. This under-estimation of k is thought to be primarily due to the overprediction of the ²³⁸U epithermal neutron capture as is evidenced in the comparison of the calculated values of ρ^{28} with measured data.

Some of the approximations used in the analyses were investigated including the use of alternate treatments in the resolved energy range, the angular quadrature in the cell calculation, whether the number of thermal groups in the cell calculation (32-group) was enough to eliminate spectrum

*SCAMP, in cylindrical geometry, is a modification of the TOPIC⁽¹⁾ program.

effects in derivation of thermal constants and the importance of the outer-boundary condition chosen for return of neutrons from the fictitious cylindrical boundary in the cell calculation. For those alternate methods investigated none would significantly affect the conclusions concerning the use of Version III data in low-enriched thermal systems. Effects that were not investigated included the adequacy of the P_1 approximation for the angular scatter distribution, the use of asymptotic thermal spectra at the fuel-reflector interface, the cylindricalization of the outer boundary of the cell and the isotropic assumption for the energy distribution of the source to the thermal groups.

(B) Summary of Methods and Results

The analyses of the TRX reactor benchmarks essentially consisted of four steps:

1. Processing the ENDF/B data into problem-independent library files
2. Use of these library files with spectrum and resonance codes to obtain problem-dependent 97-group cross sections for subsequent cell calculations (32 thermal groups)
3. Unit cell calculations using S_n theory
4. Homogenized full-core 68-group calculations to obtain final results

For step one, the ENDF/B data were processed using the ETOP⁽⁴⁾ and FLANGE II⁽⁵⁾ codes.

For step two, quarter-lethargy cross sections in the fast energy range were obtained using modified versions of the PHROG⁽⁶⁾ and RABBLE codes. The PHROG resolved-resonance treatment was bypassed in favor of the resonance self-shielding as calculated with the RABBLE treatment. The INCITE⁽⁷⁾ code, in the B-1 approximation, was used to obtain the 32-group thermal cross section set used in the cell calculations.

For steps three and four, S_n unit-cell calculations were performed, using the 97-group cross section set, in the S_6 , P_1 approximation with a semi-isotropic outer boundary condition and a leakage correction (DB^2) in the fast-energy groups. Subsequent full-core calculations (S_6 , P_1) were performed using cross sections from the cell problem coalesced over space and thermal energy to form a 68-energy group set with one thermal group below .625 eV. Fast and thermal cross sections for the H₂O reflector were obtained from the PHROG and INCITE spectrum codes assuming asymptotic

water spectra. The comparison of the calculated results with experimental data is given in Table I.

TABLE I
CALCULATION / EXPERIMENT

	TRX-1	TRX-2
K_{eff}	.9741	.9823
δ^{25}	1.039	1.018
δ^{28}	.986	.976
ρ^{28}	1.097	1.092
CR	1.016	1.040

(C) Details of the Computational Models

The ETOP code represents an extensive modification of the ETOG⁽⁸⁾ package. Since the changes in ETOP affect the calculational results, these will be briefly outlined.

Problems in data processing originate from two principal sources. The first is incompatibilities between ENDF/B format and the physical approximations incorporated into the spectrum code. The second arises from numerical limitations and inaccuracies over specified energy ranges in ETOP.

ETOP now performs no preliminary processing of ENDF/B unresolved capture, fission and scatter data except for the case where there are several isotopes specified for a single ENDF/B material. In this case, both the resolved and unresolved range parameters are processed at infinite dilution into smooth cross sections for PHROG. At present only a few ENDF/B materials fit into this category. The output smooth data files, in the resolved-resonance range, contain only the averaged data from File 3 plus the contribution from p-wave resonances and the tails of s-wave resonances that do not lie within the energy bounds of the resolved range. This contribution is computed assuming infinite dilution.

The original limitations on energy mesh were found to result in serious numerical problems in the calculation of resonance cross sections and elastic-scattering matrices in the resolved-resonance range. The original coding was adequate for version I data when less than 10 or 12 resonances occurred per quarter-lethargy group. With the advent of version II data, several isotopes exceeded these safe limits. A large number of resolved p-wave resonances are present in ^{238}U , for example. A redefinition of the integration intervals was made to reduce numerical error. Mesh problems still exist under the most severe conditions and the only real solution to the problem in these instances is to increase the total number of mesh points in the offending groups. This will require a major modification of the processing code.

The calculation of the elastic scattering matrices in the resolved resonance region is based on a special semi-analytical subroutine⁽⁹⁾ which improves the accuracy of the Legendre matrix elements several orders of magnitude for the case of isotropic scattering in the CM system. This is almost always the intended scattering law in the resolved resonance region.

For this situation, the total Legendre moment of the cross section is known analytically for any order l ⁽⁹⁾. For isotopic mass exceeding $A=16$, only one group downscatter is possible for the 0.25 lethargy-group structure and this downscatter term is easily calculated. The diagonal within-group term is then obtained by subtracting the outscatter term from the total Legendre moment which is obtained analytically. This technique permits a great simplification in the resolved-resonance range since the within-group term presents the greatest numerical difficulty. The extreme mesh requirement for this Legendre convolution is thus avoided entirely where many resonances are involved in the within-group term. At higher energies, where the scattering is not isotropic, numerical integration of the within-group term is necessary.

The FLANGE II code was used to process thermal data into a 101-energy-point library below 2.38 eV for use with the INCITE thermal-spectrum code. INCITE is a program to calculate energy-dependent thermal-neutron spectra and appropriate average-multigroup cross sections using arbitrary scattering kernels. The program employs a normalized Gauss-Seidel iteration technique to solve the energy-dependent integral form of the B-1 approximation to the Boltzman transport equation.

For the treatment in the fast-energy range, a variation of the MC² equations for the unresolved range was incorporated into the PHROG II code and the modified RABBLE package to make them completely compatible to the ENDF/B unresolved-range format. Tables of $J(\theta, \beta)$ were added to treat shielding and temperature effects in unresolved data. Both codes preprocess the unresolved data into self-shielded quarter-lethargy cross sections before performing the final spectrum calculations.

The RABBLE resonance calculation was performed for the cylindricalized cell using an isotropic outer-boundary condition. An interval width of 0.001 was used to determine the lethargy mesh in the transport calculation. At each energy point, the ²³⁸U cross sections were determined using the sum of the Breit-Wigner single-level cross sections for the three nearest (in energy) resonances. In the case of ²³⁵U, cross sections were summed over the 20 nearest resonance levels at each energy point. The smoothed background cross sections and the cross sections for the non-resonance isotopes in the cell were the quarter-lethargy values output by the ETDP code.

The 97-group, SCAMP-cell calculations were performed assuming 12 spatial intervals in the fuel, 25 in the water and 1 each in the gap and cladding. The S_6 (6 intervals on the azimuthal-angle halfspace) approximation was used with 4 Gauss-quadrature points on the polar-angle halfspace. Scatter was assumed to be linearly-anisotropic and a leakage term was applied in the fast groups through a DB^2 term. Upscatter was treated to 0.876 eV and molecular binding effects in water were treated to 2.38 eV. At the outer boundary of the cell the return current was treated using a semi-isotropic reflection albedo which assumes mirror return in the polar angle and isotropic return in the azimuthal angle.

The SCAMP code has an option to compute average cross sections coalesced over energy and space. This option was used to obtain cross sections for the cell, homogenized over all regions and collapsed over the thermal groups to 0.625 eV forming a 68-group cross section set for input to the full-core calculations.

For TRX-1, a SCAMP zero-leakage cell calculation was performed and compared to the full-core calculation to determine the magnitude of the leakage correction for each of the parameters of interest. The results, shown in Table II, indicate that the leakage effect is small for the central reaction-rate ratios and only about 15% for the multiplication factor.

TABLE II
TRX-1 LEAKAGE EFFECT

Parameter	Zero-Leakage Cell Calculation	Full-Core Calculation	Ratio Full-Core/Cell
K	1.1511	0.9741	0.8462
δ^{25}	0.0999	0.1019	1.0200
δ^{28}	0.0835	0.0901	1.0790
ρ^{28}	1.4070	1.4380	1.0220
CR	0.7962	0.8050	1.0110

(D) Alternate Resolved Resonance Treatments

Since resonance shielding is very important in these lattices, calculations were made to compare results obtained using alternate treatments in the resolved-resonance range. The PHROG II code was used to investigate the following effects.

1. The comparison of results obtained using the approximations in the PHROG II resonance treatment and the RABBLE treatment.
2. The errors resulting from the use of 3 neighboring levels in ^{238}U and 20 neighboring levels in ^{235}U when computing pointwise cross sections.
3. Comparison of PHROG II results with those obtained using pointwise ^{235}U cross sections computed by the ACSAP⁽¹⁰⁾ code using both the Breit-Wigner single-level formalism (SL) and the Reich-Moore formalism (RM).

The major modifications that form the PHROG II package were in the treatment of the resonance shielding where the numerical accuracy was improved. Also, the code was made compatible with ENDF/B data. The original PHROG coding treated resonance absorption by means of a direct numerical solution, formulated by Nordheim,⁽¹¹⁾ to the neutron collision density equations. A serious limitation of the ETOP-PHROG package was that the elastic-scattering matrices were pre-computed by ETOP. The compound-elastic contribution from the resolved and unresolved range was calculated at infinite dilution

precluding the possibility of shielding the compound elastic resonance data. This is a very important effect for ^{238}U in low-enriched thermal systems. Added to the library file for those isotopes with resonance parameters is a file containing the background P_0 and P_1 scatter matrix computed from the data on the ENDF/B version III tape. This background matrix allows the generation of a problem-dependent self-shielded scatter matrix which represents an improvement over the PHROG representation of the scatter matrix as constant data.

Other improvements in the resolved resonance calculation are (1) the inclusion of overlap effects due to neighboring resonances of an individual isotope and (2) a user-specified option allowing the selection of either the asymptotic $1/E$ flux or the depressed lump flux in the definition of the quarter-lethargy group cross section output from the resonance routines.

The physical model employed in the PHROG II resolved-resonance calculations assumes a $1/E$ slowing down flux above the upper-energy cutoff of the resolved energy range. The geometry may be homogeneous or a lump surrounded by an external moderator. The geometry of the lump may be either slab, cylindrical, or spherical, and up to three scattering nuclides (in addition to the absorber atom) may be present, providing a slowing-down source within the absorber lump. The flux in the range of integration is computed assuming a slowing-down density determined by the flux above the range of integration and a $1/E$ flux in the external moderator, if present. A correction to the magnitude of the source from the external moderator is required in a tight lattice because of mutual "shadowing" of the absorber lumps. This shadowing is approximately taken into account by a redefinition of the escape probability which makes use of the Dancoff-Ginsburg correction.

The general procedure used in obtaining the solution over each range of integration is as follows. The energy interval over which the range of integration is chosen is determined by points midway in energy between the resonance peak of the level associated with the interval and its adjacent neighbors. For the highest energy resonance, the upper cutoff of the interval is determined by the upper cutoff of the resolved-energy range; and for the lowest-energy resonance, the lower cutoff of the resolved-energy range or 0.414 eV, whichever is lower. For this range, a lethargy width is chosen which limits the point-to-point cross section variation due

to Doppler broadening (see reference 11). At each mesh point across this interval, Doppler-broadened absorption, fission, and scatter cross sections are computed assuming the Breit-Wigner single-level formulation and a Maxwellian distribution of absorber velocities. The cross sections at each point are accumulated for N neighboring resonances where N is input by the user. Then, beginning at the uppermost energy of the range, E_1 , the pointwise flux in the absorber medium is computed from the scatter source within the medium and the external source from the moderator, if any. The contribution to each interaction cross section is then accumulated for each PHROG II group which intersects the integration interval, by means of trapezoidal integration.

Multigroup (67 fast, 1 thermal) SCAMP-cell calculations were performed using regionwise cross sections generated entirely by PHROG II with the depressed lump flux used in the denominator of the equations defining the average cross sections in the resolved range. Comparison with results using the RABBLE treatment showed no significant difference for the TRX-1 lattice (the leakage-corrected k was increased by ~0.04%). Thus, for this lattice, the effects due to interference between ^{235}U and ^{238}U and the asymptotic spectra assumption in the moderator are apparently small.

The effect of the number of resonance levels used to define the pointwise resolved cross sections was investigated for the TRX-1 cell. The effect due to increasing the number of neighboring levels from 3 to 5 for ^{238}U was to increase the shielded resonance integral by 0.017 barn, a 0.1% change. The effect due to increasing the number of neighbors from 20 to 128 (all levels) in ^{235}U was to increase the fission integral by nearly 1.6 barns, a 0.6% change. Thus, the calculated value of δ^{25} would increase from the reported value of 0.1019 to a value of 0.1025, and an increase in k of ~0.01% would result had all the neighboring levels in ^{235}U been included in the definition of the pointwise cross sections.

The ^{235}U self-shielding in these lattices is small and therefore the multilevel effect is correspondingly small. However, calculations were run to determine this effect in TRX-1 and to compare results using the ACSAP code to determine the pointwise cross sections in the resolved range. Single-level and multi-level (RM) cross sections for ^{235}U were generated with ACSAP using all levels to define the cross sections at each energy point. The multi-level parameters used were taken from an evaluation by Smith. The cross sections were input to the PHROG II code using a special option and a shielding calculation was performed for each case.

Even though the smooth file is self-shielded, the use of ACSAP single-level cross sections resulted in a fission integral 2.7 barns higher than obtained from a comparable PHROG II calculation, thus ACSAP SL cross sections would predict about a 1% higher δ^{25} .

When the results of the multi-level calculation were compared to single-level results no significant effects were seen in integral results although groupwise cross sections varied by as much as 6%.

(E) Summary of Sensitivity Studies in the Thermal Range

The effects due to some of the approximations employed in the thermal energy range were investigated for the TRX-1 cell. Briefly these were:

1. An S_{10} cell calculation was performed. The change in computed reaction rates, compared to the S_6 calculation, was very small (~0.02%).
2. A cell calculation was performed employing an isotropic outer-boundary condition. The computed fuel disadvantage factor was ~0.07% higher than that obtained using the semi-isotropic albedo.
3. The assumption that the 32-group structure was adequate to assure problem-independency of the group cross sections was investigated by means of an INCITE problem in which space and energy self-shielding factors were applied by region and group. Subsequent SCAMP cell calculations, using cross sections from this INCITE case, showed changes in the reaction rates ~0.1% indicating some problem dependency, however final results would be affected only slightly.

REFERENCES

1. G. E. Putnam, "TOPIC--FORTRAN Program for Calculating Transport of Particles in Cylinders," IDO-16968, Phillips Petroleum Company (April 1964).
2. D. Klein, A. Z. Kranz, G. G. Smith, W. Baer, and J. DeJuren, "Measurements of Thermal Utilization, Resonance Escape Probability, and Fast Effect in Water-Moderated, Slightly-Enriched Uranium and Uranium Oxide Lattices," Nucl. Sci. Eng. 3 403-427 (1958).
3. P. H. Keir and A. A. Robba, "RABBLE-A Program for Computation of Resonance Absorption in Multiregion Reactor Cells," ANL-7326 (1967).
4. G. L. Singer, "ETOP-ENDF/B to PHROG," Unpublished, Aerojet Nuclear Corporation.
5. H. C. Honeck and D. R. Finch, "FLANGE-II (Version 71-1), A Code to Process Thermal Neutron Data from an ENDF/B Tape," DP-1278, E.I. duPont de Nemours & Co. (Oct. 1971).
6. R. L. Curtis, G. L. Singer, F. J. Wheeler, and R. A. Grimesey, "PHROG-A FORTRAN IV Program to Generate Fast Neutron Spectra and Average Multigroup Constants," IN-1435, Idaho Nuclear Corporation (1971).
7. R. L. Curtis and R. A. Grimesey, "INCITE--A FORTRAN-IV Program to Generate Thermal Neutron Spectra and Multigroup Constants Using Arbitrary Scattering Kernals," IN-1062, Idaho Nuclear Corporation (1967).
8. D. E. Kusner and S. Kellman, "ETOG-1, A FORTRAN IV Program to Process Data from the ENDF/B File to the Muft, GAM and ANISN Formats," WACP-3845-1 (ENDF 114), Westinghouse Atomic Power Divison (1969).
9. R.A. Grimesey, W. Serrano, R. A. Dannels, "Legendre Moments of the Elastic-Scattering Cross Section for S-Wave Neutrons," Nucl. Sci. Eng. 41, 140 (1970).
10. N. H. Marshall et al., "An Automated Cross Section Analysis Program (ACSAP)," ANCR-1042, Aerojet Nuclear Company (1972).
11. L. W. Nordheim, "A Program of Research and Calculations of Resonance Absorption," GA-2527, General Atomics Corporation (1961).

The Current UK Position on Uranium-238 Resonance Capture

J R Askew

AEE, Winfrith

April 1975

Abstract

The paper reviews the large body of integral evidence on Uranium-238 resonance capture accumulated since 1966, when attention was first drawn to a discrepancy between integral evidence and calculated results based upon differential data. The experiments cover many reactor types, laboratories and measurement techniques, and include studies of isotopic composition of discharged fuel.

It is shown that the discrepancy still exists, although changes in other data (particularly Uranium-235 resonance capture) have reduced the size of the deduced discrepancy to 4-8%. (Note added in proof: As the ENDF B IV data appears to give a higher resonance integral than the 'basic' differential data chosen here, the correction required would be greater).

It is argued that the differences are within the uncertainties of measurement of parameters for the low lying resonances which dominate thermal reactor calculations. These were originally believed to be more accurate because it was thought acceptable to assume capture widths invariant and to average them over many resonances. Once this is not permitted the differences become explicable.

The Current UK Position on U-238 Resonance Capture

J R Askew

1. Introduction

At the 1966 ANS Topical Meeting on Reactor Physics in the Resonance and Thermal regions two papers from the UK (1, 2) drew attention to the discrepancies between prediction and observation in lattice experiments which were ascribed to errors in the data for resonance capture in Uranium-238.

It appeared that a 10% reduction in resonance capture was required to give agreement with both reaction rate and reactivity for the range of light water and graphite moderated lattices studied, which included both metal and oxide fuels.

Since that time more experimental data have become available and more systematic analyses performed. Some changes in data for other nuclides - especially for Uranium-235 - will affect the results obtained. This paper sets out to describe the position now reached in this area, which is that the discrepancy still exists but is smaller than originally estimated, lying in the range 4-8%.

2 Differential Data

Table 1 shows the resonance parameters for the resolved region used in the original studies, and compares them with data due to Nordheim (3). These were shown to give very similar results.

To investigate the hypothesis that an independent compilation of resonance parameters might significantly modify the nature of an inferred correction to resonance integrals, a recent re-evaluation of GENEX cross-sections based on parameters chosen by James (12) has been evaluated in the WIMS context. The new parameters for the resolved region which now extends to 5 keV are listed in Appendix 2. The intention in this compilation was to reproduce the U²³⁸ capture cross-sections at higher energies (ie at energies of a few keV) which have been inferred from Fast Reactor integral data studies (13), and which over an appropriate energy range would be approximately 10% lower than an evaluation by Sowerby, Patrick and Mather (14). Below 5 keV the recent measurements of Rahn et al (15) have been used which have been augmented with p-wave and small s-wave resonances generated randomly from suitable distributions. In the unresolved region, above 5 keV, both s- and p-wave neutron widths were then adjusted to give the desired average capture cross-section. The adjustments were all within the known statistical uncertainty for such a generating process. For all resonances for which the capture width Γ_γ had not been measured, a value of 23.0 meV was assumed. This includes the important 6.7 eV resonance. The other mean parameters were taken to be:

Mean resonance spacing for s-wave resonance (\bar{D}) = 22.5 eV

s-wave strength function S_0 = 0.93×10^{-4}

p-wave strength function S_1 = 1.8×10^{-4}

The previous WIMS U²³⁸ group cross-sections are compared with values obtained from this compilation, and also with the Sowerby et al energy variation in Fig 2. On average, the James' parameters have given about 7% reduction in the keV region. The SDK homogeneous resonance integrals for a temperature of 900°K obtained from the new GENEX tape are compared in Table 2 with the standard uncorrected resonance integrals available in the WIMS library.

Table 1

Resolved Resonance Parameters for Uranium-238

NORHEIM data							
E	Γ_n	Γ_p		E	Γ_n	Γ_p	
6.70000E 00	1.52000E-01	2.46000E-01		2.7430E 2	2.7000E -2	2.5000E -2	
2.10000E 00	8.90000E-01	2.46000E-02		2.8113E 2	2.19000E -2	2.5000E -2	
3.67000E 01	3.25000E-04	2.46000E-02		3.1232E 2	2.10000E -3	2.5000E -2	
6.63000E 01	2.50000E-04	2.46000E-02		3.4850E 2	2.57000E -2	2.5000E -2	
4.63000E 01	2.10000E-03	2.46000E-02		3.7850E 2	2.14000E -3	2.5000E -2	
4.60000E 01	4.00000E-04	2.46000E-04		3.9900E 2	2.73000E -3	2.5000E -2	
1.02500E 02	6.50000E-02	2.46000E-02		4.1150E 2	2.13000E -2	2.5000E -2	
1.16500E 02	1.50000E-02	2.46000E-02		4.3550E 2	2.97000E -3	2.5000E -2	
1.45600E 02	8.00000E-04	2.46000E-02		4.5550E 2	2.46950E -4	0.0250E 0	
1.65200E 02	3.50000E-03	2.46000E-02		4.6450E 2	2.51000E -3	2.5000E -2	
1.40600E 02	1.35000E-01	2.46000E-02		4.7900E 2	2.33000E -3	2.5000E -2	
2.08500E 02	5.50000E-02	2.46000E-02		4.8900E 2	2.66340E -4	0.0250E 0	
2.37500E 02	3.20000E-02	2.46000E-02		5.1950E 2	2.44000E -2	2.5000E -2	
2.44500E 02	2.10000E-04	2.46000E-02		5.3650E 2	2.79000E -2	2.5000E -2	
2.74000E 02	2.70000E-02	2.46000E-02		5.5750E 2	2.72430E -3	0.0250E 0	
2.91000E 02	1.90000E-02	2.46000E-02		5.8700E 2	2.34000E -2	2.5000E -2	
3.11500E 02	1.00000E-03	2.46000E-02		5.9800E 2	2.80000E -2	2.5000E -2	
3.48000E 02	4.50000E-02	2.46000E-02		6.0500E 2	2.59000E -4	0.0250E 0	
3.77000E 02	1.50000E-03	2.46000E-02		6.2200E 2	2.32000E -2	2.5000E -2	
3.98500E 02	1.00000E-02	2.46000E-02		6.3050E 2	2.73000E -3	2.5000E -2	
4.11000E 02	1.70000E-02	2.46000E-02		6.6450E 2	2.16400E -1	2.5000E -2	
4.38000E 02	1.40000E-02	2.46000E-02		6.9650E 2	2.53500E -2	2.5000E -2	
4.55000E 02	7.00000E-04	2.46000E-02		7.1150E 2	2.21500E -2	2.5000E -2	
4.64000E 02	7.00000E-03	2.46000E-02		7.2400E 2	1.13000E -3	0.0250E 0	
4.70000E 02	4.50000E-03	2.46000E-02		7.3300E 2	2.93000E -3	2.5000E -2	
4.90000E 02	1.00000E-02	2.46000E-02		7.5600E 2	2.16000E -4	2.5000E -2	
5.19000E 02	3.70000E-02	2.46000E-02		7.6700E 2	2.67000E -3	2.5000E -2	
5.36000E 02	5.40000E-02	2.46000E-02		7.9300E 2	2.20400E -3	2.5000E -2	
5.57000E 02	1.00000E-03	2.46000E-02		7.9300E 2	2.76000E -3	2.5000E -2	
5.81000E 02	4.20000E-02	2.46000E-02		8.0900E 2	2.10000E -3	2.5000E -2	
5.96000E 02	6.70000E-02	2.46000E-02		8.2500E 2	2.66000E -2	2.5000E -2	
6.05000E 02	6.00000E-04	2.46000E-02		8.5550E 2	2.1200E -1	2.5000E -2	
6.21000E 02	3.00000E-02	2.46000E-02		8.6050E 2	1.2700E -1	2.5000E -2	
6.29000E 02	9.00000E-03	2.46000E-02		8.6950E 2	2.2120E -3	0.0250E 0	
6.43000E 02	1.25000E-01	2.46000E-02		8.9850E 2	2.1240E -3	0.0250E 0	
6.40000E 02	1.30000E-03	2.46000E-02		9.1150E 2	2.67000E -2	2.5000E -2	
6.95000E 02	8.70000E-02	2.46000E-02		9.3050E 2	2.14000E -2	2.5000E -2	
7.10000E 02	1.70000E-02	2.46000E-02		9.4213E 2	1.6800E -1	2.5000E -2	
7.23000E 02	1.47000E-02	2.46000E-02		9.6200E 2	2.15400E -1	2.5000E -2	
7.32000E 02	4.25000E-03	2.46000E-02		9.8300E 2	2.94060E -4	0.0250E 0	
7.46000E 02	9.00000E-03	2.46000E-02		9.9700E 2	2.37700E -1	2.5000E -2	
7.42000E 02	3.00000E-03	2.46000E-02		1.0140E 3	6.00000E -4	2.6000E -2	
7.92000E 02	1.10000E-02	2.46000E-02		1.0290F 3	1.9000E -2	2.6000E -2	
8.25000E 02	6.00000E-02	2.46000E-02		1.0470E 3	2.70000E -4	2.5000E -2	
8.55000E 02	1.30000E-01	2.46000E-02		1.0610E 3	2.1000E -2	2.6000E -2	
8.59000E 02	6.00000E-02	2.46000E-02		1.1100E 3	7.0000E -3	2.6000E -2	
8.67000E 02	7.70000E-03	2.46000E-02		1.1140E 3	5.7000E -3	2.6000E -2	
8.99000E 02	1.30000E-03	2.46000E-02		1.1490E 3	2.74000E -1	2.6000E -2	
9.09000E 02	9.00000E-02	2.46000E-02		1.1760E 3	4.3000E -2	2.6000E -2	
9.38000E 02	3.70000E-02	2.46000E-02		1.1860E 3	3.0000E -2	2.6000E -2	
9.40000E 02	1.95000E-01	2.46000E-02		1.2040E 3	5.7000E -2	2.6000E -2	
9.60000E 02	1.90000E-01	2.46000E-02		1.2210E 3	1.4000E -2	2.6000E -2	
9.63000E 02	1.00000E-03	2.46000E-02		1.2550E 3	2.3400E -1	2.6000E -2	
9.95000E 02	4.00000E-01	2.46000E-02		1.2740E 3	2.5000E -2	2.6000E -2	
				1.2810E 3	2.7000E -2	2.6000E -2	
				1.2920E 3	5.0000E -3	2.6000E -2	
				1.3040E 3	1.0000E -2	2.6000E -2	
				1.3750E 3	2.0700E -2	2.6000E -2	
				1.4040E 3	2.9500E -1	2.6000E -2	
				1.4190E 3	9.8000E -2	2.6000E -2	
				1.4280E 3	2.0000E -2	2.6000E -2	
				1.4370E 3	8.0000E -2	2.6000E -2	
				1.4550E 3	2.5000E -2	2.6000E -2	
				1.4870E 3	8.0000E -2	2.6000E -2	
				1.5160E 3	2.0000E -2	2.6000E -2	
				1.5390E 3	1.7100E -1	2.6000E -2	
				1.5540E 3	4.0000E -2	2.6000E -2	
				1.5600E 3	5.0000E -2	2.6000E -2	
				1.5740E 3	7.0000E -2	2.6000E -2	
				1.6400E 3	1.5000E -1	2.6000E -2	
				1.6800E 3	1.0000E -1	2.6000E -2	
				1.7100E 3	4.6000E -2	2.6000E -2	
				1.7300E 3	2.7000E -2	2.6000E -2	
				1.7400E 3	2.0000E -2	2.6000E -2	
				1.7750E 3	1.1500E -1	2.6000E -2	
				1.8000E 3	8.7000E -1	2.6000E -2	

U.K. data			
E	Γ_n	Γ_p	
6.6800E 0	1.4400E -3	2.5000E -2	
1.0200E 1	1.2770E -6	0.0250E 0	
2.1000E 1	4.0000E -3	2.5000E -2	
3.6800E 1	1.3340E -2	2.5000E -2	
6.6300E 1	2.3000E -2	2.5000E -2	
8.1200E 1	2.0000E -3	2.5000E -2	
9.0000E 1	7.5870E -5	0.0250E 0	
1.0200E 2	6.6000E -2	2.5000E -2	
1.1690E 2	1.4000E -2	2.5000E -2	
1.4580E 2	8.0000E -4	2.5000E -2	
1.6350E 2	4.0000E -3	2.5000E -2	
1.9050E 2	1.4400E -1	2.5000E -2	
2.1000E 2	5.3000E -2	2.5000E -2	
2.3920E 2	3.6000E -2	2.5000E -2	
2.6400E 2	2.2750E -4	0.0250E 0	

Table 2

Comparison of Resonance Integrals (0.55 eV-2 MeV)
Obtained from James Compilation
with Basic WIMS Library Data

(Note temperature 900°K)

σ_p barns	James RI barns	WIMS RI barns
15.53	13.95	14.52
31.49	18.44	19.20
53.40	23.07	24.05
65.34	25.22	26.30
146.2	36.70	38.36
261.3	48.89	50.87
∞	266.51	273.41

It will be seen that this evaluation gives a 4% reduction in resonance integral over the range of practical interest in power reactors, at the expense of a reduction in the infinitely dilute resonance integral which seems unlikely to be consistent with integral data. None the less, it is encouraging that some link between fast and thermal reactor requirements for data adjustment can be seen, even if the proposed route is tenuous by virtue of the dominant effect of the 6.7 eV resonance in the thermal system.

The epithermal data for Uranium-235 originally used were due to Brookes(16) and resulted in a capture/fission ratio of 0.64 above 0.5 eV. Subsequent integral studies (4) showed that this was in error, and the data currently in use correspond to a value of 0.5. The point is discussed in Reference 5.

Epithermal cross-sections for moderating materials have also changed, as is illustrated in Table 3.

Table 3

Cross-Section of Moderating Materials in the
Resolved Resonance Region (σ_s , Barns)

	Hydrogen	Deuterium	Carbon
Ankew 2 (1966)	20.50	3.40	4.70
Fayers 5 (1967)	20.00		
Chawla 6 (1972)	20.30	3.35	4.75

It will be seen that these changes are not large compared to the discrepancies under consideration.

3. Calculational Models

The integral comparisons reported here have all been carried out using the lattice code WIMS (7). This is described in References 7 and 8 with some minor improvements to the resonance treatment detailed in Reference 5. The WIMS scheme is based upon a 69-group data library and allows space/energy solutions in various degrees of complexity including full collision probability modelling of doubly heterogeneous cluster geometries. Because of its direct relevance to the problem of Uranium-238 resonance capture we shall sketch briefly the model used for this purpose.

The energy range from 4eV to 9.118 keV is divided into 13 groups of irregular width, so arranged that resonances of the most important nuclides are either central or uniformly spaced within them. Group data are tabulated as partial resonance integrals for a mixture of the resonance absorber with Hydrogen as a function of the effective potential cross-section of the mixture per absorbing atom (Σ_p) and temperature T.

For application to simple model problems, such as regular pin-lattices an equivalent value of Σ_p is determined taking into account the effective contribution of intermediate mass nuclides mixed with the absorber (including Oxygen) and a geometric term depending upon the mean chord length of the pin, together with Dancoff and Bell factors. The former term representing pin-to-pin interactions, the latter allowing for departures from the black limit in integrating the collision probability equations over energy.

The model permits first order representation of the effects of overlapping of resonances of different nuclides on a statistical basis.

The partial resonance integrals are converted to cross-section using an internally consistent model for the flux depression caused by the resonances, so that used consistently in a few group spatial solution the correct reactions are preserved.

A small correction is made to group removal cross-sections to allow for the depletion of the slowing down density due to the resonance absorption. The model is valid for cluster geometries including those with more than one moderating material.

The basic features of the model were validated by extensive comparisons of each step against more detailed methods. The overall process was demonstrated to have a precision of better than 1% of total resonance captures for a range of systems when compared to detailed Monte Carlo calculations using the identical cross-sections used to generate the WIMS library for a range of moderators, fuel mixtures and geometries as shown in Table 4 below, reproduced from Reference 9.

Table 4

Comparisons of WIMS Resonance Captures
in U238 with MOCUP and SDR Results
Resonance Regions:
5.53 keV to 4 eV for Comparison with MOCUP
75.5 eV to 4 eV for Comparison with SDR

Lattice description	Method of calculation		
	WIMS	MOCUP	SDR
Light water and 3% UO2 regular rod array. Volume ratio 1:1 As above	0.2136 0.1859	0.2122 ± 0.0014	0.1850
Light water and 3% UO2 regular rod array. Volume ratio 4:1 As above	0.07268 0.06269	0.0720 ± 0.0006	0.06117
Heavy water and 3% UO2 regular rod array. Volume ratio 4:1 Graphite and 1.6 Co metal rod array. Volume ratio 12.7:1	0.3328 0.3308	0.3302 ± 0.0016 0.3315 ± 0.0017	
21 rod cluster, 3% UO2 air cooled and graphite moderated	0.1161	0.1167 ± 0.0014	
19 rod cluster, natural UO2 air cooled and D2O moderated	0.1681	0.1696 ± 0.002	
28 rod cluster, natural UO organic cooled and D2O moderated	0.1204	0.1193 ± 0.002	
74 rod cluster, 1.3% UO2, H2O cooled and D2O moderated	0.1220	0.1229 ± 0.002	
U238/H regular slab array, N238.t _f = 0.008489, N _H .t _m = 0.048506	0.1055		0.1051
U238/H regular slab array, N238.t _f = 0.002472, N _H .t _m = 0.007705	0.1866		0.1874
U238/H regular slab array, N238.t _f = 0.009391, N _H .t _m = 0.007705	0.3294		0.3302

More recently an alternative method of determining effective resonance data, based upon sub-group arguments, has been developed and tested (10). The advantages of this is its ability to model rather general geometries, including parts of pins (for example, distinguishing the outward facing skin in an edge pin where the Plutonium build-up will be greater). This model is regarded as very promising for engineering applications, but post-dates the results reported here.

4. Comparisons with Hellstrand Correlation

Although comparison with measurements of relative conversion ratio in lattice configurations probably provide the most reliable evidence of the adequacy of resonance data for U^{238} , further checks are provided by Hellstrand's integral experiments. These experiments have been designed to provide a direct measure of resonance integral (ie resonance capture resulting from a $1/E$ -source) and thus the resulting correlation should in principle be appropriate for direct comparison with the WIMS library.

In practice some difficulties in detail arise in making the comparison. Hellstrand's own experimental results have been modified (11) to take into account the results from other integral experiments. The resulting best fit formulae for the energy range 0.55 eV - 2.0 Mev are:

U-Metal Rods

$$RI = 4.25 + 26.8 \sqrt{S/M}$$

U-Oxide

$$RI = 5.60 + 26.3 \sqrt{S/M}$$

We note that Hellstrand's original interpretation of his measurements on metal rods was subsequently adjusted upwards by about 4.1% in the light of later results.

The resonance integrals in the WIMS library were deduced from SDR calculations of resonance captures by using the basic formula derived in Ref (7),

$$\sum_a^g = \frac{N_g I_g^g}{\tau_g - \frac{N_g I_g^g}{\sum_p}}$$

where \sum_a^g is the group effective absorption cross-section, I_g^g and N_g the group shielded resonance integral and number density of U^{238} respectively, \sum_p is the potential scattering cross-section of U^{238} with admixed hydrogen in the SDR calculation, and τ_g the group lethargy width. This is a general approximation appropriate to all types of moderators, which is also invoked within WIMS to relate effective cross-sections to the tabulated resonance integrals. Thus cancelling effects are likely to occur if any error is associated with deducing resonance integrals from the SDR calculations using it. On the other hand, for the purposes of a comparison with Hellstrand's correlations, it is questionable whether the classical exponential formula

$$p = 1 - c = \exp\left(-\frac{\tau}{\sum_p}\right)$$

which is exact for mixtures of hydrogen and an infinite mass absorber should be preferred. In practice it is found that for large values of σ_p the two formulae give the same numerical values. The difference becomes just noticeable at low σ_p values, thus at $\sigma_p = 16$ barns the use of the exponential form reduces the inferred resonance integral by 0.3 barns. The results discussed in the following comparison all refer to use of the WIMS equation.

Hellstrand's correlation being given in terms of S/M, the surface to mass ratio, it is necessary to relate this ratio to the σ_p basis of the WIMS library. In order to relate σ_p to S/M we are obliged to use the WIMS equivalence principle.

$$\sigma_p = \frac{a}{N_0 \bar{l}} + \sum_i \lambda_i \sigma_{pi}$$

where a is the Bell factor, N_0 is the number density of U^{238} atoms, \bar{l} is the mean chord of the rod ($2r_0$), σ_{pi} is the potential scattering cross-section of an admixed element i in the fuel, and λ_i is the Goldstein-Cohen factor for intermediate resonance effects. The currently recommended values* of λ and σ_p for U^{238} in the WIMS library are 0.2 and 10.636 barns, while for oxygen the appropriate values (18) are 0.94 and 3.7 barns. The summation terms in Eq. (6) give 2.13 barns for U-metal and 9.08 barns for U-oxide. The Bell factor 'a' is itself a weak function of σ_p , and should be evaluated using the universal curve given in Ref. 8. The appropriate relationship with S/M obtained is

$$\sigma_p = \frac{aA}{4A_v} S/M + \sum_i \lambda_i \sigma_{pi}$$

where A_v is Avogadro's number and A the molecular weight.

The high-energy spectrum which is pertinent to Hellstrand's experiments is in some doubt. Simulation of the lattice conditions in the measurements by a WIMS calculation (2) suggests that the spectrum cut-off lies in the range 100-500 keV. Various calculated spectrum corrections have been made to the sets of measurements underlying the best fit correlations in order to give the proper $\frac{1}{E}$ -integral up to 2.0 MeV (see Ref. (11)). The uncertainty in resonance integrals arising from the correction appears to be about $\pm 2\%$ and the total uncertainty from all causes is quoted by Hellstrand as $\pm 3.5\%$.

The results of the comparison are shown in Table 5.

The ranges over which the correlations were actually fitted are marked '[]' in the table. In the central portion of these ranges we see that the WIMS resonance integrals are about 1% higher than the U-oxide correlation and about 4% lower than the U-metal correlation. There appears to be about 5% discrepancy

*An exact value for σ_p for U^{238} is not necessary since provided the other aspects of the equivalence theorem are valid, this parameter merely serves as a link to the appropriate SDR homogeneous calculation.

between the two correlations, although this is probably within the claimed accuracies for the correlations (the consistency would be improved by returning to Hellstrand's older interpretation of his U-metal experiments). Since for the application to power reactor lattices we are concerned with oxide fuels, we see that the conclusions deduced from relative conversion ratio measurements are in excellent agreement with the appropriate Hellstrand correlation.

Table 5

Comparison of WIMS Resonance Integrals
(-0.7b Corrected Set)
with Hellstrand Correlations

ρ_p	WIMS RI	Oxide Rods			Metal Rods		
		S/M	Hellstrand RI	WIMS error	S/M	Hellstrand RI	WIMS error
15.53	12.95	0.0538	11.70	+ 1.25	0.1190	13.50	- 0.55
31.49	17.10	0.1776	16.68	+ 0.42	0.2573	17.84	- 0.74
53.40	21.28	0.3457	21.06	+ 0.22	0.4474	22.18	- 0.90
65.34	23.19	0.4373	22.99	+ 0.20	0.5516	24.15	- 0.96
146.2	33.05	1.0548	32.61	+ 0.44	1.2572	34.30	- 1.25
251.3	43.14	1.9402	42.23	+ 0.91	2.2615	44.55	- 1.41
1000	81.37	7.6225	78.21	+ 3.16	8.7074	83.33	- 1.86
3600	141.96	27.6225	143.82	- 1.86	31.3950	154.41	- 12.45

Comparisons have also been made between the WIMS prediction of temperature broadening and the inferred values of β from hot experiments, where β is defined by

$$RI(T) - \delta = (RI(T_0) - \delta) [1 + \beta(\sqrt{T} - \sqrt{T_0})]$$

δ is the "1/v" portion of the resonance integral above 0.55 eV, and T and T_0 are expressed in $^{\circ}K$. The results are given in Table 6. Over the ranges of the measurements the agreement between WIMS and experimental β -values is very good, with WIMS showing a tendency to a small over-prediction.

Table 6
 Comparison of $\beta \times 10^2$ for U-Oxide and U-Metal Rods

WIMS	Oxide Measurements				Metal Measurements			
	S/M	Hellstrand et al	Pettus et al	Pelovitch and Frantz	S/M	Hellstrand et al	Pettus et al	Pelovitch and Frantz
0.59	0.050	0.59	0.54	-	0.118	0.57	0.52	-
0.69	0.173	0.67	0.62	-	0.257	0.64	0.60	0.53
0.80	0.341	0.75	0.70	0.69	0.448	0.73	0.72	-
0.85	0.433	0.80	0.75	0.59	0.552	0.78	0.78	-
1.06	1.055	1.11	1.06	-	1.258	1.14	1.20	-
1.31	1.941	1.55	1.50	-	2.263	1.64	1.80	-
1.63	7.623	4.39	3.89	-	8.709	4.86	5.65	-

The original comparison of WIMS data against Hellstrand results, reported in Reference ² was for a metal sample, and showed good agreement with basic resonance parameters (unmodified data). We see that this is consistent with our data here. The inconsistency appears to arise between the metal and oxide results, despite the demonstrated capability of the WIMS model to reproduce the change from metal to oxide consistently by comparison with Monte Carlo results, and to fit integral experiments on both systems with a single data modification.

We conclude that the Hellstrand "world-best" correlations for oxide are consistent with our other integral observation, whilst those for metal differ by an amount of the same order as the 3.5% uncertainty ascribed to them.

5. Evidence from Zero Power Measurements

5.1 Reactivity measurements

Chawla has summarized the evidence obtained for a wide range of systems analysed using WIMS. We reproduce below the reactivity results for various sets of these when using the basic WIMS data reduced by approximately 5%. (The actual model used is described in Appendix I, and corresponds to a uniform 0.1 barn reduction in cross-section. It corresponds more closely to a reduction of 0.7 barns in resonance integral at all rod sizes than to a constant percentage).

Table 7

"Best-Value" WIMS Reactivity
Estimates for Single-Rod Lattices

Lattice	Fuel/Moderator	(ν_m/ν_f)	k	keff
Wur 8	Nat. U/D ₂ O	19.4	1.143	0.991
Wur 12	Nat. U/D ₂ O	44.8	1.221	0.987
Wur 16	Nat. U/D ₂ O	80.5	1.211	0.985
SRL 1-7-I	Nat. U/D ₂ O	53.1	1.229	0.989
SRL 1-8-I	Nat. U/D ₂ O	71.1	1.230	0.990
SRL 1-9-II	Nat. U/D ₂ O	95.2	1.222	0.993
SRL 1-12-F	Nat. U/D ₂ O	161.5	1.182	0.991
R1/100H	3% en.U/H ₂ O	1.00	1.260	1.000
R2/100H	3% en.U/H ₂ O	3.16	1.328	0.993
R3/100H	3% en.U/H ₂ O	0.78	1.212	1.000
BICEP 76	Nat. U/C	76.7	1.059	0.994
BICEP EMR 24/5	1.2% en U/C	26.8	1.172	0.997

The 4 sets of experiments are:

Wurenlingen natural uranium rods of 10 mm diameter at various square pitches in D_2O moderator

Savannah River similar fuel in critical assemblies on a hexagonal pitch

Winfrith R/100H series of 3% enriched oxide pins in light water

Winfrith natural and slightly enriched metal fuel in graphite - part of the sequence reported in Reference 1.

It will be seen that the variations of reactivity with pitch - and hence with resonance capture - reported in the earlier study have been removed by the data changes proposed here. A further illustration is provided in Figure 3 from Reference 5 which shows Brookhaven exponential experiments on Uranium metal fuel in light water analysed with and without the modified U-238 data.

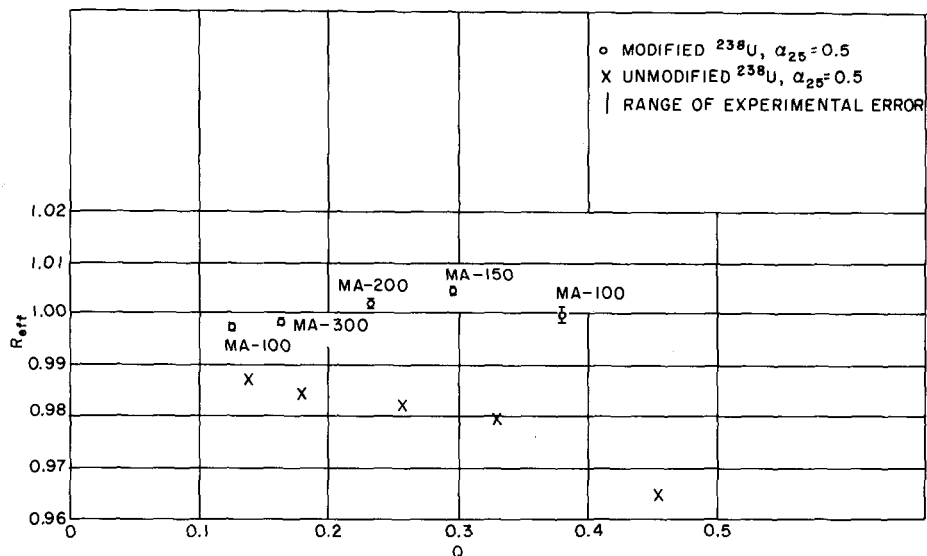


Figure 3. Plot of Reactivities Predicted by Two Data Options in WIMS for BNL Exponential Experiments with Uranium Metal.

5.2 Relative conversion ratio measurements

The technique of measuring Relative Conversion Ratio has been developed to a very high degree, and it is now believed that accuracies better than 1% can be achieved. Although most measurements undertaken at AEE Winfrith have been in the geometrically more complex SGHW and HTR systems, one series of regular light water lattices has been measured. The results are shown in Table 8 below.

Table 8
Influence of U^{238} Resonance Data on
Predicted RCR'S in Winfrith Lattices

Core Designation	H_2O/UO_2 Vol. Ratio	RCR		
		Exp.	WIMS	
			8% corr.*	4% corr.+
SS1/100H	4:1	2.040 ± 0.03	2.035	2.057
SS3/100H	2.6:1 (triangular pitch)	2.497 ± 0.03	2.476	2.511
R1/100H 20°C	1:1	4.158 ± 0.03	4.103	4.203
R1/100H 80°C	1:1	4.263 ± 0.05	4.212	4.305
R3/100H	0.78:1	4.789 ± 0.05	4.741	4.873

* hydrogen scattering cross-section normalised to 20.0 barns

+ hydrogen scattering cross-section normalised to 20.3 barns

It will be seen that the 0.1 barn (approx 4%) corrected set of data which reproduces the change in reactivity with pitch gives consistently good results, although a rather larger correction would be even better:

The same set of data have been applied to HTR lattices where, as has been noted, there is double heterogeneity, the spherical fuel kernel being packed into cylindrical or annular pins. Tables 9 and 10 show that both the effect of variations in kernel size and packing density and the effect of temperature changes up to 400°C are well reproduced, although again the reduction of 0.1 barn (approximately 2-3% of resonance integral in these lattices) is not sufficient to give a best fit.

For SGHW cluster lattices the coolant inside the cluster of pins may be varied. A typical sequence going from air-filled to water-filled cluster, via an intermediate state of mixture of heavy and light water in roughly equal proportions to give the equivalent of operating water density, is reported by Chawla (6) and shown below using the 0.1 b reduced cross-section set.

Table 9
 Comparison Between Measured and Calculated RCR
 for Different Particle and Lattice Dimensions

Kernel diameter (μ)	544	544	544	800	803	803	803	806	822	806
Particle diameter (μ)	970	970	970	1180	1200	1200	1200	1666	1120	1666
Heavy metal density in fuel zone (gm/cm^3)	0.95	0.95	0.95	1.58	1.52	1.52	1.52	0.5	2.5	0.5
N_c/N_u in lattice	270 ^a	270	610	360	164	164 ^b	175 ^c	470	100	470 ^a
RCR measured	4.591 \pm 0.028	3.968 \pm 0.024	2.486 \pm 0.015	2.900 \pm 0.020	4.880 \pm 0.029	5.243 \pm 0.036	4.861 \pm 0.028	3.856 \pm 0.023	6.117 \pm 0.037	3.682 \pm 0.022
RCR Theory/Experiment	0.987 \pm 0.006	1.012 \pm 0.006	1.003 \pm 0.006	1.005 \pm 0.007	1.014 \pm 0.006	1.010 \pm 0.007	1.014 \pm 0.006	1.001 \pm 0.006	0.996 \pm 0.006	1.018 \pm 0.006

NOTES: a Non-asymptotic lattice
 b Fuel with Cu inserts
 c Fuel with graphite inserts

Table 10
Effect of Temperature on RCR Comparisons with Theory

Reactor	No. of Fuel Channels in Heated Zone	Temperature (°C)	RCR Measured	RCR Theory/Experiment
HECTOR	8	45	4.444 ± 0.044	1.003 ± 0.010
		428	5.291 ± 0.053	1.003 ± 0.010
HECTOR	85	20	4.942 ± 0.050	1.010 ± 0.010
		425	5.346 ± 0.050	1.013 ± 0.010
ZENITH	324	18	5.770 ± 0.040	1.015 ± 0.007
		373	6.525 ± 0.030	1.010 ± 0.005

Table 11

Relative Conversion Ratio for SG3 Lattices

Coolant	Relative Conversion Ratio	
	Calculated	Measured
Air	1.978	1.987 \pm .017
Mixture	1.872	1.894 \pm .019
Water	1.694	1.707 \pm .018

These results are broadly in line with the much wider study undertaken by Kenshell (17) in which he includes a range of Canadian cluster lattices ranging from 7 to 28 pins having air, heavy water and organic coolants. The conclusion of this study was that the originally proposed 0.2 barn reduction in the resonance cross-section was a slight over-estimate of the required correction.

Over all systems it was concluded that the smaller reduction of 0.1 barns in cross-section ($\sim 0.7b$ in resonance integral) gave the best fit to experiment.

6. Comparisons with Isotopic Composition Data from Power Reactors

The WIMS U^{238} data with the approximate 4% correction of resonance integrals (ID 3238.5) is normally the preferred option used in design calculations for LWR's. Halsall has completed an LWR-WIMS evaluation of the isotopic depletion of fuel discharged from the Yankee-Rowe reactor which gives good agreement with the measured Pu/ U^{238} discharge composition. The comparison between measurement and prediction for both the 4% and 8% corrected data is shown in Fig 1, which indicates a preference for the smaller correction. Also shown in Fig 1 are the LASER results which indicate that the combination of resonance cross-sections and shielding factors used in the MUFT section of LASER are equivalent* to a resonance integral some 3% lower than the WIMS 4% corrected data.

Further evidence on the preference on resonance integrals is obtained from WIMS analysis of the isotopic depletion of the Canadian NPD and Winfrith SGHW Reactors. Although the moderation by heavy water in these reactors could lead to some systematic differences relative to observations in LWR's, the results should still be useful from the standpoint of establishing absolute resonance integral data. The NPD results associated with 8% corrected U^{238} data

*The broad assumption has been made that the principal difference between WIMS and LASER characteristics lies in the conversion ratio, since both codes obtain quite good agreement on the composition of the plutonium produced.

Table 12

Comparison of WIMS Isotopic Compositions
for NPD Bundle 2
(Burnup 39600 MWD/TelU)

Isotopic Ratio	Centre Pin			Middle Pins			Outer Pins			Cluster Average		
	Expt.	WIMS Error %		Expt.	WIMS Error %		Expt.	WIMS Error %		Expt.	WIMS Error %	
		Data Set 1	Data Set 3		Data Set 1	Data Set 3		Data Set 1	Data Set 3		Data Set 1	Data Set 3
$U^{235}/U^{238} \%$	0.2109	- 4.3	- 4.2	0.1879	- 3.2	- 3.1	0.1275	+ 2.8	+ 2.9	0.1510	0.0	0.0
$U^{236}/U^{238} \%$	0.0787	+ 2.6	- 2.0	0.0816	+ 2.3	- 2.3	0.0894	+ 1.0	- 3.7	0.0864	+ 1.4	- 3.2
Pu/U %	0.385	+ 2.8	+ 4.4	0.402	+ 0.9	+ 2.5	0.453	+ 0.2	+ 1.7	0.433	+ 0.6	+ 2.1
Pu^{239}/Pu	0.6657	- 0.1	0.0	0.6496	0.0	0.0	0.6021	+ 0.8	+ 0.9	0.6181	+ 0.7	+ 0.7
Pu^{240}/Pu	0.2732	- 0.6	- 0.7	0.2852	- 1.4	- 1.4	0.3064	- 1.3	- 1.2	0.2986	- 1.3	- 1.3
Pu^{241}/Pu	0.4705	+ 2.1	+ 1.8	0.5096	+ 1.3	+ 1.0	0.6334	- 0.6	- 0.8	0.5895	0.0	- 0.3
Pu^{242}/Pu	0.1400	+ 7.9	+ 7.4	0.1694	+ 4.5	+ 4.0	0.2818	- 2.8	- 3.2	0.2422	- 1.2	- 1.5

$$\text{WIMS Error \%} = \frac{\text{WIMS-EXPT.} \times 100}{\text{EXPT.}}$$

Table 13

Comparison of WIMS Isotopic Compositions
for SCWR Cluster LO9
(Burnup ~7285 MWD/TeU)

Isotopic Ratio	Inner Ring			Middle Ring			Outer Ring			Cluster Average		
	Expt.	WIMS Error %		Expt.	WIMS Error %		Expt.	WIMS Error %		Expt.	WIMS Error %	
		Data Set 1	Data Set 3		Data Set 1	Data Set 3		Data Set 1	Data Set 3		Data Set 1	Data Set 3
$U^{235}/U^{238} \%$	1.107	+ 0.8	0.8	1.045	- 0.4	- 0.4	0.850	- 0.1	- 0.2	0.958	0.0	0.0
$U^{236}/U^{238} \%$	0.102	+ 2.0	- 0.6	0.114	+ 0.5	- 2.2	0.140	+ 1.8	- 1.1	0.111	+ 1.4	- 1.4
$Pu/U^{238} \%$	0.324	- 2.5	- 1.1	0.327	+ 0.0	+ 1.6	0.378	- 1.7	- 0.4	0.352	- 1.4	+ 0.6
Pu^{239}/Pu	0.820	+ 1.4	+ 1.4	0.797	+ 1.4	+ 1.4	0.747	+ 0.4	+ 0.4	0.775	+ 0.6	+ 0.6
Pu^{240}/Pu	0.136	- 4.6	- 4.7	0.153	- 3.7	- 3.8	0.186	+ 0.3	+ 0.2	0.168	- 1.2	- 1.2
Pu^{241}/Pu	0.0408	- 14.1	- 14.1	0.0459	- 12.8	- 12.6	0.0579	- 5.5	- 5.2	0.0515	- 8.3	- 8.0
Pu^{242}/Pu	0.0035	- 10.9	- 10.9	0.0047	- 7.6	- 7.4	0.0088	- 1.9	- 1.5	0.0066	- 2.1	- 1.7

$$\text{WIMS Error } \% = \frac{\text{WIMS-EXPT.}}{\text{EXPT.}} \times 100$$

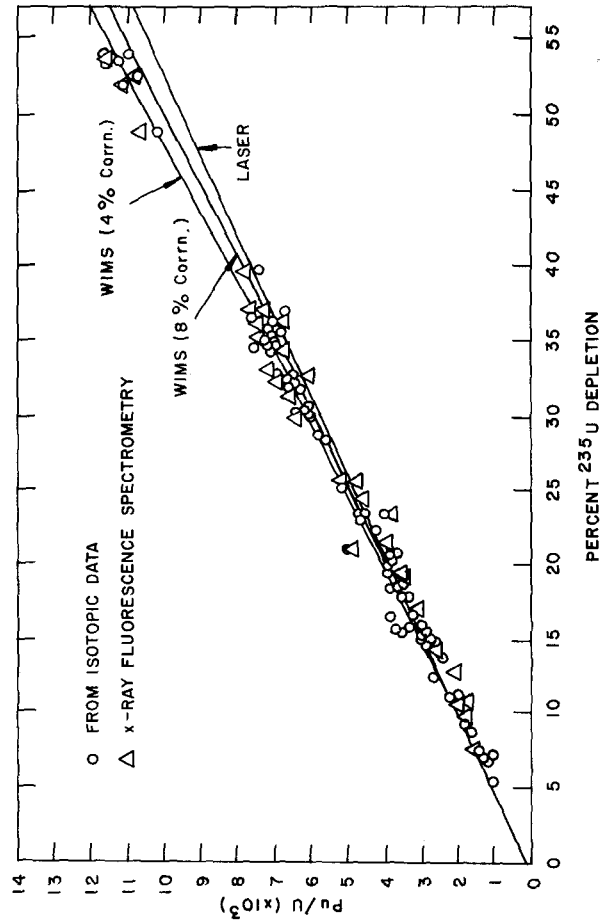


Figure 1. Plutonium-to-Uranium Ratio as a Function of ²³⁵U Depletion in Yankee Pwr.

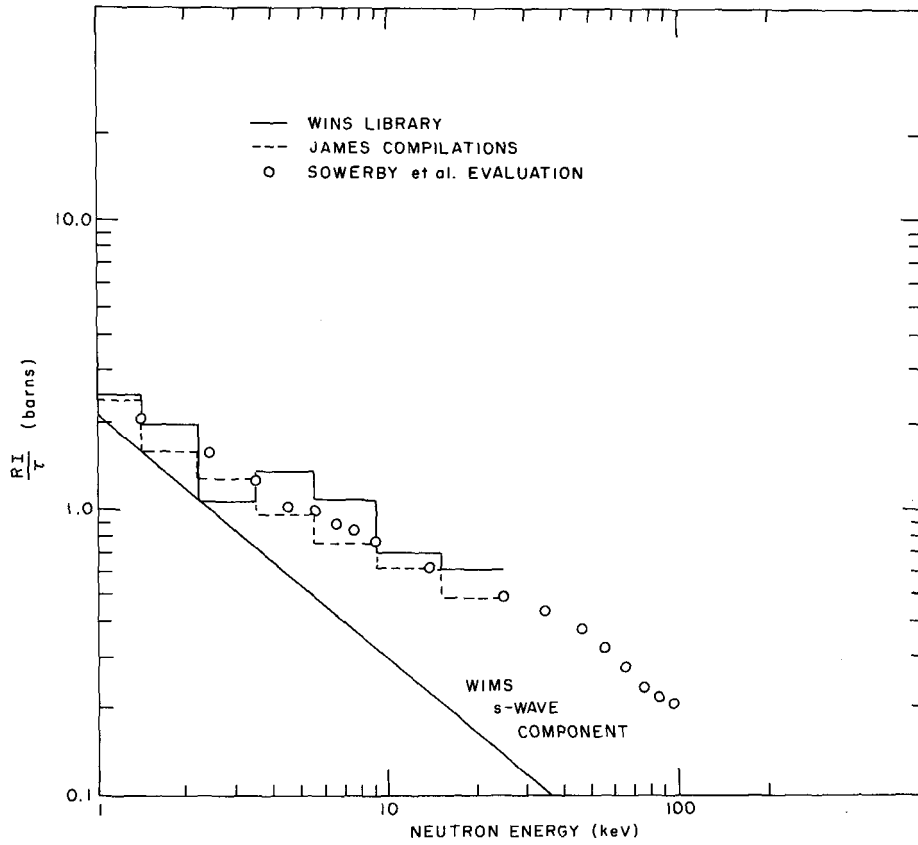


Figure 2. Comparison of WIMS Library Cross-Sections with Recent Evaluations.

which also shows the results associated with use of the 4% option. We see that with the latter the plutonium production is too high by about 2%. The equivalent results for SGHWR were discussed in Ref (10) and are given in Table 5, which indicates that the conversion ratio associated with the 4% modification is slightly too high by approximately 0.6%. Thus we find that although the 4% corrected U^{238} data essentially satisfied both the RCR's under cold conditions and the isotopic depletion in Yankee and SGHWR, the conversion ratio implied by the Pu/U ratio in the NFD reactor requires a somewhat larger correction than 4%. This lack of consistency in results remains to be resolved at the present time, although it is possible that systematic errors in the measurements could be contributing to the difficulty. It is noticeable that the preference towards 8% corrected data becomes stronger as the power reactor spectrum softens, which might be taken to imply an error in the U^{238} thermal cross-section. However the large range of spectra in cold lattices for which good agreement has been obtained on RCR measurements militates against an error in thermal cross-section. On balance the 4% correction to resonance integrals is preferred for all types of WIMS calculations.

7. Effect of Variations in Conversion Ratio on Cycle Length

Calculations on typical light water reactor lattices show that changes in resonance capture have a rather similar effect on cycle length and plutonium discharge for both PWR and BWR systems. Typically our 0.1 barn cross-section reduction (4% in resonance integral) will increase cycle length by 3.7% and reduce Plutonium concentration at a given discharge irradiation (30,000 MWD/Te) by 3.5%.

8. Summary and Conclusions

Since the original discussion of discrepancies between differential and integral data a large number of additional experiments have been studied, especial attention being paid to the determination of relative conversion ratio. Additional information on isotopic composition has become available for different types of reactor.

Changes to other data - especially the epithermal capture integral in Uranium²³⁵ - have reduced the magnitude of the discrepancy observed, from 10-15% in resonance integral down to 4-6% which is now seen to cover the majority of observations.

The Hellstrand correlations for resonance integral have an associated uncertainty of $\pm 3.5\%$ which is rather high for our purpose. The oxide data are, however, in good agreement with the position deduced here, whilst the metal data are slightly outside the range preferred.

In the differential data field it has become accepted that the resonance capture width may vary from resonance to resonance. Once it is not acceptable to average measurements over a large number of resonances the accuracy of determination is no longer adequate for thermal reactor applications. The dominant effect of the lowest (6.7 eV) resonance - which is much the most difficult to measure - gives expected overall precisions only of the order of $\pm 8\%$, and it is therefore no longer appropriate to regard the difference between integral and differential data as a discrepancy. The one remaining problem

in this area is that most proposed routes to change the resonance integral by varying capture widths change the infinitely dilute integral by an unacceptable amount, and it would be encouraging to have an alternative model for the changes.

We therefore conclude that an adjusted set of resonance data for Uranium²³⁸, used in conjunction with up to date data for other nuclides is capable of predicting observed results on a wide range of reactor designs. The majority of results fall within $\pm 2\%$ consistent with a standard deviation of the order of 1% - 1.5%.

(Note added in proof. It appears that ENDF B III and IV data lead to resonance integrals 0.5 barns higher than the 'uncorrected' values used in this paper, and thus the discrepancy would be greater using this data source.)

APPENDIX 1

Approximate influence on Resonance Integral
from a uniform shift in differential cross-sections (J. R. Askew)

We assume that the constant shift in cross-section to be introduced is $\Delta\sigma$, then the resonance integral shifts from

$$I = \int \frac{\sigma_a \sigma_p}{\sigma_a + \sigma_p} \frac{dE}{E}$$

to

$$I' = \int \frac{(\sigma_a + \Delta\sigma) \sigma_p}{(\sigma_a + \Delta\sigma + \sigma_p)} \frac{dE}{E}$$

$$= \frac{\sigma_p}{\sigma_p + \Delta\sigma} \left\{ I(\sigma_p + \Delta\sigma) + \Delta\sigma \left(\tau - \frac{I(\sigma_p + \Delta\sigma)}{\sigma_p + \Delta\sigma} \right) \right\}$$

Now if we take $I \approx I_0 \sigma_p^{-\frac{1}{2}}$, we obtain

$$\Delta I = I' - I = \frac{\sigma_p}{\sigma_p + \Delta\sigma} \frac{I_0 \sqrt{\sigma_p + \Delta\sigma}}{\sigma_p + \Delta\sigma} \left\{ 1 - \frac{\Delta\sigma}{\sigma_p + \Delta\sigma} \right\}$$

$$- I_0 \sqrt{\sigma_p} + \frac{\Delta\sigma \sigma_p}{\sigma_p + \Delta\sigma} \tau$$

If $\frac{\Delta\sigma}{\sigma_p}$ is small, then expanding gives

$$\Delta I = \sqrt{\sigma_p} I_0 \left\{ 1 - \frac{3\Delta\sigma}{2\sigma_p} - 1 \right\} + \Delta\sigma \tau \left(1 - \frac{\Delta\sigma}{\sigma_p} \right)$$

Hence

$$\frac{\Delta I}{\tau} = \Delta\sigma \left(1 - \frac{3I(\sigma_p)}{2\sigma_p \tau} \right)$$

APPENDIX 2

RESOLVED RESONANCE PARAMETERS FOR U ²³⁸ IN JAMES' COMPILATION						
ENERGY(eV)	$g\Gamma_n$ (meV)	Γ_T (meV)	ENERGY(eV)	$g\Gamma_n$ (meV)	Γ_T (meV)	
6.65±.10	1.40±.05		397.39±.35	6.0±.5	22.±6.	
10.22±.10	.0018±.0008		407.64±.36	.08±.03		
19.50±.10	.0014±.0007		410.18±.36	19.±2.	18.±2.	
20.90±.10	8.5±.8	24.±2.	433.70±.40	8.8±1.0	20.±2.	
36.80±.07	38.±2.	23.±2.	439.7±.4	.16±.04		
45.19±.07	.0020±.0015		454.1±.4	.40±.10		
63.54±.07	.006±.003		462.8±.4	4.6±.5		
65.10±.15	28.±2.	21.±2.	477.0±.4	3.0±.5		
72.46±.07	.001±.001		485.4±.4	.03±.03		
74.67±.07	.001±.001		488.2±.5	.45±.05		
80.70±.07	1.7±.2		488.9±.5	.08±.04		
83.57±.07	.004±.002		518.27±.25	49.±5.	24.±2.	
85.06±.07	.001±.001		523.21±.25	.20±.07		
89.19±.07	.09±.01		527.43±.25	.03±.03		
99.19±.07	.001±.001		535.21±.25	45.±5.	23.±2.	
102.47±.09	73.±4.	28.±3.	542.34±.27	.05±.03		
111.27±.09	.001±.001		555.90±.30	.80±.25		
116.82±.11	37.±3.	20.±2.	579.87±.30	41.±4.	21.±2.	
121.61±.11	.006±.003		584.80±.31	.05±.04		
124.30±.12	.012±.005		592.10±.31	.05±.04		
127.32±.13	.004±.002		594.84±.31	85.±5.	20.±2.	
145.57±.15	.90±.05		606.12±.34	.25±.08		
152.42±.17	.04±.02		619.75±.35	28.±3.	19.±2.	
158.89±.18	.007±.003		624.80±.35	1.0±.2		
160.65±.18	.005±.003		628.29±.35	5.2±.5		
165.21±.19	3.1±.4	18.±5.	660.9±.4	138.±15.	23.±3.	
173.11±.21	.025±.012		668.4±.4	.25±.08		
177.38±.22	.001±.001		677.5±.4	.70±.25		
182.03±.22	.003±.002		692.9±.4	42.±5.	22.±2.	
189.80±.23	188.±15.	27.±3.	707.9±.4	19.±2.	21.±2.	
196.14±.24	.001±.001		712.4±.4	.25±.15		
198.57±.24	.003±.002		720.9±.4	1.3±.2		
200.54±.24	.008±.003		728.4±.4	.7±.2		
202.30±.24	.04±.02		732.5±.4	1.0±.2		
208.49±.25	62.±5.	22.±4.	743.2±.4	.3±.3		
214.97±.28	.04±.02		756.0±.5	.45±.15		
218.04±.28	.010±.005		764.8±.5	8.0±1.0	18.±2.	
237.20±.16	35.±4.	24.±3.	778.8±.5	1.8±.2		
242.60±.17	.15±.03		790.4±.5	.60±.4		
253.88±.18	.10±.03		808.2±.5	.4±.2		
255.37±.18	.06±.03		815.3±.5	.20±.10		
257.10±.19	.92±.01		820.9±.5	62.±7.	20.±2.	
263.91±.19	.25±.04		832.4±.5	.25±.10		
273.56±.20	28.±3.	23.±3.	846.9±.5	1.0±.3		
275.76±.20	.08±.06		850.6±.5	55.±5.	23.±2.	
282.29±.21	.06±.03		856.1±.5	81.±7.	23.±2.	
291.01±.21	17.±2.	22.±3.	866.0±.5	5.0±.5		
294.96±.22	.03±.02		888.6±.5	.15±.15		
311.13±.25	1.05±.10		890.6±.5	.8±.2		
337.19±.26	.05±.02		904.5±.3	49.±3.	22.±2.	
347.74±.28	85.±7.	28.±4.	909.5±.3	1.3±.3		
351.75±.30	.06±.03		924.5±.3	2.0±.8	28.±3.	
354.66±.30	.05±.03		932.3±.3	.3±.2		
377.05±.32	.50±.10		936.6±.3	144.±12.	25.±2.	

ENERGY(eV)	g_n^{Γ} (meV)	Γ_T (meV)	ENERGY(eV)	g_n^{Γ} (meV)	Γ_T (meV)
940.1±.4	.3±.2		1565.1±.4	4.5±1.5	
958.0±.4	203.±20.	21.±2.	1597.5±.5	375.±25.	20.±4.
964.9±.4	.20±.10		1622.3±.5	70.±14.	19.±3.
976.8±.4	.6±.3		1637.4±.5	50.±8.	19.±3.
985.6±.4	.3±.2		1646.1±.5	1.0±.5	
991.4±.4	390.±25.	30.±5.	1662.0±.5	170.±20.	24.±4.
1000.5±.4	.10±.05		1688.3±.5	92.±10.	19.±3.
1005.9±.4	.10±.05		1709.0±.5	80.±8.	28.±5.
1010.5±.4	1.5±.5		1722.2±.5	15.±2.	
1014.4±.4	1.6±.5		1744.9±.5	2.0±.4	
1022.9±.4	8.2±1.5		1755.2±.5	90.±10.	27.±4.
1028.6±.5	2.5±1.0		1782.1±.5	655.±80.	
1031.1±.5	1.0±.6		1797.5±.5	3.0±1.0	
1054.0±.5	89.±8.	27.±2.	1807.9±.5	14.5±3.5	17.±5.
1062.3±.5	.7±.3		1845.5±.5	13.±5.	15.±5.
1067.6±.5	1.0±.6		1868.0±.5	4.±2.	
1071.0±.5	.3±.3		1902.4±.5	34.±4.	19.±4.
1081.1±.5	.7±.3		1912.6±.5	.5±.3	
1094.4±.5	1.3±.5		1916.5±.5	25.±3.	19.±5.
1098.1±.5	17.±3.	22.±3.	1953.4±.5	3.0±1.0	
1102.7±.5	2.0±.5		1968.6±.5	665.±120.	30.±10.
1109.9±.5	27.±4.	24.±2.	1974.3±.5	515.±80.	
1131.1±.5	1.8±.6		2022.8±.6	220.±30.	20.±4.
1139.9±.5	220.±20.	23.±2.	2029.8±.6	61.±18.	18.±5.
1147.0±.5	.3±.2		2070.9±.6	.3±.2	
1154.6±.5	.4±.2		2088.1±.6	23.±5.	22.±4.
1166.9±.5	85.±5.	23.±2.	2095.9±.6	13.±3.	
1175.6±.5	60.±5.	22.±2.	2123.8±.6	3.0±1.5	
1194.5±.5	89.±5.	19.±2.	2144.6±.6	62.±8.	15.±5.
1210.5±.5	7.0±.8		2152.2±.6	240.±35.	32.±8.
1217.9±.5	.4±.2		2175.2±.6	1.5±.7	
1237.9±.5	.4±.2		2186.0±.6	620.±80.	29.±7.
1244.9±.5	280.±35.	24.±2.	2200.6±.6	127.±17.	26.±5.
1256.5±.6	.2±.2		2229.3±.6	4.0±1.0	
1266.8±.6	22.±3.	21.±2.	2235.1±.6	4.7±1.0	
1272.7±.6	27.±3.	24.±2.	2258.8±.6	86.±15.	
1298.1±.3	4.5±1.0		2265.9±.7	210.±30.	20.±5.
1316.5±.3	4.0±.8		2281.7±.7	135.±20.	18.±5.
1332.7±.6	1.6±.6		2288.9±.7	.9±.5	
1363.4±.6	1.1±.5		2314.5±.7	21.±4.	
1371.6±.6	.6±.4		2336.9±.7	8.±4.	
1381.6±.6	.6±.4		2352.8±.7	47.±10.	28.±5.
1393.2±.3	162.±20.	28.±3.	2355.3±.7	61.±10.	24.±5.
1405.2±.3	70.±8.	25.±2.	2391.4±.7	26.±4.	
1416.5±.6	.4±.3		2410.8±.7	4.±2.	
1416.3±.3	1.8±.5		2425.7±.7	125.±18.	
1419.2±.3	9.0±1.0		2445.5±.7	195.±25.	
1427.4±.4	33.±4.	26.±3.	2454.8±.7	19.±3.	
1443.5±.4	18.±3.	22.±3.	2488.4±.7	88.±13.	
1473.4±.4	121.±10.	28.±3.	2520.7±.8	8.±3.	
1522.3±.4	240.±15.	30.±7.	2547.2±.8	550.±50.	
1532.3±.4	.4±.3		2558.5±.8	230.±30.	
1545.8±.4	2.5±1.0		2579.9±.8	315.±30.	
1549.8±.4	1.2±.4		2586.5±.8	670.±45.	

Acknowledgements

In the preparation of this paper extensive use has been made of data compiled by F J Fayers, M J Halsall and M J Roth. The conclusions remain the responsibility of the author.

References

1. J G TYROR et al
Resonance Capture Calculations for Gas-Cooled Reactors
Vol II, p 371, Reactor Physics in the Resonance and Thermal Regions.
MIT Press, 1966
2. J R ASKEW
Some Problems in the Calculation of Resonance Capture in Lattices
ibid, p 395.
3. L W NORDHEIM
A program of Research and Calculation of Resonance Absorption
GA-2527, August 1961.
4. F FEINER, L ESCH
Survey of Capture and Fission Integrals of Fissile Materials
(As Ref 1, p 299P)
5. F J FAYERS et al
An Evaluation of Some Uncertainties in the Comparison Between Theory and
Experiment for Regular Light Water Lattices
Journal Brit. Nucl. Energy Soc, 6, 2, April 1967
6. R CHAWLA
An Assessment of Methods and Data for Predicting Integral Properties for
Thermal Reactor Physics Experiments
AEEW - R 797, 1974
7. J R ASKEW et al
A General Description of the Lattice Code WIMS
Jour. Brit. Nucl. Energy Soc, 5, 4, October 1966
8. J R ASKEW
The Calculation of Resonance Captures in a Few-Group approximation
AEEW - R 489, 1966
9. F J FAYERS, G H KINCHIN
Uranium and Plutonium Lattices with Graphite and Water Moderation -
A Comparison of Experiment and Theory
The Physics Problems in Thermal Reactor Design
ENES London 1967, p 15
10. M J ROTH
Resonance Absorption in Complicated Geometries
AEEW - R 921

11. E HELLSTRAND
Measurement of Resonance Integrals
(As Ref 1) p 151
12. M F JAMES
Private Communication
13. Report of the Evaluation Working Group Meeting held on 26-28 January 1972
at AERE Harwell, EANDC 90L
14. M G SOWERBY et al
To be Published
15. F J RAHN et al
Knoxville Conference CONF 710301 Vol 2 p 658, 1971
16. F D BROOKS
Measurements of Alpha and Eta in the Intermediate Energy Range
(As Ref 1, p 193)
17. P B KEMSHELL
Some Integral Properties of Nuclear Data Deduced from WIMS Analysis of
Well Thermalized Uranium Lattices.
AEEW Report R786 1972. See also R549 1969.

ATOMIC ENERGY OF CANADA LIMITED

ANALYSIS OF THE "FOUR-FUEL" EXPERIMENTS USING HAMMER

by

D.S. Craig

The object of this paper is to draw your attention to measurements which have been made by A. Okazaki et.al at Chalk River on a series of 37 element clusters using different fuels— UO_2 , UC, U-Si-Al, and U. The cluster geometry was identical for all fuels, the moderator was D_2O and measurements were made using four different coolants—air, D_2O , H_2O , and HB40 (an organic). The geometry of the cluster is shown in Figure 1. Although it is very complicated, the calculation of reactivity for the air and D_2O lattices depends primarily on the reaction rates in U235 and U238. The absorptions in other materials is small—worth about 50 mk of which 40 mk is in the aluminum pressure and calandria tubes. With H_2O and HB40 coolants, the parasitic absorption increases by about 70 mk. Of interest to the seminar on U238 resonance capture are measurements which have been made of the ratio of captures in U238 to fissions in U235.

I have used the Savannah River Laboratory cell code HAMMER and the ENDF/B-IV data for U235 and U238 to calculate parameters for these lattices. However, before presenting the results, I would like to draw your attention to Tables I and II giving the results I have obtained for the thermal test lattices TRX and MIT, as well as an AECL lattice ZEEP. The latter lattice uses natural uranium rods, 32.57 mm in diameter, clad in aluminum and with a D_2O moderator so that the geometry is particularly simple. It is important to see how well these calculations handle these simple lattices before considering the more complicated 37-element clusters.

The HAMMER values of k_{eff} are low by 9 to 17 mk. In general, the Savannah River Laboratory code RAHAB gives better values. This improvement arises from a better calculation of δ^{28} , the ratio of fission in U238 to that in U235. Values of this ratio were not available from these particular RAHAB runs. However, in Table III, I compare RAHAB and HAMMER calculations for a 7-element cluster. The results are seen to be similar except that RAHAB gives a higher value of δ^{28} . The calculated value of the conversion ratio is high for ZEEP by 2 percent—for the other lattices it is within twice the estimated error. However the calculated value of ρ^{28} , the ratio of epithermal to thermal captures in U238 are all 6-10 percent high.

I have not attempted to calculate the "Four-Fuel" lattices using the cluster geometry. Instead, the calculations were made with the fuel pins being represented by concentric tubes of fuel separated by coolant. Thus, geometric effects may contribute to the trend indicated in Table IV where the ratio of the calculated to experimental values of the conversion ratio are given for these lattices where measurements were available. The experimental values are estimated to be accurate to 1 percent. Also given are k_{eff} and the estimated values of k_{eff} which would be obtained if the resonance integral of U238 were adjusted to make the calculated value of the conversion ratio agree with the experimental value. Because of a 0.1 m^{-2} uncertainty in the buckling measurements and a 1 percent uncertainty in the conversion ratio, this estimated value of k_{eff} is uncertain by about 7 mk.

In general, it appears that errors in the calculated conversion ratios (all high) correlate well with errors in k_{eff} indicating that the absorption rate in U238 is being constantly overestimated for all the fuels, coolants and lattice pitches considered, when using the ENDF/B-IV data files.

On Figure 2 are shown the calculated values of k_{eff} for the complete 32 lattices. Measurements were made at pitches of 245 mm and 310 mm. The results are better for the 310 mm pitch. They also appear better for the H₂O and HB40 coolants. There is also a general trend to get worse as the density of the fuel increases.

Thus the general conclusion is that where the absorption rate in U238 is relatively high (tight pitch, poor coolant moderation, high density fuel) the errors in our estimates become larger.

TABLE I
 A Comparison of Experimental and Calculated Values of Reactivities and Bucklings
 Using ENDF/B-IV Nuclear Data†

LATTICE	PITCH mm	VOLUME RATIO MODERATOR FUEL	k _{eff}			k _∞		B ² m ⁻²		
			EXP.	HAMMER	RAHAB	HAMMER	RAHAB	EXP.	HAMMER	
TRX U-H ₂ O										
	1	18.06Δ	1.000	0.9829	0.9804	1.1665	1.1671	57.00 +1.00	51.04	
2	21.74Δ	4.02	1.000	0.9898	0.9884	1.1583	1.1580	54.69 ±0.36	50.99	
MIT U-D ₂ O										
	1	114.3Δ	20.8	1.000	0.9829	0.9888	1.1547	1.1647	8.48 +0.10	7.55
	2	127.0Δ	25.9	1.000	0.9829	0.9899	1.1839	1.1912	8.56 +0.10	7.82
3	146.05Δ	34.6	1.000	0.9850	0.9916	1.2099	1.2166	8.15 +0.08	7.52	
ZEEP U-D ₂ O	200Δ	40.4	1.000	0.9917	0.9978	1.2244	1.2276	6.95 ±0.06	6.66	

†HAMMER only uses ENDF/B-IV data for U235 and U238

TABLE II

A Comparison of Experimental and Calculated Values of Some Lattice Parameters Using ENDF/B-IV Nuclear Data for U235 and U238

LATTICE	PITCH MM	CAPTURES 28 FISSIONS 25		EPITHERMAL CAPTURES 28 THERMAL CAPTURES 28		EPITHERMAL FISSIONS 25 THERMAL FISSIONS 25		FISSIONS 28 FISSIONS 25	
		EXP	HAMMER	EXP	HAMMER	EXP	HAMMER	EXP	HAMMER
TRX U-H ₂ O									
1	18.06Δ	0.792 ±0.008	0.810	1.311±.020	1.433	0.0981 ±0.001	0.111	0.0914 ±0.002	0.0937
2	21.74Δ	0.646 ±0.002	0.647	0.830±.015	0.882	0.0608 ±0.0007	0.067	0.0667 ±0.002	0.0661
MIT U-D ₂ O									
1	114.3Δ	1.017 ±0.023	0.975	0.498±.008	0.528	0.0447 ±0.0019	0.0520	0.0597 ±0.002	0.0554
2	127.0Δ	0.948 ±0.020	0.921	0.394±.002	0.433	0.031 ±0.003	0.0424	0.0596 ±0.0017	0.0539
3	148.05Δ	0.859 ±0.016	0.865	0.305±.004	0.337	0.0248 ±0.001	0.0327	0.0583 ±0.0012	0.0527
ZEEP U-D ₂ O	200Δ	0.6996 ±0.002	0.718*					0.0676 ±0.0014	0.0642

* Capture 28/absorption 25, for $\Sigma_a(U238)/\Sigma_a(U235)=0.5578$ in a 20° Maxwellian

TABLE III

A COMPARISON OF LATTICE PARAMETERS FOR A 7-ELEMENT
 UO₂ CLUSTER, 220 nm PITCH, CALCULATED USING RAHAB AND HAMMER

k_{∞}	k_{eff} at Exp. B ² of 5.923 m ⁻²	$\frac{\text{CAPTURES U238}}{\text{ABSORPTIONS U235}}$	$\frac{\text{CAPTURES U238}}{\text{NON-THERMAL THERMAL}}$	$\frac{\text{FISSIONS U238}}{\text{FISSIONS U235}}$
--------------	---	--	---	---

USING ENDF/B-III VALUES FOR ALL NUCLIDES IN RAHAB, FOR U235 AND U238 IN HAMMER

HAMMER	1.229	0.976	0.854	0.549	0.0594
RAHAB	1.130	0.982	0.851	0.551	0.0535
EXP		1.000	0.811 ± 0.010		0.0550 ± 0.0015

USING ENDF/B-IV VALUES FOR U235 AND U238 IN HAMMER, AND IV U235 FISSION SPECTRUM

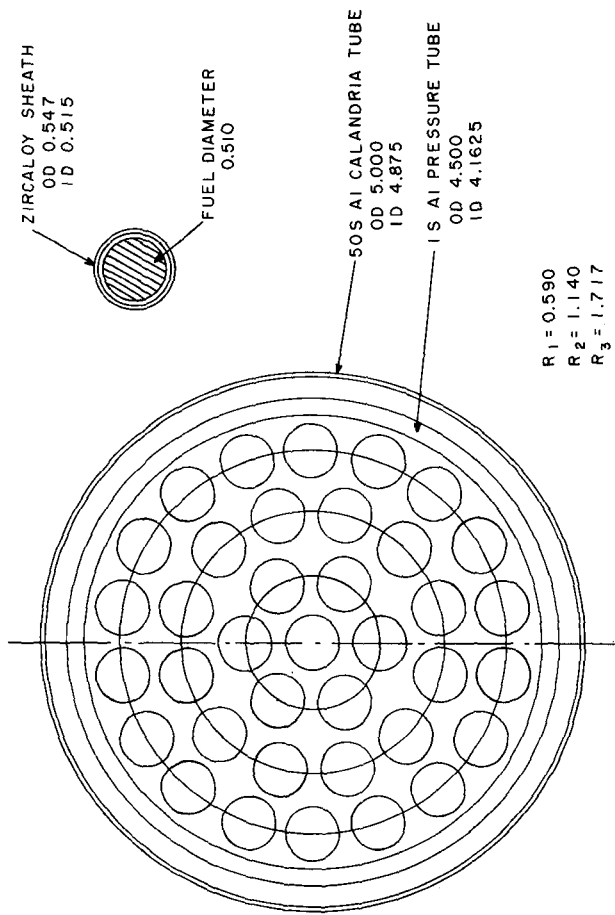
HAMMER	1.139	0.989	0.831	0.530	0.0527
--------	-------	-------	-------	-------	--------

TABLE IV

A COMPARISON OF THE EXPERIMENTAL AND HAMMER CALCULATED
VALUES OF THE REACTIVITY AND THE CONVERSION RATIO FOR
SOME OF THE FOUR FUEL LATTICES

FUEL	LATTICE		Δ PITCH IN MM	γ † CAL/EXP	k_{eff}^* ΔT EXP B ²	ESTIMATES k_{eff} FOR CAL/EXP VALUES OF γ EQUAL TO 1
	FUEL	COOLANT				
UO ₂	AIR		245	1.044	0.980	0.988±.007
			310	1.005	0.987	0.989
D ₂ O			245	1.058	0.971	0.993
			310	1.040	0.983	0.999
H ₂ O			245	1.029	0.992	1.004
			310	1.038	0.993	1.010
UC	AIR		310	1.015	0.982	0.986
	HB40		310	1.025	0.986	0.994
U-Si-Al	AIR		245	1.035	0.976	0.993
			310	1.012	0.986	0.990
D ₂ O			245	1.059	0.967	0.990
			310	1.040	0.978	0.992
U	D ₂ O		310	1.057	0.968	0.992
	H ₂ O		245	1.056	0.977	1.002

† γ = (captures U238/fissions U235)/(capture U238/fissions U235) Maxwellian at 20°
* These values of k_{eff} have been corrected for bundle end effects and the discrepancies in the HAMMER values of (fissions in U238/fissions in U235)



37 - ELEMENT BUNDLE DIMENSIONS

Figure 1

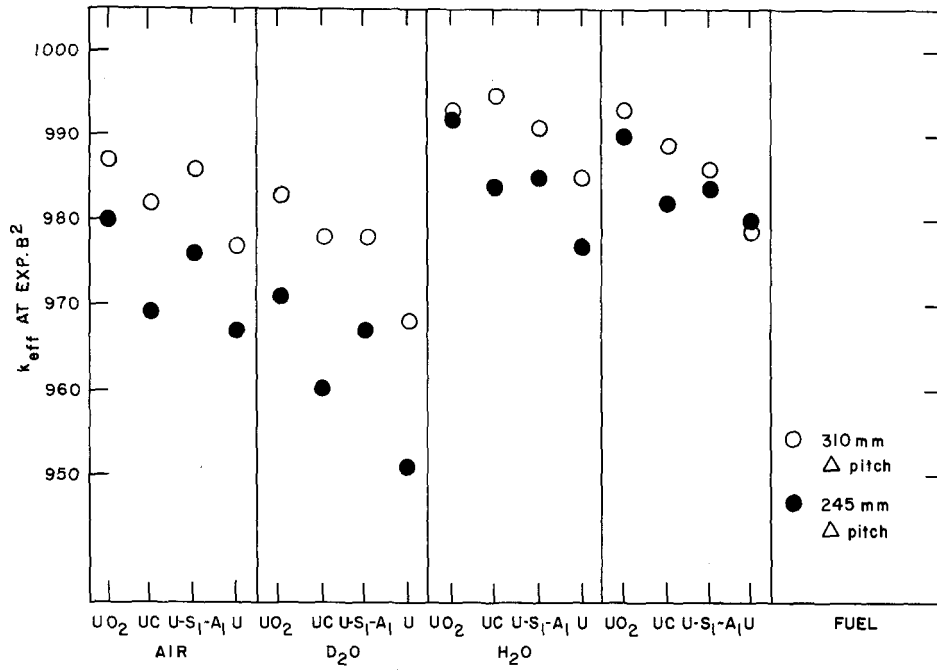


Figure 2

EFFECTIVE U238 RESONANCE INTEGRALS IN CLUSTERS OF
NATURAL URANIUM FUELPINS DERIVED FROM CRNL LATTICE MEASUREMENTS

J. Griffiths, AECL

INTRODUCTION

Lattice parameters fast fission ratio, initial conversion ratio, thermal neutron fine structure, thermal neutron spectrum parameters and buckling, have been measured at CRNL for a wide range of natural uranium lattices. The lattices consisted of regular arrays of fuel clusters, containing natural Umetal, UO_2 , UC, U_3Si/Al cooled by D_2O , AIR, organic liquid and in a few cases H_2O , in D_2O moderator, for a wide range of lattice pitches.

U238 resonance absorption rates in these lattices can be derived from the lattice parameters. These absorption rates have been related to effective U238 resonance integrals by means of the EPITHET⁽¹⁾ computer code.

METHOD

Using the cross-sections given in table 1a and assuming values for the cross-section ratios given in table 1b, it is fairly evident that the lattice parameters can be manipulated to give resonance absorption rates in U238.

The cross-sections given in table 1a are those used by the AECL lattice code LATREP. The cross-section ratios of table 1b are obtained from representative cases run on the LATREP code. To determine resonance integrals from the resonance absorption rates obtained from the lattice parameters, use has been made of the EPITHET code. This is a multigroup, multiannular region code which can be operated in several modes. The mode chosen for this work is a coarse group

Table 1a

Cross-Sections*

U235 2200m/s absorption	679.9 barns
U235 2200m/s fission	579.5 barns
U238 2200m/s absorption	2.72 barns
U238 effective fast capture	0.2446 barns
U238 effective fast fission	0.551 barns
U235 γ thermal	2.43
U235 γ fast	2.80
U238 γ fast	2.801

* The excessive number of decimal places given for some values does not imply high accuracy, but reproduces values given in certain CRNL lattice codes.

Table 1b

Assumed cross-section ratios

<u>Fast neutron absorption in cell</u> Fast neutron absorption in U238	1.2 \pm 10%
<u>U235 fast fission cross-section</u> U235 thermal fission cross-section	0.0009 \pm 50%
<u>U235 fast absorption cross-section</u> U235 thermal absorption cross-section	0.0008 \pm 50%

mode with U238 absorption represented by resonance integrals. In all 33 groups span the energy range 10 Mev to 1.4 ev. Previous work using EPITHET has established how the total U238 resonance integral should be distributed among the energy groups comprising the resonance region. Using this energy split, an iterative series of calculations using EPITHET can be performed. In these iterative calculations, the total resonance integral is changed until the calculated resonance absorptions agree closely with the values derived from the measured lattice parameters.

An error analysis was performed for the resonance absorption rates, which included the experimental errors and the errors assigned to the assumed ratios of table 1b. The error in the resonance integral due to these error accumulations was estimated by performing the resonance integral evaluation three times, once for the nominal absorption rate and once for each of the nominal value plus and minus the accumulated errors.

RESULTS

In these well moderated lattices, the effective resonance integral is not expected to vary with lattice pitch. The results derived bear out this expectation. Where results are available for more than one lattice pitch, the resonance integrals have been averaged to obtain a mean value and at the same time the standard deviation about this mean value has also been obtained. In table 2, effective resonance integrals averaged over lattice pitch are given for each lattice. Cluster average values, values for each ring of fuel pins, along with the error derived from the experimental errors and the standard deviation about the mean value over the pitch, can be found in that table.

Quite large uncertainties are generated from the experimental errors, typically 20-30%. However, the results are much more consistent than these errors would indicate. Standard deviations about the mean over several pitches being typically 3 to 4%. A well known source of experimental effective resonance integrals is the experimental data of Hellstrand. In figure 1 both the effective resonance integrals in UO_2 derived here and the UO_2 values of Hellstrand are plotted against $\sqrt{\frac{S}{M}}$. Here S is an effective fuel surface area and M the mass of fuel. S is derived from a CRNL recipe and no doubt contributes to the scatter evident in figure 1. It is apparent that the values derived here are in good agreement with those measured by Hellstrand. Some confidence, therefore, can be placed in these results for both the UO_2 fuel and the other fuel materials.

Table 1.

Effective Resonance Integrals
Derived from ZED-2 Lattice Measurements

Number of Rings	Fuel	Coolant	Cluster Average	Effective Resonance Integrals			
				Ring 1	Ring 2	Ring 3	Ring 4
7	UO ₂	D ₂ O	11.47, 3.15, 0.35	8.94, 2.57, 0.75	11.89, 3.25, 0.56		
		Void	10.23, 2.09	8.37, 1.80	10.55, 2.13		
		HB40	12.00, 2.97, 0.56	10.76, 2.57, 1.14	12.21, 3.03, 0.57		
19	UO ₂	D ₂ O	12.49, 3.10, 0.35	9.89, 2.51, 0.27	10.50, 2.67, 0.26	13.70, 3.37, 0.43	
		Void	11.13, 2.98, 0.44	8.49, 2.48, 0.40	8.81, 2.57, 0.62	12.50, 3.22, 0.37	
		HB40	14.56, 3.36, 0.39	12.45, 2.76, 0.28	13.16, 2.96, 0.32	15.44, 3.61, 0.42	
28	UO ₂	D ₂ O	14.15, 2.98, 0.48	12.11, 2.45, 0.41	12.39, 2.61, 0.52	15.54, 3.29, 0.52	
		Void	11.77, 2.67, 0.32	8.94, 2.19, 0.32	9.61, 2.33, 0.24	13.56, 2.95, 0.53	
		HB40	16.14, 3.12, 0.46	14.17, 2.50, 0.60	15.49, 2.84, 0.41	16.96, 3.41, 0.56	
19	U	D ₂ O	9.35, 2.01, 0.08	7.31, 1.51, 0.15	7.78, 1.65, 0.11	10.31, 2.23, 0.14	
		Void	8.86, 2.10, 0.26	6.74, 1.66, 0.31	7.12, 1.75, 0.16	9.90, 2.31, 0.18	
37	UO ₂	D ₂ O	12.25, 1.76, 0.10	9.56, 1.39, 0.17	9.95, 1.45, 0.25	10.64, 1.58, 0.10	14.24, 2.01, 0.05
		Void	11.07, 1.61, 0.72	8.36, 1.31, 0.50	8.53, 1.34, 0.48	9.32, 1.44, 0.68	13.24, 1.83, 1.05
		H ₂ O	14.55, 2.21, 0.59	12.07, 1.68, 0.67	12.77, 1.78, 0.44	13.55, 2.00, 0.73	15.96, 2.53, 0.54
37	U	D ₂ O	8.30, 1.23	6.23, 0.87	6.49, 0.91	6.92, 1.02	9.93, 1.50
		Void	7.53, 1.04	5.38, 0.83	5.53, 0.86	6.13, 0.89	9.26, 1.22
		H ₂ O	10.13, 1.38	8.67, 1.10	8.90, 1.14	9.71, 1.13	10.90, 1.53
37	UC	Void	10.27, 1.63	7.23, 1.23	7.47, 1.27	8.40, 1.41	12.62, 1.91
		HB40	13.08, 1.99	10.36, 1.41	11.29, 1.54	12.00, 1.75	14.54, 2.32
37	U ₃ Si/Al	D ₂ O	9.61, 1.33, 0.35	7.27, 1.01, 0.17	7.50, 1.04, 0.48	8.19, 1.15, 0.26	11.39, 1.56, 0.37
		Void	8.76, 1.32, 0.08	6.69, 1.20, 1.16	6.29, 1.03, 0.03	6.95, 1.12, 0.08	10.92, 1.55, 0.05

Key: a, b, c

a - Effective resonance integral mean over several pitches where data exist.

b - Error estimated from experimental errors.

c - Where data from several pitches exist, standard deviations about the mean value a.

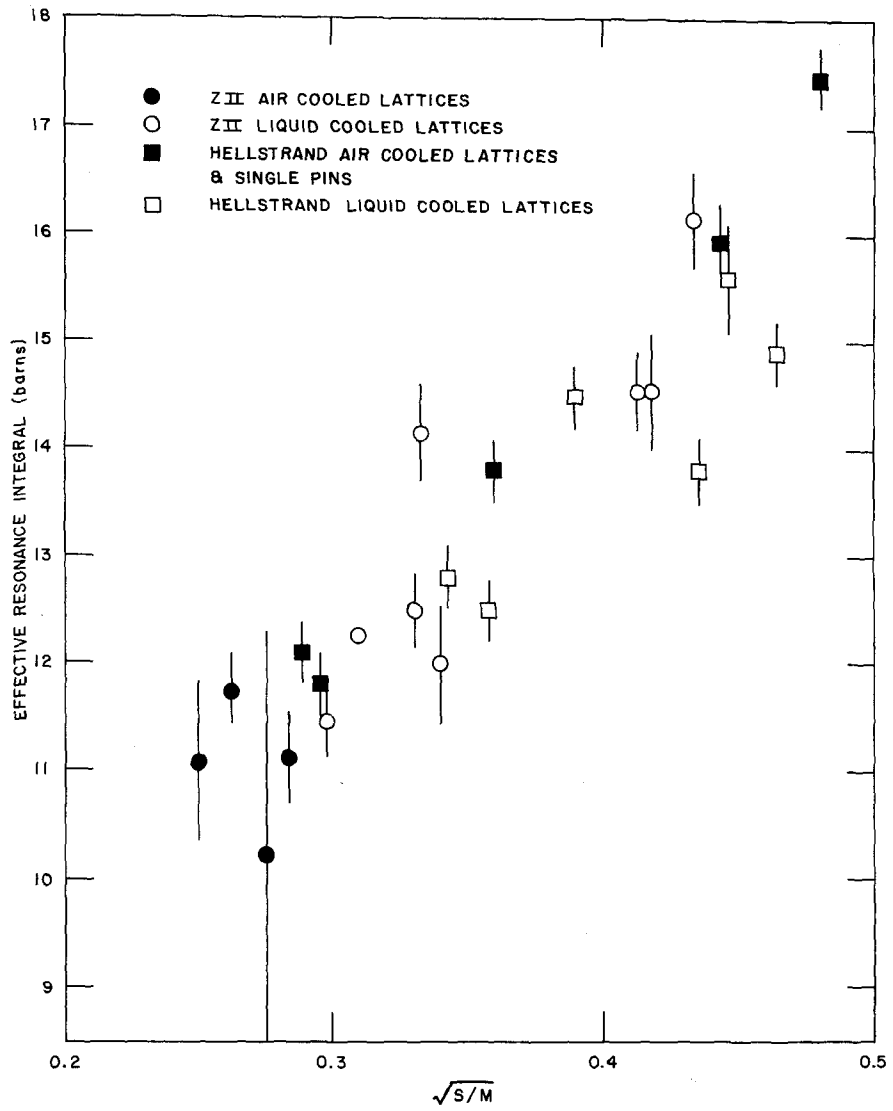


Figure 1

Adjustment of the effective ^{238}U resonance integral to
force agreement with integral data

By Malte Edenius, AB ATOMENERGI, Studsvik, SWEDEN

1. Introduction

As is well known even the most advanced cell codes fail to predict the reactivity for instance of LWR lattices correctly without some adjustments to group cross section data generated from basic nuclear data files. In particular it has been found necessary to lower the ^{238}U capture cross section calculated from basic data in the ENDF/B libraries to get results consistent with integral data from lattice measurements. The purpose of the present note is to use the resonance treatment in an advanced cell code (CASCO [1]) developed at AB Atomenergi to calculate the resonance absorption in isolated fuel rods surrounded by a large moderating region and to normalize the calculated resonance integrals to experimentally determined expressions for the resonance integral. The latter have been taken from the review article in [2]. Different forms for a correction to the effective ^{238}U resonance integral are suggested to force agreement with the experimental values and some examples are given of how such corrections improve the lattice calculations.

2. Calculational method

Effective cross sections in the resonance region are obtained using an equivalence theorem which relates the heterogeneous problem to an equivalent homogeneous problem. Expressing the fuel-to-fuel collision probability, P_{ff} , as a sum of rationals

$$P_{ff} = x \sum_n \frac{\beta_n}{x + \alpha_n} \quad \text{with} \quad \sum_n \beta_n = 1 \quad (1)$$

($x = 4V_f \Sigma_f / S_f$, V_f is the fuel volume, S_f the fuel surface and Σ_f the total cross section. α_n and β_n are fitting parameters.)

one obtains the resonance integral of the heterogeneous system, RI, as a sum of homogeneous integrals, RI_h

$$RI = \sum_n \beta_n RI_h(\sigma_p + \alpha_n \sigma_e) \quad (2)$$

σ_p is the fuel potential scattering cross section per absorber atom and $\sigma_e = S_f / 4V_f N$, N being the absorber number density. The equivalence theorem is based on the narrow resonance approximation, but by a suitable modification of σ_p it is also valid in the intermediate resonance approximation.

The CASCO code uses a rational approximation for the fuel self collision probability suggested by Carlvik [3]

$$P_{ff} = \frac{2x}{x+2} - \frac{x}{x+3} \quad (3)$$

which is more accurate than approximations based on a single rational.

The resonance energy region (4 eV - 9 keV) was in the calculations divided into 13 energy groups and groupwise tabulations of RI_h as function of temperature and background cross section were used in the equivalence

relation. The ^{238}U data in the CASCO library is generated from the ENDF/B-III resonance data using the Studsvik code system ETOS, SPENG and DORIX [4].

The Doppler broadened line shape was obtained using the ψ - and χ -functions, i.e. a Maxwellian velocity distribution was assumed for the absorbing nuclei. This is a good approximation for U-metal, but in UO_2 due to crystalline binding the uranium atoms vibrate with an average kinetic energy larger than that in a free gas state. This is approximately accounted for in CASCO by use of an effective Doppler temperature, T_{eff} , which is higher than the true temperature, T , of the fuel [5]

$$T_{\text{eff}} = \frac{3}{2} \theta_D \int_0^1 x^3 \coth\left(\frac{x\theta_D}{2T}\right) dx \quad (4)$$

where the Debye temperature, θ_D , in UO_2 is put equal to 620 K [6].

3. Comparison with measured resonance integrals

Calculated resonance integrals and their temperature dependence were compared with experimental integrals and Doppler coefficients for UO_2 rods and U-metal rods with two different radii. The smaller UO_2 radius is typical for a BWR-rod and the larger one gives background cross sections corresponding to a Dancoff factor of 0.5.

The expressions recommended in [2] for the room temperature integrals are

$$\begin{aligned} \text{RI} &= 5.60 + 26.3 \sqrt{S/M} && \text{for } \text{UO}_2 \\ \text{RI} &= 4.25 + 26.8 \sqrt{S/M} && \text{for U-metal} \end{aligned} \quad (5)$$

S/M is the surface to mass ratio of the fuel expressed in cm^2/gram .

The experimental temperature dependence is described by

$$RI(T)-\delta = [RI(T_0)-\delta][1+\beta(\sqrt{T}-\sqrt{T_0})] \quad (6)$$

where T and T_0 are expressed in K and δ is the $1/v$ -contribution to RI above 0.55 eV. The experimental value of the temperature coefficient, β , which was assumed to be independent of temperature was taken from [7]

$$\begin{aligned} \beta &= (0.58 + 0.5 \text{ S/M}) \cdot 10^{-2} && \text{for } UO_2 \\ \beta &= (0.51 + 0.5 \text{ S/M}) \cdot 10^2 && \text{for U-metal} \end{aligned} \quad (7)$$

The experimental results in Table 1 were obtained by use of expressions (5) and (7). The experimental uncertainties are about 4 % in the resonance integrals and about 10 % in the Doppler coefficients.

Calculated resonance integrals and Doppler coefficients are compared with experimental values in the first column of Table 2. The resonance integral comparison is done for $T = 300$ K. The comparison of Doppler coefficients shows the average deviation in the interval 300-1000 K.

The calculated resonance integrals are 7-10 % larger than the measured values, whereas the Doppler coefficients agree within the experimental uncertainty. The use of T_{eff} given by Eq. (4) reduces the Doppler coefficient by about 20 % at room temperature in the UO_2 cases and by a few per cent at high temperature, giving an average correction of about 10 % in the interval 300-1000 K.

4. Adjustment of the resonance integral

In order to force agreement with integral data, the ^{238}U cross sections in the energy region 4 eV - 9 keV were reduced in the calculations. Three different types of corrections were tested, viz.

Corr. 1	$\Delta\sigma_a = -0.26 b$
" 2	$\Delta\sigma_a = -0.26 [1+0.007(\sqrt{T}-\sqrt{300})] b$
" 3	$\Delta RI = -0.09 RI$

The relation between $\Delta\sigma_a$ and RI in energy group g is obtained by differentiating

$$\sigma_{a,g} = \frac{RI_g}{\Delta U_g - \frac{RI_g}{\sigma_{p,g}}} \quad (8)$$

i.e.

$$\frac{\Delta RI_g}{\Delta U_g} = \Delta\sigma_a \left[1 - \frac{RI_g}{\Delta U_g \cdot \sigma_{p,g}} \right]^2 \quad (9)$$

Correction 1 has the advantage that the unshielded resonance integral is reduced by only 2.0 b which is within the experimental uncertainty. Using this correction the calculated resonance integral at room temperature is within 1 % of the experimental value for the UO_2 rods and within about 3 % for the U-metal rods. The calculated Doppler coefficient is, however, increased by 10-16 % so that the temperature dependence in the U-metal rods is overestimated. In order to preserve the temperature dependence of the uncorrected resonance integral correction 2 was tested. This correction is identical with correction 1 at 300 K but does not change the \sqrt{T} -dependence of the resonance integral. A drawback is, however, that although the Doppler coefficient for the whole resonance energy region is not changed, $\Delta RI_g / \Delta T$ in individual energy groups will be erroneous. For example, in a group without any resonance, where $\Delta RI_g / \Delta T$ should be equal to zero, one obtains $\Delta RI_g / \Delta T < 0$. Correction 3 also leaves the Doppler coefficient unchanged but gives a value of the unshielded resonance integral which lies outside the experimental uncertainty.

5. Criticality in LWR-lattices

Table 3 shows calculated values of k_{eff} for some uniform pin cell lattices in the KRITZ-facility at Studsvik. In the UO_2 cases the reactivity is underpredicted by 1.4-1.9 % using the unmodified ^{238}U data. Using corrected data the reactivity is increased by about 2 % giving a slightly overestimated k_{eff} . The change is about the same for the three tested types of corrections. The table illustrates the results obtained with correction 1. The influence of the resonance absorption on reactivity is much smaller in the overmoderated PuO_2 case. In this lattice k_{eff} was increased by 0.7 % when the resonance integral was reduced. We note that the spread in predicted reactivities is much smaller after than before the correction of the ^{238}U data. Similar results are obtained for a number of different lattices studied in KRITZ.

6. Conclusions

Using the methods described in the paper it is shown that calculated shielded resonance integrals for ^{238}U with cross sections from ENDF/B-III are 7-10 % larger than measured resonance integrals and calculations using uncorrected ^{238}U data underpredict the reactivity in LWR-lattices. By normalizing the calculated effective resonance integrals to measured integrals for isolated fuel rods calculated reactivities in much better agreement with experimental results were obtained for a large number of different lattices. The three tested types of corrections give about the same results in typical LWR-lattices.

Using correction 1 the calculated Doppler coefficient is about 10-15 % larger than what is obtained with the other two suggested corrections or with unmodified data. However, all calculated Doppler coefficients except that for the U-metal rods with correction 1 lie within the experimental uncertainties.

References

1. Å Ahlin, M Edenius, E Hellstrand, H Häggblom
Few group cross sections for power reactor calculations
Deutsches Atomforum, Reaktortagung, Nürnberg, April 1975 (RF-75-7079)
2. E Hellstrand
Measurements of resonance integrals.
Reactor physics in the resonance and thermal regions.
Proc of the National Topical Meeting, San Diego, February 1966
Vol II, p 151
3. I Carlvik
Internal report, AB Atomenergi (1962)
4. H Häggblom
The ETOS and DORIX Programmes for processing ENDF/B Data
Seminar on Nuclear Data Processing Codes, Ispra, Dec 1973. EACRP-U-52
5. W Lamb
Phys. Rev. 55 (1939) 190
6. G Dolling et al.
Can. J. of Physics 43 (1965) 1397
7. E Hellstrand, P Blomberg, S Hörner
Nucl. Sci. Eng. 8 (1960) 497

Table 1: Measured ^{238}U resonance integrals and Doppler coefficients for isolated fuel rods

Fuel	Radius (cm)	RI _{exp} 300 K	$\beta \cdot 10^2$
UO ₂	0.52	21.7	.77
UO ₂	1.04	17.0	.67
U-metal	0.50	16.7	.73
U-metal	1.00	13.0	.62

Table 2: Comparison between calculated and measured ^{238}U resonance integrals

	Fuel	Radius (cm)	No corr	Corr 1	Corr 2	Corr 3
$\frac{\text{RI}_{\text{th}}}{\text{RI}_{\text{exp}}} - 1$ (%)	UO ₂	0.52	+ 8.9	+ 0.4	+ 0.4	+ 0.2
	UO ₂	1.04	+ 9.6	- 0.7	- 0.7	+ 1.3
	U-metal	0.50	+ 7.4	- 3.4	- 3.4	- 1.1
	U-metal	1.00	+ 8.8	- 3.0	- 3.0	+ 0.7
$\frac{\text{RI}_{\text{exp}}(\Delta\text{RI}/\Delta\text{T})_{\text{th}}}{\text{RI}_{\text{th}}(\Delta\text{RI}/\Delta\text{T})_{\text{exp}}} - 1$ (%)	UO ₂	0.52	- 3	+ 7	- 3	- 3
	UO ₂	1.04	-10	+ 2	-10	-10
	U-metal	0.50	+ 5	+18	+ 5	+ 5
	U-metal	1.00	- 2	+14	- 2	- 2

Table 3: Calculated k_{eff} using uncorrected and corrected ^{238}U resonance integrals

Fuel	V_m/V_f	k_{eff}	
		Uncorr ^{238}U	Corr 1
UO ₂ 1.35 % enr	1.4	0.982	1.001
UO ₂ 1.9 % enr	1.2	0.981	1.004
"-	1.7	0.986	1.003
1.5 % PuO ₂ in depl UO ₂	3.3	0.997	1.004

PRECISE MEASUREMENT AND CALCULATION OF ^{238}U NEUTRON TRANSMISSIONS*

D. K. Olsen, G. de Saussure, E. G. Silver, and R. B. Perez

Oak Ridge National Laboratory

Oak Ridge, Tennessee 37830

We have measured above 0.5 eV the total neutron cross section of ^{238}U in precise transmission experiments and have compared the results with ENDF/B-IV. Special emphasis was placed on measuring transmissions through thick samples in order to obtain accurate total cross sections in the potential-resonance interference regions between resonances. These total cross sections are important in computing shielded resonance capture integrals. It has been observed¹ that such shielded integrals are overestimated by ENDF/B-IV.

The neutron energies were determined by time of flight along a 41.68 m flight path at ORELA. The detector was a 7.62-cm diameter, 1.0-mm thick Li-glass disk viewed edge-on by two RCA-7585 phototubes. At 20 m from the neutron source isotopically-enriched, room-temperature ^{238}U disks with inverse thicknesses of $1/n = 5405, 1603, 807, 266, 80.7, 19.2,$ and 5.7 barns/atom were alternated in and out of the beam with 10 minute cycles. At least four separate transmission measurements with various combinations of Cd, In, Co, Al, Mn, and Au beam filters were made for each sample thickness. Blackened resonances from these filters aided in estimating the background levels both as a function of energy and sample thickness. In the resolved resonance region, the experimental resolution was limited by the neutron slowing down time in the H_2O moderator and was approximately given by $\Delta E/E \approx .0012$. After

subtracting the background (1.0 to 2.0%) and deadtime-correcting the sample-in and sample-out time-of-flight spectra, the resulting transmissions for each sample thickness were combined. The transmissions through the three thickest samples are compared in Figs. 1 to 3 with resolution-broadened transmissions calculated from the ENDF/B-IV total cross section which was Doppler broadened to 300°K.

In particular, Fig. 1 shows the experimental transmission up to 4000 eV through the .254-cm-thick sample of ^{238}U ($1/n = 80.7$ barns/atom). The smooth curve is the corresponding transmission from ENDF/B-IV radii, resonance parameters, and single-level Briet-Wigner, SLBW, formalism. Below 1000 eV no major discrepancies are observed between the calculated and measured transmission dips of the strong s-wave resonances. A few disagreements exist between the measured and calculated transmission dips of the weak, low-energy, p-wave resonances. Figure 2 shows the transmission through the 1.08-cm-thick sample (19.2 barns/atom). Above 1000 eV the measured transmission dips are either equal to or larger than those from ENDF/B-IV indicating that a resonance-by-resonance analysis of these data would perhaps give neutron widths equal to or larger than those contained in ENDF/B-IV. Figure 3 shows the transmission through the thickest sample (3.62 cm). These data are very sensitive to the cross section between resonances and the s-wave interference minima. Between 2000 and 4000 eV the ENDF/B-IV total cross section reproduces the measured transmission reasonably well. Between 40 and 2000 eV ENDF/B-IV consistently underestimates the total cross section giving a transmission larger than that which is measured experimentally. In fact, in some s-wave minima ENDF/B-IV gives a total cross section which is negative resulting in a transmission greater than unity.

These discrepancies are perhaps clearer in Fig. 4, which shows the experimental transmission from 50 to 300 eV through the thickest sample. The upper smooth curve, as before, is the corresponding transmission calculated from the ENDF/B-IV radii, resonance parameters, and SLBW formalism. The lower smooth curve shows the transmission as obtained from a more exact calculation of the total cross section using:

- (1) the Reich-Moore formalism;²
- (2) the resonance parameters and scattering radius ($.9185 \times 10^{-12}$ cm) from ENDF/B-IV; and
- (3) the "ladder approximation" (levels with uniform spacings and widths) to make an end effect correction for resonances outside the resolved resonance region, that is, a "ladder" from $-\infty$ to 0.0 eV and from 4.0 keV to $+\infty$.

This more exact calculation of the total cross section reproduces the measured transmission much better and does not yield negative cross sections. In particular, the inclusion of multilevel effects with the Reich-Moore formalism² removes the negative cross sections in the s-wave minima, but does not significantly reduce the overall discrepancy between resonances. This discrepancy is removed by the end-effect correction which includes levels outside the resolved resonance region with the "ladder approximation."

The increase in the total cross section between resonances as required by the experimental transmissions will reduce strongly self-shielded capture resonance integrals. In particular, Table I compares such integrals for various dilutions, σ_0 , calculated with the SLBW approach of ENDF/B-IV and the Reich-Moore formalism with the ladder approximation. The limits

of integration are taken from 100 to 680 eV. In this energy region the smooth background file (file #3 of ENDF/B-IV) is zero. The last column of Table I is the ratio of the third column to the second column. In particular, the capture integral from 100 to 680 eV shielded down to 10.0 barns decreases by 4.4% when the Reich-Moore formalism with the ladder approximation is used in place of ENDF/B-IV procedures. A more complete description of the experimental aspects of this work will be given in an Oak Ridge National Laboratory internal report.

TABLE I. $\int_{100 \text{ eV}}^{680 \text{ eV}} \frac{\sigma_{n\gamma}(E)}{\sigma_{n\gamma}(E) + \sigma_0} \cdot \frac{dE}{E}$

σ_0 (barns)	SLBW	RM with ladders	Ratio
1	.011673	.008632	.7395
3	.008164	.007190	.8807
10	.005482	.005240	.9559
20	.004274	.004170	.9757
30	.003668	.003607	.9834
100	.002264	.002252	.9947

* Research sponsored by the Energy Research and Development Administration under contract with the Union Carbide Corporation.

¹J. Hardy, private communication; see also Nucl. Sci. and Eng. 40, 101 (1970).

²C. W. Reich and M. S. Moore, Phys. Rev. 111, 929 (1958).

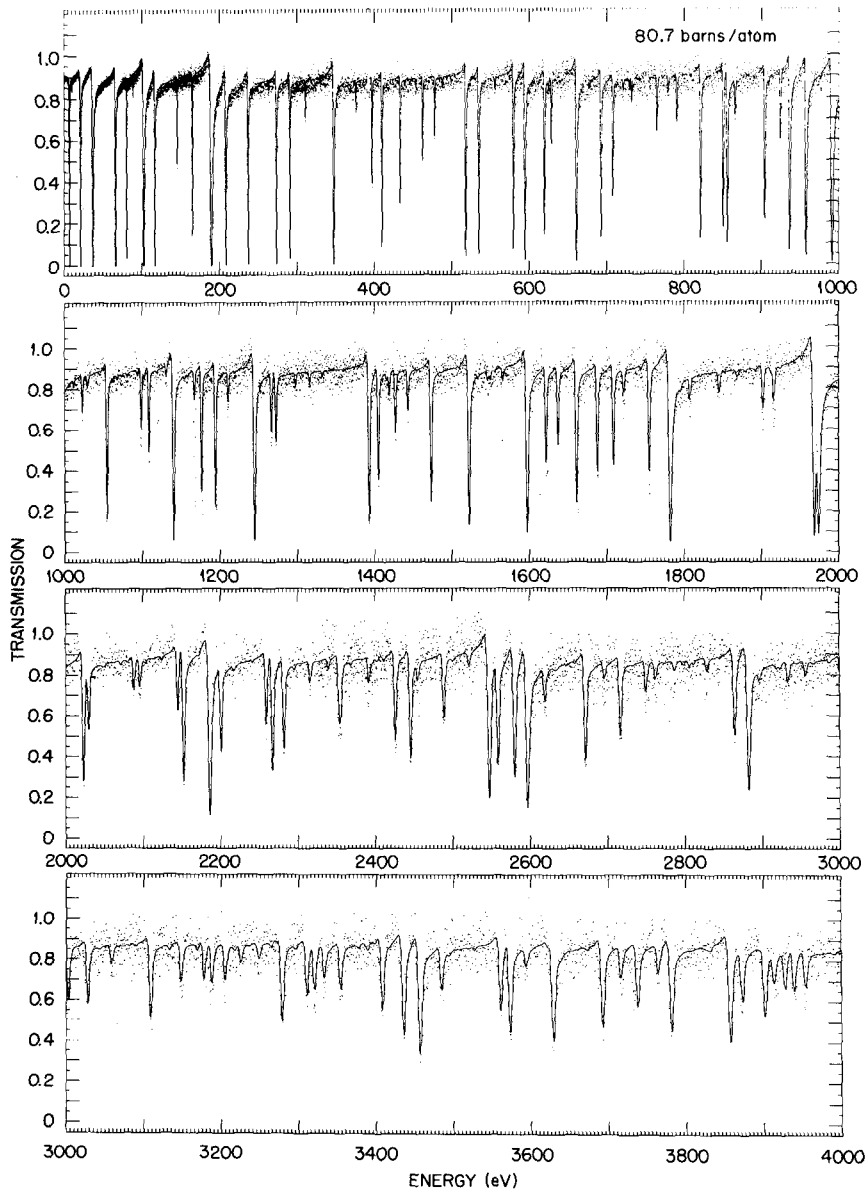


Fig. 1 Measured transmission of 0.5- to 4000.0-eV neutrons through 0.254 cm of ^{238}U ($1/n = 80.7$ barns/atom). The smooth curve is the corresponding transmission from ENDF/B-IV.

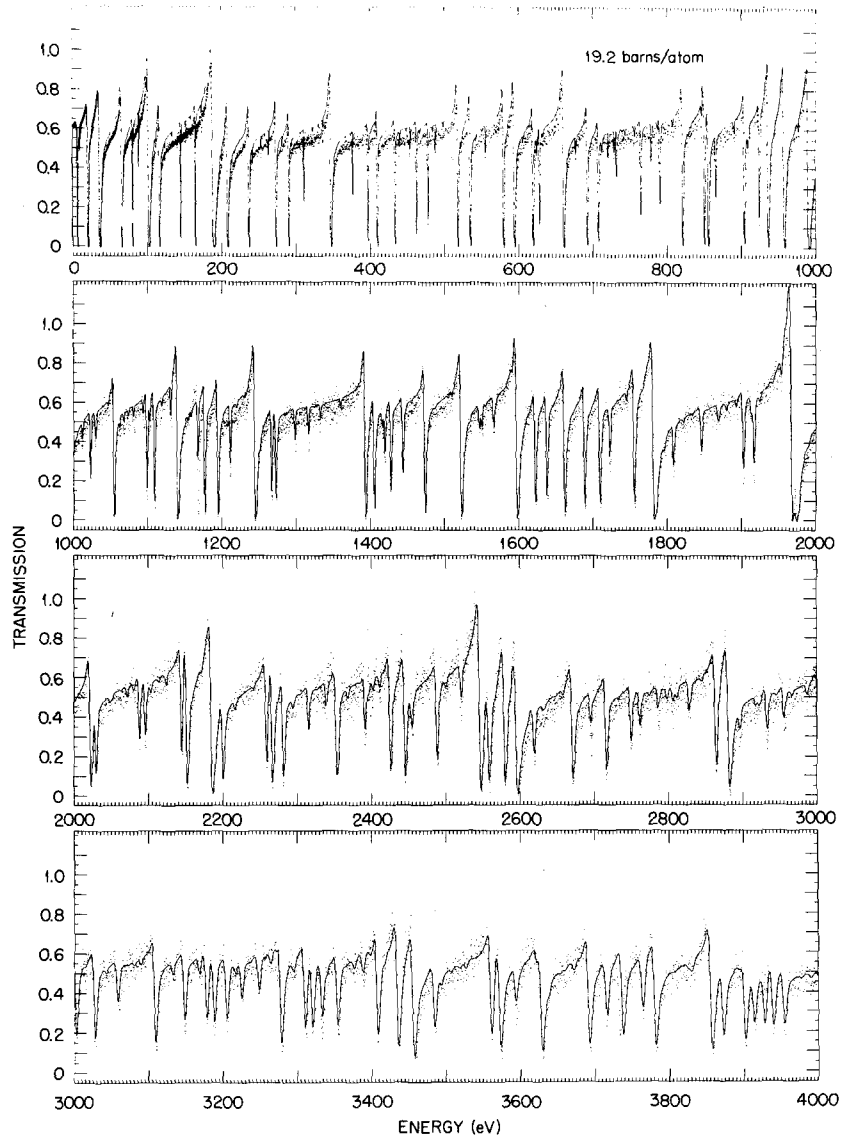


Fig. 2 Measured transmission of 0.5- to 4000.0-eV neutrons through 1.08 cm of ^{238}U ($1/n = 19.2$ barns/atom). The smooth curve is the corresponding transmission from ENDF/B-IV.

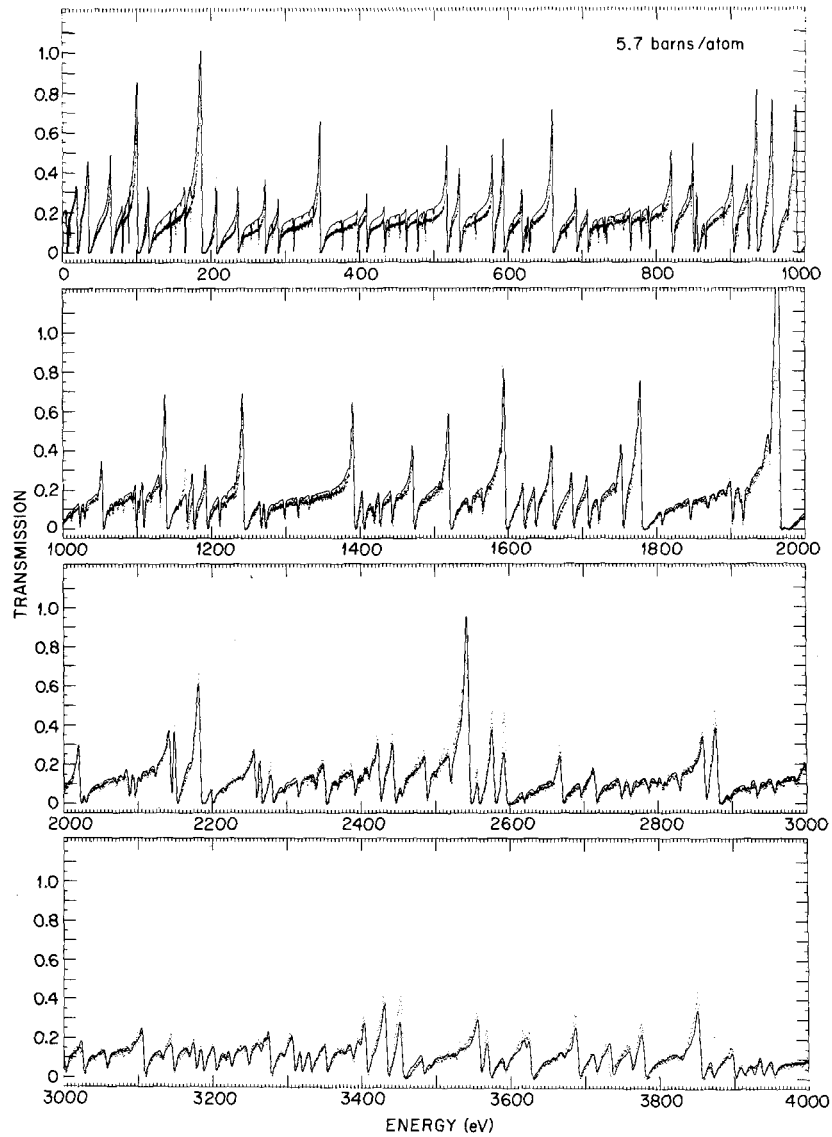


Fig. 3 Measured transmission of 0.5- to 4000.0-eV neutrons through 3.62 cm of ^{238}U ($1/n = 5.7$ barns/atom). The smooth curve is the corresponding transmission from ENDF/B-IV.

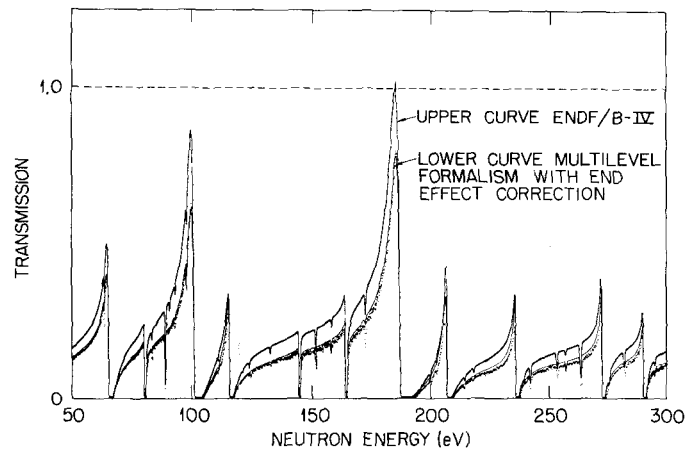


Fig. 4 Measured transmission of 50.0- to 300.0-eV neutrons through 3.62 cm of ^{238}U ($1/n = 5.7$ barns/atom). The upper smooth curve is a resolution-broadened transmission calculated from the ENDF/B-IV total cross section Doppler broadened to 300°K. The lower smooth curve is a similar transmission obtained from the Reich-Moore multilevel formalism using the "ladder" approximation for levels outside the resolved resonance region.

THE $^{238}\text{U}(n,\gamma)$ CROSS SECTION ABOVE THE RESONANCE REGION*

R. B. Perez, R. R. Spencer, and G. de Saussure

Oak Ridge National Laboratory
Oak Ridge, Tennessee 37830

Recent ^{238}U capture cross section measurements quote uncertainties in the 5% to 10% range, but often discrepancies between data are larger, indicating that some sources of error have not been properly identified.

Before 1970 all the measurements of the ^{238}U capture cross section but one, that of Moxon,¹ had been done with nearly monoenergetic neutron sources and most of those measurements had been done relative to the ^{235}U fission cross section. The interpretation of such measurements is complicated not only because of the structure in the ^{235}U fission cross section, but also because the ^{238}U capture cross section has considerable structure which needs to be measured more accurately and evaluated.

In Fig. 1 we compare the 1970 evaluation of Davey² to ENDF B-IV in the region below 100 keV. We also show some typical experimental data. Data obtained before 1970 are represented by full figures, recent data by open figures. Some error flags have been omitted so as not to overcrowd the figure. Data derived from ratios of the ^{238}U capture to the ^{235}U fission or absorption cross sections have been recomputed using ENDF B-IV values of the ^{235}U cross sections.

As can be seen on Fig. 1, there are large uncertainties in the data and discrepancies between measurements. ENDF/B-IV is lower than Davey's evaluation partly because the ^{238}U capture cross section is correlated to the ^{235}U fission cross section by the ratio measurements, and the ENDF/B-IV value of the latter cross section is lower than that evaluated by Davey.³

* Research sponsored by the Energy Research and Development Administration under contract with the Union Carbide Corporation.

The recent measurement of Panitkin et al.⁴ extends from 24 to 145 keV and was done with nearly monoenergetic neutrons from the ${}^7\text{Li}(p,n)$ reaction, and relative to the ${}^{235}\text{U}$ fission cross section. The point of Block et al.⁵ was obtained at 24.3 keV with an iron-filtered beam, and relative to Au. As we have already mentioned, these data must be interpreted in the light of the structure in the ${}^{235}\text{U}$ fission and ${}^{235}\text{U}$ and Au capture cross sections. The data of Chelnokov et al.⁶ were also obtained relative to the ${}^{235}\text{U}$ fission cross section, using a lead slowing down spectrometer.

Only four measurements done with a white neutron source and the time-of-flight technique have been reported before 1974. The data of Moxon¹ extend to 200 keV and have uncertainties ranging from 4% to 8%; the data of Fricke et al.^{7,21} extend to 1 MeV with errors of the order of 12%; the data of de Saussure et al.⁸ extend to 100 keV, the errors range from 5% to 10%; finally the measurement of Spencer and Kappeler⁹ covers the range 20 to 550 keV, but the results are still preliminary. The three first measurements were done with a Linac, were normalized by the saturated resonance technique at 6.7 eV, and were relative to the ${}^{10}\text{B}(n,\alpha)$ or ${}^{10}\text{B}(n,\alpha\gamma)$ reaction up to 80 keV. The results of these three measurements averaged over decimal intervals up to 100 keV are compared in Fig. 2 where we also show ENDF/B-IV.

Figure 2 shows that there are discrepancies between the results of the three measurements. Those discrepancies are substantially larger than the known uncertainties and do not show a consistent pattern: below

5 keV the ORELA data agree within 6% with those of Moxon but are 25% larger than those of Fricke et al.; above 50 keV the ORELA data and those of Fricke et al. agree to within 3% but are 20% larger than those of Moxon!

In Fig. 3 we compare the 1970 evaluation of the ^{238}U capture cross section above 100 keV by Davey⁷ with the recent evaluation by Sowerby et al.¹⁰ and with ENDF/B-IV.¹¹ Some typical experimental data are also shown, the data older than 1970 as full figures, the recent data as open figures; data derived from ratio measurements with respect to the ^{235}U fission cross section were recomputed using the ENDF/B-IV value of the ^{235}U cross section. The considerable differences in the three evaluations below 2 MeV reflect the considerable uncertainty in the cross section; the agreement between the evaluations above 2 MeV reflects the lack of measurements in that region!

The errors in the ^{238}U capture cross section are strongly correlated to those in the ^{235}U fission cross section, not only by the precise measurements of the ratio of those two cross sections, such as that of Poenitz,¹² but also because some authors have measured the absolute ^{238}U capture cross section and ^{235}U fission cross section using the same techniques and the same detectors to determine the incident neutron flux. If an evaluator favors a given set of data for the ^{235}U fission cross section, it is logical that he should also give much weight to the ^{238}U capture cross section obtained in the same installation, by a similar technique.

In the region from .1 to .5 MeV the data of Menlove and Poenitz¹³ are about 17% lower than those of Barry, Bunce and White.¹⁴ Davey gave

much weight to the data of White¹⁵ in his evaluation of the ^{235}U fission cross section.³ Since the data of White and the data of Barry et al. were obtained "from the same flux," Davey also weighted the data of Barry et al. in his ^{238}U capture cross section evaluation,² and he re-normalized the values of Menlove and Poenitz to agree better with those of Barry et al. Sowerby et al.¹⁰ performed a simultaneous evaluation of several cross sections including ^{238}U capture and ^{235}U fission. For this evaluation they choose to treat the data of Barry et al. as ratio measurements relative to the fission data of White. ENDF/B-IV choose to give more weight to recent data which are mostly independent of the ^{235}U fission cross section: the data of Fricke et al.,⁷ of Ryves et al.¹⁶ and the preliminary data of Pearlstein and Moxon.¹⁷

Sowerby et al.¹⁰ estimate that the ^{238}U capture cross section is known to 7% from .1 to 1 MeV; in the same range ENDF/B-IV¹¹ estimates an uncertainty of 5%. We think that these estimates are very optimistic, considering that there is more than 20% discrepancy around 1 MeV between the 1973 evaluation of Sowerby et al. and ENDF/B-IV!

The lack of agreement in the value and shape of the neutron capture cross section of ^{238}U below 100 keV among the three linac experiments suggests further measurements. Spencer and Kappeler⁹ performed a measurement with the pulsed 3-MV Van de Graaff at Karlsruhe, making use of the $^7\text{Li}(p,n)^7\text{Be}$ reaction. The idea was to provide a degree of experimental independence and in that way resolve previous difficulties. For example the Van de Graaff technique has no interfering gamma flash and, due to the very fast timing employed, background considerations are different and less complex. The detector utilized in this experiment was an 800-liter liquid scintillator tank. Both a standard gold capture

sample and a ^{235}U fission chamber were employed as flux monitors in an attempt to obtain a partially independent verification of the measured capture yield shape. Hence this measurement should be considered as a shape determination only.

The data were normalized to a value of 200 mb for the interval 90 to 100 keV. This is the value reported in an evaluation of Sowerby et al.¹⁰ Below 200 keV the gold cross section of Kompe¹⁸ was used to derive a ^{238}U capture cross section (see Table I). Above 200 keV a recent measurement of Le Rigoleur et al.¹⁹ was used which agrees well with the data of Kompe¹⁸ in the region of overlap. Recent gold measurements of Macklin et al.,²⁰ which are normalized by means of the "black resonance" technique at 4.9 eV are in agreement ($\pm 3\%$) with the Kompe and Le Rigoleur results, and therefore add justification to the use of these particular sets of data.

Table II shows the results of the ^{235}U fission chamber reference data. To obtain the $^{238}\text{U}(n,\gamma)$ cross section shape the ^{235}U fission cross section evaluation of Sowerby et al.¹⁰ was used.

The estimated error of around 11% is mainly due to the normalization value. The shape is believed to be accurate within 5%. Below 100 keV the shapes of the ^{238}U capture cross section derived from both the gold reference cross section and the ^{235}U fission cross section as reference are in excellent agreement with the results of de Saussure et al.⁸ and in fair agreement with Moxon's¹ data. Below 50 keV there are substantial shape deviations with the measurement of Friesenhahn et al.²¹

A similar neutron source, the ${}^7\text{Li}(p,n){}^7\text{Be}$ reaction with incident protons from the Argonne tandem-dynamitron, was used by Poenitz²² for his measurement of the ${}^{238}\text{U}$ capture cross section. The capture gamma-ray detector was a 1300 liter tank filled with a liquid scintillator. The Grey Neutron Detector, or some times the Black Neutron Detector or a ${}^6\text{Li}$ -glass detector were used as neutron monitors. Similar to the Spencer and Kappeler⁹ experiment, the ratio ${}^{238}\text{U}$ to ${}^{197}\text{Au}$ capture cross section ratio was measured. Then absolute measurements of the ${}^{197}\text{Au}$ capture were performed to obtain the ${}^{238}\text{U}(n,\gamma)$ cross section. The results of Poenitz measurements are in good agreement with the activation results of Ryves.¹⁶ They differ in shape from the results of Friesenhahn *et al.*^{7,21} and although about 7% lower than the ORELA⁸ results, there is in general good shape agreement with the ORELA measurement.

The latest measurement available is due to Le Rigoleur *et al.*²³ who used a total energy weighting technique in conjunction with the capture gamma-ray detector, Macklin and Gibbons.²⁴ The neutron flux was measured with a ${}^{10}\text{B}$ NaI(Tl) detector with a ${}^6\text{Li}$ -glass scintillator. The results were averaged over 10 keV energy intervals below 100 keV and in 20 keV intervals above 100 keV. Some of the data are shown in Fig. 4. Below 100 keV Le Rigoleur's results are 6% to 8% below those of ORELA,⁸ between 10% and 20% higher than Moxon's data and agree $\pm 5\%$ with the results of Friesenhahn *et al.*²¹ Between 120 and 250 keV, they fall lower than any previous measurement in this energy range. For example, when compared with Ryves¹⁶ activation measurements, one observes that Le Rigoleur's measured points lie lower by 15% than Ryves results at 160 keV and by 6% at 238 keV. But there is better agreement above 400 keV.

We now turn our attention to the considerable experimental evidence of long range fluctuations in the ^{238}U capture cross section shown by the recent high resolution experiments. This structure is illustrated in Fig. 5, from a recent paper by Spencer and Kappeler.⁹ In that figure the authors have compared the shape of their preliminary data to that obtained in the ORELA measurement.⁸ Both sets of data have been averaged over intervals of .5 to 1 keV width. The KFK data in this figure have been arbitrarily normalized, so that the agreement in magnitude is not significant. We have added to the figure the ENDF/B-IV evaluation.¹¹ Below 45 keV the evaluation is represented by statistical parameters so that some structure is implied, but clearly the details of this structure are important and need to be represented more directly by the evaluation.

To test whether or not the observed long-range fluctuations in capture represent departures from the compound nucleus model, the Wald-Wolfowitz²⁵ runs and correlation tests were applied to Monte-Carlo generated ^{238}U capture cross sections and to the ORELA⁸ measurements. Both the mock-up cross sections, computed on the basis of the compound nucleus model, and the actual data were averaged in energy intervals ranging from 600 eV up to 3 keV. The measured and mocked-up capture data averaged over 1200-eV intervals are shown in Fig. 6, together with the fits to the s-wave and p-wave strength functions.

The results of the Wald-Wolfowitz tests (Table 3) show with a high confidence limit that the fluctuations in the $^{238}\text{U}(n,\gamma)$ data cannot be accounted for by the compound nucleus model. Possible explanations for the presence of the observed intermediate structure are based on the Strutinsky double-humped fission barrier or the existence of "door-way"

states in the entrance reaction channels or perhaps a combination of both. Theoretical considerations²⁵ lead to the concept of modulated strength functions due to local enhancements of the partial reaction widths. The ORELA data, averaged over 1200 eV, were fitted with the modulated strength function model. The result of this procedure is shown in Fig. 7. In this figure the solid line represents the intermediate structure. When this structure was removed from the data, the Wald-Wolfowitz tests showed that the remaining structure behaved randomly.

Conclusions.

A number of measurements of the $^{238}\text{U}(n,\gamma)$ cross section above the resonance region have been completed in the past few years. In the keV region these measurements suggest a considerable amount of intermediate structure.

An idea of the present status of affairs is given by inspection of Fig. 8. The low resolution shape of the ^{238}U capture seems to be reaching a "consistent" status with the exception of the Friesenhahn et al.^{7,21} measurement, and two points (at round 35 and 85 keV) in the results of Moxon. Large differences in normalization are still present. However the results seem to settle above the ENDF/B-IV evaluation between the high ORELA data and the low Moxon data set. This trend will help to obtain better agreement between the calculated and measured value of the dilute capture resonance integral. The presence of intermediate structure has several implications:

- (a) Effects on the validity of activation measurements and "spot" normalization procedures of the capture cross section, especially at neutron energies such as 24 and 30 keV, where large fluctuations exist.

- (b) One may question the validity of the present statistical representation of the unresolved region. For example, corresponding to the 24-keV iron window, there is a large enhancement of the ^{238}U capture cross section. Hence, the actual detailed behavior of the intermediate structure should be included in the representation of the $^{238}\text{U}(n,\gamma)$ cross section. At ORNL we are presently in the process of testing the effect of these fluctuations in fast reactor calculations.

In summary taking into account that fast breeders are mostly lots of iron with a sprinkle of plutonium and a heavy blanket of ^{238}U for breeding, the neutron capture of this important material has to be known better than at least 3%. It is then clear that considerably more work will be needed to achieve this goal.

ACKNOWLEDGMENT

We would like to thank C. Le Rigoleur and W. P. Poenitz for their communications on their most recent work on the $^{238}\text{U}(n,\gamma)$ cross section measurements.

REFERENCES

1. M. C. Moxon, AERE-R-6074 (1969).
2. W. G. Davey, Nucl. Sci. Eng. 39, 337 (1970).
3. W. G. Davey, Nucl. Sci. Eng. 26, 149 (1966); also Nucl. Sci. Eng. 32, 35 (1968).
4. Y. G. Panitkin et al., IAEA-CN-26 II, 57 (1970).
5. R. C. Block et al., Conf-720901, II, 1107 (1972)..
6. V. B. Chelnokov et al. Preprint USSR Institute of Physics and Power Engineering (1973).
7. M. P. Fricke et al., IAEA-CN-26 II, 265 (1970).
8. G. de Saussure et al. Nucl. Sci. Eng. 51, 385 (1973).
9. R. R. Spencer and F. Kappeler, Proc. Conf. Nuclear Cross Sections and Technology, Washington, D. C., 1975, to be published.
10. M. G. Sowerby et al., AERE-R7273 (1973).
11. ENDF/B-IV, MAT 1262 (1974).
12. W. P. Poenitz, Nucl. Sci. Eng. 40, 383 (1970).
13. J. O. Menlove and W. P. Poenitz, Nucl. Sci. Eng. 33, 503 (1968).
14. J. F. Barry et al., J. Nucl. Energy 18, 481 (1964).
15. P. H. White, J. Nucl. Energy 19, 325 (1965).
16. T. B. Ryves et al., J. Nucl. Energy 27, 519 (1973).
17. S. Pearlstein and M. C. Moxon, Nuclear Data Progress Report, U. K. 1973.
18. D. Kompe, Nucl. Phys. A133, 513 (1969).
19. C. LeRigoleur et al., CEA-N-1662 (1973).
20. R. L. Macklin et al., Phys. Rev. C (to be published).
21. S. J. Friesenhahn et al., GA-10194 (1970).
22. W. P. Poenitz, to be published in Nucl. Sci. Eng.
23. C. Le Rigoleur et al., Proc. Conf. Nuclear Cross Sections and Technology, Washington D. C., 1975, to be published.
24. R. L. Macklin and J. H. Gibbons, Phys. Rev. 159, 1007 (1967).
25. R. B. Perez and G. de Saussure, Proc. Conf. Nuclear Cross Sections and Technology, Washington D. C. (1975), to be published.

TABLE I. Gold Reference

E (keV)	$\frac{\sigma_Y(^{238}\text{U})}{\sigma_Y(^{197}\text{Au})}$	Std. Dev. (statistics) %	$\sigma_Y(^{197}\text{Au})$ mb	$\sigma_Y(^{238}\text{U})$ mb	Estimated $\frac{\Delta\sigma_Y}{\sigma_Y} (^{238}\text{U})$ ±%
20-30	0.8630	0.4	667	576	11
30-40	0.8704	0.3	546	475	11
40-50	0.8856	0.3	467	413.5	11
50-60	0.7823	0.4	409	320	11
60-70	0.7263	0.4	377	274	11
70-80	0.6635	0.4	357	237	11
80-90	0.6543	0.4	328	215	11
90-100	0.6430	0.5	311	200	10
100-120	0.6202	0.3	295	183	11
120-140	0.6015	0.4	277	167	11
140-160	0.5728	0.4	269	154	11
160-180	0.5694	0.5	258	147	11
180-200	0.5510	0.5	254	140	11
180-223	0.5689	1.0	251	143	11
223-264	0.5607	1.0	232	130	11
264-309	0.6104	1.0	216	132	11
317-373	0.6816	0.5	174	119	11
387-431	0.7872	0.5	158	124	11
423-467	0.7851	0.5	146	115	11
438-483	0.9092	0.5	142	129	11
483-529	1.0115	0.5	134.5	136	11
508-564	1.0735	0.5	125	134	11

TABLE II. ^{235}U Fission Reference

E (keV)	$\frac{\sigma_Y(^{235}\text{U})}{\sigma_f(^{235}\text{U})}$	Std. Dev. (statistics) %	$\sigma_f(^{235}\text{U})$ mb	$\sigma_Y(^{235}\text{U})$ mb	Estimated $\frac{\Delta\sigma_Y}{\sigma_Y} (^{235}\text{U})$ ±%
20-30	0.2476	4	2148.3	532	12
30-40	0.2342	4	2010.7	471	12
40-50	0.2159	4	1908.4	412	12
50-60	0.1694	4	1871.4	317	12
60-70	0.1581	4	1808.8	286	12
70-80	0.1421	4	1714.1	243.5	12
80-90	0.1279	4	1681.0	215	12
90-100	0.1225	4	1632.2	200	10
100-120	0.1200	4	1542	185	12
120-140	0.1165	4	1493	174	12
140-180	0.1123	5	1424	160	13
180-223	0.1106	5	1343	148	13
223-264	0.1102	5	1295	143	13
264-309	0.0969	4	1262	122	12
317-373	0.0948	4	1223	116	12
387-431	0.0932	4	1180	110	12
423-467	0.0964	4	1162	112	12
438-483	0.1013	3	1155	117	12
483-529	0.1085	4	1134	123	12
508-564	0.1083	2	1126	122	12

Table III. Results of the Wald-Wolfowitz Correlation and Runs Tests for the Measured and Mock-Up ^{235}U Capture Cross Section.

Width (keV)	Capture (Measured)				Capture (Mock-Up)			
	ϵ_c	$P(\epsilon_c)$	ϵ_R	$P(\epsilon_R)$	ϵ_c	$P(\epsilon_c)$	ϵ_R	$P(\epsilon_R)$
.6	5.9	$<10^{-5}$	4.5	$<10^{-5}$.52	.60	.03	.98
.9	6.1	$<10^{-5}$	3.9	2.7×10^{-3}	.20	.84	.96	.34
1.0	5.9	$<10^{-5}$	4.6	$<10^{-5}$.37	.71	.68	.50
1.2	6.2	$<10^{-5}$	5.6	$<10^{-5}$.65	.52	.34	.73
1.5	5.3	$<10^{-5}$	4.8	$<10^{-5}$.31	.76	.002	.99
1.8	2.2	2.7×10^{-2}	3.6	$<2.7 \times 10^{-3}$.97	.33	1.11	.27
2.0	4.9	$<10^{-5}$	3.8	$<2.7 \times 10^{-3}$.22	.82	1.2	.23
3.0	3.9	2.7×10^{-3}	1.8	7.2×10^{-2}	1.1	.27	.006	.99

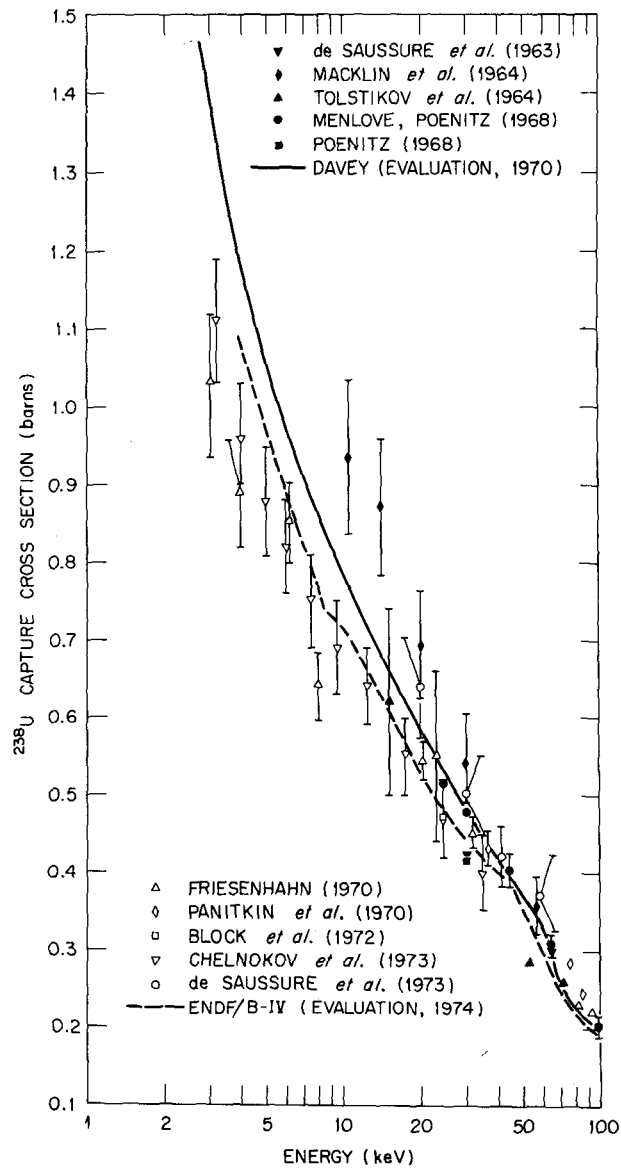


Figure 1

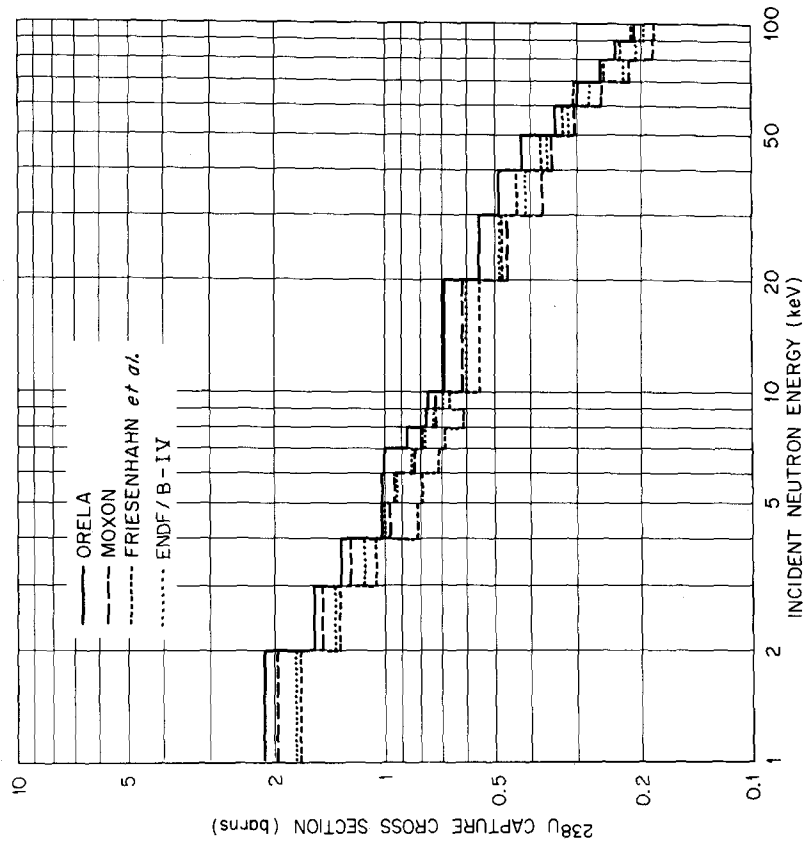


Figure 2

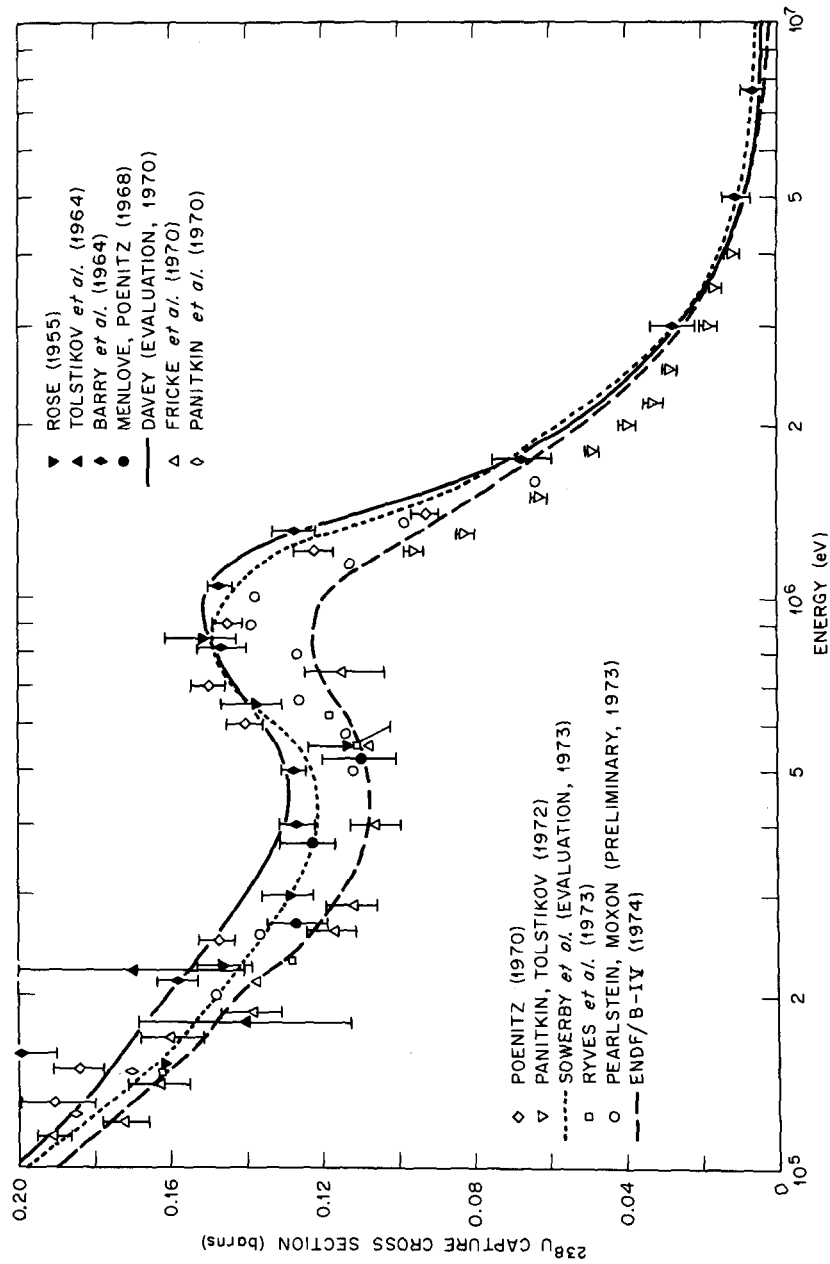


Figure 3

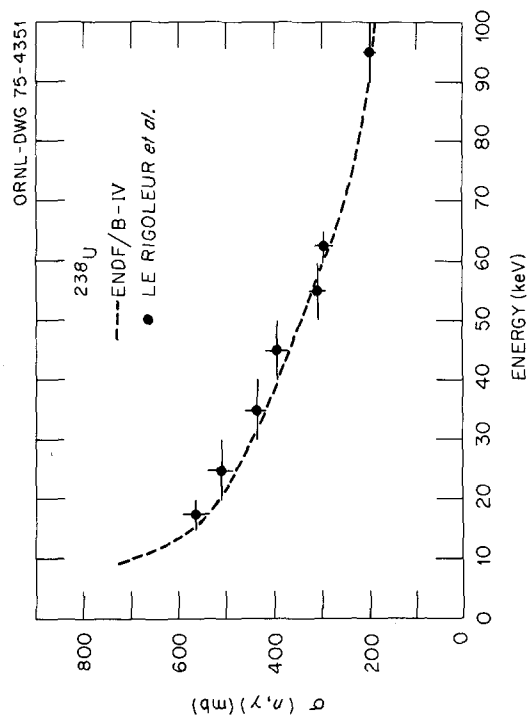


Figure 4

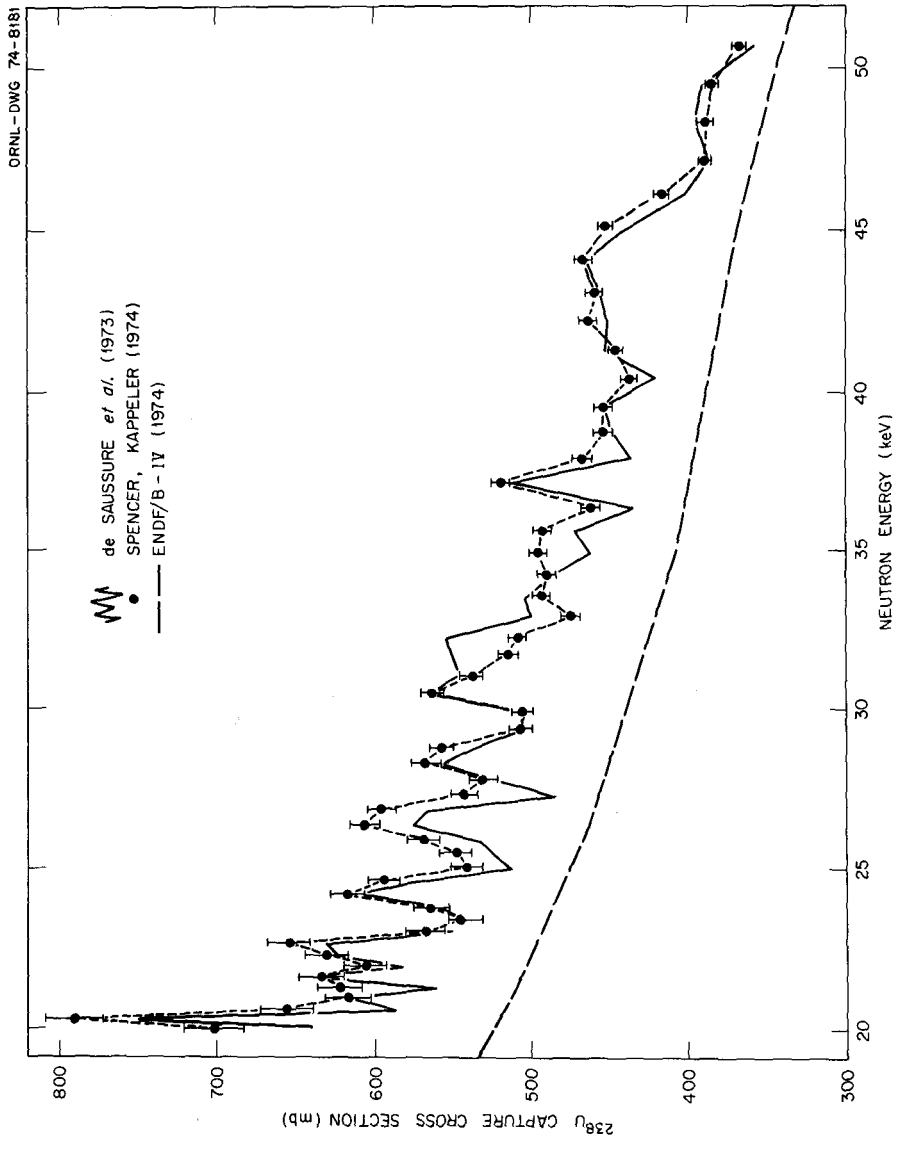


Figure 5

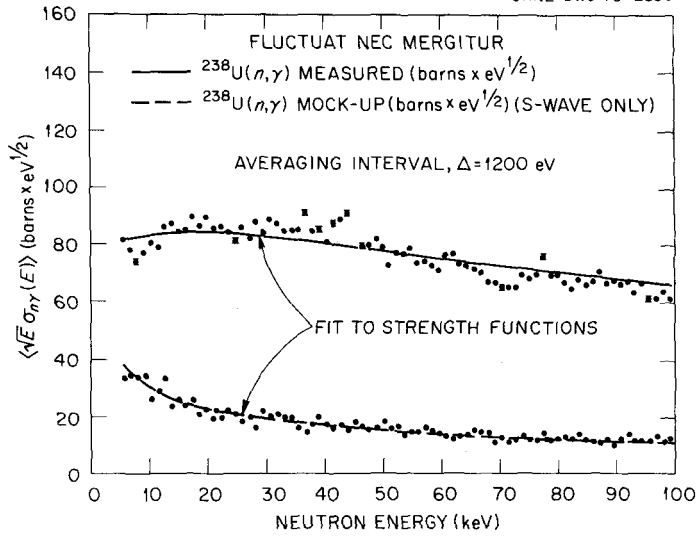


Figure 6

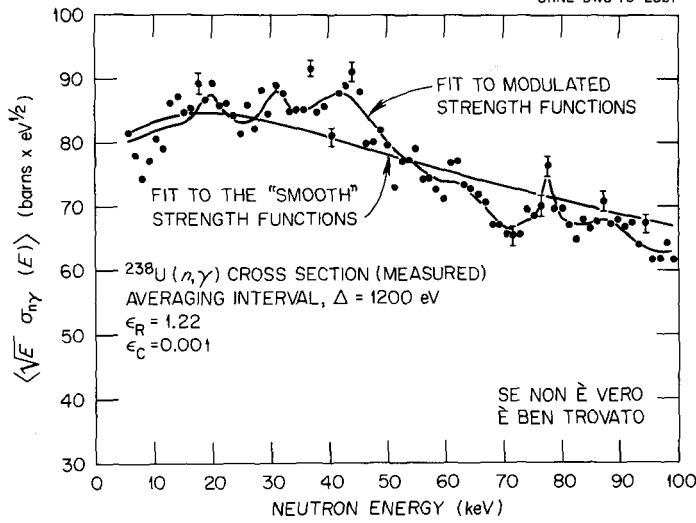


Figure 7

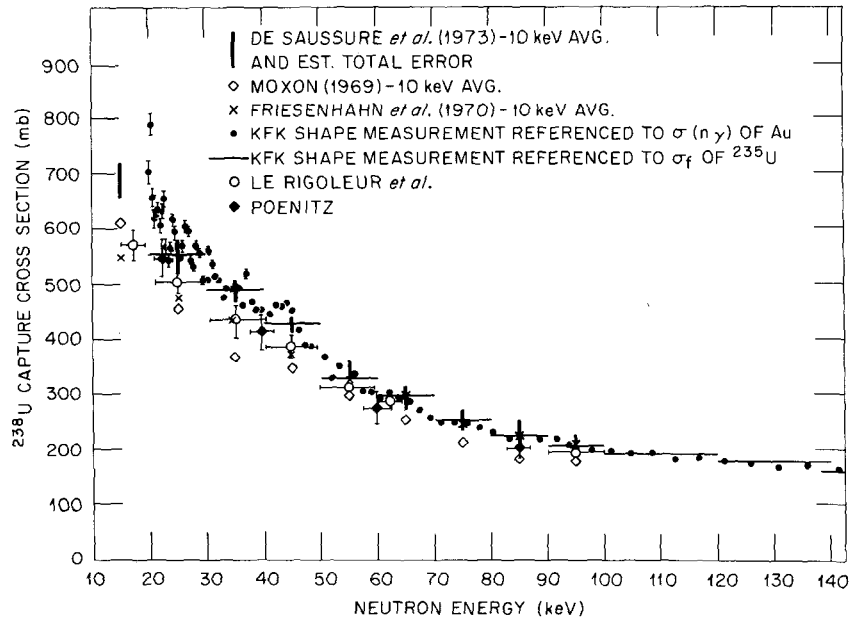


Figure 8

EVALUATION OF ^{238}U CROSS SECTIONS FOR ENDF/B-IV

F. J. McCrosson

Savannah River Laboratory
E. I. du Pont de Nemours & Co.
Aiken, South Carolina 29801

INTRODUCTION

In this paper, the evaluation of the ^{238}U cross sections below 4 keV for ENDF/B-IV will be discussed. These cross sections were reevaluated because the Data Testing Subcommittee of the Cross Section Evaluation Working Group (CSEWG) found ENDF/B-III did not accurately predict several important parameters for thermal systems. For example, in both D_2O - and H_2O -moderated lattices of natural or slightly enriched uranium rods, k_{eff} is underpredicted using Version III by 1.5%. This underprediction has been attributed to a 10% overprediction of ^{238}U epithermal neutron capture.¹

These thermal data testing results have raised questions concerning the ENDF/B-III cross sections because the calculational methods used in the analysis of the benchmark experiments generally have been considered adequate. Several possible deficiencies in the Version III ^{238}U cross sections have been

The information contained in this article was developed during the course of work under Contract No. AT(07-2)-1 with the U. S. Energy Research and Development Administration.

By acceptance of this paper, the publisher and/or recipient acknowledges the U. S. Government's right to retain a nonexclusive, royalty-free license in and to any copyright covering this paper, along with the right to reproduce and to authorize others to reproduce all or part of the copyrighted paper.

proposed; e.g., the existence of systematic errors or spurious p-wave resonances could give rise to excessive ^{238}U neutron capture.

This paper discusses the thermal cross sections; the epithermal cross sections, particularly the s- and p-wave resonances and the background cross sections; and the impact of the new ENDF/B-IV evaluations on thermal lattice calculations.

DISCUSSION

Thermal Cross Sections ($E < 1.0$ eV)

The thermal region in the evaluation spans energies below 1 eV. The cross sections in this region are tabulated in File 3. The evaluation for the thermal cross sections followed the procedures used in the Version II and Version III evaluations; i.e., the evaluation used a multi-level Breit-Wigner formulation that incorporated the first nine low-energy s-wave resonances plus an appropriate complement of bound levels.² The Version IV thermal evaluation differs from ENDF/B-III in two respects: First, the differential capture cross sections were normalized to 2.70 barns at 0.0253 eV, rather than to 2.72 barns. Second, the thermal breakpoint was lowered from 5 to 1 eV to avoid possible problems in accounting for resonance self-shielding for the 6.67-eV resonance.

The lower capture cross sections are in better agreement with the 1969 measurements of Hunt et al.³ of 2.69 ± 0.03 barns and improve prediction of criticality in the thermal benchmark

lattices. They are, however, in poorer agreement with the measurements of Bigham et al.,⁴ which yielded a value of 2.721 ± 0.016 barns.

In addition, the thermal cross sections should include the contributions associated with subthreshold fission as measured by Block et al.,⁵ but these were inadvertently omitted from File 3. The cross section for fission at 0.0253 eV should be 1.918×10^{-6} barn.⁶

Epithermal Cross Sections ($1 \text{ eV} < E < 4 \text{ keV}$)

The epithermal cross sections between 1 eV and 4 keV are described in terms of single-level, Breit-Wigner, s- and p-wave resonance parameters (File 2) and smooth background cross sections (File 3). Table 1 lists the measurements used in the evaluation of the s-wave resonances.⁹⁻¹⁴

One objective of the present evaluation was to minimize systematic differences between the various experiments as much as possible. Perhaps this could best be done by reanalyzing each of the measurements on a resonance-by-resonance basis using the same analysis technique.⁷ However, because this approach would have been too time consuming for the present evaluation, a type of regression analysis was used instead.

In the regression analysis approach, the neutron widths are normalized to a common basis.⁸ The measurements of Rahn et al.⁹ and those of Carraro and Kolar¹² each span the full energy range 1 eV to 4 keV; therefore, either could be used as the basis for

normalization. The Columbia University data⁹ were selected, however, because of the rather large strength functions associated with the Carraro and Kolar data, particularly at higher energies. The resonance energies and Γ_n values of Rahn et al. provide an appropriate standard since they were obtained from a self-consistent analysis of high resolution transmission, self-indication, and Moxon-Rae capture measurements for seven different ^{238}U sample thicknesses.

The regression analysis, of course, does not account for systematic errors within the Columbia measurement itself. A final normalization of the neutron widths was planned to improve the agreement with measured values of ρ^{28} (the ratio of epithermal-to-thermal ^{238}U neutron captures) for benchmark lattice experiments, but this was not done when the results were found to be too insensitive to be useful.

Below 1 keV, the regression analysis consisted of determining the constant C in the relation

$$Y_i = CX_i, \text{ where } i = 1, 2, \dots, N$$

In this relation, X_i denotes the ratio Γ_n/E_0 determined by Rahn et al. for the s-wave resonances, and Y_i denotes the same ratio but as determined from one of the other experiments in Table 1. The index N denotes the number of s-wave resonances below 1 keV. A similar procedure was used to normalize the Carraro and Kolar data to the Rahn et al. data between 1 and 4 keV. The values of C determined from the regression analysis are given in Table 2.

Values of C greater than unity indicate measurements having neutron widths that are on the average greater than those of Rahn et al. The neutron widths of each of the experiments were therefore multiplied by the reciprocal of C to remove the systematic differences.

After the neutron widths were normalized by the regression analysis, the resonance parameters were evaluated on a resonance-by-resonance basis to determine E_0 , Γ_n , and Γ_γ . As part of the evaluation process, the capture resonance integral and the peak capture and total cross sections for each of the various normalized experiments were compared. Tables 3, 4, and 5 give the resonance energies, the normalized neutron widths, and the capture widths for each of the s-wave resonances below 1 keV. The corresponding values for the capture resonance integral and the peak capture and total cross sections for each of these resonances are listed in Tables 6, 7, and 8.* The appropriate formulas are:

$$\text{Capture integral} \quad I_\gamma = \frac{a\pi}{2} g \frac{\Gamma_n \Gamma_\gamma}{\Gamma E_0^2}$$

$$\text{Peak capture cross section} \quad \sigma_0^\gamma = a g \frac{\Gamma_n \Gamma_\gamma}{E_0 \Gamma^2}$$

$$\text{Peak total cross section} \quad \sigma_0^{\text{total}} = a g \frac{\Gamma_n}{E_0 \Gamma}$$

where the left-hand side of each of the equations is in barns,

* Tables 6, 7, and 8 do not indicate the resonance parameters below 100 eV because these parameters are unchanged from Version III.

energy is in eV, g is the statistical spin factor,

$$\Gamma = \Gamma_n + \Gamma_\gamma, \text{ and}$$

$$a = 2.6032 \times 10^6.$$

The resonance parameters that yielded the most consistent values for Γ_γ , σ_0^γ , and σ_0^{total} were selected for the ENDF/B-IV evaluation. Special attention was given to maintaining the coupling between Γ_n and Γ_γ determined in the individual experiments.

The ORELA capture measurements¹⁰ are not reported in terms of resonance parameters; therefore, these measurements had to be factored into the evaluation by an indirect method. The measured capture probabilities as a function of energy below 4 keV have been compared to Monte Carlo calculations using ENDF/B-III data (Figure 1). These comparisons of the capture probabilities together with the Version III resonance parameter information in Tables 3 through 8 provided the needed link to at least qualitatively include the inferences of the ORELA measurements.

Table 9 summarizes the evaluation of the s-wave resonances. Version III and Version IV evaluations differ very little. The infinite dilution resonance integrals in Table 9 were calculated using the narrow resonance approximation. The small differences between the Version III and Version IV infinite dilution resonance integrals probably translate to even smaller differences for effective integrals with high self-shielding.

The current File 2 resonance parameters contain an error, which causes the representation of the subthreshold fission

widths (Γ_f) in ENDF/B-IV to be incorrect. Under the assumption that Γ_γ is 23 meV, the ENDF/B-IV compilation gives fission widths of 0.29 and 0.051 meV for the 720- and 1210-eV resonances, respectively. But in Reference 5, these fission widths correspond to Class II levels with radiation widths of 4.9 meV. When the resonances are assigned to the first well of the double-humped fission barrier, Γ_γ is 23 meV, and Γ_f is 1.2 and 0.12 meV for the 720- and 1210-eV resonances, respectively.

The measurements used in the evaluation of the p-wave resonances are listed in Table 10.^{9,10,15,16,17}

Table 11 gives a partial list of the experimentally determined neutron widths (multiplied by the statistical spin factor, g)* and the resonance energies. The ENDF/B-III p-wave parameters were derived almost entirely from the data of de Saussure et al.¹⁰ and hence provide a measure of the neutron widths for that experiment.

Although the experiments themselves do not isolate the s- and p-wave resonances, it is generally easy to distinguish them because the p-wave levels are typically much weaker. As indicated in Table 11, some experimenters have differed in the assignment of some of the resonances that can be considered as strong p-wave or weak s-wave resonances. With the exception of the resonance at

* The experiments cannot determine g , which can equal 1 or 2 depending on the spin of the compound nucleus.

263.9 eV, the ENDF/B evaluation has used the statistical analysis of Rahn et al.⁹ to distinguish weak levels as p or s. The 263.9-eV resonance must be p-wave to conserve parity since measured spectra for the resonance exhibit E1 radiative transitions to the $5/2^+$ ground state of ^{239}U .¹⁸

In the evaluation below 1200 eV, a supposed p-wave resonance of an experiment was considered spurious and hence ignored if it was not substantiated by another of the experiments considered. For each established p-wave resonance, the neutron width was determined by weighting the measured values according to their reported experimental precision. The Version IV p-wave parameters between 1.2 and 4 keV are almost the same as those in Version III, but with minor modifications to improve the agreement with the ORELA capture cross section measurements.

The p-wave resonance parameter evaluation is summarized in Table 12. Again, only small differences are observed between the Version III and Version IV evaluations. The ENDF/B-IV strength function of 1.89×10^{-4} is based on the p-wave resonances below 500 eV. This value, determined using a channel radius of 8.4 fermi, is consistent with the p-wave strength function obtained from the cross sections in the 10-40 keV range.

The background cross sections between 1 eV and 4 keV that went into File 3 will now be described. A scattering cross section of approximately 2.5 barns was added between 1 eV and the first resonance to provide continuity across the breakpoint

at 1 eV. This addition is required because File 2 includes only the positive energy resonances with their associated interference scattering terms. A similar spectrum of bound level resonances exists and is the origin of this additional 2.5 barns contribution. Capture cross sections between 1 and 100 eV were also added to account for the bound level contribution.

In addition, background cross sections between 0.68 and 4.0 keV were added to account for missed p-wave resonances in the resolved region. These background cross sections are compared with those in Version III in Table 13.

CONCLUSION

ENDF/B-III and ENDF/B-IV calculations of k_{eff} and ρ^{28} for ten CSEWG thermal benchmark experiments are given in Tables 14 and 15.

The five unreflected spheres of uranyl nitrate solution contain 93 wt % ^{235}U and serve as a test of the H_2O and ^{235}U cross sections. The relatively good prediction of criticality for the spheres, particularly for Version IV, indicates no severe problems with H_2O and ^{235}U cross sections in thermal systems.

The two H_2O -moderated lattices of slightly enriched uranium and three D_2O -moderated lattices of natural uranium rods test the ^{238}U thermal and resonance region capture cross sections, in addition to the ^{235}U and moderator cross sections. Although the improvement over Version III is significant, the Version IV calculations still underpredict criticality. Again, this can be

traced to the overprediction of ρ^{28} . Reasonably good predictions of criticality would be achieved if the required reduction in epithermal-to-thermal ^{238}U captures could be accomplished.

Good prediction of criticality could therefore be achieved for the uranyl nitrate solutions and the lattice experiments if epithermal neutron capture in ^{238}U were reduced to yield agreement with ρ^{28} measurements. In light of the present evaluation, however, the required reductions of the epithermal ^{238}U capture cross sections appear to be below the bounds established by the precision of present differential measurements. Thus, the difficulties encountered in thermal data testing may be arising, at least in part, from sources other than cross sections.

REFERENCES

1. F. J. McCrosson, "Thermal Data Testing of ENDF/B-III and Prognosis for ENDF/B-IV," *Trans. Am. Nucl. Soc.*, **18**, 352 (1974).
2. B. R. Leonard, Jr., *Thermal Cross Sections of the Fissile and Fertile Nuclei for ENDF/II*, USAEC Report BNWL-1586 (1971).
3. J. B. Hunt, J. C. Robertson, and T. B. Ryves, "A Measurement of the Thermal Neutron Radiative Capture Cross Section of ^{238}U ," *J. Nucl. Energy*, **23**, 705 (1969).
4. C. B. Bigham, R. W. Durham, and J. Ungrin, "A Direct Measurement of the Thermal Neutron Conversion Ratio of Natural Uranium," *Can. J. Phys.*, **47**, 1317 (1969).
5. R. C. Block, R. W. Hockenbury, R. E. Slovacek, E. B. Bean, and D. S. Cramer, "Subthreshold Fission Induced by Neutrons on ^{238}U ," *Phys. Rev. Letters*, **31**, 247 (1973).
6. R. C. Block, Rensselaer Polytechnic Institute, Troy, N. Y., private communication, March 18, 1975.
7. M. Derrien and P. Ribon, "On the Shape Analysis of Various ^{232}Th and ^{238}U Transmission Data," *Specialists Meeting on Resonance Parameters of Fertile Nuclei and ^{239}Pu* , Saclay, May 20-22, 1974, Report NEANDC(E) 163U, p. 63 (1975).
8. T. A. Pitterle and N. C. Paik, "Studies of Applications of Cross Section Data and Critical Experiment Data to Reactor Design," *Quarterly Progress Report for Period Ending April 30, 1972*, USAEC Report WARD-3045T4B-2 (1972).
9. F. Rahn et al., "Neutron Resonance Spectroscopy. X. ^{232}Th and ^{238}U ," *Phys. Rev.*, **6**, C1854 (1972).
10. G. de Saussure, E. G. Silver, R. B. Perez, R. Ingle, and H. Weaver, *Measurement of the ^{238}U Capture Cross Section for Incident Neutron Energies up to 100 keV*, USAEC Report ORNL-TM-4059 (1973).
11. M. Asghar, C. M. Chaffey, and M. C. Moxon, "Low-Energy Neutron Resonance Parameters of ^{238}U ," *Nucl. Phys.*, **85**, 305 (1966).
12. G. Carraro and W. Kolar, "Neutron Widths of ^{238}U from 60 eV to 5.7 keV," *Nuclear Data for Reactors, Helsinki, Vol. 1*, 403 (June 1970); and "Total Neutron Cross Section Measurements of ^{238}U ," *Proc. Third Conf. Neutron Cross Sections and Technology*, Knoxville, Tenn., March 15-17, 1971, USAEC Report CONF-710301 (Vol. 1).

13. G. Rohr, H. Weigmann, and J. Winter, "Resonance Parameters from Neutron Radiative Capture in ^{238}U ," *Nuclear Data for Reactors, Helsinki, Vol. 1*, 413 (June 1970).
14. Kh. Malétski, L. B. Pikelner, I. M. Salamatin, and É. I. Sharapov, "Radiative Widths of ^{238}U Neutron Resonances," *Soviet Atomic Energy*, 32, 45 (1972).
15. L. M. Bollinger and G. E. Thomas, "p-Wave Resonances of ^{238}U ," *Phys. Rev.*, 171, 1293 (1968).
16. J. B. Garg et al., "Neutron Resonance Spectroscopy. III. ^{232}Th and ^{238}U ," *Phys. Rev.*, 134, B985 (1964).
17. N. W. Glass et al., " ^{238}U Neutron Capture Results from Bomb Source Neutrons," *Proc. 2nd Conf. Neutron Cross Sections and Technology*, Washington, D. C., USAEC Report CONF-680307-20 (1968).
18. O. A. Wasson, R. E. Chrien, G. G. Slaughter, and J. A. Harvey, "Distribution of Partial Radiation Widths in ^{238}U (n, γ) ^{239}U ," *Phys. Rev.* 4, C900 (1971).

TABLE 1		
Sources of Data for Evaluation of s-Wave Resonances		
<i>Experimenters</i>	<i>Type of Measurement</i>	<i>Energy Range</i>
Total and Capture		
Rahn et al. ⁹	Transmission Self-Indication Capture	0-4 keV
de Saussure et al. ¹⁰	Capture	0-4 keV
Asghar et al. ¹¹	Scattering Capture	0-823 eV
Carraro and Kolar ¹²	Transmission	0-4 keV
Rohr et al. ¹³	Capture	66-1055 eV
Maletski et al. ¹⁴	Transmission Capture	66-1197 eV
Fission		
Block et al.	Subthreshold Fission	

TABLE 2					
Normalization Constants for Γ_n					
$\Delta E, \text{ keV}$	<i>Rahn</i> ⁹	<i>Carraro</i> ⁴	<i>Rohr</i> ¹³	<i>Maletski</i> ¹⁴	<i>Asghar</i> ¹¹
0-1.0	1.0	0.962	0.948	0.919	0.772
1.0-1.5	1.0	1.005			
1.5-2.0	1.0	1.074			
2.0-2.5	1.0	1.022			
2.5-3.0	1.0	1.131			
3.0-3.5	1.0	1.200			
3.5-4.0	1.0	1.245			

TABLE 3
Energies of s-Wave Resonances, eV

RAW	FCR	CARRARO	MALETSKI	ASGHAR	ENDF/B-III
0.1025E 03	0.1026E 03	0.1025E 03	0.1024E 03	0.1026E 03	0.1026E 03
0.1169E 03					
0.1456E 03	0.0	0.1456E 03	0.1459E 03	0.0	0.1456E 03
0.1652E 03	0.0	0.1653E 03	0.1656E 03	0.0	0.1653E 03
0.1858E 03	0.1856E 03	0.1866E 03	0.1895E 03	0.1896E 03	0.1856E 03
0.2085E 03	0.2085E 03	0.2084E 03	0.2084E 03	0.2085E 03	0.2084E 03
0.2372E 03	0.2373E 03	0.2373E 03	0.2376E 03	0.2373E 03	0.2373E 03
0.2736E 03	0.2736E 03	0.2736E 03	0.2739E 03	0.2736E 03	0.2736E 03
0.2910E 03	0.2908E 03	0.2908E 03	0.2912E 03	0.2908E 03	0.2908E 03
0.3111E 03	0.0	0.3112E 03	0.3117E 03	0.0	0.3112E 03
0.3477E 03	0.3478E 03	0.3478E 03	0.3481E 03	0.3478E 03	0.3478E 03
0.3779E 03	0.0	0.3768E 03	0.3770E 03	0.0	0.3768E 03
0.3514E 03	0.3576E 03	0.3576E 03	0.3981E 03	0.3976E 03	0.3576E 03
0.4102E 03	0.4102E 03	0.4102E 03	0.4107E 03	0.4102E 03	0.4102E 03
0.4337E 03	0.4341E 03	0.4342E 03	0.4346E 03	0.4341E 03	0.4341E 03
0.4541E 03	0.0	0.4537E 03	0.0	0.0	0.0
0.4628E 03	0.0	0.4632E 03	0.4641E 03	0.0	0.4632E 03
0.4770E 03	0.0	0.4783E 03	0.4794E 03	0.0	0.4783E 03
0.5183E 03	0.5183E 03	0.5183E 03	0.5190E 03	0.5183E 03	0.5183E 03
0.5352E 03	0.5352E 03	0.5352E 03	0.5362E 03	0.5352E 03	0.5352E 03
0.5559E 03	0.0	0.5561E 03	0.0	0.0	0.0
0.5792E 03	0.5800E 03	0.5800E 03	0.5807E 03	0.5800E 03	0.5800E 03
0.5948E 03	0.5950E 03	0.5950E 03	0.5948E 03	0.5950E 03	0.5950E 03
0.6158E 03	0.6158E 03	0.6158E 03	0.6210E 03	0.6198E 03	0.6198E 03
0.6283E 03	0.0	0.6285E 03	0.6250E 03	0.0	0.6285E 03
0.6605E 03	0.6611E 03	0.6611E 03	0.6620E 03	0.6611E 03	0.6611E 03
0.6529E 03	0.6530E 03	0.6530E 03	0.6940E 03	0.6930E 03	0.6530E 03
0.7079E 03	0.7080E 03	0.7080E 03	0.7050E 03	0.0	0.7080E 03
0.7205E 03	0.0	0.7214E 03	0.0	0.0	0.7214E 03
0.7325E 03	0.0	0.7321E 03	0.7330E 03	0.0	0.7321E 03
0.7648E 03	0.0	0.7652E 03	0.7670E 03	0.0	0.7651E 03
0.7788E 03	0.0	0.7795E 03	0.0	0.0	0.7788E 03
0.7504E 03	0.0	0.7510E 03	0.7920E 03	0.0	0.7510E 03
0.8209E 03	0.8218E 03	0.8218E 03	0.8220E 03	0.0	0.8218E 03
0.8506E 03	0.8514E 03	0.8514E 03	0.0	0.0	0.8514E 03
0.8561E 03	0.8563E 03	0.8563E 03	0.0	0.0	0.8563E 03
0.8660E 03	0.0	0.8668E 03	0.8690E 03	0.0	0.8668E 03
0.9045E 03	0.9054E 03	0.9054E 03	0.9070E 03	0.0	0.9054E 03
0.9245E 03	0.0	0.9254E 03	0.0	0.0	0.9254E 03
0.9372E 03	0.9372E 03	0.9372E 03	0.9390E 03	0.0	0.9372E 03
0.9566E 03	0.9589E 03	0.9589E 03	0.9600E 03	0.0	0.9589E 03
0.9580E 03	0.9589E 03	0.9589E 03	0.0	0.0	0.9580E 03
0.9514E 03	0.9519E 03	0.9519E 03	0.0	0.0	0.9519E 03

TABLE 4
Normalized s-Wave Neutron Widths, eV

102.47	BAHN	0.7600E-01	ROHZ	0.7658E-01	MALETSKI	ASGHAR	ENDE/B-II
116.82		0.3500E-01		0.2821E-01	0.7617E-01	0.7596E-01	0.4550E-01
145.57		0.6400E-03	0.0	0.2944E-01	0.2944E-01	0.2992E-01	0.2720E-01
165.21		0.3680E-02	0.0	0.9252E-03	0.5140E-03	0.0	0.8500E-03
185.80		0.1790E 00	0.0	0.1784E 00	0.1784E 00	0.1725E 00	0.1650E 00
208.49		0.5900E-01	0.5145E-01	0.5509E-01	0.5223E-01	0.6489E-01	0.5300E-01
237.20		0.3500E-01	0.2753E-01	0.2511E-01	0.2538E-01	0.3238E-01	0.2823E-01
273.56		0.2690E-01	0.2760E-01	0.2692E-01	0.2394E-01	0.2689E-01	0.2550E-01
291.01		0.1110E-01	0.1698E-01	0.1553E-01	0.1764E-01	0.1810E-01	0.1500E-01
311.13		0.1560E-02	0.0	0.1142E-02	0.5733E-03	0.0	0.1100E-02
347.74		0.8200E-01	0.8618E-01	0.8690E-01	0.8487E-01	0.7435E-01	0.8360E-01
377.03		0.9700E-02	0.0	0.1313E-02	0.5753E-03	0.0	0.1260E-02
357.35		0.6330E-02	0.6751E-02	0.6580E-02	0.5114E-02	0.6412E-02	0.6330E-02
410.18		0.1500E-01	0.2059E-01	0.2141E-01	0.2176E-01	0.1843E-01	0.2060E-01
433.70		0.8750E-02	0.1065E-01	0.9979E-02	0.8735E-02	0.1319E-01	0.9603E-02
454.10		0.4300E-03	0.0	0.4762E-03	0.0	0.0	0.0
462.80		0.4500E-02	0.0	0.5765E-02	0.5440E-02	0.0	0.5550E-02
477.51		0.3850E-02	0.0	0.4127E-02	0.3808E-02	0.0	0.3970E-02
518.27		0.4890E-01	0.5158E-01	0.5763E-01	0.4570E-01	0.5065E-01	0.5550E-01
535.21		0.4310E-01	0.4536E-01	0.4659E-01	0.5985E-01	0.5026E-01	0.4523E-01
555.50		0.7470E-02	0.0	0.7276E-03	0.0	0.0	0.0
579.87		0.4090E-01	0.4483E-01	0.4584E-01	0.3917E-01	0.4863E-01	0.4410E-01
594.84		0.8510E-01	0.8587E-01	0.8773E-01	0.1012E 00	0.9248E-01	0.8443E-01
619.75		0.2150E-01	0.2144E-01	0.3378E-01	0.3591E-01	0.3303E-01	0.3250E-01
628.25		0.5560E-02	0.0	0.6548E-02	0.7617E-02	0.0	0.6700E-02
660.50		0.1380E 00	0.1300E 00	0.1372E 00	0.1632E 00	0.1356E 00	0.1320E 00
652.90		0.4210E-01	0.4442E-01	0.4553E-01	0.4352E-01	0.4406E-01	0.4380E-01
707.90		0.2100E-01	0.2352E-01	0.2308E-01	0.2176E-01	0.0	0.2420E-01
726.90		0.1340E-02	0.0	0.1518E-02	0.0	0.0	0.1460E-02
732.50		0.1080E-02	0.0	0.1653E-02	0.3808E-02	0.0	0.1590E-02
764.80		0.8020E-02	0.0	0.5509E-02	0.7617E-02	0.0	0.8207E-02
778.80		0.1470E-02	0.0	0.1575E-02	0.0	0.0	0.2209E-02
790.40		0.5600E-02	0.0	0.7173E-02	0.6525E-02	0.0	0.6009E-02
823.90		0.6560E-01	0.6312E-01	0.7063E-01	0.7181E-01	0.0	0.6530E-01
856.60		0.5510E-01	0.5669E-01	0.6757E-01	0.0	0.0	0.6300E-01
856.10		0.8110E-01	0.8270E-01	0.5663E-01	0.0	0.0	0.8633E-01
866.00		0.5400E-02	0.0	0.6861E-02	0.5440E-02	0.0	0.5700E-02
904.50		0.4300E-01	0.5200E-01	0.5673E-01	0.4352E-01	0.0	0.5620E-01
924.50		0.5730E-02	0.0	0.1507E-01	0.0	0.0	0.1391E-01
936.60		0.1440E 00	0.1366E 00	0.1507E 00	0.1306E 00	0.0	0.1376E 00
958.00		0.2030E 00	0.1904E 00	0.2225E 00	0.1415E 00	0.0	0.1960E 00
951.40		0.3900E 00	0.3599E 00	0.4200E 00	0.0	0.0	0.3770E 00

TABLE 5
s-Wave Capture Widths, eV

102.47	RAHN	0.2800E-01	ROHR	0.2610E-01	CARRARO	MALETSKI	ASGHAR	ENDF/B-III	1
116.82		0.2000E-01		0.2430E-01	0.2355E-01	0.2300E-01	0.2595E-01	0.2610E-01	2
145.57		0.2355E-01		0.0	0.2355E-01	0.2300E-01	0.2572E-01	0.2430E-01	3
155.21		0.1800E-01		0.0	0.2355E-01	0.2355E-01	0.0	0.2350E-01	4
185.83		3.2700E-01		0.2470E-01	0.2355E-01	0.2200E-01	0.2321E-01	0.2470E-01	5
208.45		0.2200E-01		0.2240E-01	0.2355E-01	0.2600E-01	0.2149E-01	0.2350E-01	6
237.20		3.2300E-01		0.2450E-01	0.2355E-01	0.2600E-01	0.1953E-01	0.2450E-01	7
273.56		0.2300E-01		0.2355E-01	0.2355E-01	0.2500E-01	0.2391E-01	0.2350E-01	8
291.01		0.2200E-01		0.2355E-01	0.2355E-01	0.2300E-01	0.2240E-01	0.2350E-01	9
311.13		0.2355E-01		0.2355E-01	0.2355E-01	0.2200E-01	0.0	0.2350E-01	10
347.74		0.2600E-01		0.2355E-01	0.2355E-01	0.2200E-01	0.2040E-01	0.2500E-01	11
377.03		0.2355E-01		0.0	0.2355E-01	0.2355E-01	0.0	0.2350E-01	12
387.36		3.2300E-01		0.2520E-01	0.2355E-01	0.2355E-01	0.3750E-01	0.3000E-01	13
410.18		0.1800E-01		0.2260E-01	0.2355E-01	0.2500E-01	0.2661E-01	0.2350E-01	14
433.70		0.2000E-01		0.2650E-01	0.2355E-01	0.2355E-01	0.2510E-01	0.2650E-01	15
454.13		0.2355E-01		0.0	0.2355E-01	0.0	0.0	0.0	16
462.80		0.2355E-01		0.0	0.2355E-01	0.2355E-01	0.0	0.2350E-01	17
477.00		0.2355E-01		0.0	0.2355E-01	0.2355E-01	0.0	0.2350E-01	18
518.27		0.2400E-01		0.2440E-01	0.2355E-01	0.2300E-01	0.5120E-02	0.2440E-01	19
535.21		0.2300E-01		0.2470E-01	0.2355E-01	0.2300E-01	0.2930E-01	0.2470E-01	20
555.90		0.2355E-01		0.0	0.2355E-01	0.0	0.0	0.0	21
575.67		0.2100E-01		0.2610E-01	0.2355E-01	0.2300E-01	0.2200E-01	0.2610E-01	22
594.84		0.2000E-01		0.2310E-01	0.2355E-01	0.2400E-01	0.2179E-01	0.2350E-01	23
615.75		0.1900E-01		0.2460E-01	0.2355E-01	0.2400E-01	0.3310E-01	0.2460E-01	24
628.25		0.2355E-01		0.0	0.2355E-01	0.2355E-01	0.0	0.2350E-01	25
660.90		0.2500E-01		0.2600E-01	0.2355E-01	0.2200E-01	0.2312E-01	0.2600E-01	26
652.50		0.2200E-01		0.2410E-01	0.2355E-01	0.2400E-01	0.2020E-01	0.2410E-01	27
707.90		0.2100E-01		0.2850E-01	0.2355E-01	0.2600E-01	0.0	0.2850E-01	28
720.52		3.2355E-01		0.0	3.2355E-01	0.0	0.0	0.2350E-01	29
732.50		0.2355E-01		0.0	0.2355E-01	0.2355E-01	0.0	0.2350E-01	30
764.80		0.1700E-01		0.0	0.2355E-01	0.0	0.0	0.2850E-01	31
778.80		0.2355E-01		0.0	0.2355E-01	0.0	0.0	0.2350E-01	32
790.40		0.2355E-01		0.0	0.2355E-01	0.2355E-01	0.0	0.2850E-01	33
820.90		0.2000E-01		0.2600E-01	0.2355E-01	0.2400E-01	0.0	0.2600E-01	34
850.60		0.2500E-01		0.3090E-01	0.2355E-01	0.0	0.0	0.3090E-01	35
856.10		0.2300E-01		0.2360E-01	0.2355E-01	0.0	0.0	0.2350E-01	36
866.00		0.2355E-01		0.0	3.2355E-01	0.2355E-01	0.0	0.2350E-01	37
504.50		0.2200E-01		0.2680E-01	0.2355E-01	0.2500E-01	0.0	0.2680E-01	38
924.50		0.2500E-01		0.0	0.2355E-01	0.0	0.0	0.2350E-01	39
936.63		3.2500E-01		0.2360E-01	0.2355E-01	0.2400E-01	0.0	0.2350E-01	40
558.00		0.2100E-01		0.2270E-01	0.2355E-01	0.2200E-01	0.0	0.2350E-01	41
551.40		0.3000E-01		3.3070E-01	0.2355E-01	0.0	0.0	3.3070E-01	42

TABLE 6
s-wave Capture Integrals, barns

	RAM	BOHR	CARRARO	MALTSKI	ASCHAR	ENDE/R-III
132.47	0.7789E 01	0.7561E 01	0.8008E 01	0.7555E 01	0.7532E 01	0.7371E 01
116.82	0.3814E 01	0.4008E 01	0.3848E 01	0.3510E 01	0.4159E 01	0.3840E 01
145.57	0.1565E 00	0.0	0.1718E 00	0.1652E 00	0.0	0.1654E 00
165.21	0.3543E 00	0.0	0.4601E 00	0.4289E 00	0.0	0.4445E 00
189.80	0.2663E 01	0.2467E 01	0.2361E 01	0.2230E 01	0.2327E 01	0.22451E 01
208.45	0.1507E 01	0.1470E 01	0.1536E 01	0.1634E 01	0.1519E 01	0.1533E 01
237.20	0.1035E 01	0.9414E 00	0.9451E 00	0.9991E 00	0.8847E 00	0.9520E 00
273.56	0.6598E 00	0.6801E 00	0.6851E 00	0.6665E 00	0.6914E 00	0.6730E 00
291.31	0.4645E 01	0.4733E 00	0.4536E 00	0.4846E 00	0.4840E 00	0.4427E 01
311.13	0.4285E 01	0.0	0.4404E 01	0.3957E 01	0.0	0.4437E 01
347.74	0.6640E 00	0.6242E 00	0.6265E 00	0.5895E 00	0.5411E 00	0.6506E 00
377.03	0.2680E 01	0.0	0.3627E 01	0.2709E 01	0.0	0.3444E 01
387.35	0.1221E 00	0.1371E 00	0.1330E 00	0.1084E 00	0.1416E 00	0.1352E 00
410.18	0.2246E 00	0.2645E 00	0.2725E 00	0.2829E 00	0.2646E 00	0.2668E 00
433.70	0.1323E 00	0.1645E 00	0.1520E 00	0.1376E 00	0.1573E 00	0.1529E 00
454.10	0.8374E 02	0.0	0.5305E 02	0.0	0.0	0.0
462.63	0.7213E 01	0.0	0.8033E 01	0.4359E 01	0.0	0.8557E 01
477.00	0.4553E 01	0.0	0.6276E 01	0.5831E 01	0.0	0.6071E 01
518.27	0.2451E 00	0.2521E 00	0.2246E 00	0.2325E 00	0.7078E 01	0.2580E 00
535.21	0.2174E 00	0.2283E 00	0.2239E 00	0.2363E 00	0.2642E 00	0.2280E 00
555.90	0.9083E 02	0.0	0.5234E 02	0.0	0.0	0.0
579.87	0.1687E 00	0.2005E 00	0.1891E 00	0.1742E 00	0.1841E 00	0.1993E 00
594.84	0.1871E 00	0.2123E 00	0.2145E 00	0.2242E 00	0.2037E 00	0.2123E 00
619.75	0.1203E 00	0.1473E 00	0.1477E 00	0.1525E 00	0.1760E 00	0.1490E 00
628.23	0.4454E 01	0.0	0.5564E 01	0.5948E 01	0.0	0.5357E 01
650.90	0.2243E 00	0.2027E 00	0.1881E 00	0.1809E 00	0.1983E 00	0.2032E 00
682.90	0.1231E 00	0.1332E 00	0.1321E 00	0.1315E 00	0.1153E 00	0.1324E 00
737.53	0.8568E 01	0.1051E 00	0.5508E 01	0.8637E 01	0.0	0.1668E 00
720.90	0.5576E 02	0.0	0.1120E 01	0.0	0.0	0.1080E 01
732.50	0.7870E 02	0.0	0.1178E 01	0.2495E 01	0.0	0.1136E 01
764.80	0.3810E 01	0.0	0.3118E 01	0.4000E 01	0.0	0.4363E 01
778.80	0.1051E 01	0.0	0.1226E 01	0.0	0.0	0.1354E 01
780.40	0.3088E 01	0.0	0.3593E 01	0.3322E 01	0.0	0.4082E 01
820.90	0.5281E 01	0.1059E 00	0.1070E 00	0.1089E 00	0.0	0.1126E 00
850.60	0.9271E 01	0.1142E 00	0.8551E 01	0.0	0.0	0.1169E 00
856.10	0.5557E 01	0.1024E 00	0.1054E 00	0.0	0.0	0.1030E 00
866.00	0.2249E 01	0.0	0.2891E 01	0.2393E 01	0.0	0.2497E 01
904.50	0.7589E 01	0.8822E 01	0.8384E 01	0.7853E 01	0.0	0.9052E 01
924.50	0.3551E 01	0.0	0.4388E 01	0.0	0.0	0.4170E 01
936.60	0.5530E 01	0.9368E 01	0.5482E 01	0.5402E 01	0.0	0.9339E 01
958.00	0.6479E 01	0.9020E 01	0.9470E 01	0.6447E 01	0.0	0.9332E 01
991.40	0.1155E 00	0.1176E 00	0.5269E 01	0.0	0.0	0.1180E 00

TABLE 7

s-Wave Peak Capture Cross Sections, barns

	RAHN	ROHR	CARRARO	MALETSKI	ASGHAR	ENDF/B-III
102.47	0.5185E 04	0.4810E 04	0.4706E 04	0.4823E 04	0.4816E 04	0.5036E 04
116.82	0.5157E 04	0.5509E 04	0.5522E 04	0.5565E 04	0.5535E 04	0.5549E 04
145.57	0.5547E 03	0.0	0.6504E 03	0.6421E 03	0.0	0.6286E 03
165.21	0.1566E 04	0.0	0.1787E 04	0.1683E 04	0.0	0.1739E 04
185.80	0.1582E 04	0.1465E 04	0.1421E 04	0.1382E 04	0.1435E 04	0.1528E 04
208.49	0.2470E 04	0.2634E 04	0.2620E 04	0.2712E 04	0.2533E 04	0.2658E 04
237.20	0.2648E 04	0.2733E 04	0.2712E 04	0.2729E 04	0.2574E 04	0.2729E 04
273.56	0.2348E 04	0.2364E 04	0.2368E 04	0.2375E 04	0.2370E 04	0.2373E 04
291.01	0.2201E 04	0.2186E 04	0.2145E 04	0.2195E 04	0.2213E 04	0.2129E 04
311.13	0.3449E 03	0.0	0.3694E 03	0.3201E 03	0.0	0.3573E 03
347.74	0.1384E 04	0.1260E 04	0.1256E 04	0.1223E 04	0.1265E 04	0.1326E 04
377.03	0.2623E 03	0.0	0.3497E 03	0.2647E 03	0.0	0.3337E 03
387.39	0.1103E 04	0.1091E 04	0.1118E 04	0.1181E 04	0.1164E 03	0.9420E 03
410.18	0.1585E 04	0.1564E 04	0.1583E 04	0.1577E 04	0.1534E 04	0.1580E 04
433.70	0.1271E 04	0.1266E 04	0.1253E 04	0.1180E 04	0.1232E 04	0.1171E 04
454.10	0.1010E 03	0.0	0.1119E 03	0.0	0.0	0.0
462.80	0.7976E 03	0.0	0.8883E 03	0.8551E 03	0.0	0.8686E 03
477.00	0.5540E 03	0.0	0.6505E 03	0.6507E 03	0.0	0.6729E 03
518.27	0.1109E 04	0.1355E 04	0.1034E 04	0.1117E 04	0.4188E 03	0.1065E 04
535.21	0.1088E 04	0.1110E 04	0.1082E 04	0.9736E 03	0.1132E 04	0.1111E 04
555.80	0.1325E 03	0.0	0.1361E 03	0.0	0.0	0.0
573.87	0.1066E 04	0.1044E 04	0.1006E 04	0.7609E 01	0.9626E 03	0.1048E 04
594.84	0.6743E 03	0.7117E 03	0.7308E 03	0.6782E 03	0.6752E 03	0.7453E 03
615.75	0.1012E 04	0.1034E 04	0.1016E 04	0.1007E 04	0.1050E 04	0.1030E 04
628.29	0.6184E 03	0.0	0.7295E 03	0.7642E 03	0.0	0.7150E 03
660.90	0.5652E 03	0.5470E 03	0.4523E 03	0.4116E 03	0.5192E 03	0.5413E 03
652.90	0.8455E 03	0.8554E 03	0.8449E 03	0.8554E 03	0.8302E 03	0.8601E 03
707.50	0.5193E 03	0.5108E 03	0.9191E 03	0.9107E 03	0.0	0.5131E 03
720.90	0.1839E 03	0.0	0.3053E 03	0.0	0.0	0.1987E 03
732.50	0.1490E 03	0.0	0.2179E 03	0.6256E 03	0.0	0.2111E 03
764.80	0.7413E 03	0.0	0.3227E 03	0.6267E 03	0.0	0.5823E 03
778.80	0.2057E 03	0.0	0.2384E 03	0.0	0.0	0.2614E 03
790.40	0.5276E 02	0.0	0.5889E 03	0.5586E 03	0.0	0.5632E 03
820.90	0.5706E 03	0.6676E 03	0.5538E 03	0.5946E 03	0.0	0.6452E 03
850.60	0.6359E 03	0.6510E 03	0.5860E 03	0.0	0.0	0.6751E 03
856.10	0.5234E 03	0.5251E 03	0.4820E 03	0.0	0.0	0.5114E 03
866.00	0.4342E 03	0.0	0.5247E 03	0.4547E 03	0.0	0.4718E 03
904.50	0.6155E 03	0.6453E 03	0.5874E 03	0.6651E 03	0.0	0.6286E 03
924.50	0.5679E 03	0.0	0.6659E 03	0.0	0.0	0.6569E 03
936.60	0.3489E 03	0.3489E 03	0.3246E 03	0.3664E 03	0.0	0.3471E 03
558.00	0.2305E 03	0.2564E 03	0.2350E 03	0.2599E 03	0.0	0.2355E 03
991.40	0.1742E 03	0.1901E 03	0.1320E 03	0.0	0.0	0.1827E 03

TABLE 8
s-Wave Peak Total Cross Sections, barns

	BAHN	FCR	CARRARO	MALETSKI	ASGHAR	ENDF/B-III
102.47	0.1815E 05	0.1852E 05	0.1518E 05	0.1895E 05	0.1891E 05	0.1845E 05
116.82	0.1418E 05	0.1228E 05	0.1215E 05	0.1136E 05	0.1158E 05	0.1176E 05
149.57	0.6159E 03	0.0	0.5759E 03	0.6671E 03	0.0	0.6524E 03
165.21	0.2502E 04	0.0	0.2059E 04	0.1948E 04	0.0	0.1990E 04
189.30	0.1192E 05	0.1206E 05	0.1211E 05	0.1223E 05	0.1210E 05	0.1158E 05
208.45	0.5055E 04	0.8710E 04	0.8749E 04	0.8340E 04	0.9379E 04	0.8654E 04
237.20	0.6510E 04	0.5804E 04	0.6063E 04	0.5812E 04	0.6843E 04	0.5870E 04
273.54	0.5259E 04	0.5128E 04	0.5075E 04	0.4649E 04	0.5036E 04	0.4588E 04
291.01	0.3912E 04	0.3753E 04	0.3566E 04	0.3906E 04	0.4000E 04	0.3488E 04
311.13	0.3404E 03	0.0	0.3673E 03	0.3334E 03	0.0	0.3743E 03
347.74	0.5653E 04	0.5881E 04	0.5890E 04	0.5939E 04	0.5873E 04	0.5762E 04
377.03	0.2731E 03	0.0	0.2698E 03	0.2757E 03	0.0	0.3516E 03
557.35	0.1404E 04	0.1383E 04	0.1430E 04	0.1167E 04	0.1560E 03	0.1141E 04
410.18	0.3259E 04	0.3056E 04	0.3022E 04	0.2950E 04	0.22597E 04	0.2964E 04
433.70	0.1827E 04	0.1720E 04	0.1784E 04	0.1617E 04	0.1732E 04	0.1555E 04
454.10	0.1528E 03	0.0	0.1142E 03	0.0	0.0	C.0
462.80	0.5624E 03	0.0	0.1106E 04	0.1053E 04	0.0	0.1074E 04
477.00	0.658E 03	0.0	0.8115E 03	C.7559E 03	0.0	0.7865E 03
518.27	0.3369E 04	0.3410E 04	0.3567E 04	0.3337E 04	0.4561E 04	0.3489E 04
535.21	0.3221E 04	0.3149E 04	0.3240E 04	0.3507E 04	0.3073E 04	0.3145E 04
555.90	0.1365E 03	0.0	0.1403E 03	0.0	0.0	0.0
579.87	0.2566E 04	0.2837E 04	0.2565E 04	0.2622E 01	0.3090E 04	0.2820E 04
594.84	0.3544E 04	0.3480E 04	0.3449E 04	0.3538E 04	0.3541E 04	0.3422E 04
615.75	0.2499E 04	0.2363E 04	0.2475E 04	0.2513E 04	0.2058E 04	0.2351E 04
628.25	0.7565E 03	0.0	0.5453E 03	0.1011E 04	0.0	0.5189E 03
660.90	0.3255E 04	0.3281E 04	0.3361E 04	0.3465E 04	0.3322E 04	0.3293E 04
682.53	0.2468E 04	0.2439E 04	0.2471E 04	0.2418E 04	0.2518E 04	0.2423E 04
707.90	0.1839E 04	0.1663E 04	0.1820E 04	0.1673E 04	0.0	0.1688E 04
720.90	0.1944E 03	0.0	0.2182E 03	0.0	0.0	0.2111E 03
732.50	0.1558E 03	0.0	0.2332E 03	0.4944E 03	0.0	0.2253E 03
764.80	0.1091E 04	0.0	0.6450E 03	0.8294E 03	0.0	0.7457E 03
778.80	0.2213E 03	0.0	0.2584E 03	0.0	0.0	0.2859E 03
750.40	0.658E 03	0.0	0.7683E 03	0.7134E 03	0.0	0.7213E 03
820.90	0.2425E 04	0.2211E 04	0.2376E 04	0.2374E 04	0.0	0.2266E 04
850.63	0.2159E 04	0.2002E 04	0.2267E 04	0.0	0.0	0.2051E 04
856.10	0.2569E 04	0.2365E 04	0.2438E 04	0.0	0.0	0.2389E 04
866.00	0.5264E 03	0.0	0.6775E 03	0.5622E 03	0.0	0.5868E 03
924.50	0.1866E 04	0.1857E 04	0.1059E 04	0.1823E 04	0.0	0.1947E 04
936.60	0.7889E 03	0.0	0.1059E 04	0.0	0.0	0.1045E 04
958.00	0.2368E 04	0.2368E 04	0.2406E 04	0.2342E 04	0.0	0.2371E 04
991.40	0.2438E 04	0.2418E 04	0.2485E 04	0.0	0.0	0.2424E 04
						0.2427E 04

TABLE 9		
Summary of s-Wave Resonances		
	<i>ENDF/B-III</i> ^a	<i>ENDF/B-IV</i>
No. of Resonances	199	190
$\langle \Gamma_{\gamma} \rangle$, meV	23.5	23.5
S_0 , 10^{-4}		
0-1 keV	1.002	1.005
1-2 keV	1.083	1.109
2-3 keV	1.119	1.122
3-4 keV	0.974	1.013
0-4 keV	1.045	1.062
$\langle D \rangle$, eV		
0-1 keV	20.0	21.3
1-2 keV	20.8	21.3
2-3 keV	18.9	20.8
3-4 keV	20.8	20.8
0-4 keV	20.1	21.05
I_{γ} , barns		
0-1 keV	269.77	269.37
1-2 keV	1.15	1.12
2-3 keV	0.49	0.45
3-4 keV	0.25	0.25
0-4 keV	271.63	271.19

^a. From Reference 8.

TABLE 10
Sources of Data for Evaluation of p-Wave Resonances

<i>Experimenters</i>	<i>Type of Measurement</i>	<i>Energy Range</i>
Bollinger and Thomas ¹⁵	Transmission	0-174 eV
Rahn et al. ⁹	Transmission Self-Indication Capture	0-4 keV
de Sausurre et al. ¹⁰	Capture	0-4 keV
Garg et al. ¹⁶	Transmission	0-4 keV
Glass et al. ¹⁷	Capture	30-2050 eV

TABLE 11
Comparison of p-Wave Resonances

E_0, eV	$g\Gamma_n, 10^{-6} eV$				
	<i>Bollinger</i> ¹⁵	<i>Glass</i> ¹⁷	<i>Rahn</i> ⁹	<i>ENDF/B-III</i>	<i>Recommended</i>
10.22	1.56 ±0.01		1.77 ±0.36	1.50	1.56
11.00				0.3064	-
11.32	0.358 ±0.006				-
16.30	0.053 ±0.015				-
19.50	1.0 ±0.1		1.37 ±0.57	0.97	1.00
45.19	0.83 ±0.15	1.0 ±0.5	2.0 ±1.0	3.00	1.00
47.5		1.8 ±0.8		0.80	-
49.5	0.68 ±0.23	0.5 ±0.3		1.50	0.60
56.4		0.6 ±0.2		1.20	-
57.9	0.48 ±0.08				-
63.54	5.5 ±1.5	4.8 ±2.0	6.0 ±2.6	17.2	5.50
72.8		10.8 ±5.0		5.215	-
74.4		2.7 ±1.0			-
83.57	7.0 ±0.7	6.4 ±1.0	4.0 ±2.0	12.93	6.30
89.19	85.0 ±4.0	85.0 ±3.0	89.8 ±10.9	96.00 ^a	90.00
91.0		6.0 ±6.0		6.00	6.00
93.3	3.0 ±0.6	4.0 ±2.0		12.11	5.00
98.2		4.8 ±1.0		13.09	8.00

a. Treated as s-wave in ENDF/B-III

TABLE 12

Summary of p-Wave Resonances

	<i>ENDB/B-III</i>	<i>ENDF/B-IV</i>
No. p-Wave Resonances	258	220
S_1 , 10^{-4} (Below 500 eV)		1.89
I_γ , barn (p-Wave Resonances)		
0 -1.0 keV	0.403	0.369
1.0-2.0 keV	0.106	0.108
2.0-3.0 keV	0.036	0.050
3.0-4.0 keV	0.033	0.034
0 -4.0 keV	0.578	0.561

TABLE 13

Background Cross Sections Between 0.68 and 4.0 keV

Energy, eV	Capture Cross Section, barn	
	<i>ENDF/B-III</i>	<i>ENDF/B-IV</i>
680	0	0
700	0.005	0.005
980	0.05	0.02
1000	0.08	0.05
2000	0.16	0.11
2100	0.17	0.12
2500	0.22	0.15
3000	0.25	0.17
4000	0.28	0.19
I_γ , barn (0.68-4.0 keV)	0.255	0.171

TABLE 14

Criticality

Benchmark	Description	k_{eff}							
		ANL	BAPL	ORNL	GGA	ORNL	SRL	ENDF/B-III	ENDF/B-IV
ORNL	Unreflected spheres of uranyl nitrate solution								
-1	H/ ²³⁵ U = 1378; R = 34.595 cm		0.9965		0.9999		0.9973		0.9996
-2	H/ ²³⁵ U = 1177; R = 34.595 cm		0.9963		0.9995				
-3	H/ ²³⁵ U = 1033; R = 34.595 cm		0.9933		0.9963				
-4	H/ ²³⁵ U = 971; R = 34.595 cm		0.9947		0.9980		0.9958		0.9976
-10	H/ ²³⁵ U = 1835; R = 61.011 cm		0.9931		0.9956		0.9935		0.9951
TRX	H ₂ O-moderated U lattices								
-1	Mod/Fuel = 2.35	0.9741	0.9872	0.9808	0.9791	0.985	0.9766	0.9875	
-2	Mod/Fuel = 4.02	0.9823	0.9913	0.9876	0.9924	0.998	0.9859	0.9941	
MIT	D ₂ O-moderated U lattice								
-1	Mod/Fuel = 20.74			0.9801	0.9888	0.984	0.9735	0.9883	
-2	Mod/Fuel = 25.88			0.9804	0.9925	0.974	0.9752	0.9888	
-3	Mod/Fuel = 34.59			0.9826	0.9996	0.975	0.9788	0.9911	

TABLE 15
Ratio of Epithermal-to-Thermal ²³⁵U Captures^a

Benchmark	Exp	^ρ ₂₈							
		ANC	ENDE/B-III BAPL	ORNL	GGA	ORNL	SRL	ENDE/B-IV SRL	
TRX-1	1.311 ± 0.020	1.438	1.422	1.419	1.416	1.44	1.454	1.417	
TRX-2	0.830 ± 0.015	0.906	0.899	0.874	0.877	0.91	0.890	0.868	
MIT-1	0.498 ± 0.008			0.5319	0.534	0.535	0.5683	0.5464	
MIT-2	0.394 ± 0.002			0.4365	0.435	0.430	0.4659	0.4483	
MIT-3	0.305			0.3400	0.334	0.346	0.3624	0.3490	

^a. Thermal cutoff energy = 0.625 eV

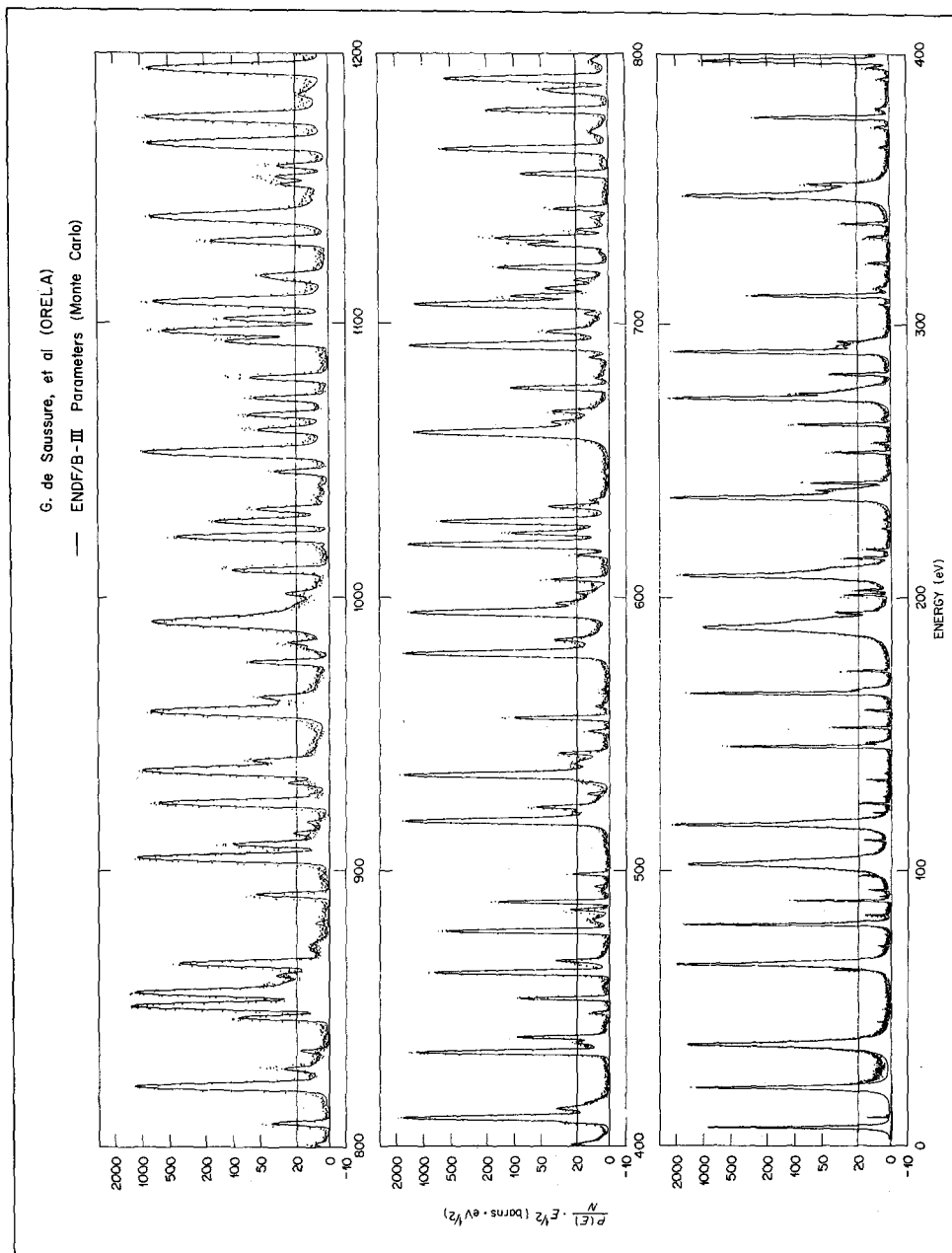


FIGURE 1 Comparison of ENDF/B-III and ORELA Capture Measurements

Comments on the U-238 Discrepancy

R. E. Chrien
Brookhaven National Laboratory

The performance of thermal reactors using light water moderation and slightly enriched uranium fuel is not well predicted from microscopic nuclear parameters. The problem lies in neutron capture by U-238. The capture is overpredicted using commonly accepted resonance parameters from the ENDF-B IV file, and as a consequence the predicted critical eigenvalue for thermal critical assemblies is significantly less than one.

Because the uranium is present in lumped fuel elements, the quantity of most importance is the heavily shielded resonance capture integral. Phrased in another way, it is the cross section between resonances which assumes crucial importance in this instance. Since the dilute resonance integral is fixed to the measured thermal capture cross section, through the device of assuming a sufficient bound level cross section, we can be reasonably sure that the cross section in the thermal region, and below the first resonance at 6.67 eV, is adequately represented by the parameters.

Above the 6.67 eV resonance however, there is a mechanism which could lead to an over estimate of the true capture cross section, if the parameters have been selected to produce the correct thermal cross section. This mechanism is the existence of an asymmetry in the 6.67 eV capture resonance. Now, in fact, the symmetry imputed to a capture resonance is essentially approximate in character, resulting from the large number of exit channels available for radiative capture. The radiative width amplitudes have random signs, and the sum of a large number of these causes approximate cancellation of level-level interference effects.

In U-238, however, it is well known^{1,2} that the capture from thermal to the first resonance exhibits an anomalously high probability for populating the 720 keV $1/2^-$ state of U-239. At thermal this 4059 keV line represents $\sim 11\%$ of total capture, far larger than any of the others. Accordingly, the presence of this anomalous transition may introduce a significant asymmetry in the shape of the first resonance. The interference associated with this transition is constructive below the 6.67 eV resonance, and destructive

above.¹ Since a fit to total capture is forced at thermal, the result of this asymmetry is a reduction of the cross section above the resonance. Use of a normal Breit-Wigner curve will consequently over-predict the cross section above 6.67 eV.

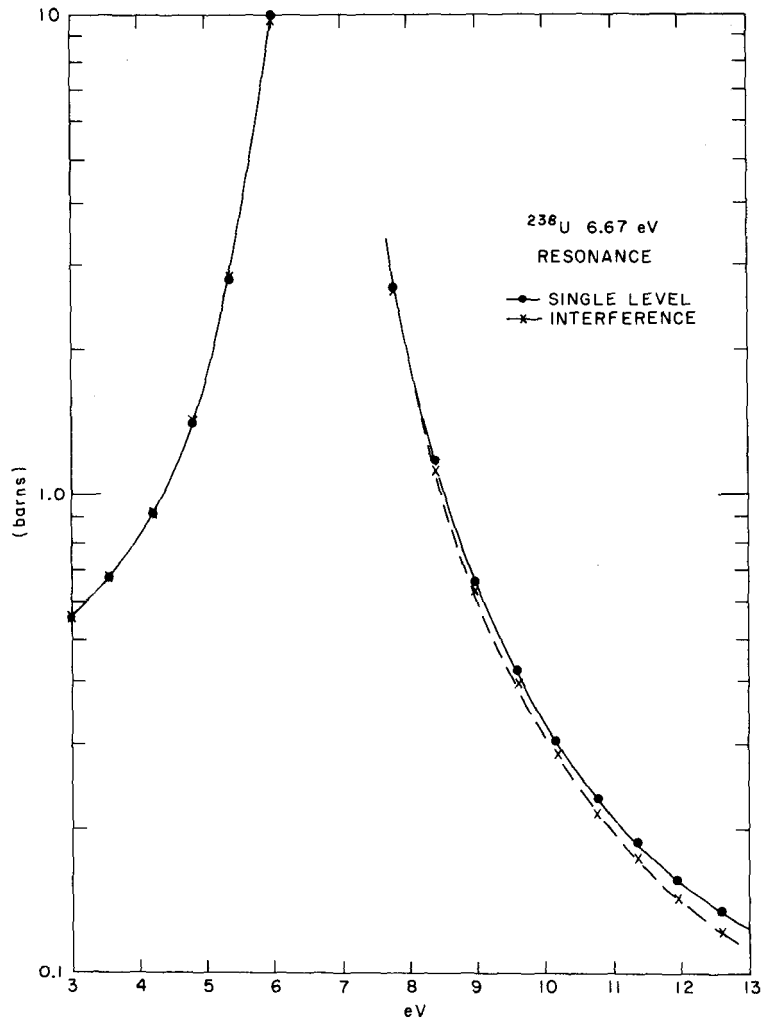
The effect has been estimated as follows: We assume the asymmetry is due only to the 4059 keV γ -ray populating the 720 keV $1/2^-$ state; all others are assumed to sum to zero. We use the resonance parameters of BNL 325 and the previously measured resonance partial widths.¹ We assume the γ -ray transition strengths as measured by Sheline et al.²

The resulting curves and tables are included in this report. As expected, there is very little effect below 6.67 eV. Above this energy there is a significant reduction in capture cross section due to destructive interference. The effect is largest near the interference minimum at 10.2 eV (the p-wave resonance near this energy has been ignored). The effect while small in cross section, is a large fractional effect--about 7%--in the region near 10 eV.

Two experiments can be done with the equipment at HFBR which are crucial in resolving the U-238 capture discrepancy. The first is to do a precise measurement of the capture cross section in the wings of the U-238 resonance; i.e. from 0.0253 eV to about 3 or 4 eV, and from 8 eV up to about 15 eV. I propose to do this by the activation technique using the monochromatic beam from the crystal monochromator at H-1A. From these experiments the degree of asymmetry of the 6.67 eV resonance can be determined, and a precise value of the thermal capture cross section of U-238 obtained. While the presently-accepted number, 2.7 is reputedly known to 1%, the value should be checked as it is crucial to the calculation of capture in this region. The second experiment is a precise measurement of the total radiation width of the 6.67 eV resonance, and possibly the 20.9 eV resonance. These resonances contribute a major share of the resonance capture integral of U-238, and their values should be determined to 5%. It seems almost certain that if the discrepancy in U-238 capture can be attributed to the microscopic cross sections, then it is this energy region where the parameters are in error. The measurement is to be done by measuring total cross section, capture, and self-indication areas of these resonances, using the HFBR fast chopper.

REFERENCES

1. D. L. Price et al., Nucl. Phys. A121, 630 (1968).
2. R. K. Sheline et al., Phys. Rev. 151, 1011 (1966).



LIST

PR: BASIC V01-05

```
100 REM INTERFERENCE PLUS SINGLE RESONANCE
110 REM PLUS BACKGROUND CALCULATION
200 PRINT "TYPE TOTAL, TOTAL GAMMA, PARTIAL GAMMA, REDUCED NEUTRON"
205 PRINT "WIDTHS"
210 INPUT G, G3, G1, G0
215 LET G2=SQR(G1+G0)
220 PRINT "TYPE DIRECT AMPLITUDE, THERMAL CAPTURE CROSS SECTION"
230 INPUT A, S1
240 PRINT "TYPE INITIAL, FINAL, STEP IN ENERGY"
250 INPUT E1, E2, E3
260 PRINT "TYPE RESONANCE ENERGY"
270 INPUT E0
274 X1=FNB(.0253)
276 X2=FNB(.0253)
277 C1=X1*((G2+(G2+E0)/X2+A)^2+(G2*G/2/X2)^2)
278 C2=X1*G0*G3/X2
279 PRINT "ENERGY", "TOTAL", "PARTIAL", "RATIO"
280 FOR E=E1 TO E2 STEP E3
282 LET X1=FNB(E)
284 LET X2=FNB(E)
286 LET X3=X1*((G2*(E-E0)/X2+A)^2+(G2*G/2/X2)^2)
288 LET X4=X1*G0*G3/X2
292 LET X5=FNE(E)
294 LET X6=X3+X4+X5
300 PRINT E, X6, X3, X3/X6
310 NEXT E
320 GO TO 200
330 DEF FNA(E)=650750/SQR(E)
340 DEF FNB(E)=(E-E0)*(E-E0)+G*G/4
350 DEF FNE(E)=(S1-C1-C2)*SQR(.0253)/SQR(E)
390 END
```

TYPE TOTAL, TOTAL GAMMA, PARTIAL GAMMA, REDUCED NEUTRON
WIDTHS

7.02752, .02537, .00063, .000589

TYPE DIRECT AMPLITUDE, THERMAL CAPTURE CROSS SECTION

7.00018, 2.7

TYPE INITIAL, FINAL, STEP IN ENERGY

7.0253, 13.6

TYPE RESONANCE ENERGY

76.67

ENERGY	TOTAL	PARTIAL	RATIO
.0253	2.7	.301963	.111838
.6253	.605272	.0648762	.107185
1.0253	.492035	.0500842	.10179
1.8253	.470984	.0450235	.0955945
2.4253	.493788	.0437323	.0885649
3.0253	.558616	.0450839	.0807064
3.6253	.684937	.0493701	.0720797
4.2253	.928237	.0583097	.0628177
4.8253	1.4513	.0771159	.0531357
5.4253	2.88874	.125177	.0433326
6.0253	9.92777	.3353	.0337739
6.6253	1771.16	44.0287	.0248586
7.2253	11.9881	.203448	.0169709
7.8253	2.68972	.0280513	.0104291
8.4253	1.14903	6.25539E-03	5.44404E-03
9.0253	.638455	1.33949E-03	2.09802E-03
9.6253	.410963	1.43280E-04	3.48645E-04
10.2253	.291	1.53707E-05	5.28202E-05
10.8253	.220379	2.20748E-04	1.00167E-03
11.4253	.175427	5.18623E-04	2.95635E-03
12.0253	.145082	8.23724E-04	5.67764E-03
12.6253	.123636	1.10607E-03	8.94618E-03

TYPE TOTAL, TOTAL GAMMA, PARTIAL GAMMA, REDUCED NEUTRON
WIDTHS

7.02752, .026, 0, .000589

TYPE DIRECT AMPLITUDE, THERMAL CAPTURE CROSS SECTION

76.27

TYPE INITIAL, FINAL, STEP IN ENERGY

7.0253, 13.6

TYPE RESONANCE ENERGY

76.67

ENERGY	TOTAL	PARTIAL	RATIO
.0253	2.7	0	0
.6253	.602577	0	0
1.0253	.487759	0	0
1.8253	.465078	0	0
2.4253	.485991	0	0
3.0253	.548452	0	0
3.6253	.671601	0	0
4.2253	.910288	0	0
4.8253	1.42586	0	0
5.4253	2.84874	0	0
6.0253	9.84639	0	0
6.6253	1770.04	0	0
7.2253	12.0916	0	0
7.8253	2.74155	0	0
8.4253	1.18444	0	0
9.0253	.665771	0	0
9.6253	.43345	0	0
10.2253	.310268	0	0
10.8253	.237345	0	0
11.4253	.190659	0	0
12.0253	.15896	0	0
12.6253	.136424	0	0

NOTE ON THE CAPTURE WIDTH OF THE 6.67 eV LEVEL IN ^{238}U *

G. de Saussure and R. B. Perez
Oak Ridge National Laboratory
Oak Ridge, Tennessee 37830

At a recent "Seminar on ^{238}U Capture" the suggestion¹ was made that the capture width of the 6.67-eV level in ^{238}U might be appreciably smaller than the value 25.6 meV evaluated in Versions III and IV of ENDF/B.

The suggestion was based, in part, on a comparison between a Monte Carlo calculation and a measurement of the capture probability in a thick sample of ^{238}U .² For the level at 6.67 eV the calculation indicated a broader peak than the measurement (Fig. 1).

In this note we present a few comments on this argument.

1. The measurement and calculation referred to (illustrated in Fig. 1) were not done for the purpose of determining the capture width of the 6.67-eV levels, but were done to normalize a time-of-flight measurement by the saturated resonance technique. For such normalization, the only quantity of importance is the value of the capture probability on the "flat top" of the peak, and this quantity is insensitive to the value of the capture width.

The relative energy scales of the calculation and of the measurement shown in Fig. 1 were not well aligned, and the calculation was made assuming a disk of infinite radius, whereas the measurement was done with a disk of 7.65 cm diameter. Hence, it seems unwise to conclude from Fig. 1 that the capture width of the 6.67-eV level is smaller than that used in the calculation (25.6 meV).

* Research sponsored by the Energy Research and Development Administration under contract with the Union Carbide Corporation.

2. An attempt was made to see if our previous measurements of the capture probability in the saturated 6.67-eV level could yield information of the capture width of that level, in spite of the fact that the intent of the measurements was not to determine that width.

The Monte Carlo program was refined to include the effect of the finite size of the capture sample, and calculations were done with capture widths of 21, 23, and 25.6 meV for sample thicknesses of .002849 a/b and .000789 a/b.

The calculations were compared with a set of nine measurements recently done with those two sample sizes.³ The experimental background could not be measured directly with sufficient precision, so the calculations were fitted to the measurement and a "free" background. The results of this comparison are illustrated in Table I. In Fig. 2 we compare one run with calculations done with capture widths of 21 and 25.6 meV.

As shown in Table I the data from the nine saturation measurements examined seem to favor a value of 23 meV for the capture width of the 6.67-eV level in ^{238}U . But this conclusion is barely statistically significant. Furthermore there is at least one possible experimental effect which could reduce the apparent capture in the wings of the resonances.

Neutrons with energies near 6.67 eV have a very short mean free path in the sample and hence are captured on the surface of the sample. However, neutrons in the wings of the resonance are captured nearly uniformly through the sample. Hence, the capture gamma rays produced by the

latter neutrons are perhaps more attenuated by the sample. We don't know how to compute reliably the magnitude of this effect, in the complicated geometry of the experiment and a realistic estimate should come from measurements with "split samples."

In conclusion, our previous measurements of the capture rate in thick samples of ^{238}U were not designed to determine the capture width of the 6.67-eV level and do not provide reliable information on this width. An analysis of recent measurements seems to favor a value of 23 meV for this capture width, but additional experiments especially designed for the purpose would be most desirable.

REFERENCE

1. Proc. Seminar of ^{238}U Resonance Capture, March 18-20, 1975, Brookhaven National Laboratory, to be published.
2. G. de Saussure et al., Nucl. Sci. and Eng. 51, 385 (1973).
3. G. de Saussure, J. Halperin, N. W. Hill, R. L. Macklin, and R. B. Perez, to be published.

Table 1. Comparison of Calculation and Measurements of the Capture Rate in the 6.67 eV in ^{239}Pu .

Run No.	Thickness (atom/b)	" χ^2 " of Fit			Background Obtained by Fit			Estimated Background
		$\Gamma_Y = 21$ meV	23 meV	25.6 meV	$\Gamma_Y = 21$ meV	23 meV	25.6 meV	
4670	.002849	1.167	1.147	1.501	2873	2839	2795	2943 \pm 200
4710	"	1.466	1.248	1.782	3630	3561	3474	3745 \pm 200
4730	"	1.261	1.098	1.657	3809	3732	3633	3972 \pm 200
4790	"	1.318	1.168	1.760	3504	3428	3354	3639 \pm 200
4900	.000789	1.407	1.192	1.450	662	643	620	650 \pm 30
5010	"	1.065	.825	.933	937	910	876	918 \pm 50
5050	"	1.177	1.094	1.164	1103	1076	1039	1076 \pm 50
5060	"	1.146	.982	1.234	1470	1434	1390	1444 \pm 50
5070	"	1.072	.800	1.105	1205	1174	1134	1178 \pm 80

The experimental data were fitted to a function $A \cdot S(E, \Gamma_Y) + B$ where $S(E, \Gamma_Y)$ is the capture probability computed for a given value of Γ_Y by a Monte Carlo program.

The number in columns 3 to 5 are proportional to the weighted sums of the residual for the fit. The numbers in columns 6 to 8 are the values of B obtained by the fits. In column 9 is given one estimate of B obtained independently of the fit (with a "background scaler").

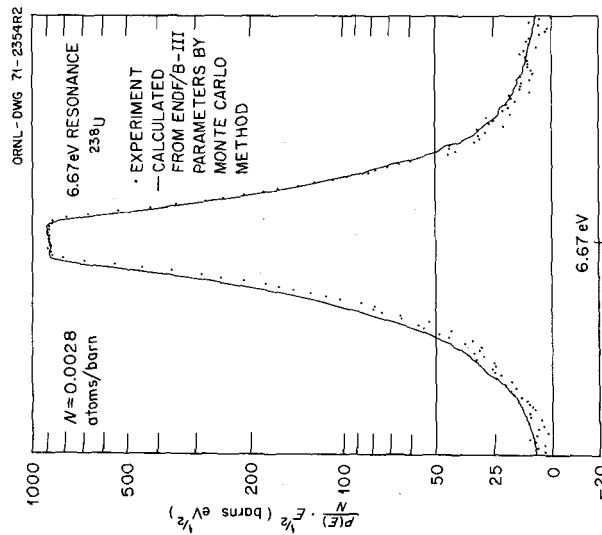


Fig. 1. Probability of capture in a 25-mil sample of ^{238}U at the 6.67 eV resonance. The ordinate is the probability of capture multiplied by the square root of the energy and divided by the sample thickness in atoms/barn. The calculation was done with the Monte Carlo code MULTSCA using the resonance parameters of ENDF/B-III. Note that the ordinate is linear from -20 to +50 barn $\cdot eV^{1/2}$ and logarithmic above 50 barn $\cdot eV^{1/2}$.

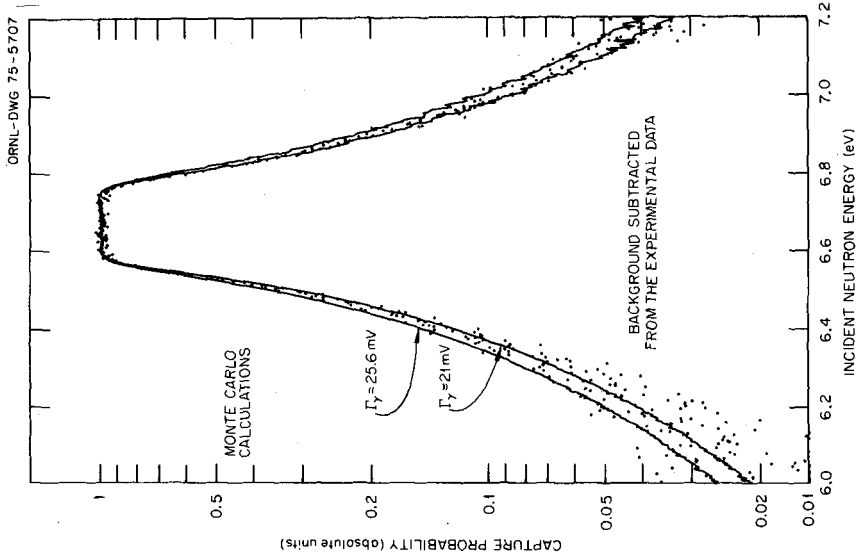


Fig. 2. Capture Probability in the 6.67 eV Level of ^{238}U ; Sample of 0.002845 atom/b.

COMMENTS ON ^{238}U NEUTRON WIDTH EVALUATIONS

H. DERRIEN

CEN - SACLAY, FRANCE

The present situation of ^{238}U resonance parameters as it is seen by European experimenters and users is reported in the proceedings of the Specialist meeting on "Resonance Parameters of fertile nuclei and ^{239}Pu " held at Saclay on 20-22 May 1974 [1]. At this meeting a new evaluation of the ^{238}U resonance parameters has been proposed by M. MOXON [2]. Some preliminary results concerning new measurements in progress at Geel have been given by POORTMANS et al [3]; other details about these new measurements were given by F. CORVI et al at the last Washington Conference [4].

The parameters recommended by M. MOXON are an average of all the weighted values presently available in the literature (from all the measurements performed since 1955). The high χ^2 value he obtained from the comparison of the various sets of neutron widths (2422.1 for 679 degrees of freedom) indicates that there are some systematic differences in these sets of data or that some of the uncertainties have been underestimated. As a matter of fact, MOXON has shown, by checking "the fractional difference FN in Γ_n between the data from a given reference and the weighted mean value from the other available data", that correlation exists for some data sets between FN and the neutron energy (for instance negative correlation in the GARG data [5] and positive correlation in the CARRARO data [6]). The origin of these systematic differences, as MOXON pointed out, could be found in: i) the type of measurement; ii) the method of analysis; iii) the Doppler and resolution effects. There is however a lack of information concerning the possible source of errors (background determination, self-screening correction, multiple scattering, effective temperature of the sample, influence of the finite cut off to the resonance areas...). In view of this situation, MOXON has concluded that it is not possible to make a choice among the various sets of data. According to MOXON, the best set of resonance parameters which can be recommended at the present time is obtained by averaging all the available values, with large error bars on each averaged value.

This rather pessimistic conclusion only shows that the problem of ^{238}U resonance parameters is still far from being solved. Yet, the most recent measurements reviewed in the MOXON evaluation have been made with very high resolution with the purpose of obtaining very accurate resonance parameters i.g the Columbia measurements, as reported by RAHN et al [7] and the Geel measurements, as reported by CARRARO et al [8] , [6] . These works took advantage of all the improvements of the last few years in the time of flight techniques and in the method of analysis ; the results should therefore be better than those from the earlier experiments. Still, at least beyond 1.5 KeV neutron energy, severe discrepancies exist between the Γ_n values obtained by RAHN and CARRARO. And now, the problem is : will the new measurements in progress at Geel give an explanation to these discrepancies or will they provide one more set of parameters different from the others ?

Indeed, performing new measurement can be useful if one can trust the results and if one knows *why* the new results should be better than the older ones ; this was probably MOXON ' s feeling when he did his evaluation. But there is another way of checking the existing data, before deciding about the necessity of a new measurement : it is to use the same analysis technique for several sets of experimental data. Of course, it would be a very lengthy procedure if all data had to be re checked in this way. But it seems to us that checking simultaneously the Columbia and the Geel transmission measurements would provide an accurate set of Γ_n values. In the last few years, we have shown that the best and quickest way to do this kind of evaluation is to use least square shape analysis method [9] , [10] , which is able to bring out the systematic errors in the transmission experiments (mainly in the background evaluation and in the normalization). Furthermore, the difficulties arising from the contribution of neighbouring resonances, the Doppler and resolution effects, the knowledge of the effective potential scattering can be easily canceled in the shape analysis. For instance, the code used at Saclay allows simultaneous analysis of 5 transmission series and 100 resonances. Such work, on Columbia and Geel transmissions would take three or four months for an evaluator and would be much less expensive than a new measurement.

We have tried this method in two energy intervals of the Columbia and Geel data. But before giving comments on the results, one remark is of interest : the situation when comparing the Columbia and Geel Γ_n values is not too bad up to 1.5 KeV neutron energy. Table I shows how the sum of Γ_n obtained from the values published by CARRARO et al. at Helsinki and the values published by RAHN at Knoxville compare each others. Only beyond 1.5. KeV the situation becomes critical and needs to be examined very carefully. Up to 1.5 KeV. average values of Columbia and Geel results would provide fairly accurate estimation of Γ_n values.

Table II and table III show the results in the two energy ranges we analysed (results shown in table II have also been published in the proceedings of the May 1974 Saclay meeting). The time for this work was about 4 days for one physicist and needed about 15 minutes of computer time on IBM-360-91 ; this gives an idea of the cost of an eventual ^{238}U Γ_n width evaluation by this method throughout the energy

range where the resonances are resolved (0 eV to 4500 eV). In the 1.4 to 1.8 KeV energy interval (table III), it appears that the values we obtain from the shape analysis of Geel and Columbia data, and the values published by RAHN (area analysis) are in agreement within less than 4% on the average, while the CARRARO values are 15 % to 20 % higher. The reason for the discrepancy between CARRARO values and the others does not appear clearly, because the background correction in the shape analysis remains negligible or weak in each case. But it seems that the RAHN values are better than those of CARRARO in this energy range.

Between 2.5 KeV and 2.8 KeV (table III) the situation is reversed. The values published by CARRARO et al. at Helsinki agree fairly well with the values obtained from our shape analysis of the Geel and Columbia data, while the RAHN values are more than 10% lower on the average. Here also, the origin of the discrepancy between the RAHN values and the others is not apparent. The shape analysis of the two sets of transmission data give consistent results while the values given by the experimenters are in discord.

From these analysis no information can be obtained concerning the Γ_γ values. At such high energies the shape analysis cannot provide accurate value of Γ_γ . The Doppler and the resolution widths are too large compared to the total width Γ of the resonances. The difference between Γ and Γ_n has the same order of magnitude than the error on the determination of Γ ; furthermore, the comparison between the Γ and Γ_n obtained is used to check the resolution width which is not always very well known. But, it must be pointed out that the discrepancies between Geel and Columbia appear particularly in the large Γ_n values. For such large neutron widths, the determination of Γ_γ from the capture area is not affected by the errors on Γ_n . An evaluation of the neutron widths by comparing the Geel and Columbia Transmissions would thus have very little consequence on the published Columbia Γ_γ values.

CONCLUSION

The above comments indicate that it is possible to improve the evaluation of ^{238}U resonance parameters by checking very carefully the existing sets of experimental data. Here, we have only considered two sets of experimental transmissions which are probably the most accurate up to now. It is obvious that the differences between the Γ_n values obtained by RAHN and CARRARO are mainly due to the analysis technique: area analysis using the intersection of curves in the $(\Gamma_n, \Gamma_\gamma)$ plan or ATTA-HARVEY least square area analysis. Other investigations have to be done concerning the capture data for which the shape analysis method cannot be used if they are not corrected for experimental effects like self-screening and multiple scattering. It would be of great interest to know the exact value of the capture area for each resonance directly from a corrected capture cross-section. Apparently that has been done by the Los Alamos physicists for ^{232}Th and ^{238}U ; for ^{232}Th the results appear to be excellent. But for ^{238}U , the Γ_γ obtained by using the Los Alamos capture area and RAHN Γ_n values are much lower than the other values. An important step in the evaluation of the ^{238}U resonance parameters will be made, if this anomaly is explained.

REFERENCES

- /1/ Specialist meeting on "Resonance parameters of fertile nuclei and ^{239}Pu ".
Saclay - May 1974 - NEANDC (E).163 U.
- /2/ M.C. MOXON,
Evaluation of U-238 resonance parameters.
See [1] page 159.
- /3/ F. POORTMANS et al.
Neutron scattering measurements on ^{238}U ...
See [1] page 149.
- /4/ F. CORVI et al.
Abstract, Washington
Conference March 1975.
- /5/ J.B. GARG et al.
P.R. 134 (1964) B.985.
- /6/ G. CARRARO et al.
Knoxville (1971) page 701.
- /7/ F. RAHN et al.
P.R., Vol 6, n°5 (Novembre 1972).
- /8/ G. CARRARO et al.
Helsinki (1970) Vol.1 page 403.
- /9/ J.P. L'HERITEAU and P. RIBON,
Knoxville (1971) Vol 1, page 438.
- /10/ H. DERRIEN and P. RIBON,
See [1] page 63.

TABLE I

COMPARISON BETWEEN $\sum_{E_1}^{E_2} \Gamma_n^\circ$ FROM GEEL AND COLUMBIA

Energy range E_1 E_2	Geel	Columbia	relative difference
66 - 500	40.23	42.41	-5.5 % (1)
500 - 1000	52.35	51.77	1.1 %
1000 - 1500	39.95	39.15	2.0 %
1500 - 2000	77.45	74.24	4.7 %
2000 - 2500	57.66	50.60	12.3 %
2500 - 3000	68.46	62.95	8 %
3000 - 3500	56.46	47.94	15 %
3500 - 4000	67.81	54.35	20 %
4000 - 4500	17.09	15.56	9 %

(1) In this energy range the difference is mainly due to the large Γ_n° value of the 189.6 eV resonance.

TABLE II

^{238}U NEUTRON WIDTHS FOR LARGE RESONANCES BETWEEN 1450 eV AND 1760 eV.

Energy eV	Shape analysis of Geel data (2 thicknesses) Γ_n , meV	Shape analysis of Columbia data (3 thicknesses) Γ_n , meV	Geel published values [Ca 71] Γ_n , meV	Columbia published values [Ra 72] Γ_n , meV
1473.4	114 \pm 2	108 \pm 2	125 \pm 8	125 \pm 10
1522.3	215 \pm 4	236 \pm 3	260 \pm 15	240 \pm 15
1597.5	309 \pm 6	352 \pm 4	351 \pm 40	355 \pm 25
1622.3	97 \pm 2	88 \pm 2	116 \pm 15	68 \pm 14
1637.4	50 \pm 1	46 \pm 2	60 \pm 5	50 \pm 8
1662.0	201 \pm 4	214 \pm 4	241 \pm 20	171 \pm 20
1687.3	98 \pm 2	97 \pm 2	104 \pm 9	92 \pm 10
709.0	81 \pm 2	77 \pm 2	94 \pm 7	86 \pm 8
1755.2	121 \pm 3	116 \pm 3	135 \pm 10	105 \pm 10
$\sum \Gamma_n$	1286	1334	1486	1292

In the shape analysis of Geel data the adjusted background parameters a were negligible ($\leq 10^{-3}$).

In the shape analysis of Columbia the adjusted background parameters a were equal to :

0.0011 for 0.084 at/b sample;
- 0.010 " 0.0348 at/b " ;
0.027 " 0.0084 at/b " .

For the signification of the parameter a see comments on table III.

TABLE III

Γ_n VALUES FOR LARGE RESONANCES BETWEEN 2.5 keV AND 2.8 keV.

Energy eV	Shape analysis on Geel transmissions	CARRARO et al. results (Helsinki)	Shape analysis on Columbia transmissions	RAHN et al. results
2547.2	716 ⁺³⁰	706 ⁺³⁶	675 ⁺²⁷	550 ⁺⁵⁵
2558.5	282 ⁺¹²	234 ⁺¹⁰	271 ⁺²⁷	230 ⁺³⁰
2579.9	439 ⁺²²	394 ⁺²⁰	436 ⁺²⁷	340 ⁺³⁹
2599.0	760 ⁺³⁸	790 ⁺⁵⁰	795 ⁺⁴²	740 ⁺⁴⁵
2671.3	281 ⁺¹⁴	280 ⁺¹⁰	265 ⁺²⁴	270 ⁺²⁰
2716.5	171 ⁺⁸	170 ⁺¹⁰	155 ⁺¹⁸	145 ⁺¹⁴
$\Sigma \Gamma_n$	2649	2574	2596	2275

COMMENTS ON TABLE III

The Geel shape analysis has been done on the 0.011 at/b sample; no background correction is needed; but the normalization coefficient is equal to 0.975. The Columbia shape analysis has been done on the 0.084 at/b and 0.035 at/b samples; the background corrections are respectively equal to 0.007 and 0.013, at 2600 eV neutron energy.

The theoretical formulation of the transmission used in the shape analysis is the following :

$$T_r = a + c \left(e^{-n\sigma\Delta} \right) * R$$

$\sigma\Delta$ is the usual Breit-Wigner one level formulation of the total cross section, broadened by the Doppler effects, plus one term taking into account the level-level interference in the neutron channel; R is the resolution function, a the background parameter and c the normalization coefficient.

Review of Benchmark Experiments

R. Sher and S. Fiarman
Stanford Univ.

This paper discusses some possible systematic errors in reaction rate measurements in lattices, which might be correctable, even at this late date. These include streaming through catcher foils or gaps, fast source perturbations due to the use of depleted uranium detectors and cadmium, and cadmium cut-off effects.

1) Streaming: Some of the lattice measurements were done with 0.001" aluminum catcher foils on either side of the detector foil. Resonance neutron streaming through the "gap" thus formed would cause increased resonance activation of the detector foil. This would make the measured value of ρ_{28} too high. There is not much data on streaming effects, but two sets of relevant measurements do exist: one, some work done by Baumann and Pellarin⁽¹⁾ at SRL in 1964, the second, some measurements done at MIT⁽²⁾. These indicate that for small gaps, the resonance activation is increased a few percent per mil. Corrections for this have not been applied to the MIT benchmark natural uranium D₂O lattices; however the MIT experiments were done in a different set of lattices (0.250" rods, UO₂).

Baumann and Pellarin's measurements were done on natural uranium metal rods of 0.350" and 1.00" diameters, and show effects of the same order of magnitude. They calculate the increase in resonance absorption by a geometric calculation in which the energy integral over an artificial resonance is used, the resonance being designed to give the proper amount of shielded resonance absorption. Essentially the calculation computes the fraction of the difference

between the rod resonance integral and the isolated foil resonance integral attributable to the gap.

We have done a similar energy integral calculation but using a simple Monte Carlo approach to treat the geometry and get good agreement with the MIT data and with the SRL data for small gaps. The Monte Carlo calculation does not agree well with Baumann's equation, but we believe we have found an error in Baumann's equation which removes the discrepancy. Since we are calculating the ratio of activation with streaming paths to without streaming paths, we feel that despite the simple method of treating the resonance region and the neutron flux, either calculational method can be applied to any given lattice. For the 1" natural uranium MIT lattices, the correction is of the order of 6% per mil.

2) Source perturbations: These fall into 2 classes: for the δ_{28} measurements, the depleted detector foil and associated catchers form a region in which there are no thermal fissions and therefore the local fast neutron flux is depressed. This lowers the value of δ_{28} . For ρ_{28} and δ_{25} the cadmium cover produces a similar effect by suppressing local thermal fissions.

Price at MIT has calculated the correction to δ_{28} in terms of a mean chord length for a fast neutron in the fuel rod. This correction applies only to the fraction of fast fissions that are caused by neutrons originating in the same fuel rod; the interaction fact is unaffected by the perturbation. He finds a correction factor

$$M_{28} = \frac{\delta_{28} \text{ (true)}}{\delta_{28} \text{ (measured)}} = 1 + \frac{\bar{\omega}}{\bar{l} + \lambda_R \frac{v_f}{v_{\text{cell}}}} \frac{1}{D_2^0}$$

where $\bar{\omega}$ is the mean chord length for fast neutrons in the detector foil and \bar{l} is the mean chord length for fast neutrons in the fuel rod.

For the benchmark lattices, M_{28} was not determined. For an isolated 1" nat. U rod, it was 1.039; this is an upper limit for the MIT benchmark lattices. This correction will worsen the existing discrepancies in δ_{28} for these lattices.

The corrections for ρ_{28} and δ_{25} arise from the suppression of the local fast neutron source caused by the presence of the cadmium. The corrections calculated by Price with a first-flight collision model are of the form:

$$\rho_{28} = \rho_{\text{meas}}^{28} + A(\delta_{28})_{\text{SR}} = \rho_{28}^{\text{meas}} + C_{28}$$

$$\delta_{25} = \delta_{25}^{\text{meas}} + B(\delta_{28})_{\text{SR}} = \delta_{25}^{\text{meas}} + C_{25}$$

where A and B are constants which depend principally on ratios of cross sections averaged over fission spectra and thermal spectrum, enrichment.

Price evaluated A and B, but used a (grossly) incorrect $(\delta_{28})_{\text{SR}}$, and then badly underestimated the effect.

For the MIT benchmark lattices, we have re-evaluated C_{28} and C_{25} and obtain $C_{28} = 0.026$, $C_{25} = 0.0019$. These are in the right direction to improve the agreement between measured and calculated values.

3) Cd cut-off: In general there has been no systematic and complete treatment of the cadmium cut-off in those benchmark measurements which determine ρ_{28} and δ_{25} by the cadmium ratio method. Hardy has pointed out that to explain the typical discrepancies between measured and calculated ρ_{28} values the Cd cut-off would have to be well above 0.625 eV. Although this may be improbable, a rigorous calculation of the Cd cut-off energy should be attempted for the benchmark lattices.

References

1. N. Baumann and D. Pellarin, SRL --
2. W. D. Ardenne et al., MIT-2344-2 (MITNE-53) 1964
3. L. Price, M.S. Thesis, MIT 1966

REACTIVITY AND REACTION RATE MEASUREMENTS
IN U-D₂O LATTICES WITH COAXIAL FUEL

D. J. Pellarin

B. M. Morris

Savannah River Laboratory
E. I. du Pont de Nemours & Co.
Aiken, South Carolina 29801

INTRODUCTION

Material bucklings and reaction rate parameters were measured for heavy water (D₂O) moderated, uniform lattices in the experimental facility (SE-SP)^{1,2} at the Savannah River Laboratory (SRL). Two different slightly enriched, coaxial, uranium fuel assemblies were examined over a wide range of triangular lattice pitches in this study. Results of experiments were compared with RAHAB computations using ENDF/B-IV cross sections.

Previous analyses of benchmark U-D₂O data involving both buckling and parameter measurements have been restricted to simple rod lattices.³ The purpose of this work was to expand the experimental data base to include uniform lattices of coaxial fuel assemblies. Assembly geometry and fuel composition are summarized in Table 1. Integral parameters are reported for inner and outer fuel separately, providing data for a more detailed and rigorous comparison with computation than previously available.

The information contained in this article was developed during the course of work under Contract No. AT(07-2)-1 with the U. S. Energy Research and Development Administration.

By acceptance of this paper, the publisher and/or recipient acknowledges the U. S. Government's right to retain a nonexclusive, royalty-free license in and to any copy-right covering this paper, along with the right to reproduce and to authorize others to reproduce all or part of the copy-righted paper.

SCOPE OF EXPERIMENTS

The lattice experiments using Type I fuel were completed at 5.5-, 6.0-, 7.0-, and 8.0-in. triangular pitches with D₂O purities ranging from 99.50 to 99.37 mol %.

The lattice experiments using Type II fuel were completed at 6.35-, 7.0-, 8.08-, 9.25-, and 14.0-in. triangular pitches with D₂O purities ranging from 99.54 to 99.13 mol %. The 6.35-in. pitch case was reassembled at the end of the experimental program, and measurements were repeated to check the experimental reproducibility. Results were duplicated within about 1-1/2%.

PARAMETERS MEASURED

Reactivity and reaction rate parameters that were calculated from experimental data are summarized below:

$$\begin{aligned} {}^{238}\text{U} \text{ (n,}\gamma\text{) Capture Ratio,} & \quad \rho_{28} = \frac{\text{Epi Cd } {}^{238}\text{U Captures}}{\text{Sub Cd } {}^{238}\text{U Captures}} \\ {}^{235}\text{U} \text{ Fission Capture,} & \quad \delta_{25} = \frac{\text{Epi Cd } {}^{235}\text{U Fissions}}{\text{Sub Cd } {}^{235}\text{U Fissions}} \\ {}^{238}\text{U} \text{ Fast Fissions,} & \quad \delta_{28} = \frac{{}^{238}\text{U Fissions}}{{}^{235}\text{U Fissions}} \\ \text{Modified Conversion Ratio,} & \quad C^* = \frac{{}^{238}\text{U Captures}}{{}^{235}\text{U Fissions}} \\ \text{Thermal Neutron Spectral} & \quad R = \frac{\left[{}^{176}\text{Lu}/{}^{63}\text{Cu} \right]_{\text{Fuel}}}{\left[{}^{176}\text{Lu}/{}^{63}\text{Cu} \right]_{\text{Thermal Ref.}}} \\ \text{Index (spectral hardening),} & \\ \text{Material Buckling,} & \quad B_m^2 = B_R^2 + B_Z^2 \end{aligned}$$

Intracell thermal neutron activation profiles also were measured.

The measurements were made in the exponential facility (SE).

DESCRIPTION OF SE-SP FACILITY

The exponential tank, 5 ft in diameter and 7 ft high, is mounted directly over the SP, a small, fully enriched, graphite-moderated reactor that supplies neutrons to the SE through a graphite pedestal. Accurate top and bottom positioning pins and spacers were used to establish the various pitches in the exponential. The SE-SP facility is shown in Figure 1.

Reference foils in the SP thermal column were irradiated by a thermal neutron flux simultaneously with the lattice irradiations in the exponential tank. A $1/v$ cadmium ratio of about 3×10^{-4} existed at the foil exposure position, so corrections for epithermal cadmium activation were not required for the reference foil activities.

Equilibrium flux spectra, characteristic of the measured lattices, existed in the central region of the SE where the foil activation experiments were made. This was affirmed by radial and axial cadmium ratio mapping measurements using gold pin detectors.

REACTION RATE MEASUREMENTS

Description of the Fuel Assembly Containing the Foils

The Type I and Type II fuel assemblies consisted of nested inner and outer fuel pairs stacked on an aluminum inner housing to produce uniform, continuous axial fuel columns.

The foil bearing irradiation assembly was placed at the center of the lattice and rotated slowly during irradiation to average any radial flux asymmetry. An inner and outer fuel pair

with accurately machined, solid angle slots to accommodate thin, bare, shaped foils and 1/2-inch-thick filler pieces were near the center of the fuel column. The shaped foils were fabricated to fit accurately in the slots, so the specific activation in the foil represented the average reaction rate in the fuel. Epicadmium activations were obtained from foils placed inside a small (0.375-in.-dia. x 0.01-in.-thick) cadmium pill box contained in a recess in the lower filler piece about 3 inches from the nearest bare foil.

Bare- and cadmium-covered lutetium-copper-lutetium foil sandwiches and copper foils were suspended in the moderator on thin polyester tape supported on an aluminum wire frame attached to the outer fuel. These data were used to obtain intracell flux and spectral index (R) profiles.

Experimental Procedures for ρ_{28} Measurements

Measurement of the ^{238}U (n, γ) capture ratio (ρ_{28}) was made by the indirect or subtraction technique that permitted the epicadmium component of the ^{238}U captures in the fuel to be determined without cadmium-covered ^{238}U foils. This method has the advantage of reducing the effect of spectrum distortion produced by cadmium.

Thin (0.003 to 0.004 in.), bare depleted and natural uranium foils were used to determine the total ^{238}U capture rate in the fuel. Identical bare foils were simultaneously irradiated at the thermal reference position (along with copper foils) to normalize the subcadmium ^{238}U capture rate in the fuel.

The neptunium decay was counted 2 to 3 days after irradiation with NaI scintillation counters biased to accept gamma energies in the interval from 90 to 116 keV. A simultaneous count representative of fission product decay activity, obtained at an integral bias of 500 keV, was used to correct for the fission product contribution to the counting rate in the window. The ratio of the fission product counting rate in the 90 to 116 keV window to the fission product counting rate at the 500 keV bias was determined for the actual counting conditions and irradiation times of each experiment. This ratio was obtained for ^{235}U fission products from the natural and depleted foils in the thermal reference position that were counted with the natural and depleted foils from the lattice. Typically, the fission product correction for the 0.019 wt % depleted foils was about 2%, and was 10% for natural uranium foils. Systematic differences were not noted in the ρ_{28} values between the two different foil types.

An auxiliary experiment was performed to obtain a factor to correct the average epicalcium specific activity of the two 0.010-in.-thick copper foils in the cadmium pill box in the fuel to the equivalent epicalcium specific activity for a single 0.010 in. copper foil under 0.030 in. of cadmium and dimensionally similar to the shaped bare copper foils contained in the fuel. This correction, about 9%, simultaneously established the effective cadmium cutoff energy for the ρ_{28} measurement at 0.625 eV, which corresponded to 0.030 in. of cadmium in slab geometry and isotropic flux with a $1/E$ energy dependence.

Small corrections of 1% for the inner fuel and 2% for the outer fuel accounted for the increase in ^{238}U resonance capture caused by the 0.001-in. gap at the interface between the foils and the fuel where aluminum was placed to prevent fission product contamination of the foils. These corrections were derived from an experiment in which known gaps of from 0.001 to 0.021 in. were introduced. The normalized (normalized to 0.001-in. gap) ^{239}Np episcadmium component of each foil was plotted against foil gap thickness and extrapolated to zero gap to obtain the correction.

Small calculated corrections of about 2% were applied to the measured ^{239}Np subcadmium activities to account for the difference between the actual average thermal flux at the foil site in the fuel, and what the true thermal flux in the fuel would have been without the foil. Calculated thermal flux depression factors were used to derive these corrections.

Calculated thermal flux depression factors were applied to the copper foils and to the depleted and natural uranium foils in the thermal reference position and in the lattice. These factors were applied consistently throughout the data analyses; therefore, the reported values of ρ_{28} are for infinitely thin ^{238}U foil detectors.

Other corrections to the experimental data accounted for:

- Differences (~4%) in gamma attenuation in the 90-116 keV window count caused by small differences in foil thicknesses between the natural and depleted uranium foils.

- Small differences in foil-to-counter geometry. Because small foil-to-counter acceptance angles were used, this correction generally was about 0.3%.
- Differences in the axial elevation of the foils in the experiment. This correction was obtained from a smooth fit of the axial flux based on bare gold pin activations in the moderator.
- Differences in moderator purity. Calculated corrections of 1 to 2% were applied to convert the measurements to 99.75 mol % D₂O.

δ_{28} Measurement

δ_{28} was measured using paired natural and depleted uranium foils in the fuel; 1/2-in.-diameter foils of similar composition and thickness were simultaneously irradiated in a δ_{28} reference geometry. The reference was taken as a 1/2-in. recess in a 1-in. natural uranium rod buried in a large graphite moderator block. The assembly was fed by thermal neutrons from the SP. Both sets of foils (i.e., those in the lattice and those in the reference) were counted for fission product activity under the same time and counting conditions. The value of δ_{28} in the lattice was derived from the known value of δ_{28} in the reference, simple ratios derived from the fission product activities, and known compositions of the foils. The δ_{28} values in the lattice are based on a δ_{28} reference value of 0.076. This value was obtained by

direct measurement using the standard double fission chamber method. As a check, a value of $\delta_{28} = 0.053 \pm 0.003$ was measured for an isolated 1-in.-diameter natural uranium rod using this reference technique. This value is in good agreement with a measurement by Bigham,⁴ giving δ_{28} as 0.050 ± 0.001 for the isolated 1-in.-diameter natural uranium rod.

δ_{25} Measurement

The ^{235}U fission capture ratio (δ_{25}) was determined by activating bare and cadmium-covered, diluted ^{235}U -Al foils in the fuel.

C* Measurement

The modified conversion ratio (C*) involved the measurement of relative ^{238}U (n, γ) capture rates and the ^{235}U fission rates in natural and depleted uranium foils. The foils were irradiated simultaneously in the lattice and in the thermal reference position.

R Measurement

The activation ratio of subcadmium captures in ^{176}Lu to subcadmium captures in ^{63}Cu within the fuel is a parameter related to the energy distribution of the neutron flux. ^{176}Lu has a resonance at 0.14 eV and ^{63}Cu is a $1/v$ absorber. Normalization to the same ratio in the Maxwellian spectrum at the thermal reference position provides a thermal neutron spectral index, R, that is a measure of the thermal neutron spectrum hardening in the fuel.

Comparison of Experimental Results with Computation

The experimental results were compared with RAHAB⁵ computations. RAHAB uses multigroup integral transport theory and the Nordheim resonance treatment to perform lattice cell computations. For uniform lattices, RAHAB is similar to the HAMMER⁶ code. ENDF/B-IV cross sections were used. The comparisons are summarized in Table 2 for the Type I fuel and in Table 3 for the Type II fuel. The standard deviations represent a one-sigma range based on the statistics of duplicate determinations.

The following observations were noted:

- For Type I fuel, ρ_{28} (outer fuel) is slightly overpredicted by about 4% on average, while ρ_{28} (inner fuel) is consistently overpredicted by about 22% on average (Figure 2).
- For Type II fuel, ρ_{28} (outer fuel) is overpredicted by about 11%, while ρ_{28} (inner fuel) is overpredicted by about 20% (Figure 3).
- Computations overpredict the ratio of episcadmium to sub-cadmium ^{235}U fissions (δ_{25}). For both Type I and Type II fuel, δ_{25} (inner fuel) is overestimated by about 23% on average; and δ_{25} (outer fuel) is overestimated by about 14%.
- C^* is overpredicted for both Type I and Type II fuel; the major disagreement again occurring for the comparison with the inner fuel.
- The RAHAB computations underestimate δ_{28} for both fuel types by about 11% for the inner fuel, and about 7% for the outer fuel.

- RAHAB overcalculates the magnitude of the spectral hardening (R) in the fuel.

In general, the discrepancies between experiment and RAHAB computation do not show a pitch dependence. The comparison between experiment and calculation is summarized in Table 4. Also the calculations do less well in predicting inner fuel parameters.

MATERIAL BUCKLING MEASUREMENTS

Experimental Procedures

Material bucklings were measured by flux mapping techniques in the cylindrical exponential facility (SE). Radial and axial curvatures were determined independently and combined to obtain

$$B_m^2 = B_R^2 + B_z^2.$$

The ratio of cadmium-covered to bare gold pin activations was determined throughout the exponential, so that regions where flux curvature was energy-dependent could be avoided.

A separate irradiation was made with a cadmium "shutter" between the critical source reactor (SP) and the SE, thereby eliminating from consideration photoneutrons resulting from the gamma field of the SP. The shutter correction also eliminated contributions from neutrons that originated in the SP and were reflected from walls into the SE.

Two methods of profiling were used to determine axial bucklings, depending on whether the material buckling was larger or smaller than the radial buckling.

Exponential profiles ($B_m^2 < B_R^2$) were measured with a traveling

ion chamber which sampled flux at 2-cm intervals over a total distance of 60 cm. The axial buckling was determined as the curvature of the best fit to the experimental data points by varying parameters in a hyperbolic cosine function. The perturbation of the flux shape from the traveling monitor itself was found to be negligible.

Cosine axial flux profiles ($B_m^2 > B_R^2$) were measured by irradiating gold pins of standardized shape and mass. The gold pins were arranged at 8-cm intervals on stringers of 70-cm length; three such stringers were used for each experiment. In such cases, the data were fitted to a cosine function. The gold pin activations were measured using NaI scintillation counters and include background, decay, and counter deadtime corrections. The traveling monitor could not be used for these more reactive lattices because of the large perturbation induced by the ion chamber.

Both the traveling monitor guide tube and gold pin stringers were near the centerline of the exponential tank. Previous experience has shown, however, that the axial buckling is independent of the radial positions at which the flux profile is measured, provided the edge of the SE is avoided.

Radial flux profiles were measured by irradiation of standardized gold pins. Pins were located at from 12 to 30 interstitial positions within a given horizontal plane, and 3 such arrays of pins at different elevations were included for each lattice pitch. The counting of the pin activations was

similar to that described for the axial measurements. The measured radial flux shapes were fit to a zero-order Bessel function to determine the radial buckling.

Comparison of Experimental Results with Computation

The results of the buckling measurements for both fuel types are given in Tables 5 and 6. Although D₂O purities varied during the experiments, corrections to a common purity of 99.75 mol % were calculated and applied to the data. Such calculated D₂O purity corrections have been verified by experimental measurements.

For both the axial and radial measurements, the standard deviation in flux was approximately 0.5%. This uncertainty in flux induces an uncertainty in buckling which is dependent on the magnitude and nature of the curvature. The standard deviation in axial buckling ranges from 0.10 to 0.20 m⁻²; and for the radial buckling, the range is from 0.20 to 0.35 m⁻². These statistical uncertainties in flux and buckling are primarily associated with uncertainties in gold pin mass, gold pin position, and position of fuel assemblies. Repetition of buckling measurements after unloading and reloading of fuel and pins indicates the bucklings can be reproduced to within 0.10 m⁻².

The major source of systematic error in these experiments is expected to be the application of exponential theory to a lattice. The detailed effects of this approximation on the buckling measurements have not been investigated. However, an SE buckling measurement was compared to a critical measurement /

of the same lattice. The test lattice was very similar to lattice types I and II. The buckling of the test lattice as measured in the critical facility was found to be lower than the SE value by 0.20 m^{-2} . No adjustment in the data of Tables 5 and 6 was made on the basis of this information; the error ranges in those tables reflect only the statistical uncertainties in the measurements.

Bucklings and k_{eff} values calculated using the integral transport theory code, RAHAB, and ENDF/B-IV cross sections are also shown in Tables 5 and 6. The differences between measured and calculated quantities increase as the lattice pitch decreases, or as the fuel-to-moderator ratio increases. In all cases, these discrepancies are significantly larger than either the experimental uncertainties or the possible bias between critical and exponential measurements.

CONCLUSIONS

The underprediction of material buckling and k_{eff} by RAHAB is consistent with the overprediction of ρ_{28} , C^* , and δ_{25} and the underprediction of δ_{28} . It is thought that the major part of these discrepancies may be attributed to the particular resonance capture models employed by RAHAB. The effects of possibly inaccurate differential or evaluated cross section data probably add a smaller contribution.

The detailed reaction rate parameters and the material bucklings presented here constitute a set of data which should complement

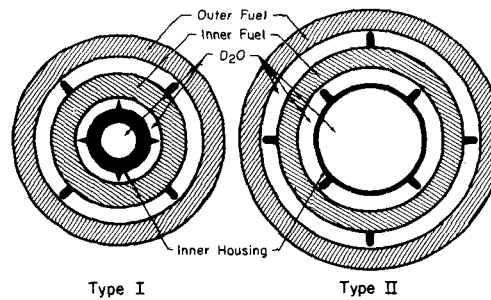
existing benchmark D₂O lattice data. Coaxial tube fuel assemblies, such as Type I and Type II, provide a more detailed set of data for comparison of calculation to experiment than is possible for simple rod lattices. Also, the Type I and Type II fuel at the experimental lattice pitches represent fuel-to-moderator ratios significantly larger than for other measured D₂O lattices. For example, the 6.35-in.-pitch Type II lattice has a ratio of uranium to deuterium which is a factor of ten larger than that of the highest uranium-to-deuterium (U/D) lattices.⁷ The significance of this is that the Type I and Type II lattices enhance the relative number of captures in ²³⁸U and thus present a more rigorous test of calculational methods for resonance capture.

REFERENCES

1. A. E. Dunklee and C. E. Jewell, *Zero Power Measurements on a High-Flux Demonstration Lattice*, USAEC Report DP-1076, E. I. du Pont de Nemours and Co., Savannah River Laboratory, Aiken, S. C. (1967).
2. R. C. Axtmann, L. A. Heinrich, R. C. Robinson, O. A. Towler, and J. W. Wade, *Initial Operation of the Standard Pile*, USAEC Report DP-32, E. I. du Pont de Nemours and Co., Savannah River Laboratory, Aiken, S. C. (1953) (declassified 1957).
3. F. J. McCrosson, "Thermal Data Testing of ENDF/B-III and Prognosis for ENDF/B-IV," *Trans. Am. Nucl. Soc.* 18, 352 (1974).
4. C. E. Bigham, *Measurement of Fast Fission Ratios in Natural Uranium*, Atomic Energy of Canada, Ltd. Report CRRP-1220 (AECL-2285), Chalk River, Ontario, Canada (1965).
5. H. C. Honeck, *The JOSHUA System*, USAEC Report DP-1380, E. I. du Pont de Nemours and Co., Savannah River Laboratory, Aiken, S. C. (1975).
6. J. E. Suich and H. C. Honeck, *The HAMMER System: Heterogeneous Analysis by Multigroup Methods of Exponentials and Reactors*, USAEC Report DP-1064, E. I. du Pont de Nemours and Co., Savannah River Laboratory, Aiken, S. C. (1967).
7. T. J. Thompson, I. Kaplan, and M. J. Driscoll (editors), *Heavy Water Lattice Project Final Report*, USAEC Report MIT-2344-12, Massachusetts Institute of Technology, Department of Nuclear Engineering, Cambridge, Massachusetts (1967).

TABLE 1. Assembly Geometry and Fuel Composition

	Type I	Type II
<u>Geometry, inches</u>		
<u>Al Inner Housing</u>		
O. D. ^a	0.8706	1.6512
I. D. ^b	0.5320	1.4730
<u>Inner Fuel Slug</u>		
<u>Al Cladding^c</u>		
O. D. ^a	1.9975	2.6787
I. D. ^b	1.166	1.958
<u>Fuel</u>		
O. D. ^a	1.914	2.605
I. D. ^b	1.226	2.018
<u>Outer Fuel Slug</u>		
<u>Al Cladding^c</u>		
O. D. ^a	3.076	3.700
I. D. ^b	2.400	3.105
<u>Fuel</u>		
O. D. ^a	3.016	3.640
I. D. ^b	2.460	3.165
<u>Fuel Composition, wt %</u>		
²³⁵ U	0.860	1.10
²³⁸ U	99.101	98.877
²³⁶ U	0.032	0.023



a. Outside diameter, includes rib volumes.
 b. Inside diameter.
 c. A thin (0.5 mil for Type I fuel; 6.41 mil for Type II inner fuel; 0.47 mil for Type II outer fuel) nickel flashing exists at the fuel-cladding interface and was homogenized in the cladding for the calculations.

TABLE 2. Type I Fuel Summary, 99.75 Mol % D₂O

Parameter	Pitch	Inner Fuel			Outer Fuel			Assembly Ava.				
		Expt.	Std. Dev.	Calc./Expt.	Expt.	Std. Dev.	Calc./Expt.	Expt.	Calc.	Calc./Expt.		
p ₂₈	5.5	2.550	±0.019	3.008	1.180	2.432	±0.016	2.504	1.030	2.472	2.676	1.083
	6.0	1.971	±0.013	2.396	1.216	1.928	±0.050	1.952	1.012	1.942	2.102	1.082
	7.0	1.388	±0.012	1.687	1.215	1.291	±0.028	1.330	1.030	1.323	1.448	1.094
	8.0	1.041	±0.016	1.299	1.248	0.905	±0.034	0.998	1.103	0.949	1.097	1.156
				Avg		Avg		Avg				
C*	5.5	1.656	±0.016	1.777	1.073	1.645	±0.024	1.634	0.993	1.649	1.684	1.021
	6.0	1.447	±0.014	1.570	1.085	1.451	±0.025	1.425	0.982	1.449	1.475	1.018
	7.0	1.190	±0.012	1.309	1.100	1.142	±0.017	1.170	1.025	1.158	1.217	1.051
	8.0	1.059	±0.011	1.154	1.090	0.998	±0.015	1.026	1.028	1.024	1.399	1.037
				Avg		Avg		Avg				
δ ₂₅	5.5	0.254	±0.003	0.313	1.232	0.205	±0.004	0.229	1.117	0.222	0.257	1.158
	6.0	0.203	±0.002	0.249	1.227	0.157	±0.003	0.178	1.134	0.173	0.202	1.168
	7.0	0.142	±0.0015	0.174	1.225	0.109	±0.002	0.121	1.110	0.120	0.138	1.150
	8.0	0.105	±0.001	0.132	1.257	0.0787	±0.0015	0.0901	1.145	0.0874	0.104	1.190
				Avg		Avg		Avg				
δ ₂₈	5.5	0.134	±0.005	0.125	0.933	0.0928	±0.004	0.0903	0.973	0.107	0.102	0.953
	6.0	0.128	±0.005	0.117	0.914	0.0878	±0.0035	0.0822	0.936	0.102	0.0943	0.925
	7.0	0.121	±0.005	0.109	0.901	0.0777	±0.003	0.0734	0.945	0.0921	0.0853	0.926
	8.0	0.115	±0.0045	0.104	0.904	0.0740	±0.003	0.0685	0.926	0.0876	0.0803	0.917
				Avg		Avg		Avg				
R	5.5	1.757	±0.017	1.811	1.031	1.628	±0.024	1.673	1.028			
	6.0	1.759	±0.017	1.749	0.994	1.575	±0.023	1.604	1.018			
	7.0	1.656	±0.016	1.655	0.999	1.477	±0.022	1.504	1.018			
	8.0	1.547	±0.015	1.590	1.028	1.407	±0.021	1.439	1.023			
				Avg		Avg		Avg				

TABLE 3. Type II Fuel Summary, 99.75 Mol % D₂O

Parameter	Inner Fuel			Outer Fuel			Assembly Avg.						
	Pitch Expt.	Std. Dev.	Calc./Expt.	Std. Dev.	Calc./Expt.	Expt.	Calc./Expt.	Expt.	Calc./Expt.				
P ₂₈	6.35	2.701	±0.026	3.235	1.198	2.367	±0.076	2.688	1.126	2.507	±0.076	2.900	1.157
	7.00	2.145	±0.013	2.558	1.193	1.878	±0.034	2.058	1.096	1.979	±0.034	2.248	1.136
	8.08	1.563	±0.013	1.896	1.213	1.311	±0.024	1.462	1.115	1.404	±0.024	1.624	1.157
	9.25	1.229	±0.015	1.494	1.216	0.983	±0.029	1.113	1.132	1.073	±0.029	1.253	1.168
	14.0	0.815	±0.019	0.945	1.160	0.611	±0.043	0.648	1.061	0.685	±0.043	0.754	1.101
			Avg	1.196			Avg	1.706					
C*	6.35	1.341	±0.013	1.470	1.096	1.269	±0.020	1.340	1.056	1.305	±0.020	1.391	1.066
	7.00	1.183	±0.012	1.289	1.090	1.094	±0.016	1.153	1.054	1.135	±0.016	1.206	1.063
	8.08	1.006	±0.010	1.096	1.089	0.922	±0.014	0.962	1.043	0.959	±0.014	1.013	1.056
	9.25	0.897	±0.009	0.972	1.084	0.810	±0.012	0.844	1.042	0.847	±0.012	0.891	1.052
	14.0	0.755	±0.008	0.789	1.045	0.666	±0.010	0.678	1.018	0.702	±0.010	0.718	1.023
			Avg	1.081			Avg	1.043					
δ ₂₈	6.35	0.252	±0.003	0.307	1.218	0.199	±0.004	0.231	1.161	0.220	±0.004	0.260	1.182
	7.00	0.195	±0.002	0.242	1.241	0.155	±0.003	0.177	1.142	0.170	±0.003	0.201	1.182
	8.08	0.148	±0.0015	0.177	1.196	0.108	±0.002	0.125	1.157	0.123	±0.002	0.144	1.171
	9.25	0.112	±0.001	0.137	1.223	0.0809	±0.0015	0.0938	1.159	0.0923	±0.0015	0.110	1.192
	14.0	0.0648	±0.001	0.0783	1.208	0.0441	±0.001	0.0504	1.143	0.0515	±0.001	0.0603	1.171
			Avg	1.217			Avg	1.152					
δ ₂₈	6.35	0.115	±0.004	0.102	0.887	0.0843	±0.003	0.0773	0.917	0.0962	±0.003	0.0872	0.906
	7.00	0.104	±0.004	0.0962	0.925	0.0731	±0.003	0.0705	0.964	0.0850	±0.003	0.0805	0.947
	8.08	0.102	±0.004	0.0909	0.891	0.0672	±0.003	0.0640	0.952	0.0801	±0.003	0.0742	0.926
	9.25	0.103	±0.004	0.0884	0.858	0.0575	±0.003	0.0504	0.895	0.0805	±0.003	0.0709	0.881
	14.0	0.0954	±0.004	0.0869	0.911	0.0520	±0.0025	0.0573	0.924	0.0741	±0.0025	0.0680	0.918
			Avg	0.894			Avg	0.930					
R	6.35	1.737	±0.017	1.800	1.036	1.586	±0.023	1.673	1.055	1.597	±0.023	1.673	1.055
	7.00	1.644	±0.016	1.734	1.055	1.539	±0.023	1.597	1.038	1.506	±0.023	1.597	1.038
	8.08	1.589	±0.016	1.649	1.038	1.419	±0.021	1.506	1.061	1.440	±0.021	1.506	1.061
	9.25	1.530	±0.015	1.585	1.036	1.378	±0.021	1.440	1.045	1.440	±0.021	1.440	1.045
	14.0	1.392	±0.014	1.459	1.048	1.267	±0.019	1.318	1.040	1.318	±0.019	1.318	1.040
			Avg	1.043			Avg	1.048					

TABLE 4. Summary of Comparison Between Calculated and Experimental Values

Parameter	Average Ratio of Calculated/Experimental Values			
	Type I Lattices		Type II Lattices	
	Inner Fuel	Outer Fuel	Inner Fuel	Outer Fuel
ρ_{28}	1.22	1.04	1.20	1.11
δ_{25}	1.24	1.13	1.22	1.15
C*	1.09	1.01	1.08	1.04
δ_{28}	0.91	0.95	0.89	0.93
R	1.01	1.02	1.04	1.05

TABLE 5. Fuel Type I Bucklings and k_{eff}^a

Lattice Pitch, inches	5.50	6.00	7.00	8.00
Axial Buckling, m^{-2}	-14.42 \pm 0.20	-8.94 \pm 0.20	-2.53 \pm 0.10	-0.28 \pm 0.10
Radial Buckling, m^{-2}	9.50 \pm 0.30	9.36 \pm 0.30	9.30 \pm 0.25	9.48 \pm 0.20
Material Buckling, m^{-2}				
Measured	- 4.92 \pm 0.36	0.42 \pm 0.36	6.77 \pm 0.27	9.20 \pm 0.22
RAHAB-ENDF/B-IV	-10.95	-4.57	2.88	6.30
k_{eff} (RAHAB-ENDF/B-IV)	0.921	0.933	0.942	0.951

a. All values correspond to 99.75 mol % D₂O.

TABLE 6. Fuel Type II Bucklings and k_{eff}^a

Lattice Pitch, inches	6.35	7.00	8.08	9.25
Axial Buckling, m^{-2}	-5.72 \pm 0.20	-1.36 \pm 0.20	2.46 \pm 0.10	4.01 \pm 0.10
Radial Bucklings, m^{-2}	8.50 \pm 0.22	9.06 \pm 0.22	9.36 \pm 0.20	9.17 \pm 0.20
Material Buckling, m^{-2}				
Measured	2.78 \pm 0.30	7.70 \pm 0.30	11.82 \pm 0.22	13.18 \pm 0.22
RAHAB-ENDF/B-IV	-2.64	3.24	8.57	10.81
k_{eff} (RAHAB-ENDF/B-IV)	0.928	0.940	0.951	0.960

a. All values correspond to 99.75 mol % D₂O.

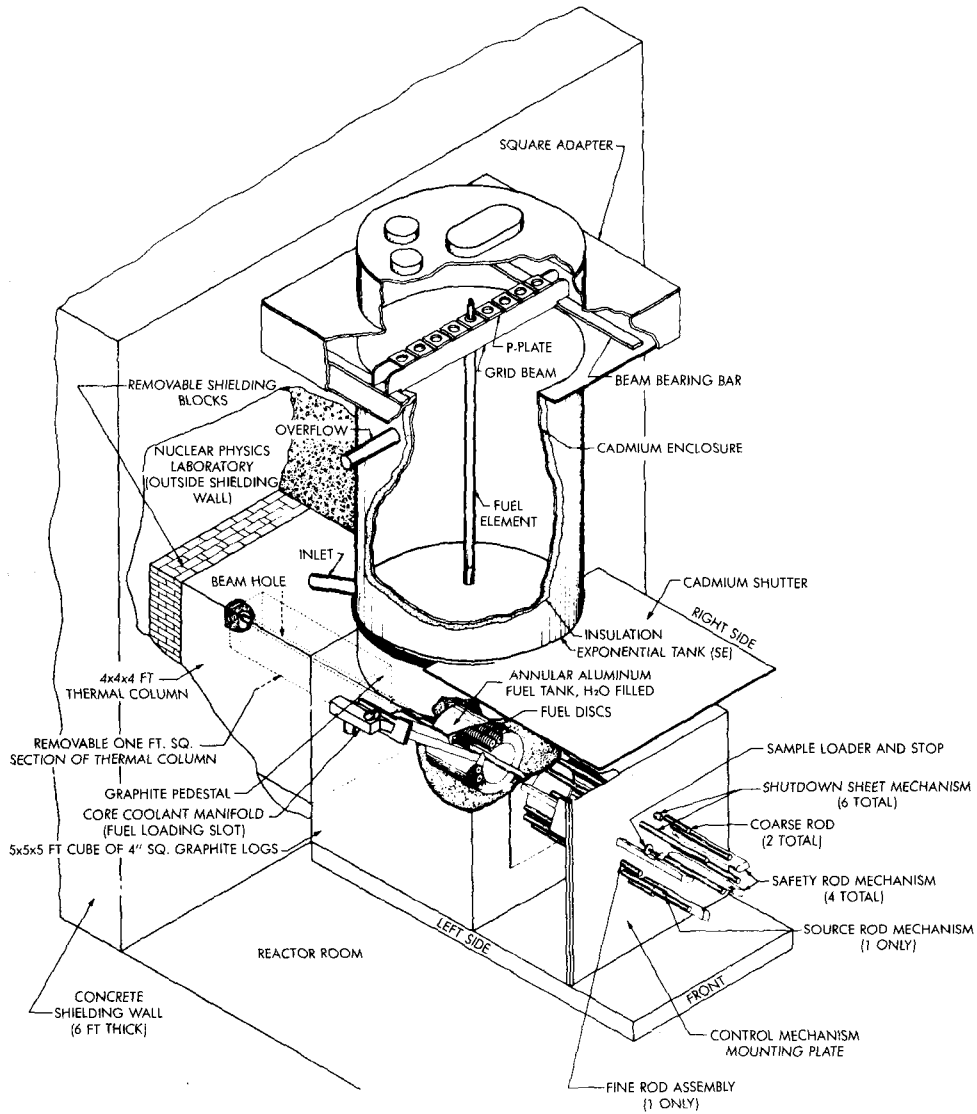


Figure 1. SE-SP facility.

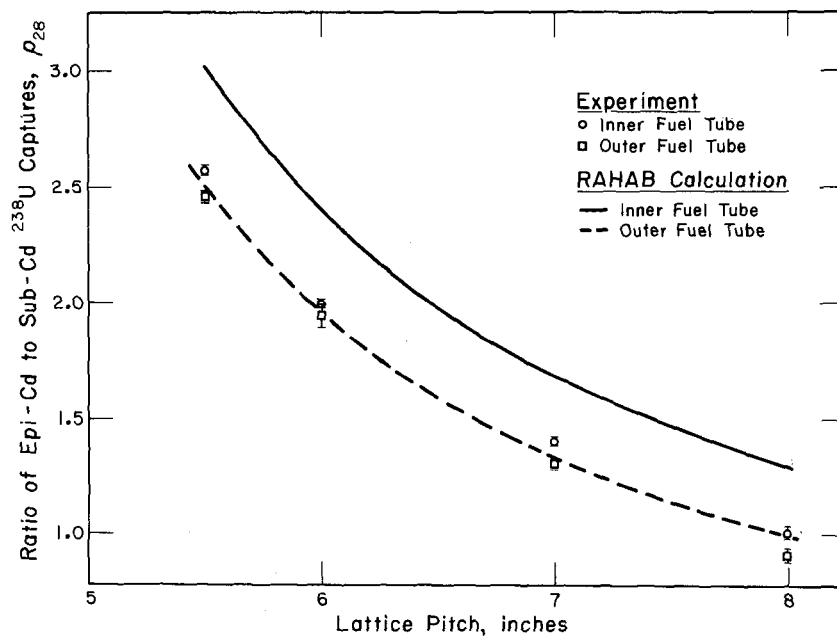


FIGURE 2 Comparison of Measured and Calculated ρ_{28} for Type I Fuel at 99.75 mol % D_2O ENDF/B-IV Cross Sections

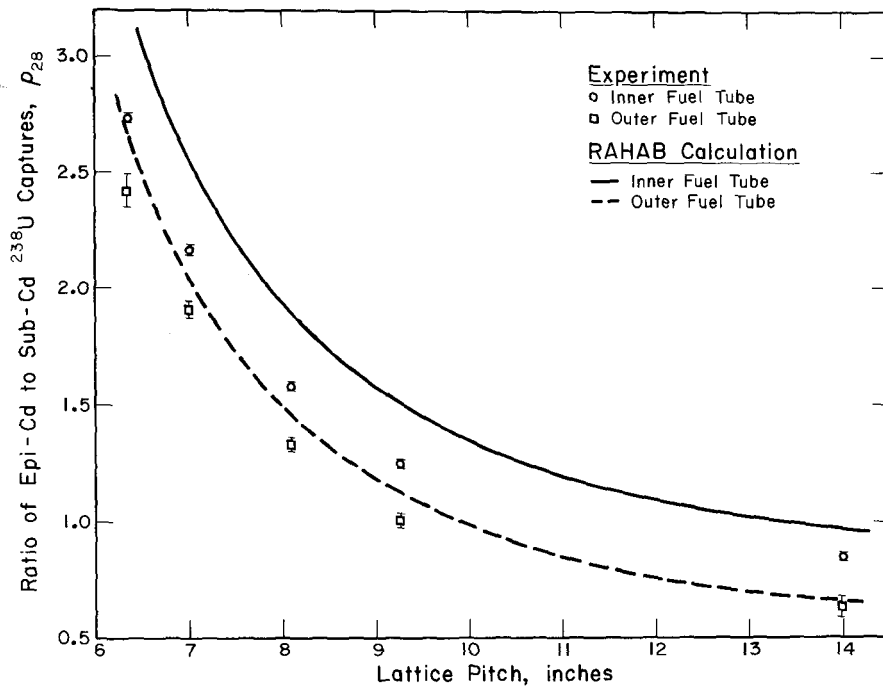


FIGURE 3 Comparison of Measured and Calculated ρ_{28} for Type II Fuel at 99.75 mol % D_2O ENDF/B-IV Cross Sections

INTERFERENCE SCATTERING EFFECTS ON INTERMEDIATE
RESONANCE ABSORPTION AT OPERATING TEMPERATURES

R. Goldstein
Combustion Engineering

The Intermediate Resonance (IR) approximation provides a relatively simple means of accurately calculating resonance integrals. The IR solution to absorption problems is accomplished through the use of interpolation parameters. Each scattering species of the system is represented by a parameter which bridges the gap between the wide resonance (WR) and narrow resonance (NR) extremes, thereby representing the more practical intermediate case. The values of the interpolating IR parameters depend on the resonance characteristics and the physical properties of the system under consideration and can be determined from analytical solutions based on a successive approximation approach or a variational procedure.

The original IR formulation¹ was carried out at zero temperature without the inclusion of interference scattering. Later the solution was extended separately to the cases including interference scattering² or Doppler broadening.³ More recently, these two effects have been treated concurrently, so that the coupling between interference scattering and Doppler broadening has been included.⁴ With this approach it is possible, therefore, to evaluate the effect of temperature on the interference between resonance and potential scattering.

The inclusion of interference scattering effects is more important for the higher energy, more strongly scattering resonances. When these effects are included, the

IR parameters sometimes fall outside the range between 0 and 1, which correspond to the first-order WR and NR approximations, respectively. This situation has been discussed in the literature.^{5,6} The actual values of the parameters are not very important, however, and less emphasis should be placed on them. The resonance integrals are the important quantities of interest, and these are still reliable, even when the parameter is less than zero or greater than unity.

Part of the problem which causes this situation and makes extrapolation necessary, is the inadequacy of the first-order WR approximation. Since the first-order WR approximation completely neglects scattering, interference effects are not reflected in it. Only to second and higher order will the WR approximation reflect scattering effects. The situation is depicted pictorially in Fig. 1. The example is for the case when the first-order WR approximation, $WR^{(1)}$, gives a larger resonance integral than the first-order NR approximation, $NR^{(1)}$. This occurs when the resonance and scattering properties are such that $s\Gamma_n > \sigma_p \Gamma_\gamma$, where s is the effective scattering of the moderator and σ_p is the potential scattering of the absorber. When interference scattering is neglected, the higher-order approximations converge to a value inside the initial range, so that the IR parameter λ and the IR absorption integral also fall within the initial range.

Figure 2 depicts how the situation becomes altered when interference scattering is included. The inclusion of interference scattering always tends to increase the resonance

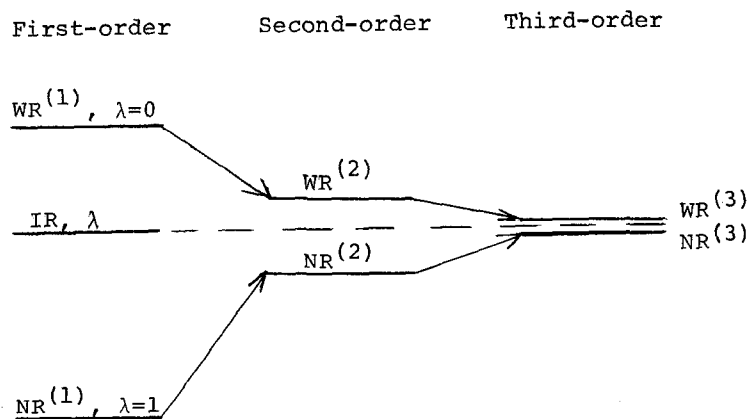


Fig. 1: Resonance Integrals Without Interference

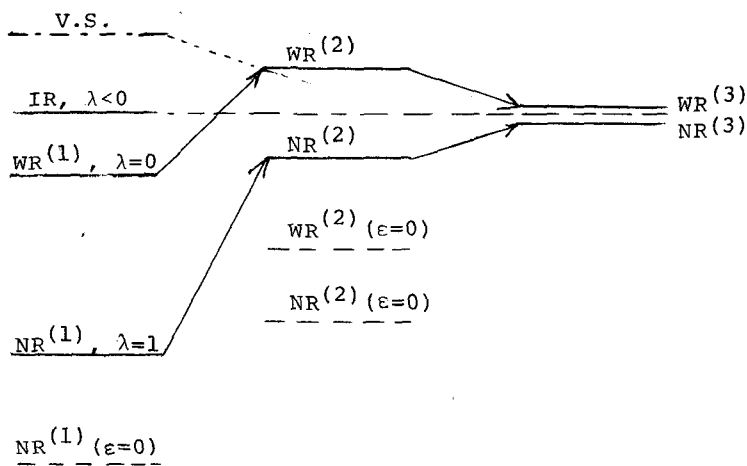


Fig. 2: Resonance Integrals With Interference Scattering Included ($\epsilon=0$ is without interference).

absorption. As already mentioned, however, the first-order WR approximation is unchanged by interference scattering. Therefore, it can happen sometimes, that the increase in resonance absorption due to the inclusion of interference scattering, causes the second-order NR and WR approximations to yield resonance integrals, both of which are greater than the first-order WR integral. When the resonance and scattering characteristics of a system cause this to occur, the situation depicted in Fig. 2 can result. Also given on the Figure for reference are the resonance integrals without interference ($\epsilon=0$).

The successive approximation approach determines that value of the IR parameter λ which equates the first- and second-order resonance integrals. For the situation given in Fig. 2, equality occurs for λ less than zero. With a well-formulated iteration procedure, the IR calculation can still provide a good approximation to the resonance integral; one which is equivalent to a higher-order calculation.

For practical uranium systems, the more common situation is for s to be greater than $s_0 = \frac{\sigma_p \Gamma}{\gamma_n}$. This is the case discussed above and depicted in Fig. 2. However, it is also possible for s to be less than s_0 , in which case the first-order NR integral is greater than the first-order WR integral. When this happens, extrapolated values of the IR parameter, which are greater than unity, can occur.

The extrapolated solution for λ which occurs in Fig. 2 could be avoided by improving the first-order WR approximation. For example, if a small but non-zero amount of scattering were included in this approximation, then the first-order WR approximation with interference scattering included could be made to exceed the second-order results, and the IR parameter would remain between zero and unity. This improved WR approximation is shown on Fig. 2 as a virtual state (V.S.).

Another way of avoiding extrapolation would be to equate second- and third-order approximations as a means of solving for the IR parameter. Since scattering is now included in all approximations, the solution will be within the initial range.

The additional work required for either of these two approaches is probably not warranted, however. Since the resonance integrals from the IR calculations are fairly reliable even when extrapolated values of the IR parameter are used, the latter are still applicable. Sometimes the solutions to the transcendental equations for the IR parameters are multiple-valued. In these cases the appropriate choice can be made on physical grounds. For example, λ less than zero or greater than unity would be chosen for those values of s that are greater or less than $\sigma_p \Gamma_\gamma / \Gamma_n$, respectively.

Since interference scattering effects decrease with increasing temperature, the inclusion of Doppler broadening

in the IR formulation mitigates the interference effects. The recent IR formalism⁴ enables one to investigate the effect of interference scattering at operating temperatures on resonance absorption. Since for the higher energy, more strongly scattering resonances, the use of the IR approximation and the inclusion of interference scattering often tend to act in the same direction of increasing the resonance absorption, it is important in determining temperature effects to evaluate these aspects for each physical system.

The IR results are summarized below for the case of an absorber with potential scattering cross section σ_p and interference scattering parameter ϵ , admixed with a non-absorbing moderator of cross section σ_m and located in an NR moderating medium of effective scattering cross section s . The temperature-dependent resonance integral may be written as

$$I_{\kappa\lambda}(\xi) = r\gamma_{\kappa\lambda}J_{\kappa\lambda}(\xi), \quad (1)$$

where

$$\gamma_{\kappa\lambda} = (s + \kappa\sigma_m + \lambda\sigma_p)\Gamma/\sigma_o(\Gamma_\gamma + \lambda\Gamma_n) \quad \text{and} \quad r = 2I^{(o)}/\pi = \sigma_o\Gamma_\gamma/E_r. \quad (2)$$

The integral J is a function of both temperature and interference and is defined by

$$J_{\kappa\lambda}(\xi) = \frac{1}{2} \int_{-\infty}^{\infty} f_{\kappa\lambda}(x, \xi) dx \quad ; \quad f_{\kappa\lambda}(x, \xi) = \psi(\xi, x) / [\gamma_{\kappa\lambda} + \psi + \zeta_\lambda \chi], \quad (3)$$

$$\zeta_\lambda = \epsilon\lambda\Gamma/(\Gamma_\gamma + \lambda\Gamma_n), \quad \epsilon = \sqrt{\sigma_p\Gamma_n\sigma_J/\sigma_o\Gamma}, \quad \xi = \sqrt{A\Gamma^2/4kTE_r}, \quad (4)$$

and ψ and χ are the symmetric and anti-symmetric Doppler-

broadened-line-shape functions.⁷

The IR solution for this case may be written as

$$\lambda = 1 - z_{\kappa\lambda} \quad \text{and} \quad \kappa = 1 - z_{\kappa\lambda}^{(m)} \quad , \quad (5)$$

$$z_{\kappa\lambda}^{(i)} = (1/z_{\kappa\lambda}^{(i)}) \tan^{-1} z_{\kappa\lambda}^{(i)} + (i_{\kappa\lambda}^{(i)}/z_{\kappa\lambda}^{(i)}) \log(1+z_{\kappa\lambda}^{(i)2}) \quad . \quad (6)$$

The IR parameters κ and λ correspond to the admixed moderator and the absorber, respectively. The superscript (i) in Eq. (6) refers to either the absorber (for which no superscript is used) or the admixed moderator (for which the superscript (m) is used). The interference quantity $i_{\kappa\lambda}^{(i)}$ in Eq. (6) is given

by

$$i_{\kappa\lambda}^{(i)} = b^{(i)} \theta_{\kappa\lambda} / (1 - 2b^{(i)} \omega_{\kappa\lambda}), \quad \omega_{\kappa\lambda} = \zeta_{\lambda} / \gamma_{\kappa\lambda}, \quad \theta_{\kappa\lambda}^2 = \beta_{\kappa\lambda}^2 - \omega_{\kappa\lambda}^2, \quad (7)$$

where

$$\beta^2 = 1 + 1/\gamma, \quad b^{(m)} = \zeta_{\lambda}, \quad \text{and} \quad b = (\epsilon\Gamma/\Gamma_n) [1 - \sigma_p \Gamma / (s + \kappa\sigma_m) \Gamma_n]^{-1}. \quad (8)$$

Using the scalar product notation to denote integration over the energy variable $x = 2(E - E_r)/\Gamma$,

$$(f, g) = \int_{-\infty}^{\infty} f(x)g(x)dx \quad , \quad (9)$$

the quantities $z_{\kappa\lambda}^{(i)}$ in Eq. (6) may be written as

$$z_{\kappa\lambda}^{(i)} = (\pi\delta_i) (f, g^{(i)}) / (f, 1) (g^{(i)}, 1) \quad ; \quad \delta_i = 2E_r(1 - \alpha_i)/\Gamma, \quad (10)$$

where

$$g_{\kappa\lambda}^{(i)} = f_{\kappa\lambda} + b^{(i)} h_{\kappa\lambda} \quad \text{and} \quad h_{\kappa\lambda}(\xi, x) = \chi(\xi, x) / (\gamma + \psi + \zeta\chi). \quad (11)$$

In Eq. (10), $\alpha_i = (A_i - 1)^2 / (A_i + 1)^2$, where A_i is the mass of either the absorber or the admixed moderator, as measured in neutron masses.

Once the set of IR equations has been solved for the

parameters κ and λ , the resonance integral is determined from Eq. (1). The integral $J = \frac{1}{2}(f,1)$ defined in Eq. (3) is the IR generalization of the tabulated temperature-dependent J-function⁷, which includes interference scattering.

Equations (5) and (6) are the generalizations of the IR solution which contain both interference and temperature effects. The coupling between temperature and interference occurs in the integrals contained in the quantity defined as z in Eq. (10). These integrals may be determined from tabulations or may be evaluated numerically. The values of the IR parameters can be determined from Eqs. (5) and (6) by iterative, graphical, or other numerical procedures.

In the extreme WR or NR limits, the solution has the appropriate behavior. In these limits, for example, the physical parameter δ in Eq. (10) becomes zero or infinite, so that $z \rightarrow 0$ (WR) or $z \rightarrow \infty$ (NR). From Eqs. (5) and (6), this means that $Z \rightarrow 1$ (WR) or 0 (NR), and the absorber IR parameter $\lambda \rightarrow 0$ (WR) or 1 (NR), which are the correct limits.

The generalized results also reduce to the previous results when temperature or interference is neglected. For example, when both effects are neglected, $z \rightarrow \delta/2\beta_\lambda = x_\lambda$, and $\lambda = 1 - (1/x_\lambda) \tan^{-1} x_\lambda$ (for a one-parameter system). If only temperature is neglected, $z \rightarrow \delta/2\theta_\lambda$, and if only interference is neglected, $z \rightarrow \pi\delta K_\lambda/2J_\lambda^2$, where $K_\lambda = \frac{1}{2}(f,f)$. All of these results are consistent with earlier solutions of the IR problem.¹⁻³

Since the Doppler motion which occurs at non-zero

temperatures tends to diminish the effect of interference scattering, it is important to evaluate the coupling between interference and temperature. The IR results given by Eqs. (1), (5) and (6) are a consistent set in that both the IR parameters and the resonance integral are functions of temperature and interference, and include the coupling between them. Calculations based on these equations should yield improved Doppler coefficients; at the same time, the need for the semi-empirical fits previously used to account for these effects^{5,8}, has been eliminated.

From the form of the IR solutions given, it is possible to make some general observations about the effects of interference scattering on resonance absorption. Consider, for simplicity, a one-parameter system (λ for the absorber). At zero temperature, the increase in absorption due to interference is a function of the magnitude of the ratio $\omega_\lambda/\beta_\lambda$. By evaluating this quantity for a particular resonance and scattering properties, an estimate of the importance of interference scattering can be obtained. Generally, this quantity becomes larger as $\lambda \rightarrow 1$ (narrower resonances), and for resonances which have both larger potential scattering (σ_p) and larger resonance scattering ($\Gamma_n/\Gamma \rightarrow 1$). For a given resonance, the interference effect decreases with increasing s ; that is to say, it is less important for more dilute systems.

When the temperature is increased from zero, the resonance broadens and the resonance integral increases,

but the effect of interference scattering tends to diminish. Equations (3) and (5) can be used to evaluate the changes in λ and J that occur with varying temperature. Because the representation of the higher energy, more strongly scattering resonances by the IR approximation (rather than the NR approximation) and the inclusion of interference scattering often tend to produce effects which act in the same direction (of increasing the resonance absorption), it is important to evaluate these effects when determining temperature-dependent quantities, especially Doppler coefficients.

REFERENCES

1. R. Goldstein and E.R. Cohen, "Theory of Resonance Absorption of Neutrons," Nucl. Sci. Eng., 13, 132 (1962).
2. R. Goldstein and E.R. Cohen, "Theory of Resonance Absorption of Neutrons II," Trans. Am. Nucl. Soc., 5, 56 (1962).
3. R. Goldstein, "Temperature-Dependent Intermediate Neutron Resonance Integrals," Nucl. Sci. Eng., 48, 248 (1972).
4. R. Goldstein, "Intermediate Resonance Absorption Including Interference Scattering and Doppler Broadening," Trans. Am. Nucl. Soc., June, 1975, to be published.
5. J. Mikkelsen, "Extrapolation and Interpolation in Calculation of the Resonance Absorption of Neutrons of Intermediate Energy," Nucl. Sci. Eng., 39, 403 (1970).
6. Y. Ishiguro, "On the Permissible Range for Parameter Used in Intermediate Resonance Treatment," J. Nucl. Sci. Technol., 5, 255 (1968).
7. L. Dresner, "Resonance Absorption in Nuclear Reactors," Pergamon Press, New York (1960).
8. Y. Ishiguro, S. Inoue and H. Takano, "Temperature Dependence of Parameters Used in Intermediate Treatment of Resonance Absorption," J. Nucl. Sci. Technol., 6, 308 (1969).

Interactive Approaches to Evaluating Methods and
Data for Self-Shielded Resonance Absorption[†]

Martin Becker
Department of Nuclear Engineering
Rensselaer Polytechnic Institute
Troy, New York 12181

A variety of measurements have been made of self-shielded resonance integrals for ^{238}U . In addition, extensive direct measurements of cross-sections and resonance parameters have been performed. However, when differential data are used to compute the self-shielded resonance integrals, discrepancies of a significant nature arise. As discussed in a number of papers at this symposium, these discrepancies have persisted for some time.

At RPI, considerable experience has built up on interpreting discrepancies between integral measurements and calculations based on differential data, including specific experience with ^{238}U . Most activity has been at moderate to high energies. Thus, resonance integral information has emphasized the unresolved resonance region. However, the approaches used in the unresolved region should also prove useful in the resolved region.

Our experience indicates that there are four ingredients to a program of interpreting integral-differential discrepancies —

- (1) The integral measurement must be well defined and of reliable accuracy.
- (2) A calculation is available that is sufficiently precise that uncertainty in calculational method can be eliminated as a cause of discrepancy.
- (3) A procedure exists for gaining understanding of the sensitivity of the integral quantities of interest to variations in key parameters.
- (4) A procedure exists for taking action in translating sensitivity information into specific conclusions and recommendations.

At RPI, fast spectrum activities have emphasized all four ingredients. Well-defined measurements of neutron spectra were performed and analyzed with precise procedures (1,2). In addition simplified analysis (1) based on generalized continuous slowing down theory (3) was used to infer general causes of discrepancies. Most recently, a capability to infer more specific causes of dis-

[†]Sponsored by USERDA under Contract No. AT(11-1)-2458

crepancy has been developed using interactive graphics (4,5). This capability has proved to be quite powerful, and also should be applicable to the low-energy ^{238}U problem and to a variety of other problems.

The interactive capability that has been developed has some unique features that are of particular importance to studying sensitivities. A variety of options useful in the construction of data files to be compared, applying modifications to a data file, calculating and displaying the consequences of these modifications, etc., have been automated through the Rensselaer Interactive Graphics Analysis System (RIGAS). A thirty-two push-button hardware dialogue unit has been constructed to facilitate exercising these options. In addition, an asynchronous communication capability has been incorporated, permitting time-sharing telephone communication with a CDC-6600 computer for situations where the speed and sophistication of the large computer are required.

The system is designed to separate general file comparison from specific application needs. Specific needs for specific applications are called by a User Routine button. The user by light pen selection picks which routines are to be executed and in which order. These user routines are then used for calculating the implications of modifications introduced into particular files. A new application requires a new set of user routines, but makes use of the automated options that are of general applicability.

Interactive sensitivity evaluation permits comparison of alternate data and of alternate approximations. In the unresolved capture region, for example, relevant comparisons include changes in data from one ENDF/B file to another, and in methodological differences from one processing code to another. The reductions in unresolved capture between ENDF/B-II and ENDF/B-III were found to be appropriate, and the methods in SUPERTOG and MC^2 -II were found to yield equivalent results.

The cross-section file for which the interactive mode has been most useful has been the inelastic scattering file, because of the sensitivity of fast spectra to this file. Interactive modi-

fications have led to a result where the inelastic cross-section is reduced substantially relative to ENDF/B files (6). The result is qualitatively similar in the low MeV range (where the inelastic scattering cross-section reaches a maximum) to the data in the independently-obtained ^{238}U evaluation for the German KEDAK-3 nuclear data library (7).

The interactive approach has the advantage of permitting on-line exercise of professional judgment. This judgment influences the magnitudes and directions of modifications and influences the consistency among several modifications. It also permits raising and answering important peripheral questions, such as sensitivity of results to uncertainty in relative normalization in files being compared.

It is likely that an approach such as the interactive one would be desirable for dealing with the self-shielded resonance integral over both unresolved and resolved resonances. As reported during this symposium, the integral measurements and the precise calculations leading to the current discrepancy have been reproduced in a number of laboratories for a number of years. A sensitivity evaluation capable of rapid investigation of the significance of a number of detailed possibilities could facilitate focusing on detailed problems, as has been the experience with fast spectra.

References

1. N. N. Kaushal, B. K. Malaviya, M. Becker, E. T. Burns, E. R. Gaerttner, "Measurement and Analysis of Fast Neutron Spectra Depleted in the Uranium-235 Isotope," Nucl. Sci. Eng. 49, 330 (1972).
2. M. Becker, N. N. Kaushal, "An Assessment of ENDF/B-III Data for Uranium-238 Based on Integral Spectrum Measurements," Nucl. Sci. Eng., 56, 307 (1975).
3. F. E. Dunn, M. Becker, "Improvements to Slowing Down Theory for Fast Reactors," Nucl. Sci. Eng. 47, 66 (1972).
4. M. Danchak, W. R. Moyer, M. Becker, "The Rensselaer Interactive Graphics Analysis System," Trans. Am. Nucl. Soc. 18, 159 (1974).

References (Continued)

5. M. Danchak, M. Becker, W. R. Moyer, "Utilization of Interactive Graphics and Continuous Slowing Down Theory," Trans. Am. Nucl. Soc., 19, 175 (1974).
6. A. Parvez, doctoral research, RPI, 1974 (in progress).
7. B. Goel, H. Kusters, F. Weller, "Recent Evaluation for the German Nuclear Data Library KEDAK-3," paper presented at the 1974 Neutron Cross-Section and Technology Conference.

EFFECTS OF THE FREE-GAS, SLOWING-DOWN MODEL

ON RESONANCE CROSS SECTIONS IN ^{238}U *

R. A. Karam

School of Nuclear Engineering
Georgia Institute of Technology
Atlanta, Georgia 30332 USA

BACKGROUND

Effective resonance cross sections used in the analysis of heterogeneous reactors have generally been obtained through the use of equivalence theory and/or integral transport theory. One fundamentally restrictive assumption common to equivalence theory and most integral transport methods is the flat-flux/flat-source approximation. The assessment of this approximation was recently completed under Contract No. AT-(40-1)-4750 with the U. S. Atomic Energy Commission and reported in ORO-4750-2, December 31, 1974. The assessment comprised the following:

- a. Comparison of the broad group cross sections of ^{238}U in the resolved resonance region using:
 1. The flat-flux/flat-source approximation;
 2. The exact source distribution;
 3. The rational approximation with Levine type factor.⁽¹⁾
- b. Comparisons in (a) for three types of reactors:
 1. Typical ZPR-assembly;
 2. LMFBR commercial power station;
 3. Light-water power reactor.

The main conclusions reported in ORO-4750-2 were:

1. Even though there were significant differences between the exactly calculated escape probabilities and those calculated with the flat-flux/flat-source approximations, additional differences between the general energy dependent reciprocity relation and the energy independent (but often erroneously applied as energy dependent) reciprocity relation almost completely compensated for the error in the flat-flux/flat-source escape

* Supported by the U.S. Energy Research and Development Administration under Contract No. AT-(40-1)-4750

probabilities. Due to this unusual and somewhat unexpected compensating effect, the effective capture cross sections of ^{238}U in the resolved resonance region, generated by the three methods stated earlier, were essentially the same (see Table 1).

2. The neutron source, $x(r,E)$, defined as

$$X(r,E) = \int \Sigma_s(r,E' \rightarrow E) \phi(r,E') dE' + Q(r,E),$$

where the symbols are standard notation, was calculated for the two-region unit cell described in Table 1. The results are shown in Fig. 1 for the 189.6 eV resonance. It is seen that the source in the absorber plate is significantly higher than that in the surrounding medium. The large σ_p of the absorber plate relative to the scattering cross sections of the surrounding medium is the reason why the source is high in the absorber. Under these conditions the resonance integral over the 189.6 eV resonance is largely determined by the source in the plate and not in the surrounding medium.

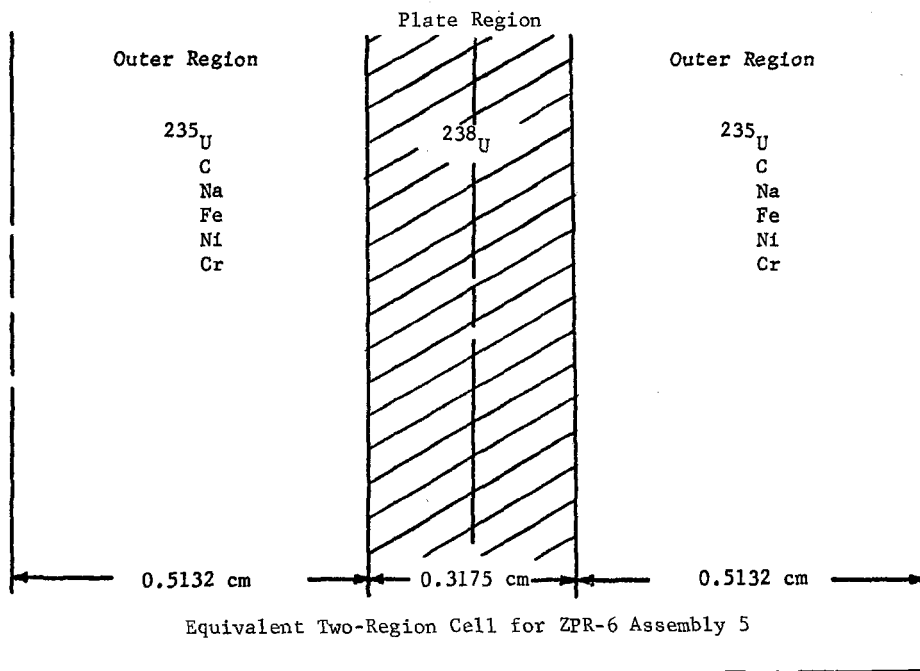
3. The magnitude of the neutron source shown in Fig. 1 is largely governed by the value of σ_p and the slowing-down process. The slowing-down process used was based on the free-gas model (i.e. the absorber atoms are free in a gaseous state) and on the assumption of isotropic elastic scattering in the center of mass coordinates. The free-gas model, as far as we know, has always been used for neutron energies above 1.0 eV. This is certainly the case in such codes as the MC², RABBLE, and GAROL.

4. The source distribution shown in Fig. 1 indicates that in order for σ_c^{238} to be too high in the resonance region, either the value of σ_p for ^{238}U would have to be too high or the resonance parameters would have

TABLE I

Effective Resonance Cross Sections for the Two-Region
 (shown below) Cell of ZPR-6 Assembly 5 (barns),
 Using ENDF/B-III Resolved Resonances

Group	E_{lower} (eV)	Equivalence Theory	Exact Flat	Nonuniform
15	4307 - 2612.	0.3875	0.3925	0.3886
16	2035.	0.5202	0.5275	0.5214
17	1234.	0.5318	0.5425	0.5350
18	961.	0.6443	0.6539	0.6466
19	582.9	0.8005	0.8121	0.8021
20	275.4	0.6871	0.6987	0.6894
21	101.3	1.1224	1.1305	1.1218
22	29.02	1.7327	1.7427	1.7318
23	13.71	2.7702	2.7852	2.7696



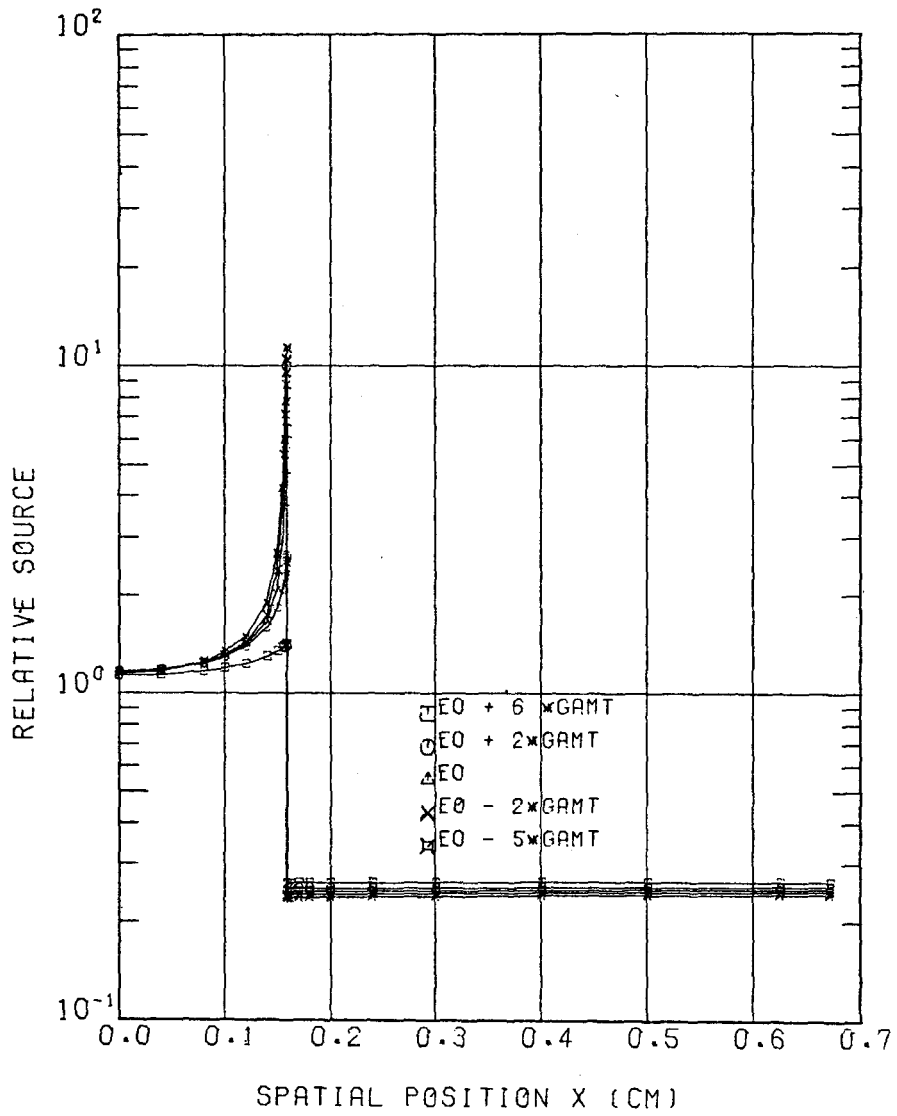


Fig. 1. Spatially Dependent Source for 189.6 eV Resonance

to be too poorly understood, and highly erroneous, or the slowing-down process would have to unrealistically produce large numbers of resonance neutrons. The potential scattering cross section is known to a good accuracy and may be ruled out as a source of major error. The picture with respect to resonance parameters is more complex especially in the unresolved region. However, the magnitude of the differential capture cross section of ^{238}U has been going upward whereas integral measurements required lower values. Whatever the error in the resonance parameter may be, this subject is left to those who measure differential cross sections. In this proposal we concentrate on the slowing-down process and show that the free-gas model for crystalline ^{238}U metal would produce large error in the effective, broad group, resonance capture cross sections of ^{238}U .

DISPLACEMENT ENERGY

The minimum energy required to displace an atom from a normal site in the crystal lattice is defined as the displacement energy, E_d . The value of E_d may be estimated⁽²⁾ by equating E_d to the energy of sublimation of an atom in the solid, designated here by E_s . For uranium, $E_s \approx 7.2$ eV; however, sublimation occurs from the surface of a solid, where it is necessary to break only half of the interatomic bonds to move the atom. By comparison, an interior atom has twice as many bonds and thus would require about 14.4 eV for displacement. According to reference (2), if an atom is moved from a lattice site to an interstitial position in the direction of least resistance, allowing time for neighboring atoms to relax, then E_d would be twice E_s . In reality, the struck atom receives a sharp blow and passes to an interstitial position in a highly irreversible way.

Consequently, it is estimated (estimates based on experimental data) that the displacement energy is 4-5 times E_s .

The minimum neutron energy required to displace an atom as a function of the atomic weight (taken from ref. 2) is shown in Fig. 2. Although there may be some uncertainty in the value of E_d for uranium it appears that the true value lies somewhere between 30-50 eV. Based on elastic scattering laws, the minimum neutron energy required to displace an atom is given by the following relationship:

$$E_{\min} = \frac{(m_1 + m_2)^2 E_d}{4m_1 m_2}$$

where m_1 and m_2 are the masses of the neutron and the nucleus, respectively. For uranium metal, the minimum neutron energy required to displace atoms lies in the range of 1.8 to 3 keV.

PHONON EXCITATION

When the neutron energy is not enough to displace atoms from normal to interstitial sites, the energy loss from the neutron would take place through phonon excitations in the crystal. Based on the Van Hove theory of space time correlations, (3) the expression relating the phonon emission to the scattering cross section is given by Bell and Glasstone (4) as follows:

$$\begin{aligned} \Sigma_s(E') f_s(\hat{\Omega}', E' - \hat{\Omega}, E) &= \frac{\Sigma_b}{4\pi} \sqrt{\frac{E}{E'}} \frac{1}{2\pi} \int_{-\infty}^{\infty} e^{-i\epsilon t/\hbar} \\ &\times \exp \left[\frac{\hbar K^2}{2Am} \int_{-\infty}^{\infty} \frac{f(\omega) e^{-\hbar\omega/2kT}}{2\omega \sinh(\hbar\omega/2kT)} (e^{-i\omega t} - 1) d\omega \right] dt \end{aligned} \quad (1)$$

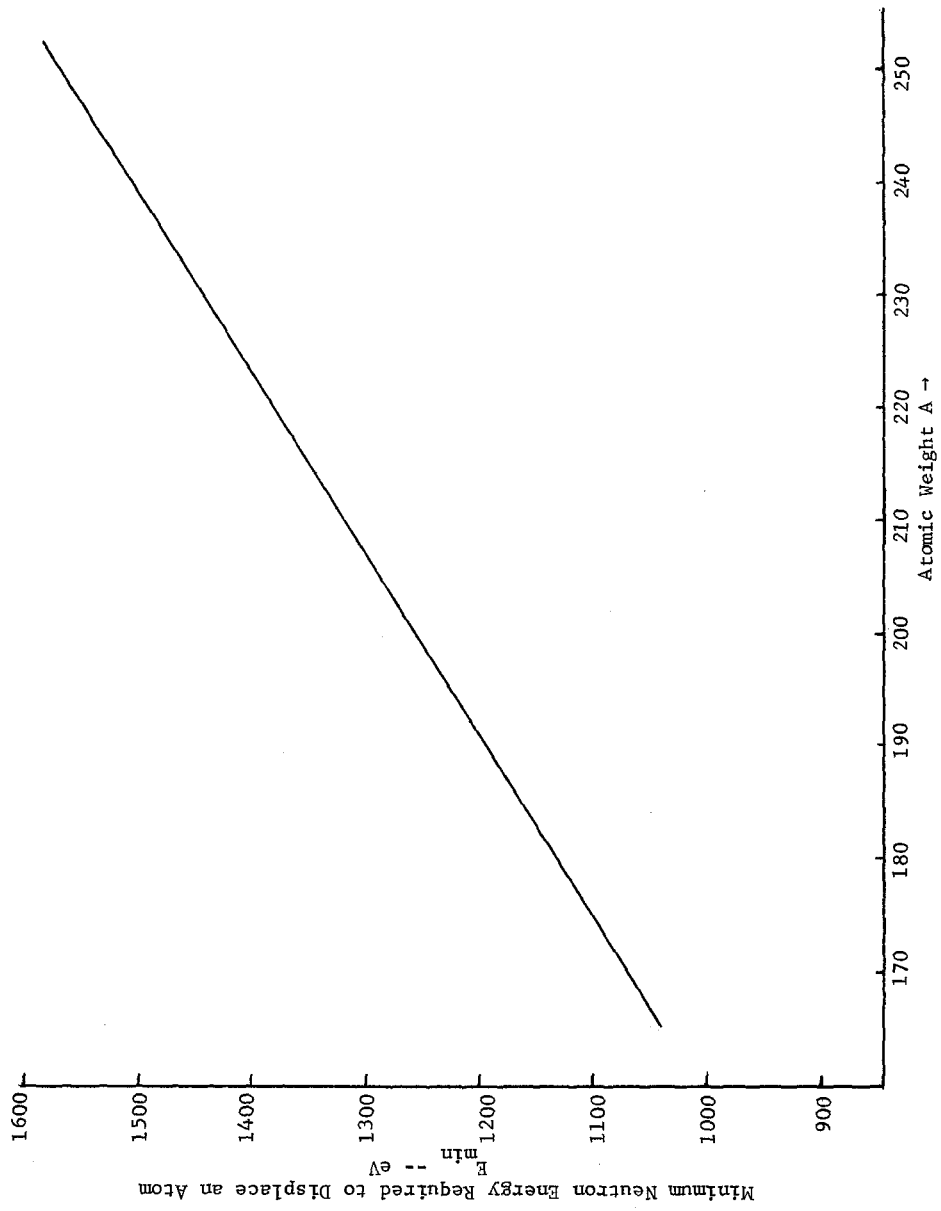


Fig. 2. Displacement Energy vs. Atomic Weight

where

Σ_s = the (macroscopic) bound cross section

$e = E' - E$ the energy transfer from the neutron (initial-final energy of neutron)

$$\hbar^2 \kappa^2 = 2m(E' + E - 2\mu_0 \sqrt{EE'})$$

μ_0 = cosine of the scattering angle (lab system)

Am = mass of crystal atoms

κ = Boltzmann constant

T = temperature °K

ω = frequency of phonon (in (rad/sec))

$f(\omega)$ = continuous phonon frequency distribution function (in units of sec)

t = time (in sec)

This formula is based on the assumption that no interference between different parts of a neutron wave incident on the crystal is present. Furthermore, the crystal is assumed to be of the simple cubic type with one atom per unit cell. The atoms, occupying the lattice positions in the crystal, are assumed to be harmonically bound to each other. Thermalization studies have yielded the phonon distribution function, $f(\omega)$ ⁽⁵⁾, which is shown in Fig. 3. It is obvious from this figure that the primary contribution to the phonon frequency spectrum is due to the two peaks centered at $2.28 \times 10^{13} \text{ sec}^{-1}$ and $3.11 \times 10^{13} \text{ sec}^{-1}$, respectively. Thus, to a first order approximation it may be assumed that $f(\omega)$ has the form

$$f(\omega) = 0.39 \delta(\omega - 2.28 \times 10^{13} \text{ sec}^{-1}) + 0.61 \delta(\omega - 3.11 \times 10^{13} \text{ sec}^{-1})$$

The coefficients of the delta functions appearing in $f(\omega)$ were chosen in such a way that

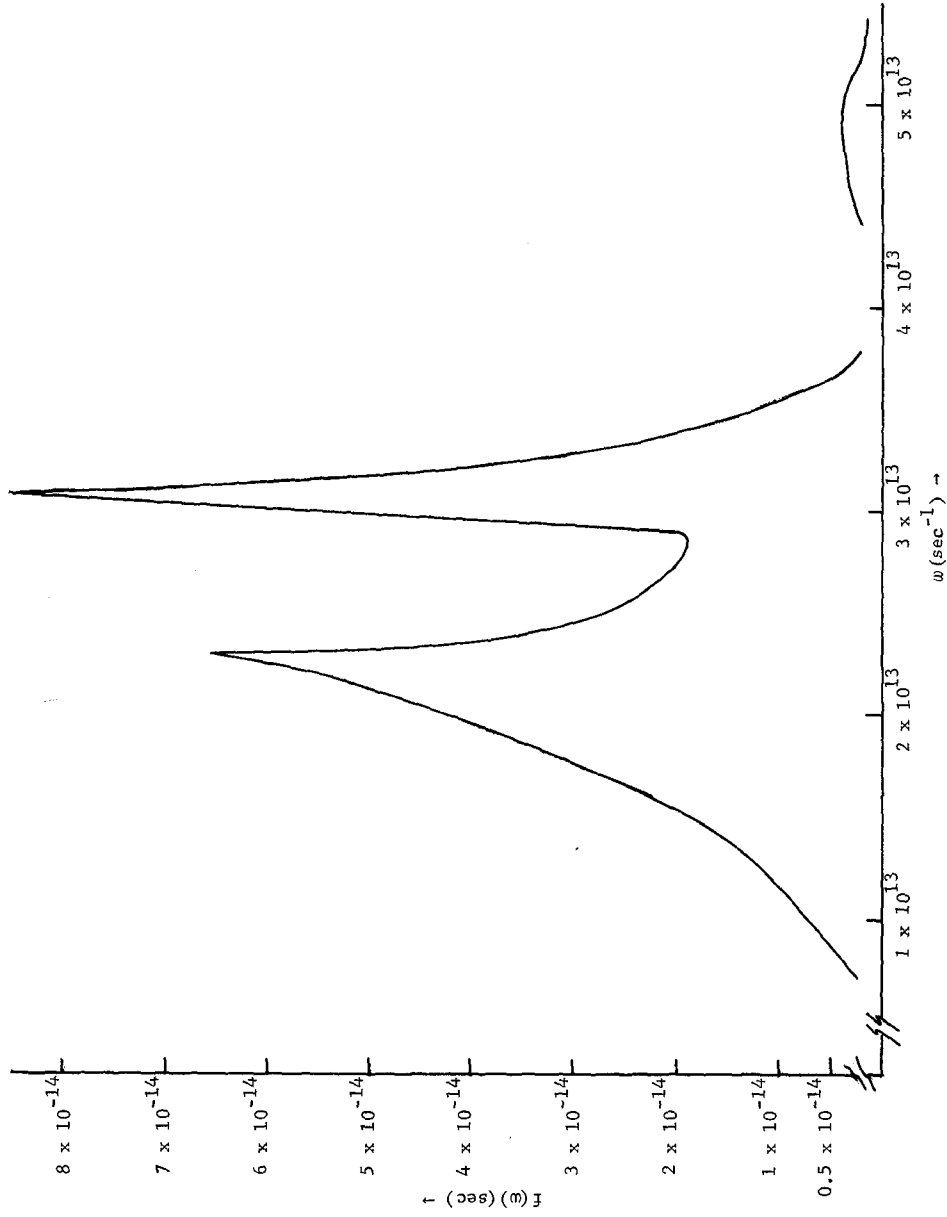


Fig. 3. Frequency Spectrum of Uranium

$$\int_0^{\infty} f(\omega) d\omega = 1,$$

a normalizing property which $f(\omega)$ is required to have. An evaluation of Eq. 1 gives a value of 0.041 eV for the maximum energy loss which can occur with 1.5 keV incident neutrons.

The energy loss through phonon excitation is obviously very small and one may choose to either ignore slowing-down in the ^{238}U plate, shown in Table I, or incorporate a fictitious mass in the free-gas, slowing-down model such that the maximum energy loss per collision does not exceed .04 eV. This last approach was tried using the RABBLE code. The atomic mass of ^{238}U was set at 1×10^4 amu (corresponding to maximum energy loss of .4 eV), and the capture cross sections in the resolved resonance region, using ENDF/B-III s-wave parameters only, were calculated. For comparison, the same cross sections were calculated in the usual manner, i.e. the mass of ^{238}U was 238 amu's. Table II shows the results. The differences are significant.

It may be argued that for the first two groups the free-gas, slowing-down model may be more appropriate. This may be the case since more work is needed to more accurately determine the displacement energy for uranium. There is no doubt, however, that below 2 keV the free-gas, slowing-down model is not appropriate. Furthermore, large and significant reduction in the σ_c^{238} is achieved with a more appropriate model. Experimentally, it has been observed⁽⁶⁾ that there are significantly more neutrons below 2 keV than calculations predict. This also supports the conclusion that below 2 keV the scattering laws in use are in error.

TABLE II
 Comparison of ^{238}U Capture Cross Sections Using the Free-gas,
 Slowing-down Model ($A=238$) and the Bound Atom in a Crystal
 Model ($A = 1 \times 10^4$); ENDF/B-III s-wave Resonance
 Parameters and about 60,000 Ultrafine Groups Were Used

Energy Group	$(\sigma_c) A = 238$	$(\sigma_c) A = 1 \times 10^4$
4.307 - 2.612 keV	0.3989	0.1653
2.612 - 2.035 keV	0.5571	0.3003
2.035 - 1.234 keV	0.5703	0.2978
1.234 - 0.9611 keV	0.7106	0.3007
0.9611 - 0.5829 keV	0.8886	0.5491
0.5829 - 0.2754 keV	0.7977	0.3752
0.2754 - 0.1013	1.284	0.6932
0.1013 - 0.02902	1.5957	0.9492
0.2902 - 0.01371	2.5779	1.3662

REFERENCES

1. R. A. Karam and K. D. Kirby. "Assessment of Flat-Flux and Flat-Source Approximations in Generating Resonance Cross Sections," ORQ-4750-2 (Dec. 1974); also to be published in NS&E
2. B. T. Kelly, "Irradiation Damage to Solids," Pergamon Press, London, 1966
3. L. Van Hove, Phys. Rev., 95, 249 (1954)
4. G. I. Bell and J. Glasstone, "Nuclear Reactor Theory," Van Nostrand Reinhold Company, New York, N. Y., 1970, p. 348
5. Gulf General Atomic, Inc., Report #GA 8774, "Reference Manual for ENDF Thermal Neutron Scattering Data," San Diego, California, 1968
6. J. C. Young *et al.*, "Measurement and Analysis of Neutron Spectra in Fast Subcritical Assembly Containing U^{235} , U^{238} , and BeO," Nucl. Sci. and Eng., 48, 45 (1972)

Technique for Simultaneous Adjustment of Large Nuclear Data Libraries
(D. R. Harris and W. B. Wilson)
Los Alamos Scientific Laboratory

Successful nuclear design requires adequate prediction of integral design quantities such as critical loading, energy deposition rate, transmutation rate, Rossi- α ., and radiation dose. Adequate prediction, in turn, requires an adequate nuclear data base, and a number of groups have attempted to achieve this by adjusting the data base to improve agreement with integral observations. These groups have in all practical cases utilized least square methods¹, and whatever the functional to be minimized they have limited the adjustment to only a portion of a large nuclear data library. Had the adjustment been applied to another portion of the nuclear data library, another result would have been obtained. The limitation of adjustment to only a portion of the nuclear data library may be justified by physical intuition, but it has also been the result of technical problems in the required inversion of large matrices¹. We show here that this inversion problem can be circumvented and arbitrarily large nuclear data libraries can be adjusted simultaneous, when, as was assumed by most groups¹, the basic nuclear data are uncorrelated. We illustrate the technique by adjusting nuclear data to integral observations (including very discrepant central worths) made on the ZPR-6-6A, ZPR-6-7, and ZPR-3-48 fast reactor benchmark critical assemblies².

Group cross sections and other data in a nuclear data library will be represented by $x_1, x_2, \dots, x_{\hat{j}}$, where \hat{j} , the number of primary parameters, may be of order 10^4 or 10^5 . Integral parameters $y_1, y_2, \dots, y_{\hat{i}}$ are computed as functions of the primary parameters, $y_i(x_1, x_2, \dots, x_{\hat{j}})$, or $y_i(x)$ in a convenient notation. Here \hat{i} , the number of integral parameters usually is of order 10 to 10^2 . From a combination of measurements, corrections, and calculations one arrives at "evaluated" observed values $x_1^e, x_2^e, \dots, x_{\hat{j}}^e$ and $y_1^e, y_2^e, \dots, y_{\hat{i}}^e$. It usually is found that $y_i(x^e)$ differs from y_i^e and we wish to reduce this discrepancy. One presumably can improve the data base by minimizing (other techniques are reviewed in Ref. 1),

$$S = \sum_{L=1}^{\hat{L}} \sum_{L'=1}^{\hat{L}} w_{y_1 y_{1'}} [y_1(x) - y_1^e] [y_{1'}(x) - y_{1'}^e] + \sum_{j=1}^{\hat{J}} \sum_{j'=1}^{\hat{J}} w_{x_j x_{j'}} [x_j - x_j^e] [x_{j'} - x_{j'}^e] + 2 \sum_{i=1}^{\hat{I}} \sum_{j=1}^{\hat{J}} x_j y_i [y_i(x) - y_i^e] [x_j - x_j^e] \quad (1)$$

subject to the requirements that

$$y_i(x) = y_i(x^e) + \sum_{j=1}^{\hat{J}} \frac{\partial y_i}{\partial x_j} \bigg|_{x^e} [x_j - x_j^e] \quad , \quad (2)$$

$$i = 1, 2, \dots, \hat{I} \quad .$$

For minimum variances in the adjusted results the weights w appearing in Eq. (1) are the elements of the inverse of the matrix of variances and covariances among the primary and secondary parameters. The use of a linear relation between $y(x)$ and x in Eq. (2) results because the computation of $y_i(x)$ and $\partial y_i / \partial x_j$ is expensive and is done infrequently, although one can of course iterate. We note here that the computation of $y_i(x)$ and $\partial y_i / \partial x_j$ (by perturbation theory) is obtained for the whole primary data base at once, not just a portion of it.

If we minimize S by obtaining \hat{J} normal equations, then the combination of these and the \hat{L} Eq. (2) represent $\hat{I} + \hat{J}$ simultaneous equations. In general the normal equations are solved by Gauss-Newton iteration³; here as in solution of the simultaneous linear Eqs. (1) and (2) large matrices, at least of order $\hat{J} \times \hat{J}$, must be inverted. But if the primary parameters are uncorrelated with each other and with secondary parameters then the normal equations

$$\sum_{i=1}^{\hat{I}} \sum_{l'=1}^{\hat{L}} w_{y_i y_{l'}} [y_i(x) - y_i^e] \frac{\partial y_{l'}}{\partial x_j} \bigg|_{x^e} + w_{x_j x_j} [x_j - x_j^e] = 0 \quad (3)$$

$$j = 1, 2, \dots, \hat{J} \quad ,$$

permit the replacement of $x_j - x_j^e$ in Eq. (2) by linear combinations of $y_i(x) - y_i^e$. There result only \hat{I} equations for $y_i(x) - y_i^e$,

$$\sum_{i'=1}^{\hat{I}} [y_{i'}(x) - y_{i'}^e] [\delta_{ii'} + \sum_{j=1}^{\hat{J}} \sum_{L''=1}^{\hat{L}} \frac{w_{L'' L''}}{w_{x_j x_j}} \frac{\partial y_{L''}}{\partial x_j} \bigg|_{x^e} \frac{\partial y_i}{\partial x_j} \bigg|_{x^e}] = y_L(x^e) - y_i^e \quad , \quad (4)$$

$$L = 1, 2, \dots, \hat{L}$$

and, because \hat{i} usually is much less than \hat{j} , the solution of Eq. (4) is a considerable computational improvement. Once the adjusted values $y_i(x)$ are computed from Eq. (4), the adjusted primary parameters are computed from Eq. (3) for the whole library at once. This adjustment technique has been coded as an option into the ALVIN sensitivity and adjustment code.

We illustrate this improved technique by adjusting nuclear data to $\hat{i}=24$ integral observations on three ZPR assemblies described by Bohn³. Bohn supplies sensitivity coefficient information for only $\hat{j}=19$ important primary nuclear data parameters so our technique is not really necessary (matrices of order $\hat{i}+\hat{j}=43$ are readily inverted), but the principle at least is demonstrated. It is convenient to allow y_i to represent the ratio of the computed value C_i of an integral parameter to its experimental value E_i , and to let x_j represent the ratio of the nuclear datum σ_j to its evaluated value σ_j^e ; then y_i^e and x_j^e are unity, and

$$\left. \frac{\partial y_i}{\partial x_j} \right|_{xe} = \left(\frac{\sigma_j}{C_i} \frac{\partial C_i}{\partial \sigma_j} \right) \bigg|_{xe} - \left(\frac{\sigma_j}{E_i} \frac{\partial E_i}{\partial \sigma_j} \right) \bigg|_{xe} \quad (5)$$

Specifically, for $i=1,2,3$ the integral parameters are the C/E values for multiplication factors of ZPR-6-6A, ZPR-6-7, and ZPR-3-48, indicated in the second column of Table I by subscripts A, 7, and 8 respectively. For $i=4,5,\dots,15$ the integral parameters are the C/E values for central worths of ^{239}Pu , ^{235}U , ^{238}U , and ^{10}B , indicated by 49, 25, 28, and B, respectively as superscripts on W; for example, the C/E value for the central worth of ^{239}Pu in the ZPR-6-7 assembly is indicated by W_7^{49} in Table I. Finally, for i greater than 15 the integral parameters y_i are C/E values of ratios of reaction rates, eg, 7^{28c}_{49f} for y_{20} represents the C/E value of the ^{238}U capture rate relative to the ^{239}Pu fission rate measured in ZPR-6-7. If y_i is $(\sigma_n/\sigma_m)/(\sigma_n/\sigma_m)E$, then to first order (unchanged flux spectrum),

$$\left. \frac{\partial y_i}{\partial x_j} \right|_{xe} = \delta_{nj} - \delta_{mj} \quad (6)$$

Table I. Integral Parameters y_i and Values $y_i(x^e)$ Computed Using Evaluated Nuclear Data Parameters x_j^e . If No Adjustment Were Necessary, $y_i(x^e)$ Would Equal Unity.

i	y_i	$y_i(x^e)$	y_i adjusted by ALVIN	y_i selected by Bohn
1	k_A	.9920±.004	.992	
2	k_7	.9924±.004	1.002	
3	k_8	.9927±.004	1.002	
4	W_A^{49}	1.10±.025	.993	1.06
5	W_A^{25}	1.15±.025	1.020	1.05
6	W_A^{28}	1.24±.035	1.103	1.09
7	W_A^B	.92±.075	.848	.96
8	W_7^{49}	1.25±.035	1.064	1.14
9	W_7^{25}	1.24±.035	1.050	1.08
10	W_7^{28}	1.16±.025	.929	.95
11	W_7^B	1.18±.035	1.033	1.17
12	W_8^{49}	1.25±.035	1.054	1.12
13	W_8^{25}	1.26±.035	1.063	1.08
14	W_8^{28}	1.27±.035	1.033	.99
15	W_8^B	1.09±.035	.951	1.06
16	A^{R25f}_{28f}	.90±.03	.947	
17	A^{R25f}_{28c}	1.03±.03	1.063	
18	7^{R49f}_{28f}	.99±.02	.973	
19	7^{R49f}_{25f}	1.05±.02	1.033	
20	7^{R49f}_{28c}	1.09±.02	1.060	
21	7^{R25f}_{28f}	.94±.02	.927	
22	7^{R25f}_{28c}	1.04±.02	1.027	
23	8^{R25f}_{28f}	.96±.05	.960	
24	8^{R25f}_{28c}	.94±.05	.927	

Table III. Primary Nuclear Data Parameters x_j , Their Uncertainties, and Their Adjusted Values

j	x_j	x_j^e	x_j adjusted by ALVIN	x_j selected by Bohn
1	σ_f^{25}	1±.1	.971	.93
2	σ_c^{25}	1±.1	.925	
3	σ_f^{49}	1±.1	.988	.97
4	σ_c^{49}	1±.1	.994	
5	σ_c^{28}	1±.15	.958	.88
6	σ_f^{28}	1±.1	.971	.97
7	σ_{inel}^{28}	1±.15	.793	.88
8	σ_{el}^{Na}	1±.1	1.068	
9	σ_{el}^O	1±.1	1.075	
10	σ_c^{Fe}	1±.1	.977	
11	σ_c^{Ni}	1±.1	1.001	
12	σ_c^{Cr}	1±.1	.995	
13	\bar{v}_d^{28}	1±.06	1.153	1.10
14	\bar{v}_d^{25}	1±.04	1.109	1.012
15	\bar{v}_d^{49}	1±.06	1.190	1.024
16	\bar{v}_d^{40}	1±.1	1.011	1.016
17	\bar{v}_d^{41}	1±.1	1.012	
18	σ_c^{Na}	1±.1	.995	
19	σ_{el}^C	1±.1	1.097	

Primary nuclear data selected by Bohn for sensitivity studies are listed in Tables II and III together with sensitivity coefficients computed by Bohn and uncertainties mostly assigned by Bohn. All Bohn's calculations utilize ENDF/B-III data as the evaluated base as processed into multigroup cross sections by SDX. All primary data were assumed to change independent of energy.

Values of primary and secondary parameters adjusted by ALVIN are listed in Tables I and III and show physically expected trends. Values selected by Bohn on the basis of the integral experiments also are listed. Our data adjustments are only illustrative of our adjustment technique. More detailed study of data uncertainties and sensitivities would be required to justify an adjusted data set for nuclear design application.

References

1. D. R. Harris, "Consistency Among Differential Nuclear Data and Integral Observations", Trans. Am. Nuc. Soc. 18, 340 (1974).
2. E. M. Bohn, "The Central Worth Discrepancy in Three Fast Reactor Benchmark Critical Assemblies", ZPR-TM-185 (1974).
3. D. R. Harris, "DAFT1-a FORTRAN Program for Least Square Fitting of 0.0253 ev Neutron Data for Fissile Nuclides", WAPD-TM-761 (1968).

ENDF/B-IV THERMAL REACTOR LATTICE BENCHMARK
ANALYSIS WITH MONTE CARLO RESONANCE TREATMENT

W. Rothenstein
Brookhaven National Laboratory
Upton, New York 11973

1. Introduction

The benchmark studies currently in progress at BNL are based on ENDF/B-IV data and the HAMMER lattice analysis code.⁽¹⁾ No data adjustments are made, but improvements are introduced into the calculational procedure wherever appropriate. In particular the resonance treatment is replaced by Monte Carlo reaction rates, attention being given to the most effective manner in which these reaction rates can be introduced into the multigroup code.

The multigroup library has been prepared in accordance with the special features of the subsequent heterogeneity, resonance, and leakage treatments. The problems which arise from the artificial separation of resonance cross sections into resonance and smooth contributions have been investigated. An account is given of the modifications which have been introduced into the processing code in order to derive the required ENDF/B-IV multigroup data.

The benchmark lattices analyzed and described in the present paper are the one region TRX-1 and TRX-2 lattices⁽²⁾ of 1.3% enriched, 0.387 inch diameter Uranium metal rods. In order to extend the range of volume ratios the two region TRX-3 benchmark has been replaced by a BNL⁽³⁾ lattice containing the same fuel and with the same water to metal volume ratio. It will be denoted by TRX-3B, and is calculated as a one region system with the experimental buckling of the BNL lattice. The other integral parameters were taken from TRX-3, where they were measured at the center of the lattice. It contained 217 rods and was surrounded by a $\text{UO}_2\text{-H}_2\text{O}$ driver zone.

The Monte Carlo code for the calculation of resonance events will be described. It makes use of ENDF/B-IV resonance profiles which are stored on tapes in standard ENDF/B format so that they can be readily replaced if modifications in the evaluated data are considered to be necessary. The code concentrates on the resolved resonance region in which most of the resonance absorption occurs. At these energies, the Monte Carlo results are used in the lattice analysis code in preference to the built in calculation of shielded resonance integrals. In the unresolved resonance region the shielding is considerably smaller and the absorption represents only a small fraction of the total resonance absorption. Consequently, the shielding calculations in the unresolved resonance region have been left unmodified in the lattice analysis. On the other hand, it is possible to introduce the effective detailed resonance profiles into the Monte Carlo code by the use of probability cables. A simple code for constructing such tables from the single level ENDF/B average resonance parameters and statistical distributions in the unresolved resonance region is described in the Appendix. The results obtained by this code have shown that cross section correlations in the unresolved resonance region at successive neutron energies during the moderating process can be ignored.

The paper contains the results of the analysis of the TRX lattices together with the effects of a number of different approximations which can be used in the calculations. The final results and conclusions take into account the discussions held at BNL during the seminar on U-238 capture in March 1975.

In general, the effective multiplication factor of the lattices is still underpredicted, but the other integral parameters are now closer to the experimental values than was frequently reported in the past.

2. Monte Carlo Code for Resonance Reaction Rates

The Monte Carlo Code (REPC) which was used to calculate resonance reaction rates utilizes detailed resonance cross section profiles prepared by the RESEND program⁽⁴⁾ from the ENDF/B-IV data.

RESEND replaces the standard ENDF/B tape by a modified library in which the File 2 resonance parameters are deleted and File 3 is extended to contain the detailed cross sections as a function of energy at 0°K throughout the resonance region. The resonance formalisms as recommended in the ENDF/B manual⁽⁵⁾ are fully implemented. In the resolved resonance region the energy mesh is constructed by selecting initially the energies of the resonance peaks and successively halving the interval between them until an interpolation accuracy criterion ϵ is met: the fractional difference between the cross sections calculated from the resonance formalism at the mesh points selected last and the value obtained by linear interpolation between the neighboring points must not exceed ϵ . For U-235 and U-238 the accuracy was taken to be $\epsilon = 0.001$. The sections for σ_g , σ_f , σ_c of the former then contained about 11000 energy points each (most of these points being in the resolved resonance region between 1.0 and 82.0 ev), while for U-238 the cross sections σ_g and σ_c were specified at about 32000 energies (most of the points being between 1.0 and 4000 ev).

The cross section tapes were subsequently Doppler broadened by the SIGMA 1⁽⁶⁾ routine. This procedure does not alter the energy mesh, and makes use of the integrals of the product of the (linearly varying) cross section between successive energy points and the Gaussian temperature broadening kernel.

To facilitate the data handling in the Monte Carlo code the sections specifying the different cross sections of each isotope are brought to a common grid (in practice the densest grid), so that the energy mesh needs to be stored only once for each isotope. In addition the grids were inverted so that the cross sections could be read from high to low energy in analogy with the neutron moderation.

In the Monte Carlo code the cross section data are stored in the extended core facility of the CDC 7600. The neutron histories are dealt with in batches (typically of 1000 neutrons each). Part of the data (a page with lowest energy E_L^i) for each nuclide i is transferred to central memory, and the entire neutron batch is processed until all the neutrons have reached an energy below the largest E_L^i stored in the core. A new page of data for this isotope i now read into central memory and the process is repeated until all the neutrons in the batch have passed the minimum energy specified for the problem.

In the unresolved resonance region the RESEND program calculates average cross sections from the specified average resonance parameters and statistical distributions. Resonance shielding is therefore not treated at these energies in a Monte Carlo code which uses the broadened RESEND cross section tapes directly. It is possible however to make use of the probability table method⁽⁷⁾ to modify the cross sections in the unresolved resonance region. The construction of the probability tables from the average resonance parameters and statistical distributions is quite straightforward when the single level resonance formalism applies. In the Appendix a code written for this purpose is described. It averages the probability tables

over many ladders. The code has been used to investigate the significance of correlations between cross sections at relatively closely spaced energy points which would be missed by the direct use of uncorrelated probability tables. It was found that for energy degradations greater than the average separation of successive resonances such correlations are entirely negligible. This condition is met for practically all neutron collisions with heavy isotopes in the energy regions where their resonances are unresolved.

The Monte Carlo Code(REPC) itself is a new version of the REPETITIOUS program⁽⁸⁾. It treats the geometry of a square or hexagonal lattice of rods, each subdivided into a number of coaxial annular regions, exactly. The neutron histories are followed between energies E_{\max} and E_{\min} in which all collisions are taken to be elastic and isotropic in the center of mass system. These conditions apply in the entire resolved and most of the unresolved energy regions. The isotropic injection routine introduces each neutron into the lattice with unit weight at the first energy with which it emerges below E_{\max} after an elastic collision above this energy, assuming that the cell flux is proportional to $1/E$ for $E > E_{\max}$. The neutron weight is degraded by the scattering probability Σ_s/Σ_t at each collision, reaction rates being obtained from $W \Sigma_x/\Sigma_t$ for the different reaction types x . For editing purposes the reaction rates are stored by regions in specified energy groups, which may be conveniently selected to coincide with the MUFT group structure. All quantities are printed out together with their probable errors at one standard deviation obtained from the results for the different batches.

In the calculations reported in the present paper the Monte Carlo runs covered the energies from $E_{\max} = 50$ kev, to $E_{\min} = 0.625$ ev, and used the Doppler broadened RESEND tapes. The Monte Carlo reaction rates were utilized only in the resolved resonance region which accounts for most of the resonance capture and fission, and where a precise determination of the shielding effect is most important. The resolved resonance region is sufficiently far below the source near E_{\max} for the results to be independent of any small approximations made in the injection routine. For the resonance reaction rates in the unresolved resonance region the standard routines in the lattice analysis code were regarded as adequate, since they are much smaller than those at lower energies, and far less affected by shielding.

A basic problem exists in the use of the cross section tapes constructed with the Breit Wigner single level resonance formalism in a Monte Carlo code. The current ENDF specifications⁽⁵⁾ do not lead to cross sections which are positive definite. The problem of negative scattering (and sometimes total) cross sections over limited energy ranges below some resonance peaks persists even after Doppler broadening. In the Monte Carlo code σ_s was set to zero whenever a negative value was encountered. Alternative libraries in which the isotopes were treated by the multilevel formalism, but without changing any of the resonance parameters, were also used; the problem of negative cross sections was then automatically eliminated. The effect of the different formalisms for the calculation of σ_s on the resonance reaction rates was investigated, and found to be very small (see paragraph 7).

3. Shielded Resonance Integrals and Resonance Reaction Rates

Different computational methods treat the resonance events by methods which are quite distinct from one another. A Monte Carlo program for example calculates the resonance reaction rates directly. They can be recorded by reaction type, by nuclide giving rise to the reaction under consideration, and in specified volumes and energy intervals. They are generally normalized to one source neutron. These reaction rates are part of those needed to specify the neutron balance in a reactor or a lattice unit cell.

Other programs such as the HAMMER lattice analysis code perform a calculation of the shielded resonance integral which must be subsequently translated into resonance reaction rates. If one treatment of the resonance region is to be substituted for another to improve the accuracy of the lattice analysis, care must be taken that the interface is handled properly.

In the HAMMER program the shielded resonance integrals are obtained from Nordheim's method⁽⁸⁾. Inherent in this treatment are a number of approximations⁽⁹⁾ which make its replacement by more precise calculations desirable. However, apart from these considerations the manner in which the Nordheim shielded resonance integrals are used in the lattice analysis code must be clarified, if this calculation is to be replaced by an alternative treatment. The calculation of the shielded resonance integral for the n th resonance is based on the relation between the collision density $F_n(u)$ at lethargy u in the resonance and the flux level ϕ_n in the absence of flux depression:

$$F_n(u) = \frac{\Sigma_a^n(u)}{\Sigma_t^n(u)} \phi(u) = N \sigma_B \phi_n \quad (1)$$

when $N \sigma_B$ is the constant macroscopic background cross section. The absorption in the resonance is then given by:

$$A_n = \int_n \frac{\Sigma_a^n(u)}{\Sigma_t^n(u)} F_n(u) du = N I_{eff}^n \phi_n \quad (2)$$

so that

$$I_{eff}^n = \int_n \frac{\Sigma_a^n(u)}{\Sigma_t^n(u)} f_n(u) du \quad (3)$$

where $f_n(u)$ is the collision density normalized to σ_B above the resonance. In Nordheim's method $f_n(u)$ is calculated for a lattice cell by solving the integral equation for the collision density numerically over a very fine mesh starting at a lethargy where the asymptotic value applies. Cell heterogeneity is taken into account by the use of region to region collision and escape probabilities. The absorption fraction in the nth resonance is

$$\alpha_n = \frac{A_n}{q_0} = \frac{N I_{eff}^n \phi_n}{q_0} \quad (4)$$

where q_0 is the slowing down source into the group in which the resonance lies. If one allows for the gradual decrease of the flux level due to absorption (but without depression due to the resonance)

$$\alpha_n = 1 - \exp\left(-\frac{N I_{eff}^n \phi_n}{q_0}\right) \quad \text{and} \quad \alpha_g = \sum_n \alpha_n \quad (5)$$

The total absorption fraction α_g per unit source into group g , obtained by replacing the ϕ_n in Eq. 5 by the average group flux ϕ_g , forms the basis of the resonance absorption treatment in the HAMMER lattice analysis code.

The resonance treatment may be replaced by a Monte Carlo calculation by correcting the resonance integrals of Eq. 3. In fact, this has frequently been done in the past. A shielded resonance integral may be calculated from the Monte Carlo resonance events by means of the group resonance escape probability

$$P_g = \exp \left[- \frac{N I_{\text{eff}}^g}{\xi \Sigma_B} \right] \quad (6)$$

This value of I_{eff}^g is based on the volume averaged slowing down powers of all the constituent nuclides of the lattice cell for a flat flux. On the other hand in Eq. 3 I_{eff} results from the (potential) scattering cross section σ_B of the fuel with its admixed nuclides, which is the asymptotic value of the collision density, as well as from collision probabilities calculated by suitable approximations. Whether the two definitions of I_{eff}^g are identical in practice is by no means certain.

For the reasons stated above the reaction fractions α_g^x per unit source into the group for each reaction type x , which are calculated directly in a Monte Carlo code, were preferred to the shielded resonance integrals as the interface for introducing the Monte Carlo results into the lattice analysis code. Even so, questions arise whether this should be done in the integral transport theory lattice heterogeneity calculation, or as a preliminary to the B-1 leakage calculation. In addition there are problems connected with the separation of smooth and resonance absorption. These points will be considered in Section 5.

4. Preparation of the Multigroup Libraries

The ENDF/B-IV epithermal multigroup library was obtained with the ETOG 3 rprocessing code⁽¹¹⁾. A number of modifications were introduced for consistency with the HAMMER analysis code⁽¹⁾. The additional options refer in particular to the resonance nuclides. They will be described with special reference to the options selected for U-235 and U-238.

The MUFT 54 epithermal group structure was used with thermal cut off at $E_c = 0.6248$ ev. The weighting function was a $1/E$ spectrum joined above $E = 6.738 \times 10^4$ ev (the low energy limit of group 20) to a simple fission spectrum $[4E/(\pi\theta^3)]^{1/2} \exp(-E/\theta)$, with $\theta = 1.323$ Mev in accordance with U-235 thermal fissions (ENDF/B-IV).

Equivalent smooth unshielded capture and fission cross sections can be constructed from the specified resonance parameters in the ENDF/B library. Alternatively the resolved s wave resonance parameters can be included in the input to the HAMMER analysis code in which case they are not entered as smooth cross sections into the multigroup library. If this option is selected one may additionally treat the unresolved s wave resonances in the same way provided they lead to only one J state of the compound nucleus; otherwise they are converted to equivalent unshielded smooth cross sections. For any resolved resonance for which resonance shielding is calculated in the HAMMER code a $1/v$ tail is subtracted from the resonance integral. It is put back as a smooth cross section in each group g in the resolved resonance region, down to the low energy limit of this region. These $1/v$ smooth tail contributions are calculated for a 2200 m/sec cross section

$$\sigma_o^R \frac{\Gamma_x}{\Gamma} \sqrt{\frac{E_R}{E_{th}}} \left/ \left[\frac{4}{\Gamma^2} (E_R - E_{th})^2 \right] \right.$$

for resonance R and reaction type x and assuming a 1/E flux in each resonance group for cross section weighting. The resolved resonance region is taken to end at the upper energy of the multigroup just below the unresolved resonance region, and a similar choice is made at the upper end of the latter region.

For U-235 only the resolved s wave resonance parameters were kept for resonance shielding calculations in HAMMER. All other resonances were converted to smooth unshielded cross sections. For U-238 the resolved and unresolved s wave resonance parameters formed part of the HAMMER input; the p wave resonances were converted to smooth cross sections. A separate calculation of the small unresolved p-wave resonance shielding was made in this case and entered into the lattice analyses as a correction. In the resonance region resonance scattering was omitted from the multigroup library since it is included in the resonance absorption calculation.

The (n,2n) cross section was added twice to the inelastic-scattering cross section and subtracted once from the capture cross section. Assuming that the spectra of the neutrons after inelastic scattering and the (n,2n) reactions are not very different this procedure accounts for the additional neutrons which are produced and preserves neutron balance in the group in which the reactions occur.

An error in the calculation of the fission spectrum in the ETOG 3 code was noticed and corrected. The original calculations had altered the shape of the fission spectrum very slightly and led to high values of the fast fissions in U-238 in the lattice analyses reported during the U-238 resonance capture seminar. The results given in the present paper are based on the corrected U-235 fission spectrum.

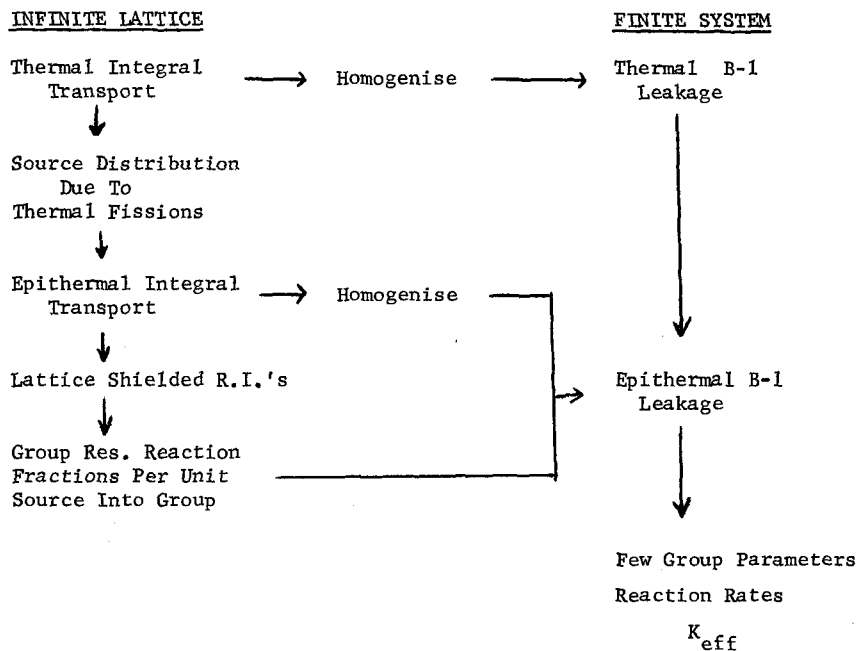
The thermal 30 group multigroup libraries for THERMOS were produced with the FLANGE-II code⁽¹²⁾ which was also used to calculate the scattering kernels⁽¹⁰⁾ for the thermal spectrum calculations. Whenever the resonance region extends into the thermal energy range, resonance scattering was included in the preparation of the thermal libraries. The thermal scattering kernels were normalized to the inelastic cross section, or the sum of inelastic and elastic scattering, according to the data specified on the ENDF/B tapes for each moderator.

5. The HAMMER Lattice Analysis Code

The HAMMER lattice analysis, including a full account of the equations involved, has been described previously⁽¹⁰⁾. In the present section only a broad outline will be given together with details of some problems which arise in the resonance treatment.

The calculations are performed in accordance with the following flow chart:

HAMMER LATTICE ANALYSIS



The lattice analysis starts with the THERMOS thermal spectrum calculation for which a spatially flat flux can be assumed for the specification of the slowing down source. In fact apart from resonance shielding the cell flux is flat already at considerably higher energies.

The integral transport treatment for the calculation of the heterogeneity effects is based on the iterative solution of the transport equation for the scalar flux

$$\phi_{ni} = \sum_{n'} T_{n n' i} \left[\sum_j P_{n' i j} \phi_{n' j} + S_{n' i} \right] \quad (7)$$

Here $T_{n n' i}$ is the transport kernel from region n' to region n in group i . It is related to the collision probability $p_{n n' i}$ in n for a flat source of unit density in n' through

$$T_{n n' i} = \frac{P_{n n' i}}{\sum_{ni} V_n}, \quad \sum_n P_{n n' i} = V_{n'} \quad (8)$$

in which \sum_{ni} is the transport corrected total cross section. In the thermal energy range $P_{n' i j}$ is the transport corrected scattering kernel from group j to group i and $S_{n' i}$ is the elastic slowing down source from epithermal energies into thermal group i . At epithermal energies $P_{n' i j}$ is replaced by the in-group scattering kernel $P_{n' i}$ and the source includes elastic and in-elastic scattering into group i as well as the fission contribution.

Some of the problems which arise in the presence of both smooth and resonance absorption in the epithermal energy groups may be seen if one specifies the source term and in-group scattering kernel in the resonance

region, where the sources due to fission and inelastic scattering are absent. Considering the entire cell and assuming all parameters to be suitably cell averaged the slowing down density $q(u)$ satisfies the approximate Greuling Goertzel integral equation⁽¹³⁾

$$q = \frac{\xi}{\lambda} \int_{-\infty}^u e^{-\frac{(u-u')}{\lambda}} \Sigma_s(u') \phi(u') du' \quad (9)$$

where ξ and $\xi\lambda$ are the mean and half the mean square lethargy increments for an elastic collision. For hydrogen moderation this equation is exact and $\xi = \lambda = 1$. If the corresponding differential equation

$$q + \lambda \frac{dq}{du} = \xi \Sigma_s \phi \quad (10)$$

is integrated over an energy group in which q_0 and q_1 refer to the high and low energy limits

$$q_1 = q_0 \frac{\lambda - \frac{\Delta u}{2}}{\lambda + \frac{\Delta u}{2}} + \frac{\xi \Sigma_s \phi \Delta u}{\lambda + \frac{\Delta u}{2}} \quad (11)$$

in which λ , $\xi \Sigma_s$ and ϕ are now group averages.

The neutron balance equation

$$\Sigma_a \phi = \frac{q_0 - q_1}{\Delta u} = \frac{q_0}{\lambda + \frac{\Delta u}{2}} - \frac{\xi \Sigma_s \phi}{\lambda + \frac{\Delta u}{2}} \quad (12)$$

or $\Sigma_{tr} \phi = P\phi + S$, $\Sigma_{tr} = \Sigma_{s,tr} + \Sigma_a$ (13)

is now fully consistent with the transport equation, Eq. 7, summed over the entire cell after multiplying by $\sum_n V_n$, if

$$P = \sum_{s, \text{tr}} \frac{\xi \sum_s}{\lambda + \frac{\Delta u}{2}} \quad \text{and} \quad S = \frac{q_0}{\lambda + \frac{\Delta u}{2}} \quad (14)$$

The absorption cross section in Eqs. 12 and 13 refers to the smooth absorption. Resonance absorption can be allowed for in different ways. The simplest method consists of accounting for it immediately at the top of the group by replacing q_0 in Eqs. 11, 12, and 14 by $q_0 (1-\alpha)$ where α is the resonance absorption per unit slowing down density at the top of the energy group, as calculated in Section 3. Neutron balance is then still preserved. This is in fact the MUFT procedure. The group flux calculated from Eq. 7 is then depressed both by smooth and by resonance absorption. Such a procedure would require calculating α first, before the source for the solution of the integral transport problem, Eq. 7, is specified. On the other hand, the current version of the HAMMER makes use of the flux distribution in the lattice cell in order to specify the collision probabilities which are needed for the calculation of α . An iterative procedure between the resonance and transport calculations would then be necessary. At present the iteration is omitted in the HAMMER code by solving the integral transport problem first, calculating α subsequently, and allowing for the resonance absorption only in the calculation of q_1 by using $q_0(1-\alpha)$ in Eq. 11. The source $S = q_0 / (\lambda + \frac{\Delta u}{2})$ is not reduced to allow for resonance absorption in the group in which the transport equation, Eq. 7, is solved. Neutron balance is therefore violated.

These difficulties do not arise in the B-1 leakage calculations for the homogenized lattice cell. Here the neutron balance equation for buckling B is

$$(BJ + \sum_a \phi) \Delta u + q_0 \alpha = q_0 - q_1 \quad (15)$$

below the fission source and in the absence of inelastic-scattering. It is solved together with the isotropic slowing down equation, Eq. 10, the B-1 equation for the current, and the anisotropic slowing down equation. If Eq. 11 is used to eliminate q_1 from Eq. 15 it is clear that the resulting relation between q_0 and the flux depends on the leakage. Consequently, in expressing the resonance absorption as a fraction of q_0 , at the high energy limit of an energy group, q_0 should be corrected for leakage. This is in fact done in MUFT-5⁽¹⁴⁾ but not in the current version of HAMMER. On the other hand the average group flux is the flux in the presence of leakage.

In the light of these considerations and the discussions during the U-238 resonance capture seminar the Monte Carlo resonance reaction rates (smooth and resonance) in the resolved resonance region were introduced into HAMMER code just before the leakage calculation for the homogenized cell. In fact, group capture and fission cross sections were defined (iteratively) in a zero buckling homogenized cell calculation so that the Monte Carlo group capture and fission rates, suitably normalized, were reproduced exactly. The effective multiplication factor and integral parameters were then obtained after the subsequent B-1 leakage calculation. In addition to the resonance shielding the reduction of the smooth capture due to flux depressions near the resonance peaks, as well as the effect of leakage on the total absorption,

were thus fully taken into account.

An additional consideration regarding the slowing down treatment refers to the heavy isotopes. If the slowing down and neutron balance equations, Eqs. 11 and 12, are solved for q_1 at the low energy limit of an energy group,

$$q_1 = \frac{\xi \Sigma_s + \Sigma_a \left(\lambda - \frac{\Delta u}{2} \right)}{\xi \Sigma_s + \Sigma_a \left(\lambda + \frac{\Delta u}{2} \right)} q_0 \quad (16)$$

When $\Delta u \gg \lambda$ spurious reductions in the slowing down density may occur.

These can be avoided by setting $\lambda = \frac{\Delta u}{2}$ so that

$$\phi = \frac{q_1}{\xi \Sigma_s + \Sigma_a \left(\lambda - \frac{\Delta u}{2} \right)} \rightarrow \frac{q_1}{\xi \Sigma_s} \quad (17)$$

which implies that the contribution to q_1 from the heavy isotopes is based, approximately, on the average group flux.

6. Effective Capture Integrals of U-238 in the TRX Lattices

The separation of the U-238 capture into smooth and resonance contributions, and the importance of shielding corrections may be seen from the following tables.

U-238 Capture Integrals (barns) Treated as Smooth Capture

1/V Tails of resolved S wave resonance	0.79
p-wave resolved resonances	0.70
p-wave unresolved resonances	0.84
File 3 Capture	<u>0.33</u>
Total	2.66

U-238 Shielded S Wave Resonance Integrals (barns)

	<u>TRX-3B</u>	<u>TRX-1</u>	<u>TRX-2</u>
Resolved Resonance Region	10.35	11.84	12.35
Unresolved Resonance Region	<u>0.55</u>	<u>0.58</u>	<u>0.59</u>
Total	10.90	12.42	12.94

Reduction of U-238 Resonance Integrals Due to Shielding (barns)

	<u>TRX-3B</u>	<u>TRX-1</u>	<u>TRX-2</u>
Resolved s Wave Resonances	260.7	259.2	258.7
Unresolved s Wave Resonances	0.24	0.22	0.21
Unresolved p wave resonances	0.06	0.05	0.05

The File 3 capture consists of a bound level contribution, p -wave resonances which were missed in the experiments, and a small d-wave resonance contribution in the unresolved resonance region.

It should be noted that more than twenty percent of the capture is treated as smooth capture and therefore does not get reduced by local flux depressions at energies close to the resonance peaks unless codes, such as Monte Carlo treatments, are used which combine smooth and resonance capture.

The s wave resolved resonances are shielded to an extremely large extent. This is particularly true for the very large low lying resonances. Unresolved resonance shielding is far less important, but even so in terms of the effective unresolved resonance integral, or even the total effective resonance integral, these shielding corrections must be taken into account.

7. Effect of Different Resonance Formalisms on U-238 Resonance Capture

In Section 2 the problems arising in Monte Carlo calculations from the use of the single level Breit Wigner formalism were discussed. In addition even a multi-level formalism does not reproduce the experimental data of the total cross section in the valleys between the resonance peaks very well. Typically the σ_t profile should be raised by about 2 barns in these energy regions. In order to examine the effect of the detailed shape of σ_s on the capture in the benchmark lattices the Monte Carlo calculations for TRX-1 were repeated under different conditions. In the following table the results are shown both for the shielded resonance integral and the capture fraction between 50 kev and 0.625 ev.

TRX-1 Monte Carlo U-238 Resonance Capture

$$E_{\max} = 5 \times 10^4 \text{ ev}, \quad E_{\min} = 0.625 \text{ ev}$$

<u>Resonance Treatment</u>	<u>Resonance Integral (barns)</u>	<u>Capture Fraction</u>
Single level (σ_s) _{min} = 0.0	14.97 ± 0.08	0.1929 ± 0.0008
Single level (σ_s) _{min} = 2.0	15.16 ± 0.15	0.1951 ± 0.0017
Single level $\sigma'_s = \sigma_s + 2.0$ for 6.67 < E < 4000 ev	14.99 ± 0.07	0.1932 ± 0.0008
Multilevel	14.84 ± 0.08	0.1918 ± 0.0008

The minimum acceptable value of σ_s is 0. In the second calculation σ_s was set equal to 2.0 barns whenever a smaller value was obtained from the ENDF/B-IV profile. In the third calculation 2.0 barns were added to σ_s at all energies in the resolved resonance region above the first resonance.

The last result relates to a multilevel profile in which the ENDF/B-IV single level parameters were left unchanged. All the results except the second were obtained for 10^5 histories involving about 1.2×10^6 moderator and 2.4×10^5 fuel collisions. In the second calculation only 20000 histories were run.

It is clear that the different shapes of σ_s in the valleys did not affect the U-238 capture by an amount exceeding the probable error at one standard deviation. The use of the ENDF/B-IV profile, in which σ_s is not allowed to become negative, appears therefore to be adequate.

The Monte Carlo estimate of the U-238 reaction rate was compared with a RECAP calculation made at Westinghouse with ENDF/B-IV data by J. Hardy. The results agreed within the statistical accuracy of both estimates.

8. Comparison of Resonance Shielding Calculations With Monte Carlo Estimates

The shielded resonance integrals as calculated by the HAMMER program can be compared with Monte Carlo values although part of the differences may arise from problems of definition of the shielded resonance integral as pointed out in Section 3.

Comparison of Shielded Resonance Absorption Integrals in the TRX Lattices
U-238 (1.0 ev - 3.35 Kev); U-235 (1.0 ev - 101 ev) (barns)

	TRX-3B	TRX-1	TRX-2
U-238 HAMMER	10.35	11.84	12.35
M.C.	9.65 ± 0.09	11.42 ± 0.11	11.87 ± 0.11
U-235 HAMMER	208.3	218.1	220.9
M.C.	177.7 ± 1.8	194.5 ± 1.9	201.6 ± 2.0

The values refer to the groups which were treated as resolved resonance groups, MUFT groups 27-53 for U-238, and 35-53 for U-235. The Monte Carlo values given in the table are those obtained after subtraction of the smooth absorption integral of the HAMMER library in the resolved resonance groups. This ensures that similar quantities are compared. The Monte Carlo values are lower by about 5 percent in U-238 and more than 10 percent for U-235.

Comparisons of the total reaction rates (smooth and resonance) are tabulated below:

Comparison of Reaction Rates in the TRX Lattices
 U-238 (1.0 ev - 3.35 Kev); U-235 (1.0 ev - 101 ev)

	<u>TRX-3B</u>	<u>TRX-1</u>	<u>TRX-2</u>
U-238 HAMMER	0.2841	0.1640	0.1065
Corrected HAMMER	0.2560	0.1552	0.1029
M.C.	0.258 ± 0.003	0.155 ± 0.002	0.1015 ± 0.001
U-235 Capture			
HAMMER	0.0267	0.0148	0.00952
Corrected HAMMER	0.0242	0.0141	0.00924
M.C.	0.0210 ± 0.0002	0.0123 ± 0.0002	0.00817 ± 0.0001
U-235 Fission			
HAMMER	0.0478	0.0264	0.0169
Corrected HAMMER	0.0435	0.0252	0.0164
M.C.	0.0401 ± 0.004	0.0235 ± 0.0003	0.0154 ± 0.0002

The corrected HAMMER values refer to the neutron balance in the integral transport calculation (see Section 5). The resonance reaction fraction per unit slowing down density at the top of each energy group is calculated in the code in relation to the group flux. This flux is calculated in the absence of resonance absorption and there is a lack of balance of the neutrons. The correction discussed in Section 3 ensures neutron balance and lowers the group

flux in accordance with the total absorptions occurring in the group. Consequently, the reaction rates are also lowered.

The table shows that the differences between the Nordheim and Monte Carlo calculations for the U-238 capture in the TRX lattices is largely eliminated if the integral transport theory neutron balance is treated as described in Section 5. This is however fortuitous. In the corrected HAMMER results smooth capture is calculated more accurately, but resonance capture is underestimated since it should refer to the group flux level in the absence of the resonances. Evidently the underestimate is just sufficient to compensate for the inaccuracies in the Nordheim treatment. Other methods for treating resonance capture in the integral transport calculation with proper neutron balance may be used. The resonances could be accounted for at the bottom of each group, so that smooth absorption would be overestimated but resonance absorption treated in accordance with Section 3. Alternatively, two flux levels could be calculated, the first based on the smooth absorption only to derive the proper resonance absorption fractions per unit source, the second to calculate the actual smooth absorptions in the presence of the resonances.

The Monte Carlo absorption rates are unambiguous since resonance and smooth data are combined at the outset in the cross section calculations. They also account for mutual shielding, in particular the reduction of the U-235 absorptions in the vicinity of the large U-238 resonances.

9. k_{eff} and Integral Parameters of TRX Lattices (HAMMER, ENDF/B-IV)

The corrections referred to in the previous section improve the agreement between the HAMMER calculations and experimental values. The quantities compared are the effective multiplication factor k_{eff} , the ratio of epithermal to thermal captures in U-238 ρ_{28} , the ratio of epithermal to thermal fissions in U-235 δ_{25} , the ratio of U-238 fissions to U-235 fissions δ_{28} , and the ratio of U-238 captures to U-235 fissions C.

Comparison of Integral Parameters for the
TRX Lattices (ENDF/B-IV, HAMMER)

		TRX-3B	TRX-1	TRX-2
k_{eff}	HAMMER	0.9600	0.9801	0.9872
	Corrected HAMMER	0.9755	0.9848	0.9890
ρ_{28}	HAMMER	3.31	1.419	0.876
	Corrected HAMMER	3.13	1.383	0.863
	Expt.	3.01 ± 0.05	1.311 ± 0.002	0.830 ± 0.015
δ_{25}	HAMMER	0.258	0.1056	0.0642
	Corrected HAMMER	0.252	0.1046	0.0639
	Expt.	0.230 ± 0.003	0.0981 ± 0.001	0.0608 ± 0.0007
δ_{28}	HAMMER	0.169	0.0944	0.666
	Corrected HAMMER	0.167	0.0941	0.0665
	Expt.	0.163 ± 0.004	0.0914 ± 0.0020	0.0667 ± 0.0020
C	HAMMER	1.303	0.813	0.649
	Corrected HAMMER	1.256	0.802	0.645
	Expt.	1.255 ± 0.011	0.792 ± 0.008	0.646 ± 0.002

The extent by which k_{eff} differs from unity is large for the tightest lattice (water to metal volume ratio 1.0). The correction described in Sections 5 and 9 have the most pronounced effect on k_{eff} for this lattice. The correction improves agreement between calculation and experiment for all the integral parameters of the above lattices.

10. TRX Benchmark Analysis With Monte Carlo Reaction Rates

The Monte Carlo reaction rates were introduced into the HAMMER analysis at zero buckling after the lattices had been homogenized by defining group fission and capture cross sections as described in Section 5. The effect of leakage was then introduced in a final iteration.

The results are compared with experiment in the following table.

TRX Lattice Calculations and Comparison with Experiment
 ENDF/B Version IV

Resonance Reaction Rates of Zero Buckling Differential Transport
 Homogenized Cell calculation set equal to M. C. values for U-235
 fission and capture (resolved resonance region) and U-238 Capture
 (resolved resonance region).

	TRX-3B* $V_w/V_f = 1.00$		TRX-1 $V_w/V_f = 2.35$		TRX-2 $V_w/V_f = 4.02$	
	ENDF/B-IV	σ_c -0.1 barn Expt.	ENDF/B-IV	σ_c -0.1 barn Expt.	ENDF/B-IV	σ_c -0.1 barn Expt.
k_{eff}	0.9764	1.0000	0.9878	0.9977	0.9920	0.9982
ρ_{28}	3.11	3.01 ± 0.05	1.366	1.291	0.845	0.802
δ_{25}	0.237	0.230 ± 0.003	0.0995	0.0990	0.0612	0.0610
δ_{28}	0.169	0.163 ± 0.004	0.0944	0.0933	0.0665	0.0661
C	1.263	1.255 ± 0.011	0.800	0.775	0.640	0.625

* results calculated for the ENL lattice
 MA-130-387-100 which has the same fuel
 and volume ratio as TRX-3

** σ_c was reduced by 0.1 barn in U-238
 for MUFT groups 27-53
 (3.35 keV - 0.83 eV)

An attempt was made to attribute the remaining discrepancy between calculation and experiment to the U-238 capture data. The calculations were repeated by subtracting 0.1 barns from the group capture cross section throughout the resolved resonance region. This amounts to a capture integral of 0.83 barns.

The results for the integral parameters ρ_{28} and C suggest that a reduction of the U-238 shielded resonance integral by about 0.4 barns would lead to the best overall agreement with experiment.

11. Further Refinements and Conclusions

The results for the TRX benchmarks presented in this paper suggest that the epithermal capture of U-238 is overpredicted to some extent by the present ENDF/B-IV data. However, the discrepancy is smaller than was reported in the past and amounts approximately to 0.4 barns of shielded resonance integral.

The k_{eff} values are generally low and specially so for the tightest lattice, even if the data for U-238 are adjusted as indicated above. An attempt was made to determine whether some of this problem might be due to the calculations in the fast region where the fission neutrons are produced in the rods. To this end the calculations were repeated with corrected fluxes in the high energy groups using the ANISN⁽¹⁵⁾ transport code.

Fluxes entered into the HAMMER calculation from a P1-S4 ANISN run for the highest 20 energy groups (down to 67 kev), or P3-S8 ANISN run for the highest 10 energy groups (down to 820 kev) did not lead to a noticeable change in the calculated parameters. In fact, the ANISN flux distributions

in space and energy in these groups were practically identical with the HAMMER integral transport fluxes.

An additional effect which was examined in the final MUFT leakage calculation was that produced by resonance scattering. As discussed in Section 4 resonance scattering of U-238 is not included in the HAMMER multigroup library, since it is treated in the resonance calculation. However, in the final B-1 leakage treatment, when the resonance capture and fission cross sections have already been defined, resonance scattering should be included as well. In order to test its effect average group resonance scattering cross sections were introduced into the computation at this stage. They increased k_{eff} by about 0.5 percent without affecting the other integral parameters significantly. However, the magnitude of the change in k_{eff} should be regarded as an upper limit since it refers to unshielded resonance cross sections. Shielding would certainly be significant, although possibly less pronounced than in the case of capture. Consequently, the results would be much closer to those in which resonance scattering is omitted altogether and which were discussed in Section 10.

In conclusion, it may be said that after reduction of the U-238 shielded resonance integral by about 0.4 barns quite good agreement of the parameters ρ_{28} , δ_{25} , δ_{28} , and C with experimental values is obtained. These parameters were measured at the center of the core. The values of k_{eff} are less than unity, especially for the tightest lattice where the discrepancy remains more than 1 percent. The multiplication factor relates to the assembly as a whole and part of its underprediction may be due to the fact that asymptotic reactor theory in the lattice analysis code is compared with experiments on assemblies with rather small cores.

References

1. Suich, J.E., Honeck, H.C., The HAMMER System. DP-1064, 1967.
2. Hardy, J., Klein, D., Volpe, J.J. A Study of Physics Parameters in Several H₂O-Moderated Lattices of Slightly Enriched and Natural Uranium. J. Nucl. Sci. and Eng. 40, 101, 1970.
3. Hellens, R.L., Price, G.A., "Reactor Physics Data for Water Moderated Lattices of Slightly Enriched Uranium." Reactor Technology, Selected Reviews, 529, 1964.
4. Ozer, O. RESEND A Program to Preprocess ENDF/B Materials With Resonance Files into Point-wise Form. BNL 17134, 1973.
5. Drake, M.K. "Data Formats and Procedures for the ENDF Neutron Cross Section Library." ENDF-102 1970.
6. Cullen, D.E., "Program SIGMA 1 (version 74-1) - A Program to Exactly Doppler Broaden Tabulated Cross Sections in the ENDF/B Format," UCID-16426, Lawrence Livermore Laboratory, 1974.
7. Levitt, L.B. The Probability Table Method for Treating Unresolved Resonances in Monte Carlo Calculations. J. Nucl. Sci. & Eng. 49, 450, 1972.
8. Davison, P., et al. The REPETITIOUS code, WCAP-1434, 1964.
9. Rothenstein, W. Discrepancies in Thermal Reactor Lattice Analysis, BNL Seminar on U-238 Resonance Capture, 1975.
10. Jabbawy, S., Karni, J., Rothenstein, W., Velner, S. Water-Moderated Reactor Analysis with ENDF/B Data. Nuclear Data in Science and Technology, Vol. II, 147, 1973.
11. Kusner, D.E., Dannels, R.A. ETOG-1, A fortran IV Program to Process Data from the ENDF/B File to MUFT, GAM, and ANISN Formats. WCAP-385-1 (ENDF-114), 1969, Suppl. 1973.
12. Honeck, H.C., Finch, D.R. FLANGE-II A Code to Process Thermal Neutron Data from an ENDF/B Tape. DP-1278, ENDF-152, 1971.
13. Fertziger, J.H., Zweifit, P.F. Theory of Neutron Slowing Down in Nuclear Reactors. MIT Press, 1966, p. 161.
14. Bohl, H., Hemphill, A.P. MUFT-5 A Fast Neutron Spectrum Program for the PHILCO-2000. WAPD-TM-218, 1961.
15. Engle, W.W. A Users Manual for ANISN. Oak Ridge, K-1693, 1967.

Appendix

Construction of Probability Tables in the Unresolved Resonance Region

The RESEND program⁽⁴⁾ prepares a library in which the ENDF/B File 2 resonance data are converted to cross sections and added to the contents of File 3. In the unresolved resonance region average unshielded cross sections are calculated at the energy points at which the average resonance parameters and the statistical distributions of the neutron widths and resonance spacings are specified.

To obtain the actual cross sections in a Monte Carlo calculation the average cross sections must be multiplied by a random number selected in accordance with the relevant probability frequency functions $P(\sigma)$. Levitt⁽⁷⁾ calculated the integrals of these functions over specified cross section intervals (bins). The choice of the required random number is then a simple matter in a Monte Carlo program when interpolation within each bin is applicable.

The probability per unit cross section interval that its value is σ , is given by

$$P(\sigma) = \frac{1}{\Delta E} \int dE \delta [\sigma - \sigma(E)] \quad (\text{A.1})$$

The numerator of this expression sums all elementary energy intervals in ΔE for which $\sigma(E)$ precisely equals σ . It leads to the correct average and higher moments of $\sigma(E)$ in ΔE . Actually when the cross section has a complicated resonance structure, $P(\sigma)$ also exhibits considerable structure, since it is large at the maxima and minima, and small when the cross section changes rapidly. In addition $P(\sigma)$ depends on the interval ΔE which has been selected, unless it contains a very considerable number of resonances for each J sequence, and on end-effects which may arise from strong resonances near the limits of ΔE .

In the unresolved resonance region one may, however, specify probability tables averaged over many resonance ladders which are free from these difficulties. A ladder may be constructed from the average resonance parameters and the statistical distributions of neutron widths and resonance spacings specified at energy E. If this ladder is placed in a random manner with respect to E the cross sections at this energy can be calculated. Averaging this process over many such ladders leads to the probability table at energy E.

In practice only the resonances closest to E contribute to the cross sections. Assuming the Wigner distribution of resonance spacings

$$p(x) = \frac{\pi}{2} x e^{-\frac{\pi x^2}{4}} \quad (\text{A.2})$$

the actual spacings of successive resonance is $\langle D \rangle x$ where x is selected from this distribution. However, the probability that E lies between a resonance pair whose peaks are separated by D_0 is also proportional to D_0 itself, since the ladder is placed randomly with respect to E. Consequently, in constructing the ladder D_0 may be selected first as $D_0 = \langle D \rangle y$ where y is a random number chosen from the probability frequency function

$$q(y) = \frac{\pi}{2} y^2 e^{-\frac{\pi y^2}{4}} \quad (\text{Modified Wigner Distribution}) \quad (\text{A.3})$$

The nearest resonance pair is then placed on the energy scale so that E lies at a random location between these two peaks. More resonances can then be located on the energy axis above and below the pair closest to E at separations $\langle D \rangle \alpha$. The reaction widths of the resonances are obtained by multiplying their average values by random numbers selected from the appropriate x^2 dis-

tributions. The cross sections at E are finally obtained from the neighboring resonances in the ladder after Doppler Broadening. For single level Breit Wigner cross sections, this can be done by means of the line shape functions.

The above construction of ladders and probability tables is consistent with the usual formula for the average resonance cross sections: The principal contributions to the cross sections at E come from the nearest resonance pair the peaks of which are separated by D_0 . This corresponds to an average level density of $\langle 1/D_0 \rangle = 1/\langle D \rangle$ from Eqs. A.2 and A.3. Consequently, the average cross section at E becomes

$$\langle \sigma_x \rangle = \frac{\pi}{2} \frac{\sigma_0}{\langle D \rangle} \left\langle \frac{\Gamma_n \Gamma_x}{\Gamma} \right\rangle \quad (\text{A.4})$$

if correlation effects due to more distant resonances are negligible.

Figs. 1 and 2 show capture and scattering cross section distribution functions $\int_0^\sigma P(\sigma') d\sigma'$ obtained by a code which uses the above algorithms. They refer to U-238 at 4 key, the low limit of the unresolved resonance region. Three neighboring resonance pairs have been included in the cross section calculations for s-wave resonances and two pairs for each J sequence of the p-wave resonances. The effect of Doppler broadening is shown: for a given random number a smaller cross section is obtained at the low temperature in the resonance wings and the converse applies near the resonance peaks. The average cross sections are also compared with the RESEND values, Eq. A.4.

The code has also been used to determine the significance of cross section correlations by determining the cross sections at energy E-d as well as those at E. The correlated frequency function

$$P_d(\sigma, \sigma') = \frac{1}{\Delta E} \int_{\Delta E} dE \delta[\sigma - \sigma(E)] \delta[\sigma' - \sigma(E-d)] \quad (\text{A.5})$$

represents the double differential probability per unit cross section intervals that their values are σ and σ' for energy difference d . The conditional probability

$$P_{\sigma,d}(\sigma') = \frac{P_d(\sigma, \sigma')}{P(\sigma)} \quad (\text{A.6})$$

expresses the chance per unit cross section interval that its value is σ' , if the cross section at an energy augmented by d is σ . In figures 3, 4, and 5 the distribution functions at E and $E-d$ are shown for capture in U-238 at $E=4$ kev and $d = 1, 5, 20$ ev below this energy. In Fig. 3 there is strong correlation: When σ is small (or large) there is a high probability that σ' will also be small (or large). At $d = 5$ ev the correlation is much less pronounced, and at $d = 20$ ev it has practically disappeared.

The figures provide quantitative evidence that cross section correlations at successive neutron collisions in the unresolved resonance region are insignificant if the neutron energy loss per collision exceeds the mean resonance spacing.

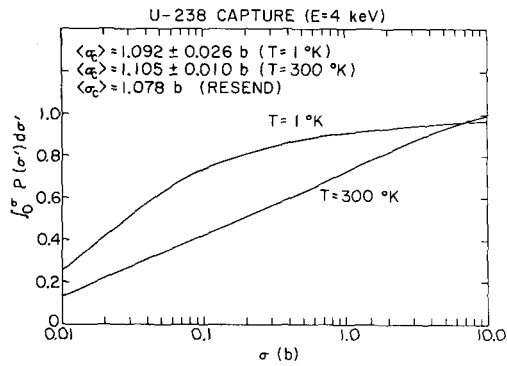


Figure 1

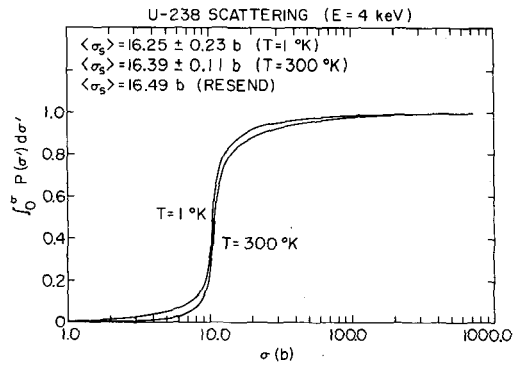


Figure 2

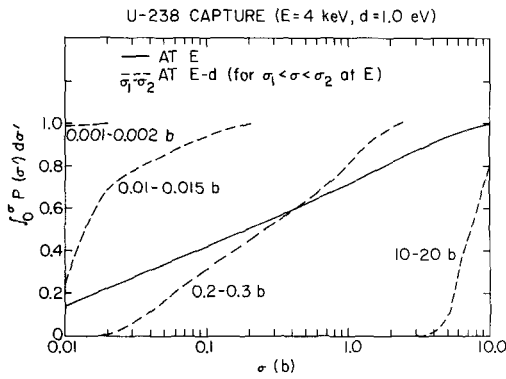


Figure 3

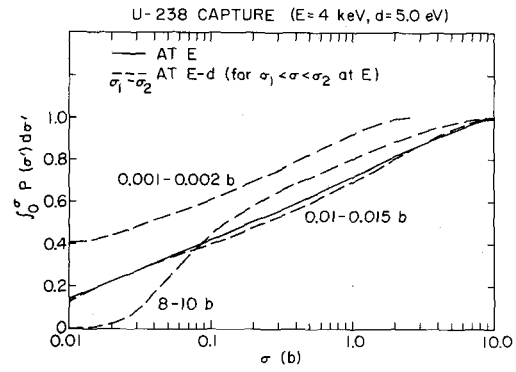


Figure 4

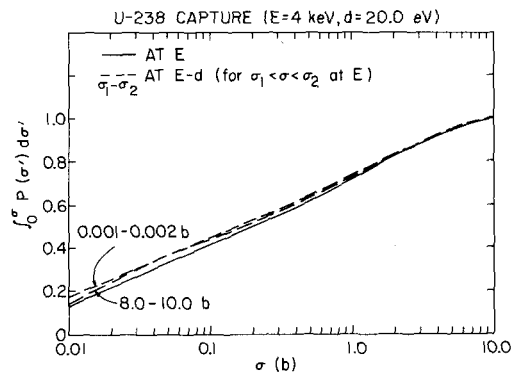


Figure 5

A Discussion of U-238 Resolved Resonance Parameters
and their Influence on Capture Cross-Sections

M. R. Bhat

National Neutron Cross Section Center
Brookhaven National Laboratory
Upton, New York 11973

April 1975

In the following, the experimental data on the resonance parameters of the first four resolved resonances of U-238 will be reviewed. The purpose of such a review is (1) to estimate the errors in the resonance parameters and (2) to determine how far the parameters could be reasonably changed within the bounds determined by the experimental uncertainties in the thermal capture cross-section and the infinitely dilute resonance capture integral. To be specific, the effect of changing the gamma width of the individual resonances will be studied and its effect on the effective resonance integral determined.

Resolved Resonance Parameters and their Error Estimates

The resonance parameters of the first four s-wave resonances of U-238 will be considered in detail as their contributions to the thermal capture cross-section and the dilute resonance capture integral account for about 90% of their experimental values. These are given in Table 1 along with the errors in these quantities as quoted by the experimenters and the type of cross-sections measured. If one of the parameters e.g. Γ_γ is enclosed in parenthesis this indicates that the value was taken over from some other experiment and was not obtained as part of the analysis involved.

An examination of these data indicate that the neutron widths obtained by Radkevich⁽⁵⁾ are consistently low for all the four resonances and lie well outside the range covered by other experiments. This may be due to some systematic error in this experiment and make the results suspect. If these numbers are left out one notices that in general Γ_γ show more of a spread in values than does Γ_n . Looking at these data sets it appears that the capture width of these resonances could have a value varying from resonance to resonance and it appears highly likely that it would lie between 22 and 26 meV. The recommended values in BNL-325⁽¹⁶⁾ for the first resonances are 26 ± 2 , 25 ± 3 , 25 ± 2 and 22 ± 2 . It is felt that the errors assigned represent a conservative lower limit and the uncertainty in the radiation widths are at least twice the values given. Though some of the authors claim errors of the order of 1% or less it is obvious that the systematic errors in these parameters are much larger than the quoted errors. The radiation widths for these resonances in the ENDF/B-IV (MAT = 1262) evaluation are 25.6, 26.8, 26.0 and 23.5 meV. The parameter Γ_n for these resonances have a narrower distribution and the recommended values in BNL-325 or the ENDF/B-IV evaluation appear reasonable. They are 1.5, 8.8, 31.1 and 25.3 meV respectively in ENDF/B-IV. In the following a value of $\Gamma_\gamma = 24$ meV will be assumed and the effect of lowering it by 9% to 22 meV on the various derived quantities will be studied.

Changes in the Capture Width and their Effect on the Thermal Capture, Dilute Resonance Integral and Effective Resonance Integral

The thermal capture cross-section of U-238 has a value of 2.70 ± 0.02 barns⁽¹⁶⁾; this is also the value used in the ENDF/B-IV evaluation (MAT = 1262).

The dilute resonance capture integral is generally accepted to be 275 ± 5 barns⁽¹⁸⁾. Any changes that are made in the capture width will therefore have to be compatible with the errors in these two experimental values. As has been mentioned in the last section, the greatest uncertainty lies in our knowledge of Γ_γ for the various resonances. Hence, it appears to be of some interest to study the effect of varying Γ_γ for the individual resonances.

In considering these changes it will be assumed that the covariance between Γ_n and Γ_γ is identically equal to zero. The fractional change in the contribution of a particular resonance to the thermal cross-section is found to be approximately equal to the fractional change in $\Gamma_{\gamma i}$; where $\Gamma_{\gamma i}$ is the radiation width of the i-th resonance.

$$\frac{\Delta \sigma_{n\gamma th}(i)}{\sigma_{n\gamma th}(i)} = \frac{\Delta \Gamma_{\gamma i}}{\Gamma_{\gamma i}} \quad (1)$$

Similarly, the fractional change in the contribution of i-th resonance to the dilute capture resonance integral is

$$\frac{\Delta I_{\gamma i}}{I_{\gamma i}} = \frac{\Delta \Gamma_{\gamma i}}{\Gamma_{\gamma i}} \frac{\Gamma_{ni}}{\Gamma_i} \quad (2)$$

where the symbols have the usual meaning. The effective or the shielded resonance integral (see Appendix) is a sum over terms of the type

$$I_{effi} = \frac{\pi}{2E_{ri}} \Gamma_{\gamma i} \sigma_{oi} \sqrt{\frac{\beta_i}{\beta_i + 1}} \quad (3)$$

each term for a resonance; where $\beta_i = \frac{\Gamma_i}{K\Gamma_{\gamma i}} \frac{\sigma_p}{\sigma_{oi}}$. Here σ_p is the potential

scattering cross-section and σ_{oi} the peak cross-section of the i -th resonance and K is defined in the Appendix. Differentiating the above expression we get,

$$\frac{\Delta I_{\text{eff}i}}{I_{\text{eff}i}} = \frac{1}{2} \frac{\Delta \Gamma_{\gamma i}}{\Gamma_{\gamma i}} \quad (4)$$

Looking at equations (3) and (4) one observes that a relatively large fractional change in the effective resonance integral can be achieved for a small change in the dilute resonance integral provided $\Gamma_{ni} \ll \Gamma_i$. This condition is fulfilled for the 6.67 eV resonance in U-238 for which $\Gamma_{ni}/\Gamma_i \sim .06$. Hence, it appears possible to bring about a substantial reduction in the contribution of the 6.7 eV resonance to the shielded resonance integral while keeping within the bounds of the error of 5 barns in the dilute resonance integral. However, such a reduction in Γ_{γ} will also cause a decrease in the value of the thermal capture cross-section which is known to 1% or an error of 0.02 barns. In such a case, it may be possible to include a bound level so that its contribution to thermal capture makes up for the decrease caused by reducing Γ_{γ} . The parameters of the bound level will have to be such that it does not in any way vitiate the $1/v$ shape of the low energy capture cross-section. It is found that a bound level of -20.0 eV can indeed be found which fulfills these requirements. Since the average spacing of the s-wave resonances in U-238 is about 18 eV; a bound level at -20.0 eV is consistent with it.

In Table 2 are shown the changes caused by decreasing the radiation width from 24 to 22 meV or by about 9%. These numbers show that a decrease of about 0.3 barns in the effective resonance integral of U-238 for a TRX-1 lattice may be

brought about for changes in the dilute resonance integral of 4.7 barns which is the same as the error in its value. The thermal capture cross-section will be reduced by 182 mb and this could be made up by including a bound level with a reduced neutron width of 0.75 meV and a $\Gamma_V = 23.5$ meV at 20.0 eV.

Acknowledgement

Some of the questions discussed here came up at the time of the U-238 Capture Seminar held here on March 18, 1975 and my thanks are due to S. Pearlstein for suggesting that they be further investigated in a parametric study.

Appendix

The following expressions were kindly supplied by Prof. W. Rothenstein; they give approximate formulae for the effective resonance integral I_{eff} for a metallic uranium rod of low enrichment.

$$I_{\text{eff}} = \frac{\pi}{2} \frac{\Gamma_{\gamma} \sigma_o}{E_r} \sqrt{\frac{\beta}{\beta+1}}$$

where $\beta = \frac{\Gamma}{K\Gamma_{\gamma}} \frac{\sigma_p}{\sigma_o}$ (wide resonance approximation)

where E_r is the resonance energy and σ_o the peak cross-section; σ_p the potential scattering cross-section Γ_{γ} and Γ are the capture and width of the resonance and

$$K = \frac{D\Sigma_p}{1-T} ; \Sigma_p = N\sigma_p = \text{macroscopic potential scattering cross-section}$$

for U-238; $N = 0.047$

D = diameter of fuel rod

T = transmission probability from rod to rod through the moderator in the lattice.

For the TRX lattices $D = 0.983$ cm. and

Lattice	V moderator/V fuel	T (low lying resonances)
TRX-1	2.35	0.146
TRX-2	4.02	0.071
TRX-3	1.00	0.349

References

1. J. E. Lynn and N. J. Pattenden, Proc. International Conf. on Peaceful Uses of Atomic Energy 4, 210 (1955).
2. J. A. Harvey, D. J. Hughes, R. S. Carter and V. E. Pilcher, Phys. Rev. 99, 10 (1955).
3. J. S. Levin and D. J. Hughes, Phys. Rev. 101, 1328 (1956).
4. R. G. Fluharty, F. B. Simpson and O. D. Simpson, Phys. Rev. 103, 1778 (1956).
5. I. A. Radkevich, V. V. Vladimirov and V. V. Sokolovsky, Jour. Nuc. Energy 5, 92 (1957).
6. L. M. Bollinger, R. E. Cote', D. A. Dahlberg and G. E. Thomas, Phys. Rev. 105, 661 (1957).
7. J. L. Rosen, J. S. Desjardins, J. Rainwater and W. W. Heavens, Phys. Rev. 118, 687, (1960).
8. M. C. Moxon and C. M. Mycock, Private Communication (1962).
9. H. E. Jackson and J. E. Lynn, Phys. Rev. 127, 461 (1962).
10. F. W. K. Firk, J. E. Lynn and M. C. Moxon, Nucl. Phys. 41, 614 (1963).
11. M. Asghar, C. M. Chaffey and M. C. Moxon, Nucl. Phys. 85, 305, (1966).
12. G. Rohr, H. Weigmann and J. Winter, Nuclear Data for Reactors, Helsinki, IAEA Vienna, I, 413 (1970).
13. G. Carraro and W. Kolar, Ibid, I, 403 (1970)
14. F. Rahn et al., Phys. Rev. 66, 1854 (1972).
15. K. L. Maletski, L. B. Pikel'ner, I. M. Salamatin and E. I. Sharapov, Sovt. Jour. At. Energy 32, 45 (1972).
16. S. F. Mughaghab and D. I. Garber, BNL-325 Third Edition Vol. 1, June 1973.

Table 1
Resonance Parameters of Low-lying s-wave Resonances of U-238

E_R (eV)	Γ (meV)	Γ_n (meV)	Γ_γ (meV)	Quantity Measured	Author, year
6.65±0.10		1.52±0.05	(23.5)	$\sigma_t, \sigma_\gamma, S.I.$	Rahn '72
6.65		1.578±0.106	23.43±10.12	σ_γ, σ_s	Asghar '66
6.65		1.52±0.01	27.2±1.5	σ_t	Jackson '62
6.68±0.06		1.48±0.05	25±2	S.I.	Rosen '60
6.690±0.025		1.15±0.04	21.15±1.30	σ_t	Radkevich '57
6.67	27.5±2.8	1.45±0.12	26.0±3.0	σ_t	Bollinger '57
6.67±0.04	27.5±1.5	1.4±0.1	26.1±1.5	σ_t	Lynn '56
6.70±0.06	26±2	1.54±0.1	24±2	σ_t	Levin '56
6.70±0.06		1.52±0.07	(24±2)	σ_t	Harvey '56
20.90±0.10		8.50±0.78	22±3	$\sigma_t, \sigma_\gamma, S.I.$	Rahn '72
20.79		9.34±0.44	33.83±3.74	σ_γ, σ_s	Asghar '66
21.0±0.3		9.0±0.3	25±2	S.I.	Rosen '60
21.00±0.14		6.35±0.59	36.0±3.5	σ_t	Radkevich '57
20.8	31.8±1.9	9.9±0.4	21.9±2.3	σ_t	Bollinger '57
21.0±0.3	37.5±2.3	8.7±0.3	28.8±2.3	σ_t	Lynn '56
21.2±0.3		10.3±2.0	25.9±12.0	σ_t	Fluharty '56
21.1±0.02	38±6	8.3±0.7	30±6	σ_t	Levin '56
20.9±0.2		8.5±0.4	25±5	σ_t	Harvey '56
36.8±0.07		37.98±2.00	23±2	$\sigma_t, \sigma_\gamma, S.I.$	Rahn '72
36.58		30.95±1.17	26.33±3.0	σ_γ, σ_s	Asghar '66
36.4	62.3±2	31.0±0.9	31.3±2.2	σ_t	Firk '63

Table 1 (Contd)

E_R (eV)	Γ (meV)	Γ_n (meV)	Γ_γ (meV)	Quantity Measured	Author, year
36.53		34.5±3.0	21.2±3.5	σ_γ	Moxon '62
36.8±0.6		33±2	26±4	S.I.	Rosen '60
37.0±0.4		22.0±3.5	34±10	σ_t	Radkevich '57
36.6	63±8	34.0±2.3	29±10	σ_t	Bollinger '57
36.8±0.15	53.5±3.9	28.6±1.5	24.9±4.2	σ_t	Lynn '56
37.0±0.6		32.6±9.0	27.7±24.0	σ_t	Fluharty '56
37.1±0.4	70±20	30±4	40±20	σ_t	Levin '56
37.0±0.3		32.5±1.9	29±9	σ_t	Harvey '56
66.10±0.15		26.02±2.03	21±2	$\sigma_t, \sigma_\gamma, S.I.$	Rahn '72
66±0.1		24±1.5	25±2	σ_t, σ_γ	Maletski '72
66.0		24.8±1.5	19.6±3.0	σ_γ	Rohr '70
66.0±0.10		25.3±1.0	(19.6±3.0)	σ_t	Carraro '70
65.95		22.74±0.77	26.07±1.67	σ_γ, σ_s	Asghar '66
66.1	50.2±1.6	25.1±1.2	25.1±1.6	σ_t	Firk '63
65.7		25.5±1.5	24.1±2.0	σ_γ	Moxon '62
66.3±1.1		23±2	20±3	S.I.	Rosen '60
67.7±0.8		19.1±4.5	25.5±12.0	σ_t	Radkevich '57
66.0	49±7	23.4±1.5	25.6±9.0	σ_t	Bollinger '57
66.2±0.4	41.2±2.3	22.6±1.5	18.6±2.7	σ_t	Lynn '56
66.0±2.5		25.4±7.0	39.1±26.0	σ_t	Fluharty '56
66.5±0.7		25±2	17±10	σ_t	Harvey '55

Table 2			
Effect of Reducing the Capture Width from 24 meV to 22 meV			
E_R (eV)	Δ_{σ_Y} (thermal)(b)	$\Delta_{\text{Res. Integral}}$ (b)	ΔI_{eff} (b)
6.67	-0.109	-0.696	-0.162
20.9	-0.036	-1.448	-0.071
36.8	-0.031	-2.014	-0.057
66.15	<u>-0.006</u>	<u>-0.518</u>	<u>-0.021</u>
	-0.182	-4.676	-0.311



